Norwegian University
of Life Sciences

Master's Thesis 2023 60 ECTS
Faculty of Chemistry, Biotechnology and Food Science (KBM)

Determination of antibiotic resistance in clinical isolates of *Pseudomonas aeruginosa*

Liv Sunniva Karlsson Lian
Biotechnology, molecular biology

Acknowledgements

The research detailed in this master project was conducted at the Protein Engineering and Proteomics (PEP) group within the Faculty of Chemistry, Biotechnology, and Food Science at the Norwegian University of Life Sciences. Dr. Gustav Vaaje-Kolstad and PhD student Per Kristian Edvardsen provided supervision for this thesis.

First and foremost, I want to express my gratitude to my main supervisor Gustav Vaaje-Kolstad for the invaluable guidance and discussions, both during the laboratory work and the writing process. From discussions of theoretical concepts and igniting a passion for the scientific field, to thorough feedback on my thesis, it has all been very much appreciated.

Second, I would like to thank my co-supervisor Per Kristian Edvardsen for all the help I got both during the laboratory work, the data processing and during the writing process. I would also like to thank Ronja Marlonsdatter Sandholm for all the help I received during the sequencing part of this thesis. Our talks and your desire to always help me has been very much appreciated.

To all the members of the PEP-group I extend my sincere thanks for your guidance and explanations of laboratory methods. A special thanks to Peter Elias Kidibule and Pascal Michael Mrozek for always taking the time to discuss both theoretical concepts, but also for lighthearted and fun moments in the laboratory.

A heartfelt acknowledgement to my fellow master students. Our shared experiences, delightful conversations, and laughter have all been cherished and will be remembered.

Lastly, I would like to give my deepest gratitude to Vetle Rakkestad for standing by my side, and providing uplifting words of affirmation as well as both support and help when I was learning LaTex and tried to navigate its many possibilities. Your presence and support has been very important to me, and I am very grateful.

Reading the thesis

Reading this thesis in a .pdf-format in a pdf-viewer (e.g., Adobe Acrobat reader) is recommended for full usage of its features. Firstly, all sections, figures, and tables listed in table of contents are clickable. Additionally, there are almost 350 cross references in the thesis. References are clickable, which sends you to the place in the thesis it was referenced to. The same is true for the citations (around 480) in the thesis. When you are done reading what was referenced to, you simply press Alt + left arrow key on your keyboard one time to go back to your original position. Alt + right arrow key can be used to go forward again, and you also have the option to go back and forth as many times as you want by using this keyboard shortcut. Lastly, some figures and tables of large size need to be zoomed in on to get all the information needed from the figure or table.

Liv Sunniva Karlsson Lian

December 2023, Ås

Abstract

The bacterium *Pseudomonas aeruginosa* is a gram-negative opportunistic pathogen that can infect immunocompromised patients such as patients born with the recessive hereditary genetic disease cystic fibrosis (CF). It is ubiquitously present, and is recognized by its high adaptability. *P. aeruginosa* is on the watch list of World Health Organization, due to antimicrobial resistance (AMR), and even multidrug resistance (MDR) emerging within the bacterial species [1]. In the cystic fibrosis lung, the pathogen is able to adapt and persist by the characteristic thick mucus lining the epithelial cells in the CF lung. Continued antibiotic exposure in an attempt to remove the pathogen, can result in the development of AMR. Understanding how the bacterium is able to achieve resistance against antibiotics is essential for development of novel antibiotics. During this master project, the antibiotic resistance properties in seven clinical isolates of *P. aeruginosa* have been characterized.

MIC was determined against three β-lactams, Piperacillin/Tazobactam (TZP), Meropenem (MEM), and Ceftazidime (CAZ), the fluroquinolone Ciprofloxacin (CIP), the aminoglycoside Tobramycin (TOB), and the polymyxin Colistin (CST). PAU5 showed to be multi-drug resistant (MDR). Interestingly, large changes in MIC value was seen between testing in Mueller-Hinton Broth and RPMI-LB10. Some isolates showed increased MIC value when in a nutrient-poor medium, while others isolates showed a reduction.

Genomic analysis showed all isolates had β-lactamases, as well as the various virulence factors and resistance genes previously identified in the species. PAU1 and PAU2 did, however, not have the efflux pump MexXY-OprM (important in efflux of aminoglycosides). The lack of this efflux pump could not be linked back to the result of the MIC determination for the two isolates. Discrepancy in genes involved in two-component regulatory system (TCS) was seen between isolates, and PAU6 had the most genes involved in TCS which might explain the low difference seen in MIC value for this isolate when changing the medium used for testing.

Finally, proteomics analysis was performed on clinical isolates PAU3 and PAU5, which had showed resistance towards two and four antimicrobial agents, respectively, during MIC analysis. Both isolates were able to grow at the highest TZP concentration tested (512/4 μg/mL). The β-lactamase ampC was the most up-regulated protein in both isolates, but additionally in PAU5, type VI secretion system was coexpressed with ampC when exposed to two different concentrations of TZP. This was not seen in PAU3. In PAU3 exposed to the highest antibiotic concentration of TZP, ampC along with protection proteins against ROS/NO damage, was seen highly up-regulated compared to control and the lowest antibiotic concentration. In the highest antibiotic concentration, PAU3 also showed up-regulation of cspD, a protein involved in persister cell formation. The conclusion was that up-regulation of the class C β-lactamase ampC was the main reason for the antibiotic resistance against TZP.

Sammendrag

Bakterien *Pseudomonas aeruginosa* er en gram-negativ opportunistisk patogen bakterie som kan infisere mennesker med nedsatt immunforsvar, slik som pasienter født med den recessivt arvelige sykdommen cystisk fibrose (CF). Bakterien er allment til stede og kjennetegnes av til høye tilpasningsevne. *P. aeruginosa* er på overvåkningslisten til Verdens helseorganisasjon, fordi antimikrobiell resistens (AMR) og til og med multiresistens (MDR) oppstår innenfor bakteriearten [1]. I lungene til pasienter med CF kan bakterien tilpasse seg og vedvare på grunn av den karakteristiske opphopningen av slim som ligger utenpå epitelcellene i lungen. Eksponering av antibiotika i forsøk på å fjerne patogenet, kan føre til utvikling av AMR. Forståelse av hvordan bakterien oppnår resistens mot antibiotika er avgjørende for utviklingen av nye antibiotika. I løpet av dette masterprosjektet har egenskapene rundt antibiotikaresistens til syv kliniske isolater av *P. aeruginosa* blitt karakterisert.

MIC ble bestemt hos alle isolatene mot de tre β-laktamene, Piperacillin/Tazobactam (TZP), Meropenem (MEM) og Ceftazidime (CAZ), et flurokinolon Ciprofloxacin (CIP), et aminoglykosid Tobramycin (TOB) og polymyxin Colistin (CST). PAU5 viste seg å være multiresistent (MDR). Interessant nok ble det observert store endringer i MIC-verdien mellom testing i Mueller-Hinton Broth medium og RPMI-LB10% medium. Noen isolater viste økt MIC-verdi i et næringsfattig medium, mens andre isolater viste en reduksjon.

Genomanalysen viste at alle isolater hadde β-laktamaser, samt ulike virulensfaktorer og resistensgener som tidligere har blitt identifisert i arten. PAU1 og PAU2 hadde imidlertid ikke efflux-pumpen MexXY-OprM (viktig for utpumping av aminoglykosider). Mangelen på denne efflux-pumpen kunne ikke knyttes til resultatet av MIC-bestemmelsen for de to isolatene. Det ble observert en forskjell i gener involvert i tokomponent reguleringssystem mellom isolatene, og PAU6 hadde flest gener involvert i TCS, noe som kan forklare den lave forskjellen sett i MIC-verdi for dette isolatet ved endring av testmedium. Til slutt ble proteomanalysen utført på isolatene PAU3 og PAU5, som viste resistens mot henholdsvis to og fire antimikrobielle midler i MIC-analysen. Begge isolatene var i stand til å vokse ved den høyeste konsentrasjonen TZP som ble testet (512/4 μg/mL). β-laktamasen ampC var det mest oppregulerte proteinet i begge isolatene, men i tillegg ble type VI-sekresjonssystemet observert i PAU5 når isolatet ble eksponert for to forskjellige konsentrasjoner av TZP. Dette ble ikke sett i PAU3. I PAU3 eksponert for den høyeste antibiotikkonsentrasjonen av TZP, ble ampC sammen med beskyttelsesproteiner mot ROS/NO-skade, sterkt oppregulert sammenlignet med kontroll og den laveste antibiotikkonsentrasjonen. I den høyeste antibiotikakonsentrasjonen viste PAU3 også oppregulering av cspD, et protein involvert i dannelse av "persister"-celler. Konklusjonen var at oppregulering av klasse C β-laktamasen ampC var hovedårsaken til antibiotikaresistensen mot TZP.

Abbreviations

A_{205}	Absorbance at 205 nanometers
ABC superfamily	ATP-Binding Casette superfamily
ABC solution	Ammonium Bicarbonate solution
ACN	Acetonitrile
AMR	Antimicrobial resistance
ATP	Adenosintrifosfat
bp	Base pairs
BUSCO	Benchmarking Universal Single-Copy Orthologs
cAMP	Cyclic Adenosine Monophosphate
CAZ	Ceftazidime
CF	Cystic Fibrosis
CFTR	Cystic Fibrosis transmembrane conductance regulator
CFU	Colony Forming Units
CIP	Ciprofloxacin
COPD	Chronic obstructive pulmonary disease
CST	Colistin sulfate salt
dH_2O	Distilled Water
DI	Deionized Water
dsDNA	Double Stranded DNA
DTT	Dithiothreitol
eDNA	Extracellular Deoxyribonucleic acid
EDTA	Ethylenediaminetetraacetic acid
EPS	Extracellular Polymeric Substances
ESBLs	Extended-Spectrum β-lactamases
EUCAST	European Committee on Antimicrobial Susceptibility Testing
ExoA	Exotoxin A
G-	Gram-negative bacteria
gDNA	Genomic DNA
HAI	Healthcare-Associated Infections
HCN	Hydrogen Cyanide
HIV	Human Immunodeficiency Virus
HMW DNA	High Molecular Weight DNA
HSI	Hcp secretion island
ILC	Innate Lymphoid Cell
IV	Intravenously
IAA solution	Iodoacetamide
kb	Kilo base pairs
kDa	Kilo Dalton
Kdp system	Potassium transport system
LB medium	Lysogeny Broth Medium
LC-MS	Liquid Chromatography Mass Spectrometry
LPS	Lipopolysaccharide

m/z	Mass-to-charge ratio
MATE family	Multidrug and Toxic Compound Extrusion family
MDR	Multi-drug resistant
MEM	Meropenem trihydrate
MFS superfamily	Major Facilitator Superfamily
MIC	Minimum Inhibitory Concentration
MSA	Multiple Sequence Alignment
NAG	N-acetylglucosamine
NAM	N-acetylmuramic acid
NCBI	National Center for Biotechnology Information
NMR	Nuclear Magnetic Resonance
NO	Nitric Oxide
OD_{600}	Optical Density at 600 nanometer
OM	Outer Membrane
PA solution	Phosphoric acid solution
PAUX	*Pseudomonas aeruginosa* Ullevaal X
PBP	Penicillin-binding proteins
Pch	Pyochelin
Pi	inorganic phosphate
PMSF	Phenylmethylsulfonyl Fluoride
Pvd	Pyoverdine
QS	Quorum sensing
RND family	Resistance-Nodulation-Division family
RNS	Reactive Nitrogen Species
ROS	Reactive Oxygen Species
RPMI medium	Roswell Park Memorial Institute Medium
SCV	Small-Colony Variant
Sec pathway	General Secretion Pathway
SMR family	Small Multidrug Resistance family
SRE	Short Read Elimination
ssDNA	Single Stranded DNA
STRING	Search Tool for the Retrieval of Interacting Genes/Proteins
STrap	Suspension trapping
TAE buffer	Tris Base, Acetic Acid, and EDTA Buffer
tat pathway	twin arginine translocation pathway
TCS	Two-component Regulatory System
TFA	Trifluoroacetic acid
timsTOF	Trapped Ion Mobility Spectrometry Time of Flight
TOB	Tobramycin sulfate salt
tRNA	transfer ribonucleic acid
TXSS	Type X Secretion System
TZP	Piperacillin Sodium Salt & Tazobactam
UV-Vis	Ultraviolet-Visible Spectroscopy
VAP	Ventilator-Associated Pneumonia

Contents

List of Figures

List of Tables

1 Introduction

1.1 General

In 1928 the scotsman Alexander Fleming made the paradigm shifting discovery of the penicillin. This marked the start of the antibiotic revolution, and the penicillin has later been termed a "miracle drug". The antibiotic completely changed the world of medicine as we know it. Fleming, according to the tales, did not yet know the colossal impact his discovery would have, but through the 1930's and 1940's an infected wound went from being life-threatening to becoming easily treatable. The antibiotic has since saved countless lives, and it has been a part of increasing the life expectancy remarkably throughout the 20^{th} century and into the 21^{st} century [2][3].

Following Fleming's discovery, a vast array of antibiotics has emerged. Antibiotics have revolutionized modern medicine and saved lives by effectively removing bacterial infections. However, their overuse and misuse has led to a growing crisis - antimicrobial resistance, often abbreviated AMR [4]. This phenomenon occurs when bacteria evolve to withstand the drugs designed to kill them, rendering previously treatable infections difficult, or even impossible, to manage. An article published in 2022 estimated that 4.95 million deaths were associated with bacterial AMR [4]. Furthermore, an estimated 1.27 million deaths were attributable to bacterial AMR [4]. These numbers are both daunting and scary.

In the realm of antibiotic resistance, some bacteria stand out as particularly concerning. These are the ESKAPE pathogens, an acronym used for the bacterial species *Enterococcus faecium*, *Staphylococcus aureus*, *Klebsiella pneumoniae*, *Acinetobacter baumannii*, *Pseudomonas aeruginosa*, and *Enterobacter* species [5]. These microbes have a knack for "escaping" the effects of antibiotics and are known for causing severe, often life-threatening infections.

This is no mere medical matter; it's a global crisis silently unfolding. The consequences of antibiotic resistance are far-reaching and alarming, leading to what some experts have termed "the silent pandemic" [6][7]. This phrase underscores the stealthy and pervasive nature of the problem. Antibiotic resistance not only threatens our ability to treat common infections, it also jeopardizes modern medical practices like surgeries, cancer treatments, and organ transplants. These life-saving procedures hinge on effective antibiotics in order to prevent and manage infections [8].

In the complex interplay between microbial pathogens and human health, one particularly significant relationship is that of the ESKAPE pathogen *P. aeruginosa* and cystic fibrosis (CF). *P. aeruginosa* is a versatile, opportunistic pathogen known for its remarkable adaptability and persistence. Cystic fibrosis, on the other hand, is a genetic disorder that profoundly affects the body and especially the respiratory system, leading to a range of debilitating symptoms. It is through the respiratory system that the bacterium *P. aeruginosa* often starts its pathogenicity route. From here it slowly progresses from an acute infection to a chronic infection where lung complications, and eventually pulmonary failure ensues [9].

The aim of this thesis is to investigate whether 7 clinical strains of *P. aeruginosa* sampled from patients with CF show resistance against different types of antibiotics, and if so, hopefully unravel the complex mechanisms by which the bacterium is able to do so. This will in turn tell us more about how the bacterium survives in the CF lung, how it adapts to different individuals of hosts, and thus offer a clearer understanding of the bacterium's ability to endure potent antibiotic treatments when exposed to them. Doing this requires us to first get a deeper understanding of the bacterium, hence the next section will give an introduction to the bacterium that is *P. aeruginosa*.

1.2 Introduction & Brief Tale About History

The discovery of *P. aeruginosa* traces back to 1882 when the French pharmacist Carle Gessard first described it. He noticed a blue and green coloration on bandages used on soldiers, and was able to identify the bacterium by isolating it from the infected wounds [10][11]. A few years later, humanity entered what historians have named the progressive era (ca. 1890-1920). This historical period witnessed revolutionary practices in health care as a whole, but also specifically in infection control. Influential figures like Joseph Lister, Ignaz Semmelweis, and Florence Nightingale pioneered the health care practices. For instance, Lister's groundbreaking contributions to disinfection protocols in hospitals brought about a lasting transformation in both wound care and operating room procedures. While these practices are now standard, they were groundbreaking during the progressive era [12][13].

As the 20^{th} century unfolded, optimism grew that infectious diseases would soon belong to the past. Antibiotic advancements, a cornerstone of this confidence, promised effective control over bacterial infections. However, this optimism was challenged as antibiotic resistance emerged and infectious diseases experienced a resurgence after antibiotics against the infectious disease had been both invented and used as treatment [14]. One of the culprits for these infectious diseases was the drug-resistant pathogen *P. aeruginosa*.

P. aeruginosa is a gram-negative, heterotrophic, facultative aerobic, and motile rod-shaped bacterium belonging to the group of γ-proteobacteria [11][15]. This resilient bacterium, often described as both antimicrobial resistant (AMR) and multi-drug resistant (MDR), is not only an ubiquitous environmental bacterium, it also stands out as a prevalent pathogen causing respiratory infections in hospitalized patients [16][17]. Multi-drug resistance is defined as a lack of susceptibility to three or more chemical classes of antibiotics [18]. *P. aeruginosa* is known to cause opportunistic infections in patients suffering from underlying medical conditions [16]. Furthermore, the bacterium is known for its metabolic versatility and for its ability to colonize many different ecological niches. It can live just as well in a soil environment or the rhizosphere, as in a water environment, and not to forget, inside a human host [15]. But how does this bacterium exhibit such apparent ease in adapting to such diverse environments?

In an attempt to deduce why this bacterium was so ubiquitously present, the complete genome was sequenced in 2000 by Stover et al. (2000) [19]. The mapping of the complete genome sequence both was and still is of crucial importance for comparing, analyzing, and evaluating the characteristics the species has [20]. Stover et al. (2000) denoted it as the

largest bacterial genome sequenced at the time, with a size of about 6.3 million base pairs (bp). They proposed that the size and the complexity of the genome gave the bacterium the opportunity to thrive in different environments, and as a result it was resistant to many antimicrobial substances [19]. Back in 2000, this bacterium was considered one of the top three causes of opportunistic human infections [19], highlighting the urgent necessity for a more profound understanding. Even today, this pathogen continues to be one of the most serious pathogens responsible for nosocomial infections [21]. *P. aeruginosa* is able to infect in several ways, and common infection routes are through burns, open wounds, post-surgery, and the respiratory system [16]. People at risk include, but are not limited to, people with urinary catheter, elderly people, people born with the recessive hereditary genetic disease cystic fibrosis (CF), people with advanced human immunodeficiency virus (HIV), or people with chronic obstructive pulmonary disease (COPD) [16]. People that are already immunocompromized often need medical care at hospitals, and one of the leading gram-negative species associated with nosocomial related infections, is just *P. aeruginosa* [22].

Before diving further into the infectivity and pathogenicity route of *P. aeruginosa* and by which virulence factors it is able to do so, a broader understanding of how the bacterium is structured and what common characteristics are present in the bacterium, is needed.

1.3 Structure and Characteristics of *P. aeruginosa*

P. aeruginosa is a heterotrophic, motile and facultatively aerobe bacterium. A facultatively aerobe means it can grow via aerobic respiration or use anaerobic respiration where nitrate serve as a terminal electron acceptor if oxygen is not available [11]. The cell size of *P. aeruginosa* is relatively small, and is in the range 0.5-0.8 μm by 1.5-3.0 μm. The typical form in which the bacteria is present, is in biofilm formation attached to a surface or substrate, but it can also be present in a planktonic and motile unicellular form [16]. In the motile life form, the bacterium expresses a polar flagellum which it moves by hydrolysis of ATP resulting in active swimming [23]. There is also substantial difference in phenotypes of *P. aeruginosa* in acute infections and chronic infections (see section 1.6.2). The acute infection phenotype expresses an array of virulence factors, while isolates sampled from cystic fibrosis (CF) lungs where the patient has chronic infection have shown to lack both flagella, pili, and other virulence mechanisms. The virulence mechanisms will be covered more in detail in section 1.7.

Morphology differs a bit between environmental and clinical isolates. Clinical cystic fibrosis isolates often have a smooth and mucoid colony type due to overproduction of alginate, and are large, with flat edges and an elevated appearance, which is not often seen in environmental isolates [11][24]. Some isolates from cystic fibrosis lungs have adopted a small-colony variant (SCV), and this has been linked to persistence of infection in a study done by A. Besse et al. (2022) [25]. In the study, environmental strains were shown to initially be larger, but to over time adopt a SCV in static cultures, showing that the environmental strains were capable of adopting the same morphology of colonies as the clinical isolates.

Because *P. aeruginosa* is a gram-negative (G-) bacterium, it has certain characteristics in the structure of the cell wall that it shares with other G- bacteria (i.e., *Escherichia coli* or the ESKAPE pathogens *Acinetobacter baumanii* and *Klebsiella pneumoniae*). The bacterium, along with the other G- species, has a cell wall that consists of a thin peptidoglycan layer surrounded by an additional outer membrane (OM). The peptidoglycan layer is of particular interest in the antibiotic field, because the synthesis of the cell wall is an often used mode of action for combating bacterial infections. Antibiotics active on the peptidoglycan layer are called β-lactams, and the theory and mechanism of β-lactam antibiotics will be described in more detail in section 1.8.2.

The layer of peptidoglycan surrounding the bacterial cell is comprised of identical subunits, and within these subunits there are two alternating sugars, called N-acetylglucosamine (NAG) and N-acetylmuramic acid (NAM). In addition to these alternating sugars, there is a peptide linked to the NAM sugar, called the stem peptide. This peptide is essential for making cross-links, or transpeptidations, between peptidoglycan chains. Figure 1.1 below shows the structure of the peptidoglycan.

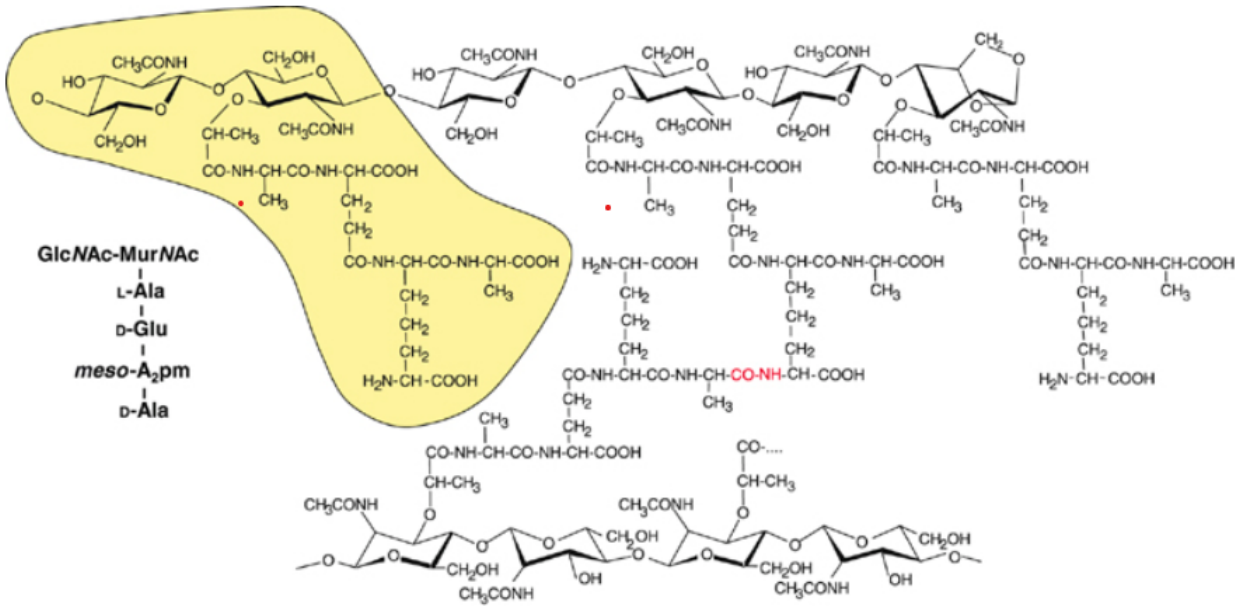

Figure 1.1. Peptidoglycan structure. Illustration of the structure of the peptidoglycan chain which is crucial for the integrity of the bacterial cell. The peptidoglycan chain at the top or the bottom of the figure, starts with a N-acetylglucosamine sugar (NAG), followed by an N-acetylmuramic acid (NAM) sugar unit which has a stem peptide with 4 amino acids chained together. The NAG, NAM, and stem peptide make up the unit that smallest repeating unit throughout the cell wall structure, and the structure is highlighted with a yellow color. CO-NH which is colored red in the middle of the figure, shows the transpeptidation that happens between stem peptides across chains. To the left, the structure of the stem peptide is shown with nomenclature. The figure is obtained from M.A. De Pedro et al. (2008) [26].

.

Figure 1.1 shows the peptidoglycan layer consists of disaccharide tetrapeptide subunits that are linked together both in long chains, but also across chains through the cross-linked stem peptides that are attached to the NAM sugar [26][27]. The stem peptides form connections by a process called transpeptidation through the amide group.

The connections between the stem peptides are crucial because it gives strength and rigidity to the cell wall. The reaction by which these connections are formed, is an often used antibiotic target in the pharmaceutical industry, and specific proteins involved in the transpeptidation of peptidoglycan chains are called penicillin-binding proteins (PBPs) [27][28]. The nomenclature of PBPs originate from their initial discovery when these proteins were identified based on their binding affinity with the β-lactam antibiotic penicillin, the antibiotic briefly discussed in section 1.1 [29].

Present between the inner membrane (IM) and the outer membrane (OM) is the periplasmic space. This space may constitute 20-40 % of the total cell volume, and many enzymes are present here (i.e., hydrolytic proteins, and transport proteins, PBPs) [30]. The periplasmic space is also where the cell wall is situated, and where components of it is added to the growing peptidoglycan chains that are bound by the stem peptides [30].

Another structure crucial to the G- bacterium is the outer membrane (OM), which surrounds the cell wall and the periplasmic space [30]. The OM is composed of both lipids, lipoproteins, and lipopolysaccharides (LPS) and it provides a first line of defense against the outside milieu. The OM is more permeable than the inner membrane due to porin and transporter proteins, and these proteins form channels across the membrane to let small molecules of up to around 600-700 Da pass. One feature of the OM is the LPS embedded in the membrane by a lipid, and the LPS serve a multitude of functions, including aiding in stabilization and maintained structural integrity of the membrane, as well as being a barrier for toxins or immune response cells [30]. The importance of LPS will be revisited in section 1.7.2.

Lipoproteins, along with LPS, are also embedded in the OM and play a role in maintaining structural integrity. These are proteins with a lipid modification to them which makes them able to anchor themselves to the membrane and at the same time be active in the extracellular, aqueous environment [31]. Lipoproteins perform many important functions for the bacterium, such as partaking in cell division, nutrient uptake, cell wall metabolism, antibiotic resistance, or adhesion to host tissues [31][32].

A rather interesting characteristic of the opportunistic pathogen, which is of importance when it comes to infection, is the fact that clinical isolates have been shown to exhibit auxotrophy [33]. Auxotrophic species or isolates are defined by being dependent on the host or the surrounding milieu for input of additional nutrients. *P. aeruginosa* is generally considered to be a prototroph. A prototroph is *P. aeruginosa* wild-type cells that are able to grow in minimal media alone, as opposed to auxotrophs that needs additional substances [33]. Adaptation towards auxotrophy happens especially in the endobronchiolar space of the cystic fibrosis lung [11][33]. This is likely a way of eliminating pathways that are not necessary so that the bacterium can allocate more energy towards other pathways in the metabolism. Other adaptations can be to develop new metabolic pathways. Some strains of *Pseudomonas* have been shown to be able to catabolize various antibiotics by using it as a carbon source, and that includes the β-lactam antibiotic penicillin [34].

A paper published in 1993 by R.F. Taylor et al. showed association between auxotrophic isolates and infection in people living with cystic fibrosis [33]. Another characteristic of importance when it comes to infection, is that isolates have been found to grow in environ-

ments depleted in oxygen, where dissolved oxygen concentrations down to less than 3 μM can be adequate for bacterial growth [35]. For comparison, at standard conditions in the atmosphere (0 °C and 1 atm), the concentration of oxygen in 1L of air is roughly 0.0094 mol or 9.4 mM (when assuming 21 % oxygen concentration) [36][37].

As explained in section 1.2, the genome size and the complexity of it (e.g., metabolic plasticity, and many two-component regulatory systems) makes *P. aeruginosa* able to adapt to many different environments, and it is able to do so quickly. The two-component regulatory system (TCS) is an important factor when it comes to quick adaptation, and the more versatile the environment the bacterium lives in, the more TCSs are necessary to yield quick adaptation. But how does it work?

The TCS is able to pick up environmental signals and quickly make modifications to gene expression if required. TCS usually consists of a sensor part that sits in the outer membrane of the bacterial cell facing the environment, and a response regulator inside the cell [38]. The sensor on the outside is a histidine kinase where auto-phosphorylation of a conserved histidine residue can happen. The phosphate is then transferred to the response regulator, where it is loaded onto another conserved residue, this time an aspartate, which again results in activation of an output domain by the response regulator [38]. The output domain is often a DNA-binding domain, and in that way the transfer of a phosphate is able to directly influence the control of gene expression [38]. This two-step response is the reason why the bacteria is able to make such quick changes to environmental cues.

One feature that is of importance, is that *P. aeruginosa* has many different antibiotic resistance mechanisms. These are both intrinsic, acquired, and adaptive mechanisms, which together confer resistance against a wide range of antibiotic classes. The various mechanisms are described in section 1.9.

1.4 Why study *P. aeruginosa*?

The effect that *P. aeruginosa* can have on a wide patient group, and the fact that most serious infections are nosocomial calls for measures to be taken to find a solution for combating this opportunistic bacterium [16]. Additionally, it is essential to understand how the bacterium is able to survive despite antibiotic treatment, because it is often seen as multi-drug resistant (MDR) [16][39]. The pathogen creates problems for hospitals worldwide, and the fact that immunocompromised patients might get infected and even more sick by being present in the place that they should be getting medical care and treatment, could create multifaceted problems that are far too complex and large to go into depth in this thesis. A study published in 2005 investigated medical institutes nationwide in Japan and the frequency of MDR *P. aeruginosa* [40]. The study found that out of 3233 strains, 89 were classified as MDR (around 2.8 %). The prevalence of MDR emphasizes the need for a deeper understanding of how the opportunistic pathogen develops, and the need for a cure before it becomes impossible to treat.

The need for developing new drugs is dire, and this is especially true in the host-microbe interface between the bacterium and people living with cystic fibrosis [41]. Measures are being taken, but at the same time progression moves slow in some areas. The way that hospitals

identify bacteria and determine whether or not it is resistant towards various antibiotics is an area that might need modernization. For the past 100 years or so, Mueller-Hinton Broth (MHB) has been used as a medium where strains of pathogens have been grown in antibiotics to see if they are able to grow [42][43]. The problem is that this is a nutrient-rich medium giving lots of nutrients and benefits to the pathogen [42]. Heightened resistance could therefore be seen which might not have been detected otherwise. When we consider that these tests are often used for choosing an antibiotic drug for treating a patient that might be suffering from a chronic infection, the protocol by which resistance is determined is of crucial importance. Not only for picking out the right drug, but also for making sure the patient does not receive a treatment that is too tough on the body, when in fact it was never needed [42][43]. In conclusion, there are two sides to the problem of *P. aeruginosa* infection treatment, and that is increased resistance against various antibiotics as well as problematic susceptibility testing.

1.5 About Cystic Fibrosis

Estimations on the number of people living with cystic fibrosis (CF) in the world varies greatly. Estimates range from 70 to 165 thousand individuals based on data from 94 countries [44]. Among Caucasians, it is the most common life-limiting autosomal recessive condition [45]. In 2019 the median life expectancy for patients living with CF was 32 years. People with CF born between 1995 and 1999 are expected to live until they are 32 years, while people born between 2015 and 2019 are expected to have a median life expectancy of 46 years [46]. The life expectancy is increasing, but still it is significantly lower than the global average life expectancy, which is above 70 years but with large differences between countries [47]. Why is the life expectancy of people living with CF so drastically reduced from the average life expectancy in the world?

CF is an inherited disorder most often due to the $\Delta F508$ mutation (in 70 % of the cases worldwide) in the Cystic Fibrosis Transmembrane Conductance Regulator (*CFTR*) gene [48], but over 1000 unique mutations can occur. The *CFTR* gene is a large gene of about 230 kb situated on the q-arm of the 7^{th} chromosome within the human genome. It consists of 27 coding exons, and upon completion of transcription the CFTR mRNA is 6.5 kb long [49]. The mRNA encodes a membrane glycoprotein, more specifically a chloride channel situated in the apical membrane[1] of epithelial cells. The CFTR channel is cAMP-regulated, and primarily it regulates chloride but it is also involved in sodium, bicarbonate, and water transport. The size of the membrane protein is 1480 amino acids with a mass of about 170 kDa [49].

Mutations in the *CFTR* gene are grouped into six categories, ranging from mutations leading to defective protein synthesis and no CFTR protein, to decreased stability of the transmembrane protein that has reduced functionality. As mentioned earlier, there are over 1000 unique mutations to this gene, and based on the categorization it is easy to understand that severity of the disease varies greatly. A defective CFTR protein affects many areas of

[1] Apical membrane means the side of the epithelial cells facing the environment for uptake or secretion of nutrients, ions, or other molecules

the body, and includes, but is not limited to, the respiratory tract, pancreas, intestine, and the genital tract [49]. What causes this is a defect in salt absorption, which again drives water into the cells causing thickened mucus [49]. In the pancreas, reduced Cl^- absorption also leads to loss of pancreatic function, and this affects the digestive system [49][50]. The extent and severity of CF tend to correlate with how well the CFTR protein functions, so the lesser the function the more severe the disease. Mortality, however, due to this disease is frequently caused by overwhelming lung infections [51]. Chronic infection often ensues when infection happens, and this leads to accumulation of tissue damage. The most common cause of mortality is due to severely limited lung capacity, ultimately leading to respiratory failure [51].

Upon lung infection of *P. aeruginosa*, the CF airways are subjected to a hyper inflammatory immune response. This, combined with repeated infections, usually leading to a chronic infection, progressively drives tissue damage in the form of lung injury. The homeostatic lung environment seen in healthy individuals where the lung environment is able to effectively remove pathogens is not the case inside a CF lung. Thick mucus, weakened immune system and reduced function of ciliary movement (the cilia is responsible for pushing pathogens and other particles out of the lung environment), combined with abnormal epithelial cells and weakened antimicrobial production make up the environment of the lung. This is, of course, not optimal for clearing an infection.

1.6 Infection & Pathogenicity of *P. aeruginosa*

1.6.1 General

P. aeruginosa has the ability to adapt to and thrive in almost any environment. This is also true when it comes to human infections. Infection by *P. aeruginosa* can often be dangerous considering that the bacterium is an opportunistic pathogen able to exploit a weakened or impaired immune system in its host. Often, people with severe infections of *P. aeruginosa* are people that are already suffering from serious underlying medical conditions [16]. The bacterium is able to enter and infect different areas of the body, but the main area of infection is the lung of immunocompromized patients. *P. aeruginosa* is one of the most common hospital pathogens, and severe *P. aeruginosa* infection is often associated with ventilator-associated pneumonia (VAP) in hospital settings. Studies done on the link between VAP and infection by *P. aeruginosa* shows that this combination has the highest mortality for all *P. aeruginosa* infections, where some studies and institutions have calculated a mortality rate of as high as 30 % [16].

A whole array of different infections can be caused by this bacterium. Figure 1.2 below gives an overview of Gellatly and Hancocks study on the common infection routes the bacterium can take, what major risk factors there are, and who are at major risk.

Common pseudomonal infections and risk factors

Infection	Major risk factors
Soft tissue	Burns, open wounds, postsurgery
Urinary tract	Use of urinary catheter
Bacteremia	Immunocompromised
Diabetic foot	Diabetes, impaired microvascular circulation
Respiratory/pneumonia	Old age, COPD, cystic fibrosis, mechanical ventilation
Otitis externa (swimmer's ear)	Tissue injury, water blockage in ear canal
Keratitis (corneal infection)	Extended contact lens wear, contaminated contact lens solution
Otitis media folliculitis (hot tub rash)	Improperly cleaned hot tubs

COPD, chronic obstructive pulmonary disease.

Figure 1.2. Common pseudomonal infections and risk factors. A picture of the table from Gellatly and Hancock's article [16], showing common infection routes, and major risk factors associated with each infection.

The figure shows *P. aeruginosa* is able to infect through both soft tissue, the urinary tract, and the respiratory system. Common pseudomonal infections for people living with cystic fibrosis are in the respiratory system, but also in the bloodstream (bacteremia). Individuals suffering from cystic fibrosis are often in a immunocompromized state due to the thick mucus hindering pathogenic removal by the immune system and ciliary clearance [16]. The immunocompromised state frequently observed in individuals with cystic fibrosis, makes them susceptible to infections [16].

A pathogen is defined as an organism that causes disease to its host [52]. Virulence, on the other hand, is described as the ability an organism has to infect a host and cause disease in the form of symptoms of varying severity [53]. For the bacterium to become highly virulent, it uses many different virulence factors. Virulence factors are different features of an organism that helps it to successfully infect a host, and these factors can be of an immunoevasive nature, or directly toxic to the host. The types of factors depend on the organism, and virulence factors are either membrane-associated, secretory, or cytosolic [53]. The types of virulence factors and how they help the pathogen sucessfully infect a host, is explained more in depth in section 1.7. In this thesis, an analysis will be performed on the potential clinical isolates of the bacterium has to resist antibiotics.

Airway infection caused by *P. aeruginosa* is either acute or chronic. An acute infection usually happens as a result of direct trauma such as burn or open wounds [16]. A chronic infection, on the other hand, arises when the body is not able to fight the acute infection, often due to an ineffective immune response. *P. aeruginosa*, being an ubiquitous bacterium and able to adapt to many different milieus, can adapt to the lung environment and start growing as a biofilm inside the patients lung [16][41]. In the cystic fibrosis lung, this infection can persist for decades [54]. But how is the bacterium able to infect a host in the first place? Let us delve deeper into the route of infection of the opportunistic pathogen.

1.6.2 Infection Route from Acute to Chronic

Upon infection of the lung, *P. aeruginosa* first enters through the nasal airways and travels down through the lung. In the cystic fibrosis lung, there is usually thick mucus present due to the defective ion channels (see section 1.5). This makes it difficult for cilia to push out the bacterium, the immune system to perform its eradication of the pathogen, and secreted antimicrobial peptides and enzymes to bind the foreign particle and promote phagocytosis. All of this increases the chance of persistence by the bacterium.

After successfully entering the host, a limiting factor when growing as a colony is that nutrients become scarce. A way to mediate this problem and provide the growing population with more nutrients, is by identifying additional sources for nutrients. This is achieved through attacking and killing adjacent epithelial cells, which leads to tissue damage, but also by killing other pathogenic bacteria that might be present in the respiratory system. The first part of successfully infecting a host includes expression of many different virulence factors that impose a lot of damage to the lung cells. Virulence factors will at the same time induce an immune response by the host, which leads to a competition between bacterial clearance by the immune system and bacterial growth by the pathogen.

The initial phase of infection includes expression of many of the virulence factors, such as LPS for interaction with host cells, pili and flagellum for motility and adhesion to host cells, and secretion of virulence factors such as exotoxins through T3SS, proteases (through T2SS), and siderophores (through T1SS) [17]. All these virulence factors combined impose such a large immune response by being highly inflammatory, that the immune cells meant to protect the lung from infection will start to inflict tissue damage on its own cells [39]. The bacterial cells responsible for the acute infection are known to be sensitive against antibiotics because they are dividing quickly and antibiotics often targets cell division (such as cell wall synthesis, or translational machinery). It has also been shown that the mutation rate is increased radically when the bacterium goes from an acute to a chronic infection, leading to hyper mutation as part of its adaptive evolution [55]. Figure 1.3 below, shows the various virulence factors expressed during acute infection and chronic infection.

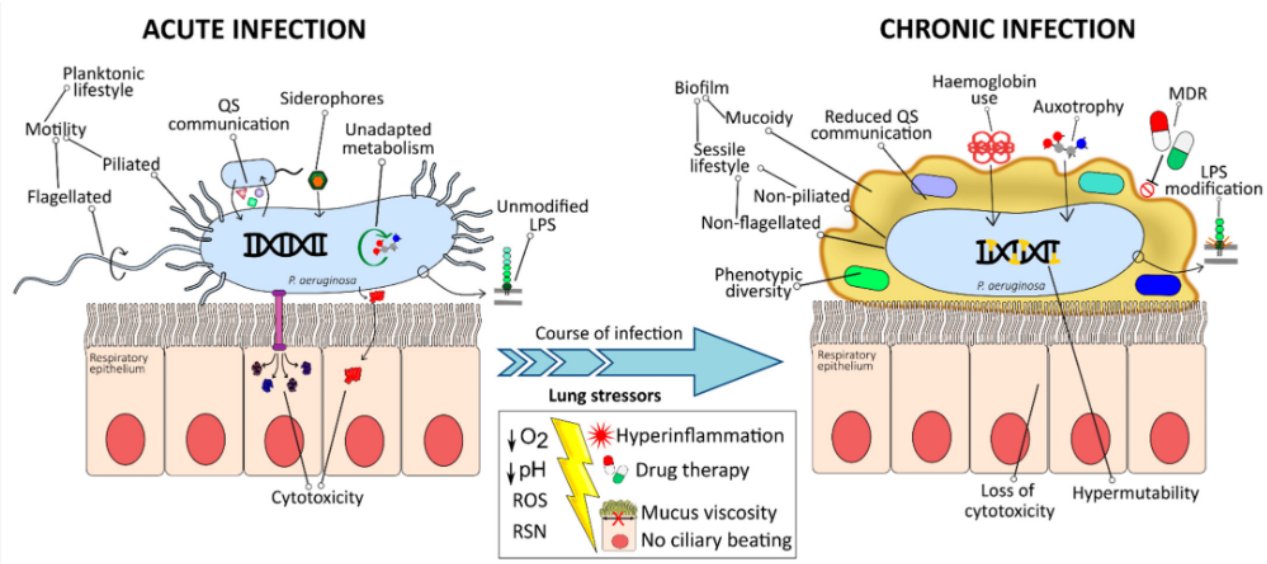

Figure 1.3. Acute to chronic infection by *P. aeruginosa*. Illustration of what virulence factors are expressed during acute and chronic infections, respectively. The figure highlights the adaptation that the bacterium undergoes in order to establish a chronic infection. QS = quorum-sensing, LPS = lipopolysaccharide, ROS = reactive oxygen species, RSN = reactive nitrogen species, and MDR = Multi-drug resistant. The illustration is obtained from I. Jurado-Martin et al. (2021) [56].

There are large changes happening when the bacterium adapts from causing an acute infection to causing a chronic infection (figure 1.3). Adaptations are being made, both on the surface by lipopolysaccharide (LPS) modification, non-piliated and non-flagellated forms, but also on the inside by adapting its metabolism. Often, this adaptation also involves switching to auxotrophy, which makes it more dependent on the host for delivery of nutrients (see section 1.2). Moreover, a down-regulation of various virulence factors is common for evasion of immune system and for allocation of energy given by the scarce nutrients available, and a less inflammatory state is commonly seen in chronic infection isolates [56].

One of the most important adaptations the bacterium makes when establishing a chronic infection in a CF lung, is to produce large amounts of biofilm. The biofilm is a self-produced extracellular polymeric matrix consisting of exopolysaccharides, proteins, extracellular DNA (eDNA), and lipids that provide many functions. First, it acts as a protection against the harsh environment in which the bacterial colony is present. Second, it stimulates to phenotypic changes due to compartmentalization within the biofilm. The reason for the compartmentalization is that the biofilm increases in size over time, making cells in different parts of the biofilm exposed to different environments. In the superficial layers of the biofilm, cells are more exposed to the surrounding environment of the biofilm, where e.g., antibiotics or the immune system is present. At the same time, the upper layers will also receive more oxygen, making it possible for aerobic respiration to be present. On the other side of the spectrum are the deepest layers of the biofilm. This is the space of the biofilm that sits against the epithelial cells within the lung. In this part oxygen availability is scarce, and this demands the bacterial cells to utilize anaerobic respiration. At the same time, nutrients are deprived, and these conditions together will trigger an adaptation of cells into a more dormant state. The cells entering a dormant state where they are less active, can go even further and

enter a state of being completely inactive. Those cells are called persisters, and they can withstand profoundly more harsh environments due to drastically lowered metabolism [57]. This, of course, also makes them resistant against many types of antibiotics. Lastly, the biofilm serves as either a blockage or a delayer for uptake of certain antibiotics making the bacterium less susceptible. Antibiotic resistance will be described in more detail in section 1.9.

1.7 Virulence Factors

1.7.1 General

Virulence factors are, as explained in section 1.6.1, important for the bacterium to infect a host, and the amount and efficacy of the virulence factors determines the ability by which the pathogen is able to do so. Generally, virulence factors are divided into subgroups. They are either membrane-associated (i.e., LPS or type IV pilus), secretory (i.e., toxins or proteases), or cytosolic (factors that mediates quick shifts in i.e., metabolism) [53]. *P. aeruginosa* uses a vast array of virulence factors. These include secretion of enzymes and toxins that can cause tissue damage, surface structures that aid in movement and anchoring to host cell surfaces, efflux pumps to effectively pump out toxins, and quorum sensing in the form of cell-to-cell signaling systems to collectively perform infection as a population or to form biofilms for protection [58, p. 445]. Virulence factors gives the bacterium the ability to perform the following tasks listed in table 1.1 below.

Table 1.1. Grouping of virulence factors. Grouping of how virulence factors can contribute to promote bacterial colonization. Table generated from list obtained from G. Kaiser [59].

1	Use motility and other means to achieve contact to host cells and disseminate within a host
2	Adhere to host cells and resist physical removal
3	Invade host cells
4	Compete for iron and other nutrients
5	Resist innate immune defenses such as phagocytosis and the complement system
6	Evade adaptive immune defenses

The various factors have widely different functions, but they are all involved in virulence and are highly expressed during initial infection. When looking at *P. aeruginosa* responsible for chronic infection, however, expression is a lot lower, and often expression of some virulence factors is completely turned off as covered in section 1.6.2 and shown in figure 1.3. In the section that follows, the goal will be to provide a clearer understanding of what the various virulence factors are and what their function is. Figure 1.4 shows the various virulence factors present in *P. aeruginosa*.

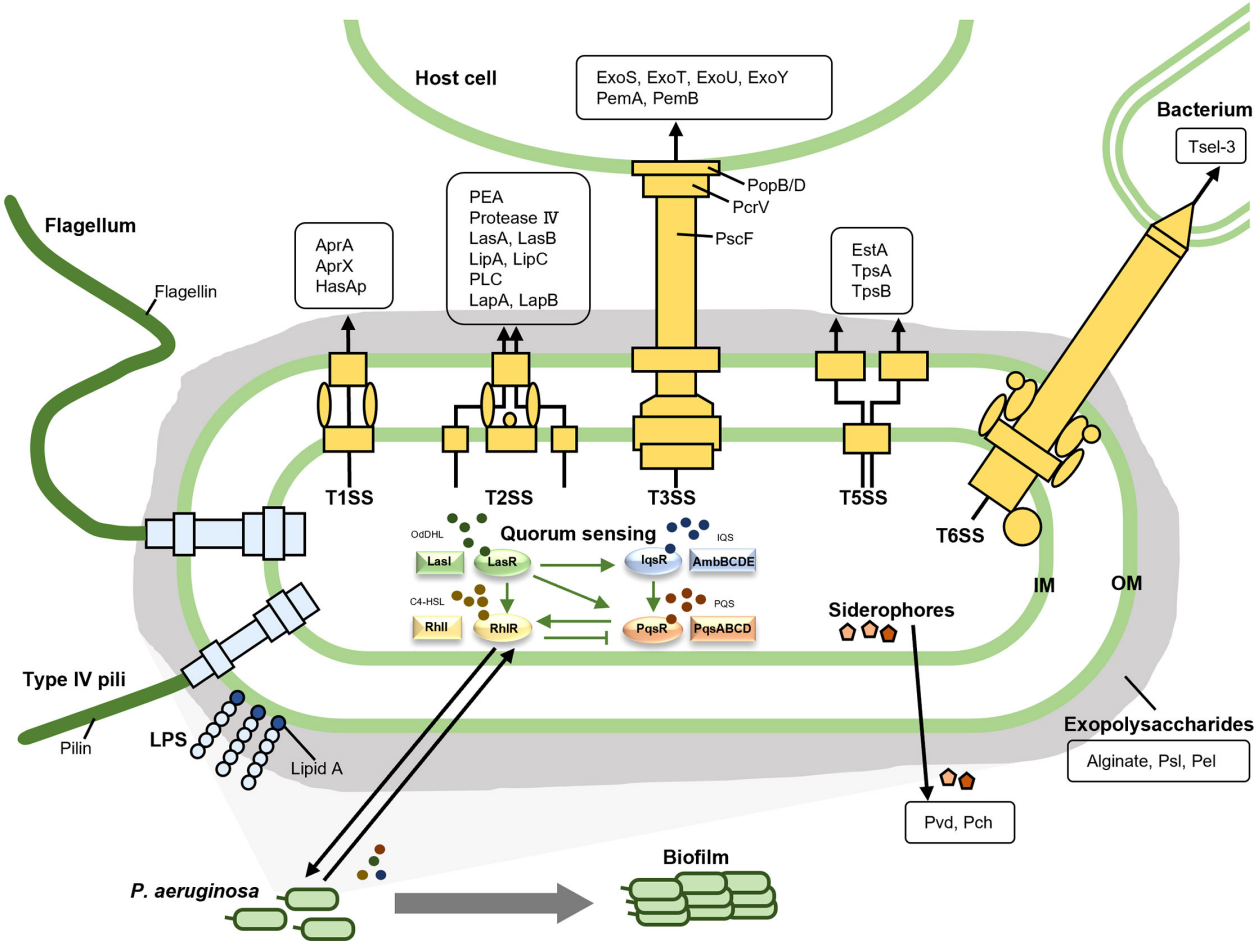

Figure 1.4. Virulence factors in *P. aeruginosa*. Illustration of the various virulence factors seen in *P. aeruginosa*. All virulence factors are explained in section 1.7. The various secretion systems are abbreviated TXSS. The illustration is obtained from C. Liao et al. (2022) [60].

1.7.2 Membrane-associated Virulence Factors

This group of virulence factors all have in common that they are situated in the membrane and in some way interact with the surrounding environment (figure 1.4). These factors do, however, have widely different functions. Some serve as anchors to adhere to surfaces, while others take part in secretion of toxins. An important class within this group are the six different types of secretion systems identified in *P. aeruginosa*. These are either one-step or two-step secretion systems. An explanation of each system will be given below, in addition to the other membrane-associated virulence factors that are important to be familiar with.

One-step secretion systems (SS):

One-step secretion systems, also called sec-independent transport, utilize a one-step translocation of the substrates across both inner and outer membrane and into the extracellular environment in one movement [61]. Sec-independent refers to this transport system not utilizing the two-step Sec translocon or Tat pathway for transport across the inner membrane and into the periplasm before subsequent transport across the outer membrane. The secretion systems that are sec-independent are type I secretion system (T1SS), type III secretion

system (T3SS), type IV secretion system (T4SS), and type VI secretion system (T6SS). T1SS is a simple secretion system, and two different types have been elucidated in *P. aeruginosa* [39][60]. T1SS secretes both proteinaceous and non-proteinaceous molecules into the extracellular space (see figure 1.4). The two T1SS combined secrete proteins such as AprA (an alkaline protease), AprX (protein with unknown function), and hasAP (extracellular heme-binding protein for iron regulation) [39][60].

The second one-step secretion system is T3SS. This is a system highly important in quorum-sensing (communication with nearby cells), and is made up of five components. The five components are the translocation apparatus, regulatory proteins, effector proteins that are secreted, chaperones, and the needle complex that can be used to penetrate host cell membranes to inject effectors into them (figure 1.4) [60]. T3SS secretes virulence effectors like ExoS/T/Y/U, PemA/B and when injected into host cells they cause disruption in the cell signaling leading to cell death. Therefore, the T3SS is important in evasion of the hosts immune response, but also to engage in invasion, colonization, and dispersion [60]. Because T3SS is so important in invasion and infection of the host, this is a widely studied system in *P. aeruginosa* virulence [62].

The third one-step secretion system is T6SS, and this has both diverse and essential functions in regards to virulence, interaction between bacteria, and competition with adjacent microorganisms [39]. When fully assembled, the complex looks similar to an inverted phage tail, with a puncturing device at the very tip of the complex [39]. This needle-like tip is used to penetrate through the membrane of adjacent cells for injection of toxins [39]. Origin of the T6SS has been shown to be related to bacteriophages, which is validated by the similarities in structure and function that bacteriophages and the T6SS has [63]. T6SS is not only able to attack nearby bacterial cells, it is also able to inject effectors into host cells [60]. The way it moves into a neighboring cell is by a contraction-based mechanism, where contraction is facilitated by an ATPase called clpV1. T6SS is highly regulated by quorum-sensing system regulators such as Las, Rhl, and MvfR [39]. Effectors secreted by the T6SS, are tse1, tse3, tse4, tse6, and tse7, and they impose various damage to the recipient cell such as degradation of peptidoglycan, essential dinucleotides (e.g., NAD^+, $NADP^+$), or DNA. *P. aeruginosa* has developed a way combat these effectors by producing immunity proteins that can bind to the effectors and neutralize them. These immunity proteins are called tsi with the same number as the effector it neutralizes behind them [64].

The T3SS and T6SS are controlled directly by the same protein. This results in the systems working in cooperation for regulation of both host and bacterial responses.The regulator is called RtcB, and is an RNA-binding protein. RtcB can therefore control colonization, establishment of infection, and pathogenicity of the entire cell. These two systems have overlapping functions, but generally T3SS directs and controls colonization, inflammation and apoptosis of host tissue and cells, while T6SS is important in biofilm formation, and removing bacterial competition (figure 1.4).

T4SS, often called type IV pili, is the last one-step secretion system found in *P. aeruginosa* (figure 1.4). T4SS is present in both gram-positive and gram-negative bacteria, as well as *Archaea*. It has a slightly different function than the other secretion systems in that it is able to transfer DNA in addition to proteins/effectors. The T4SS are divided into two subfamilies

based on its function, the conjugation system, where transfer of antibiotic resistance genes can happen, and the effector translocators, where virulence factors are injected into host cells [65]. Another important function of the T4SS, is that it has a pili, and the pili is used for twitching, motility, and adhesion to surfaces, biofilm formation, and regulation of virulence factors. Movement is achieved through cycles of extension and retraction of the hair-like appendage using cytoplasmic ATPases [60].

Two-step secretion systems:

The other type of mechanism for transport across the membrane present in gram-negative bacteria, and *P. aeruginosa* specifically, is the two-step secretion system (also called sec-dependent transport). What characterizes this system is that they lack a transporter in the inner membrane. Transport across the inner membrane therefore requires help from another system, either the Sec translocon (general secretion) pathway or the Tat (twin arginine translocation) pathway. Systems that use this mechanism are the T2SS and T5SS [61]. T2SS and T5SS has a two-step mechanism, first by transport across the inner membrane, then by transport from the periplasm across the outer membrane (figure 1.4). The Sec and Tat pathway are slightly different in mechanism of translocation. The Sec pathway performs translocation primarily on proteins still in their unfolded state [66]. Virulence proteins of various bacterial pathogens are often transported through the Sec pathway, but *P. aeruginosa* is also dependent on the Tat pathway to achieve full virulence (such as secretion of Phospholipase C, or PLC enzymes) by the T2SS [61]. The Tat pathway, in contrast to the sec pathway, transports already folded proteins. Some proteins cannot be secreted in their unfolded state e.g., because maturation of protein involves post-translational modification. This needs to happen in the cytoplasm where enzymes performing modification are present, hence a pathway for folded proteins is essential [66]. Below, T2SS and T5SS will be explained more in depth.

The T2SS directs secretion of extracellular toxins into the environment, and do so by using both the Sec and Tat pathway [39][60]. It performs various activities important for the pathogenic infection. These activities include acquiring nutrients, secretion of numerous exoproteins and toxins to contribute to virulence, but also adhesins that are important in biofilm formation [65]. A specific example is the secretion of protease IV which can digest immune response proteins like immunoglobulins produced by the host, as well as components part of the complement cascade in the human host [67].

T5SS uses the Sec pathway for the first half of transport across the membrane. This system also secretes proteins related to virulence, adhesion, and biofilm formation. A protein secreted is EstA, which is shown to increase expression of rhamnolipid, thereby contributing to biofilm formation by secretion of rhamnolipids (an exopolysaccharide) [60].

Flagella

In addition to the type IV pili that protrudes from the bacterial surface and serve in movement, the bacterium has a structure called the flagellum. The flagella is a hairlike appendage that is built from many subunits of a protein called flagellin 1.4. In addition to enable movement, it is also used for bacterial adhesion which aids in maturation of the biofilm. The flagella is recognized by the hosts immune response which elicits a large immune response to

remove the pathogen. The movement of the flagellum aids in chemotaxis, meaning movement towards areas where nutrients are available, or movement away from stressed environments or other environmental cues [60].

Lipopolysaccharide (LPS)

The last component of the membrane-associated virulence factors, is the lipopolysaccharide (LPS) (figure 1.4, lower left). The LPS is a major component of the outer membrane of *P. aeruginosa*, and is abundantly present on the surface. The LPS structure consists of three units, the lipid A, a core polysaccharide and lastly an O-antigen, and the LPS provides various functions [68]. LPS gives negative charge to the outer membrane, which serves as an effective permeability barrier against small, hydrophobic molecules that would otherwise cross the phospholipid bilayer of the outer membrane [68]. Furthermore, LPS has been pointed to as related with antibiotic tolerance and biofilm formation [39]. It also aids in both stabilization and structural integrity of the outer membrane structure, as well as being a permeability barrier for toxins secreted by other bacteria, or immune response cells trying to degrade or perform phagocytosis on the pathogen [30][60][69]. Additionally, LPS serves as a virulence factor by enabling interaction between the bacterial cell and eukaryotic cells for adhesion [39][60]. The structure of the LPS consists of a hydrophobic section called lipid A which serve as an anchor to the outer membrane, a core oligosaccharide linked to the lipid A protruding from the outer membrane, and lastly the O-antigen which is a polysaccharide attached to the core oligosaccharide. The lipid A and core oligosacharide can undergo changes, but will mostly remain the same. The O-antigen, however, can undergo many modifications in structure and composition and adapts to the environment it is exposed to. Adaptation of the O-antigen results in a way of evading the hosts immune response. The O antigen is recognized by the immune system which elicits an antibody response, but the length of the polysaccharide chain of the O-antigen can prevent the antibody from gaining access to the bacterial cell surface upon binding to the O-antigen. Release of complements for destruction of the bacterial cell might therefore be inhibited by the very structure that the antibody uses for pathogenic recognition. The O-antigen is therefore highly effective in hindering the immune response to enter the bacterial cell, even though it elicits an immune response at the same time [68].

1.7.3 Secreted Virulence Factors

In the following section, various secreted factors that *P. aeruginosa* uses as virulence factors is explained. These do not include the secreted factors already mentioned in the secretion system section (see section 1.7.2), but include the siderophores, and the exopolysaccharides.

Exopolysaccharides:

The exopolysaccharides secreted by *P. aeruginosa*, are of major importance for survival in harsh environments (figure 1.4, grey area surrounding the cell). This includes the nutrient-depleted, host immune defense-containing milieu inside the CF lung. Exopolysaccharides are extracellular macromolecules comprised of sugar moieties, and they serve as one of the main compositions for production of biofilm [60]. These sugar-based molecules increase bacterial tolerance by providing a protective layer around the bacterial cells [60]. This helps

the cells avoid oxidizing agents like reactive oxygen species (ROS) or other highly reactive compounds that could cause a lot of damage to the bacterial cell, but also the hosts defense system and desiccation [57][60]. Three exopolysaccharides have been identified in *P. aeruginosa*, and these are alginate, Pel and Psl [60]. In cystic fibrosis patients, alginate is of crucial importance for the pathology of the bacterium. This exopolysaccharide is normally only produced in strains isolated from the cystic fibrosis lung, further emphasising its importance in this environment [70]. Isolates from a cystic fibrosis lung have been shown to be specifically adapted to living in an environment surrounded by thick mucus. The cells producing this alginate-based biofilm show what is called a mucoid phenotype, which is due to the overproduction of alginate [71].

Other exopolysaccharides of *P. aeruginosa* usually present are Pel and Psl. Psl and alginate have unique chemical structures that differentiate them, while the Pel structure is yet to be fully characterized [70]. Pel and Psl has been seen to mainly be produced by isolates from the environment [70], but might be important in the biofilm of isolates inside a host.

Siderophores:

Siderophores constitutes an essential part of metal acquisition. Siderophores are iron-chelating compounds that by secretion are binds iron, and brings it back to the bacterial cell through specific uptake pathways [60]. *P. aeruginosa* produces two siderophores, pyoverdine (Pvd) and pyochelin (Pch). In the iron-depleted environment inside the CF lung, these are essential for the survival and efficacy of the bacterium in its infectivity. Iron is involved in many reactions inside the cell, therefore continuous supply of iron is essential in actively dividing cells. An example is the Fe-S containing proteins that are involved in cellular respiration [60]. Pch is used to maintain pathogenic growth in low-iron environments like the lung where there is not a lot of free iron present. Pvd has the same function as Pch, but in addition it acts as a signalling molecule for production of two virulence factors (proteinase Exotoxin A, PrpL) [72].

1.7.4 Cytosolic Virulence Factors & Intercellular Interaction

The bacterial cells have ways of interacting with one another. This is achieved through, predominantly, quorum sensing (QS), but also through the formation of biofilm. QS and biofilm are intertwined in the way that biofilm production is regulated by signals secreted by quorum sensing pathways. In this section, the function and characteristics of the QS and biofilm will be explained.

Quorum sensing (QS)

Quorum sensing (QS) is one of the communication systems used by bacteria, where the mode of communication is through signalling molecules called autoinducers. These molecules are used to perform a coordinated expression of genes across bacterial cells, and is an essential part of bacterial community behavior (figure 1.4) [60]. In *P. aeruginosa*, four different QS pathways exist, and these are Pqs, Iqs, Las, and Rhl [60]. One way the bacterium uses QS for community behavior, is by regulating expression of multiple virulence factors [60]. This can be seen as a "stronger together" behavior, where a coordinated response will be a lot

stronger and be more successful rather than each cell fighting on its own. The different QS pathways inside the cell are intertwined and are able regulate each other. OdDHL is the autoinducer for LasR, which has a stimulatory effect on RhlR. RhlR then initiates a specific virulence response (production of Pyocyanin, LasB, rhamnolipids, and HCN), in coordination with all the surrounding cells that picked up the same signal molecule from the environment. The details by which the regulatory pathways happen and what response they elicit, is not detailed in this thesis. The important take-away is that QS signals molecules coordinate a response, which is dependent on the environment. QS signalling is based on molecules that are continuously expressed, and the higher the bacterial cell density, the higher concentration of QS-molecule. When the concentration of the molecule reaches a threshold, it elicits a coordinated response between adjacent bacterial cells (as explained above) [43][60].

Biofilm

One way to "get away" from a harsh environment is by producing a biofilm. This is an aggregated form of bacteria, where the bacteria live inside extracellular polymeric substances (EPS). A biofilm consists of phenotypically diverse bacterial cells, exopolysaccharides, proteins, extracellular DNA (eDNA), and lipids (as explained in section 1.6.2) [60]. The composition of the constituents depend on the strain, growth conditions, and what maturation stage the biofilm is in [57]. The biofilm is divided in subcompartment, where cells in upper parts are more metabolically active, because more nutrients and oxygen is available [57]. Cells in deeper parts of the biofilm will be nutrient and oxygen deprived, often leading to formation of inactive bacterial cells called persisters [57]. The biofilm is highly present in chronically infected patients, as described in section 1.6.2, and the way biofilm development happens is by QS signalling molecules such as LipA and LipC (figure 1.4) [60]. Summarized, the biofilm help the pathogenic bacterium avoid and subjection to both antibiotics and the hosts immune system, giving the ability to persist as a chronic infection for years to come [60].

1.8 Antibiotics

1.8.1 General

Antibiotic treatments are crucial in the field of medicine in order to treat bacterial infections. Infections due to pathogenic bacteria can cause all sorts of illnesses, and before the discovery of antibiotics people would live their life with untreated bacterial infections such as small pox or tuberculosis. Infectious diseases had a high mortality rate, and just before the start of the 20^{th} century, the global average life expectancy was 47 years [73]. Sir Alexander Fleming and his discovery of the penicillin in 1928 marked the beginning of the antibiotic revolution [73]. Since then, many novel antibiotics has been discovered, and as of today the global average life expectancy has risen to 73.2 years [74], and treatment of disease using antibiotics has had a crucial part in increasing the average life expectancy by a staggering 26.2 years in only around 125 years. However, antibiotic resistance is becoming an increasingly larger issue due to its overuse and misuse, and certain bacterial species has gotten the label of often being multi-drug resistant (MDR). *P. aeruginosa* is one of them.

Typically, antibiotics are derived from bacteria employing compounds to out compete others for nutrients or space. These compounds often act by targeting and disrupting fundamental bacterial properties or mechanisms, such as cell wall synthesis, transcription, or translation. Antibiotics that affect these basic properties, known as broad-spectrum antibiotics, can target a wide range of bacterial species. Conversely, some antibiotics have specific bacterial targets, limiting their efficacy to only one or a few bacterial species, earning them the label of narrow-spectrum antibiotics [75][76].

In cases where the causative organism is identified, medical practitioners often opt for narrow-spectrum antibiotics due to their specificity and higher efficiency against the target bacterial species. However, when the exact bacterium is unknown, broad-spectrum antibiotics are administered. The drawback, both for broad-spectrum and sometimes narrow-spectrum antibiotics, lies in the increased risk of bacteria developing resistance during treatment. For broad-spectrum antibiotics this is because the efficacy of the antibiotic is decreased due to its broad spectrum, which increases the chance of adaptation to antibiotic exposure happens in the bacterial species [75].

One of the answers to dealing with AMR, is by making sure doctors do not prescribe antibiotics without doing thorough examinations. This alleviates the selective pressure that antibiotics naturally imposes on all bacteria subjected to the drugs. One research found that during the COVID-19 pandemic, there was an increase in frequency of prescribed antibiotics that were given without diagnostic information [7]. It is safe to say that this is very problematic when it comes to antibiotic resistance.

In this thesis, 6 different antimicrobial agents have been used to perform experiments on 7 clinical strains of *P. aeruginosa*. The antibiotics used are Ceftazidime (CAZ), Meropenem (MEM), Piperacillin and Tazobactam combination drug (TZP), Ciprofloxacin (CIP), Tobramycin (TOB), and Colistin (CST). These were chosen in order to cover a wide spectrum of antibiotics in regards to mode of action, while at the same time using antibiotics that are commonly used in treatment. The choice of antibiotics was based on antibiotic treatment used on patients living with cystic fibrosis, and the information is gathered from a Norwegian e-handbook (written in Norwegian) [77]. The handbook states that for a first time infection, a combination between Ciprofloxacin and Colistin/Tobramycin is to be used for treatment. If the patient has a chronic infection, another treatment method is suggested. An infection is considered chronic if $>$50 % of samples taken from lower airways the last year is positive, and sampling have been made at least every three months, and preferably between 7-10 samples in total. For these instances, the handbook supplied by Oslo University hospital, states to administer treatment with an aminoglycoside (i.e., Tobramycin), in combination with a β-lactam antibiotic (i.e., Ceftazidime, Aztreonam, Meropenem, or Piperacillin/Tazobactam) [77]. Lastly, it states that if there is resistance prevalent in the strain, one of either the aminoglycoside or the β-lactam can be swithed out with Ciprofloxacin (a fluoroquinolone) [77].

Below, an explanation for each antibiotic used in this study will be given, and the structure of all antibiotics will be shown (figure 1.5). The focus will be on how and where they work, as well as a classification of them.

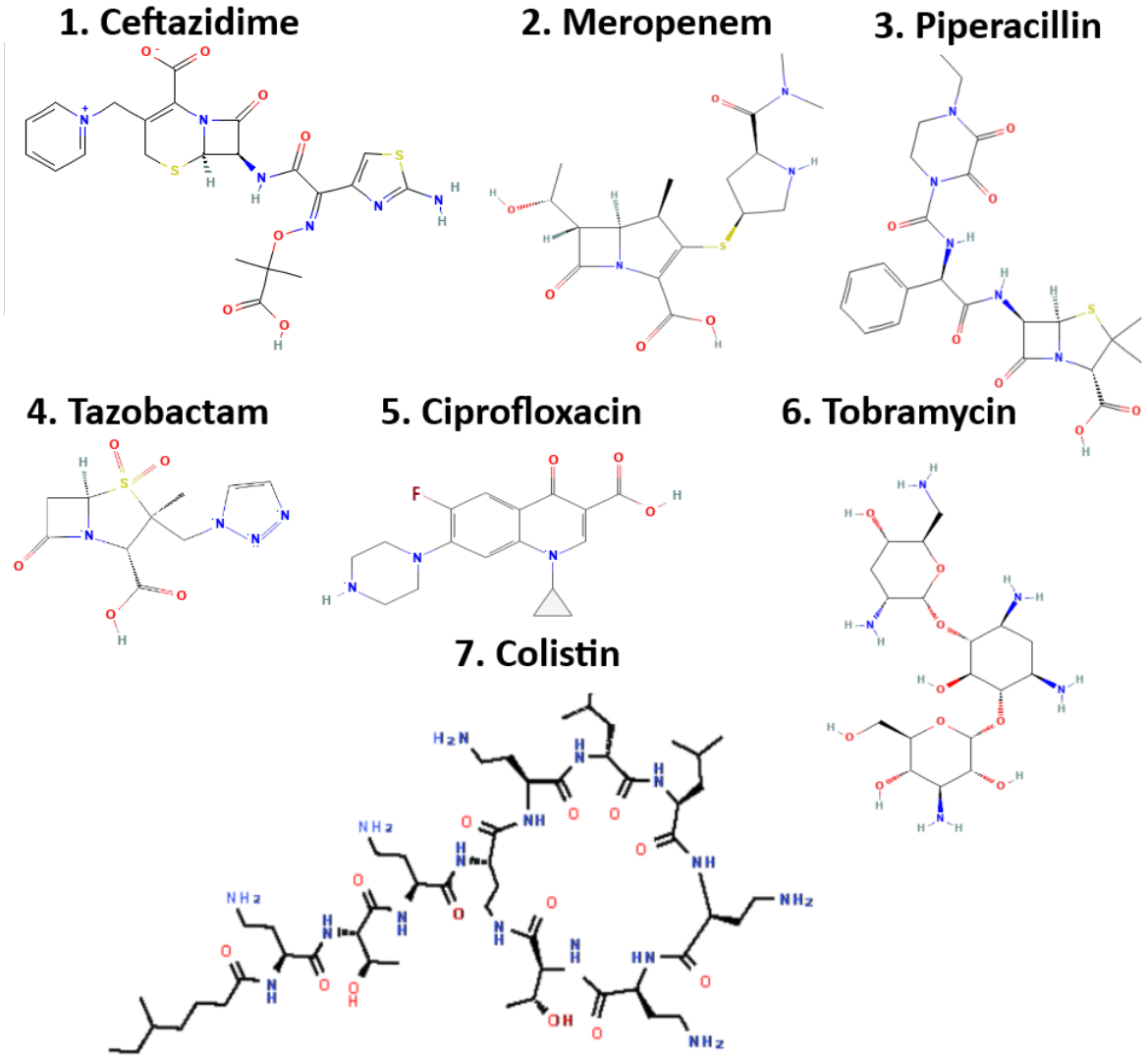

Figure 1.5. Figure with all antibiotics used. A summary image of all antibiotics used when conducting experiments. Ceftazidime, Meropenem, and Piperacillin are β-lactam antibiotics, Tazobactam is a β-lactamase inhibitor, Ciprofloxacin is a fluoroquinolone, Tobramycin is an aminoglycoside, and lastly Colistin is a polymyxin. 1: [78], 2: [79], 3: [80], 4: [81], 5: [82], 6: [83], 7: [84]

1.8.2 β-lactam Antibiotics

The antibiotic class of β-lactams is the most widely prescribed type of antibiotic [85]. The β-lactams are widely considered to be well tolerated in patients, as well as being efficient. β-lactams are characterized by having a β-lactam ring at the core, which is a four-molecule ring consisting of three carbon atoms and one nitrogen atom (figure 1.5). Surrounding the characteristic ring are additional groups, where the groups added determine what subclass the antibiotic belongs to [86]. Mode of action are penicillin-binding proteins (PBPs), which are enzymes involved in cell wall synthesis. Specifically these enzymes perform the last steps in peptidoglycan cross-linking between the stem peptides (structure of peptidoglycan explained in section 1.3) [85]. The β-lactams mimic the D-Ala-D-Ala moiety in the stem peptide, which is the natural substrate of PBPs, enabling binding and thereby inhibition of

the PBP [87]. The three β-lactam antibiotics used in this thesis are Ceftazidime, Meropenem, and the combinatory antibiotic Piperacillin/Tazobactam. Below, each antibiotic is explained more in depth.

Ceftazidime hydrate: Ceftazidime hydrate (CAZ) is a broad-spectrum antibiotic in the cephalosporin class that is especially used for Pseudomonas and other gram-negative infections (figure 1.5) [78]. The cephalosporins are grouped into five generations, and grouping is based on spectrum of bacterial coverage. Ceftazidime is a 3^{rd} generation cephalosporin, and this generation of cephalosporins are characterized by their extended gram-negative bacterial coverage [88]. One important thing about the 3^{rd} generation cephalosporins is that when given intravenously (IV), they can penetrate the blood-brain barrier and thereby treat infections in the cerebrospinal fluid (the plasma present in the brain and spine) [88][89]. Treatment of chronic *P. aeruginosa* infection often implies using this antibiotic, as explained in section 1.8.1.

Ceftazidime often comes in the hydrated form, pentahydrate where each molecule is hydrated with five water molecules. Hydration of substances, i.e., antibiotics, often help with reaction and efficacy of the substance [90]. The structure of CAZ consists of the β-lactam ring, which is surrounded by additional groups that is built from the β-lactam core. It is one of the larger 3^{rd} cephalosporins molecules with a molecular weight of 636.7 g/mol [78][85]. Ceftazidime is a hydrophilic drug with low protein binding properties [91]. Low protein binding properties entails that the drug penetrate tissue better, but it is also excreted from the body much faster. If the protein binding is more than 80-85 %, the antibiotic might bind to other proteins, making them unable to bind the penicillin-binding proteins [92].

Meropenem:

Meropenem (MEM) is a broad-spectrum carbapenem, which is another antibiotic class within the β-lactams (figure 1.5). Carbapenem has an extended spectrum of activity against both gram-positive and gram-negative bacteria. Carbapenems are characterized by their sulfur atom which acts as a linker between the two portions of the structure, and the 4:5 fused ring (which is similar to the penicillin structure) (figure 1.5). MEM is, like CAZ, also a hydrophilic antibiotic with a size of 383.5 g/mol, which is comparatively smaller than CAZ. Due to the compounds water-loving nature, it signifies that it crosses the membrane by passive diffusion through porins [93]. Meropenem also shows low protein binding, meaning it penetrates tissue better, does not bind with other proteins than the PBPs, but is at the same time excreted quicker [94].

Piperacillin and Tazobactam:

Piperacillin (PIP) and Tazobactam (TAZ) is an often used antibiotic combination to treat for instance pneumonia. PIP is a penicillin-like antibiotic, while tazobactam is a β-lactamase inhibitor (figure 1.5). This combination is often used on patients that have infection of β-lactam resistant strains (see section 1.9 for theory on resistance). It has a broad spectrum of activity against both gram-positive and gram-negative bacteria, and the tazobactam enhances the spectrum towards β-lactamase producing bacteria [95]. Tazobactam is somewhat different from the other antibiotics, because it acts as a resistance inhibitor.

TAZ contains a β-lactam ring which binds irreversibly to β-lactamases, thereby inhibiting the β-lactam resistance enzyme from attacking PIP.

PIP has the characteristic core structure of the β-lactam, with additional side groups such as an aromatic ring. This aromatic ring structure is also shared with penicillin, along with the sulfur atom present in the 5-membered ring that is fused to the β-lactam ring (see figure 1.5). Tazobactam also has the β-lactam structure fused to a 5-membered ring containing an sulfur atom, but this sulfur has two oxygen atoms bound in double bonds. This feature is thought to be important in the mechanism of binding irreversibly to the β-lactamase [96]. Both PIP and TAZ are hydrophilic compounds, and they have a low percentage of protein binding properties (30 % bound to plasma proteins) [97].

1.8.3 Ciprofloxacin

Ciprofloxacin (CIP) is a part of the class 2^{nd} generation quinolones, called fluoroquinolones, and it is a broad-spectrum antibiotic that is active against both gram-negative and gram-positive bacteria (figure 1.5). Its mode of action is the two topoisomerases DNA gyrase and topoisomerase IV. DNA gyrase is a catalyzer of ATP-driven negative super-coiling that is essential for initiation of replication, while topoisomerase IV relaxes supercoiled DNA in order for replication to happen. Without these, replication cannot happen, and CIP is able to accomplish just that [98][99, p.249, 261].

Fluoroquinolones have been an important part of antibiotic treatment for the past 5 decades due to its broad spectrum of activity against gram-negative bacteria, and especially against *P. aeruginosa*. CIP is characterized by modifications of the quinolone structure at C_7, C_6, and N_1 (figure 1.5). At C_7 there is addition of a six-membered ring with two Nitrogen-atoms (called piperazine) [100]. At C_6 there is addition of F which is specific for the fluoroquinolones (hence the name), and at N_1 there is addition of cyclopropyl (the 3-membered ring, illustrated with a equilateral triangle). The modifications that were made to produce this antibiotic compound increased the potency of the drug, and generally improved the pharmacokinetics[2] [102][103]. CIP has been shown to be hydrophilic, with a low protein binding percentage [92][104][105].

1.8.4 Tobramycin

Tobramycin sulfate (TOB) is an aminoglycoside antibiotic, that has activity against gram-negative bacteria, and especially *P. aeruginosa* (figure 1.5). Aminoglycosides work by inhibiting the translational machinery in protein synthesis [106]. Inhibition happens through binding with high affinity to the 30S ribosomal subunit, and specifically in the A-site [106]. This results in conformational changes in the A-site, where mistranslation and thereby wrong amino acids assemble into a polypeptide chain [106]. Serious side effects put limitations on the use of the agent, such as kidney damage and damage to the inner ear [83]. Due to the continued rise of MDR bacteria, and especially MDR *P. aeruginosa*, they are becoming interesting for clinical use again.

[2]Improved pharmakokinetics refers to improved interaction between the antibiotic and the patient, such as improved absorption, or activity of the drug [101]

1.8.5 Colistin

Colistin (CST), or polymyxin E, is a polycationic peptide, meaning it is a positively charged peptide (figure 1.5). CST is active against both gram-positive and gram-negative bacteria [107]. The sulfate salt of CST is used to treat intestinal or skin infections, and it has a narrow antibacterial spectrum of activity [108]. The antibiotic disrupts the cell membrane of gram-negative bacteria, and is often used as a last resort treatment against MDR bacteria, specifically. Treatment by Colistin is considered last resort due to the many side effects linked to this antimicrobial agent [42].

The mechanism by which CST disrupts the cell membrane, is by binding via electrostatic interaction to negatively charged phosphate groups in the lipopolysaccharide (LPS), specifically the hydrophobic lipid A moiety that is anchored to the membrane [109]. This binding impairs the function of the LPS, leading to permeability of the outer membrane [109]. Solubilization of the cell membrane occurs, resulting in cellular death [109]. The mechanism of action of the compound is that in the lipopolysaccharide (LPS) there are cations of Ca^{2+} and Mg^{2+} that are displaced when CST binds the lipid A of the LPS. This destroys the LPS 3-dimensional structure. Next, CST can insert the hydrophobic fatty acyl chain (which protrudes from the circular core structure of the compound) that causes an expansion of the outer membrane monolayer [109] (figure 1.5). The permeability of the outer membrane is now so altered that CST is able to pass right through the outer membrane. This results in cell lysis of the bacterial cell.

1.9 Antibiotic Resistance in *P. aeruginosa*

1.9.1 General

Antimicrobial resistance is one of the worlds most urgent health problems [110]. In 2019, antibiotic resistance was estimated to be the direct cause of 1,2 million deaths worldwide [110][111]. Another estimation states that as much as 7,7 million deaths in 2019 could be linked to bacterial infections (with bacterial infections being both directly and indirectly the cause of death) [112]. Counteracting the development of pathogens with antibiotic resistance known to cause infection and disease is required in order to keep global health care functioning. Without antibiotics, the health care system could be at risk, and medical advances such as surgery or chemotherapy might become too dangerous to carry out [113].

Nosocomial infections, often referred to as healthcare-associated infections (HAI), is one of the most common unwanted incidents in healthcare that can affect a patients safety [114]. MDR bacteria specifically, are commonly seen with HAI, and are associated with significant mortality [114]. A study from 2012 seeking to describe antimicrobial resistance patterns in the time period 2009-2010, found that nearly 20 % of all pathogens reported as HAI were multi-drug resistant. Of these 20 %, carbapenem-resistant *P. aeruginosa* accounted for 2 % of the reported findings [115]. The same study was conducted in 2011-2014, and that study found that estimations from earlier reports were similar to the new estimations for most phenotypes of pathogens. There was, however, noted an increase in resistance among *Escherichia coli* pathogens [116]. These studies highlight the problem with antibiotic resistance.

The resistance of pathogens against antibiotics is not declining, it is increasing, and the health care system is in dire need of finding a more permanent solution to the continuous race against antibiotic resistance.

There are many mechanisms of antibiotic resistance within the species *P. aeruginosa*. The mechanisms of resistance can be divided into three groups depending on how they first arose; intrinsic, adaptive, and acquired resistance [117]. In this section, the various resistance mechanisms will be covered, and tied to resistance against the 6 antibiotics explained in section 1.8.

1.9.2 Intrinsic Resistance

Intrinsic resistance is the first group of resistance mechanisms, and intrinsic resistance is defined as a trait within a species that is shared universally between all strains [118]. It is not dependent on environmental factors, such as previous antibiotic exposure or horizontal gene transfer, but rather present in the genome at all time across all strains [118]. Intrinsic resistance in *P. aeruginosa* include expression of efflux pumps that can pump antibiotics out of the cell quickly, low outer membrane permeability (i.e., due to lipopolysaccharides), and production of various enzymes that can inactivate antibiotics [1][117].

P. aeruginosa has five families of efflux pumps in its bacterial genome, that aid the bacterium in pumping out toxic compounds [1][117]. These families are called the resistance-nodulation-division (RND) family, small multidrug resistance (SMR) family, multidrug and toxic compound extrusion (MATE) family, major facilitator superfamily (MFS), and ATP-binding casette (ABC) superfamily [1][117]. When it comes to intrisic resistance, the RND family is particularly important. This family of efflux proteins consists of the familiar pumps called MexAB-OprM, MexCD-OprJ, MexEF-OprN, and MexXY-OprM. These efflux pumps are important for efflux of both β-lactams, quinolones, and aminoglycosides, giving the bacterium enhanced intrinsic resistance [1][117].

1.9.3 Acquired Resistance

Acquired resistance is all about acquisition of novel genetic material either by horizontal gene transfer (transformation, transposition, or conjugation), or through acquiring the "right" mutations [118].

Mutational changes that can happen and give acquired resistance, are mutations to porins or LPS that somehow reduce antibiotic uptake, modifications of the antibiotic target (e.g., mutations in the genomic sequence of penicillin-binding proteins), or mutations to regulators that control expression of efflux pumps, antibiotic-inactivating enzymes or other intrinsic resistance mechanisms (e.g., β-lactamases such as AmpC), leading to overexpression. Overexpression of β-lactamases can yield resistance against β-lactams, but this can also be achieved through mutations of the penicillin-binding proteins that leave the antibiotic unable to bind to the protein. As an example, deficiency in OprD has been shown to yield high level of resistance towards carbapenems (i.e., Meropenem, section 1.8.2). Other mutations yielding enhanced resistance against β-lactams (section 1.8.2) and fluoroquinolones (i.e., Ciprofloxacin section 1.8.3), are mutations leading to over-expression of the efflux pump

MexAB-OprM pump, while over-expression of the MexXY-OprM led to increased resistance against aminoglycosides (i.e., Tobramycin 1.8.4), in addition to the other two antibiotics [117].

Other modifications caused by mutations that can lead to increased resistance, are those that occur in antibacterial targets. One example is the quinolone target site (e.g., Ciprofloxacin, section 1.8.3), DNA gyrase and topoisomerase, (e.g., GyrA), resulting in decreased binding affinity to the quinolone. Modifications to the lipopolysaccharide (LPS) has been shown to result in polymyxin resistance (e.g., Colistin) [108]. Resistance can occur due to reduction of LPS, reduction in cell envelope cation contents, or lipid alterations of the lipid A moiety [108].

Like mentioned above, horizontal gene transfer is another way of acquiring antibiotic resistance. This can happen through acquisition of a resistant plasmid or free fragments of DNA from the environment [117]. Acquisition of a resistant plasmid leads to a more rapid spread of resistance compared to mutations at binding sites, because resistant plasmids can be obtained by several bacterial cells at the same time and thereby spread a lot faster than a random mutation has the ability to do [119]. Plasmids can be obtained by conjugation, while fragmented DNA can be obtained by transduction or transformation [117]. Conjugation is transfer of DNA through a sex pilus that is used for direct physical contact between two cells [117]. Transduction is transfer of DNA by bacteriophages (bacterial viruses), and transformation is uptake of DNA released into the environment by another bacterial cell [117]. All of the mechanisms result in either incorporation of DNA into the bacterial genome of the recipient cell, or acquisition of a plasmid (e.g., a plasmid with antibiotic resistance genes).

1.9.4 Adaptive Resistance

Adaptive resistance means that the bacterium makes adaptations or alterations that are not permanent, to expression levels [117]. This happens as a result of an environmental cue. Adaptive resistance is different from the acquired resistance, because once the environmental stimulus is removed, such as an antibiotic, the adaptation will also be removed and the gene or protein expression will return to the level before the stimulus (meaning it is reversible) [117].

In *P. aeruginosa*, the most known form of adaptive resistance is that of biofilm formation. The biofilm is commonly seen in chronically infected patients, especially in cystic fibrosis patients. The biofilm serves as a barrier for diffusion of antibiotics, but also delay the time it takes for the antibiotic to reach the cells (which might affect the efficacy of the antibiotic) [117]. In the deeper layers of the biofilm, oxygen is not as readily available, and this affects antibiotics that are dependent on oxygen molecules in their mechanism of inhibition or degradation (such as β-lactams, aminoglycosides, and fluoroquinolones) [57]. The biofilm, in addition to other components, consists of extracellular DNA (eDNA). The negatively charged eDNA can contribute in antibiotic resistance by capturing positively charged antibiotics and thereby reduce their activity (e.g., Colistin, Tobramycin) [57].

In the deeper layers of the biofilm, there will be reduced antibiotic activity due to lack of reactive oxygen species (ROS), because antioxidant systems (responsible for removal of ROS) in the bacterial cell will be up-regulated as a stress response due to lack of nutrients and oxygen [57]. It has been shown that induction of ROS by some bactericidal antibiotics is thought to contribute to their killing effects (e.g., with Ciprofloxacin) [57].

The persister cells present within the biofilm is of particular importance when it comes to persistence of chronic infection within the cystic fibrosis (CF) lung. These cells can withstand high concentrations of antibiotics because these cells are slow-growing, and metabolically inactive (due to target of antibiotics usually being actively dividing cells) [117]. Once the presence of the antibiotic is cleared or removed from the environment, the persister cells can shift back to actively dividing cells again [117]. In strains isolated from CF patients, it was shown that the persister cells are used for persistence of infection, and that over time (after 96 months), a 100-fold increase in persister cell levels was seen compared to the sampling at the start (month 0) [120].

1.9.5 The β-lactamases

Within the *P. aeruginosa* species, the β-lactamases are a group of enzymes that are of particular importance when it comes to resistance against β-lactams. Gram-negative bacteria that produce β-lactamases are considered one of the most harmful resistant bacteria. The β-lactamase enzymes are classified into four different classes based on their protein sequence, and there are over 1800 described variants of these antibiotic inhibitor enzymes [121]. The classes are class A (serine penicillinases), class B (metallo-β-lactamases), class C (cephalosporinases), and class D (oxacillinases). The different classes give resistance against penicillins, most β-lactams, cephalosporins (e.g., Ceftazidime), and 2^{nd} generation penicillins (e.g., Cloxacillin).

Even though resistance has emerged, researchers have found a way to counteract this emerging resistance by the use of mechanism-based inhibitors such as Clavulanic acid or Tazobactam. These inhibitors work by one of two primary mechanisms, where the first mechanism is that these inhibitors become substrates that can bind to the β-lactamase enzyme. The inhibitor and the β-lactamase will then bind with high affinity, and by doing so form sterically unfavorable interactions for subsequent reactions between the β-lactamase and a β-lactam antibiotic. One such sterically unfavorable interaction is the formation of an acyl-enzyme intermediate where the enzyme becomes hydrolytically incompetent [122][123]. Below, the different classes of β-lactamases are explained more in detail.

Class A β-lactamases are enzymes that use the amino acid serine to perform hydrolysis of the β-lactam ring. They do so by using the -OH group of the serine residue as well as a free water molecule to perform the hydrolysis on the ring, thereby inactivating the β-lactam ring [124]. This mechanism is the same as both class C and D lactamases use. Class A β-lactamases are active against penicillins and older cephalosporins, and in the beginning they worked poorly against e.g., the cephalosporin Ceftazidime. However, after using Ceftazidime against bacteria having class A β-lactamases, these bacteria accumulated mutations over time that led to increased resistance against newer cephalosporins such as Ceftazidime [121][125].

The second group of β-lactamases is the class B β-lactamases. These are called metallo-β-lactamases, and are a part of the large metallohydrolase superfamily [126]. These enzymes confer high levels of resistance towards carbapenems (e.g., Meropenem) [1]. In this class, the enzymes also catalyze a hydrolytic reaction but do so by utilising a metal-activated water nucleophile. They are Zn-dependent hydrolases, which means that in their active site there is a Zn ion that is important for the reaction mechanism of the enzyme. There can be either one or two metal ions present in the active site, and the Zn ions facilitate displacement of negative charge throughout the antibiotic in order to break the β-lactam ring [126].

Class C β-lactamases contains the enzymes denoted AmpC, and they possess an inactivation spectrum against different antibiotics, such as penicillins, cephalosporins (e.g., Ceftazidime), and cephamycins [127]. In *P. aeruginosa*, an inducible chromosomal AmpC-type enzyme has been identified, and the overproduction of this enzyme has been shown to be a major source of resistance against antibiotics such as Ceftazidime and Piperacillin [127]. In addition, it also has resistance against β-lactamase inhibitors such as Tazobactam [127]. Class C lactamases perform hydrolysis of antibiotics by the use of a nucleophilic serine and a water molecule [128]. Class C lactamases does usually not possess carbapenemase activity (e.g., against the carbapenem Meropenem) [126].

Class D β-lactamases is the last group of these β-lactam inhibiting enzymes. Class D are named using an "OXA" nomenclature, which is named after the penicillin oxacillin, because members of this class showed strong hydrolytic activity against the antibiotic [129]. This class is able to inactivate both cephalosporins, penicillins, and carbapenems, and they do so by hydrolysing the structure and cleaving the β-lactam ring [126]. At the same time as being active against several types of β-lactams, they are also uninhibited by various β-lactamase inhibitors (e.g., Tazobactam) [130]. The class D lactamases are more hydrophobic in their active site compared to class A and class C [129]. The hydrophobicity seen in the OXA enzymes is necessary for an unusual post-translational modification to occur, and that is carboxylation of a lysine in the active site for formation of a carbamate[3] functional group. The carboxy-lysine likely participates in catalysis as a general base, and by the help of an active-site water molecule, the β-lactam ring is inactivated [129].

1.10 "Omics"

1.10.1 General

"Omics" is the discipline within biological research focused on interpreting large collections of data for a better understanding of e.g., genomic adaptations made by a species to survive in a ecological niche, or to identify the response by a species when subjected to various conditions [42]. Such investigations of large pools of biological data falls within the discipline referred to as "omics" sciences. "Omics" sciences consist of several sub-disciplines called genomics, transcriptomics, phenomics, metabolomics, metagenomics, and proteomics [131]. In the following section, the branches of genomics and proteomics will be explained more in detail.

[3] $CH_2NO_2^-$ is an amino acid anion formed upon carboxylation of a lysine in the active site of class D β-lactamases

1.10.2 Genomics

Genomics is the field within the omics sciences that focus on investigating the genome of an organism. This could mean identifying genes present and their genomic neighborhood, or the structure or size of the genome, and this is achieved through determining the genomic sequence [132]. The approach for obtaining the DNA sequence of an organism starts with extracting the DNA from e.g., a bacterium. Then, many preparatory steps are performed, such as filtering out the genome from the rest of the cellular constituents, and preparing the genomic library, before sequencing using various sequencing technologies is performed. The MinION sequencing technology by Oxford Nanopore Technologies is the sequencing approach that has been used in this master project. The technology uses an ionic current by applying voltage in order to move the negatively charged, single stranded DNA (ssDNA) through a protein called a nanopore [133][134]. The ssDNA moves from the negatively charged side it is present in, to the positively charged side across the membrane, and through the nanopore protein [133]. The nanopore is embedded in a membrane, and when the ssDNA moves through the protein in a step-wise manner, there are specific changes in ionic current happening which corresponds to the nucleotide in each position [133][134]. The change in ionic current is detected by a machine that is able to translate the change into what nucleotide is present [133][134].

After detecting the entire sequence, a multitude of softwares are used in order to put the fragments of DNA back together to deduce the original sequence. There are numerous programs able to perform such a task, and each software is specialized on a few specific things (e.g., Flye assembly is better for sample with several contigs[4]) [134, (02.05.2023)]. The method of performing genomics analysis is not described more in detail in this thesis, because this was not the primary focus of the project.

1.10.3 Proteomics

Proteomics is used to investigate proteomes, where proteomes are the proteins produced or present in one organism or a system of many organisms [42][43]. Through proteomics, one can unravel the temporal and spatial aspects of protein expression, understand the roles of proteins in metabolic pathways, and decipher how an organism responds at the proteomic level to abrupt environmental changes [135]. What separates proteomics from e.g., genomics, is that the protein expression of an organism changes continuously, and the expression is largely dependent on the milieu in which it exists [135]. The genes that are present in an organism does not undergo these sudden changes as they largely stay the same over a long period of time. Proteomics wields extensive implications across medicine, biology, and biotechnology, by enriching our comprehension of the intricate and complex world of biology [136].

Within the field of proteomics there are three main approaches, where each approach focuses on distinct aspects of the complex protein landscape. The different approaches are expression proteomics, functional proteomics, and structural proteomics [135][137].

[4] A contig is overlapping DNA segments that results in a continuous genomic region

Expression proteomics seeks to comprehensively examine both the quantitative and qualitative expression of proteins under different conditions or across different biological states [135][137]. The fundamental objective of expression proteomics is to look at differences between samples subjected to distinct treatments, such as an organism exposed to antibiotics versus a control, or comparing a tumor tissue sample to a normal tissue sample. This can give insight into which proteins are up-regulated or down-regulated in the different conditions and thereby which pathways the organism utilizes within the different conditions. This insight does not merely serve an academic pursuit, it also bears the potential to yield innovative strategies for tackling pressing medical challenges, such as identifying novel targets for advancing cancer treatment methodologies, or more relevant in this case, combating antibiotic resistance [135][137].

Unlike expression proteomics, functional proteomics takes a different approach by not emphasizing variances in protein expression across various states. Instead, it is dedicated to unraveling the intricate functions of proteins and their complex interactions with both each other and other biomolecules [138]. This approach can elucidate how pathways are regulated by proteins, how the proteins contribute to different cellular mechanisms, and for annotating unknown proteins. This can again be used to make therapeutic advances in the medical field by giving insights into what drugs to utilize and what particular targets to aim for [138], or reducing the annotation gap between different proteins or protein groups and thereby obtain detailed and crucial information about what particular pathway a protein is involved in [139]. Functional proteomics finds a multitude of specific applications, each contributing to the expansive landscape of this essential research field. For instance, consider the quest to identify virulence-specific pathways in a pathogenic bacteria, such as *P. aeruginosa*, to develop tailored drugs that inhibit key proteins within these pathways, effectively mitigating the virulence of the pathogen. This example underscores the significance of functional proteomics in enabling targeted interventions and pioneering advancements in various domains.

The third, and final approach of proteomics research is the field of structural proteomics. Structural proteomics seeks to identify the three-dimensional structure of proteins, by determining the exact arrangement of the atoms in a protein [140]. Structural proteomics furthermore focuses on what interactions between proteins, or proteins and other biomolecules, look like in regards to the specific atomic interactions [140]. Techniques mostly used to achieve such detailed and precise data, are X-ray crystallography or nuclear magnetic resonance (NMR), but also the use of protein chemistry to understand how structure and bonds between atoms must be formed based on a deep understanding of limitations set by natural laws themselves [137][140].

1.10.4 LC-MS/MS

There are many ways of identifying what proteins are present in a sample. One way of achieving high-quality identification of peptides, which then can be used for identification of proteins, is the timsTOF instrument. The timsTOF machine is a sophisticated machine able to combine both liquid chromatography (LC) and mass spectrometry (MS) [141].

The timsTOF additionally adds trapped ion mobility spectrometry (TIMS) to the equation, making the results of high resolution and the ability to distinguish between isomeric compounds [142]. Liquid chromatography (LC) is a technique used for separation or isolation of compounds in a mixture. LC uses a mobile phase and a stationary phase, where the mobile phase is a solvent of some sort (e.g., water or a buffer) important for delivery of sample to the stationary phase. The stationary phase is the column in which the solvent and sample is delivered to, where interaction between each component in the sample and the column (stationary phase) will happen. Interactions will vary, and the different compounds are separated based on varying affinity for the mobile phase. When LC is coupled to a mass spectrometer, it is used to separate compounds in a sample before downstream analysis or detection by the mass spectrometer [143][144].

Mass spectrometry (MS) is a method able to detect both peptides, metabolites, lipids, proteins, and polysaccharides [145]. It can be utilized on both pure samples of a specific compound or complex mixtures such as cell lysates for identification of compounds [146]. There are many types of MS, and the technique is an intricate system where both physics and chemistry is utilized in a complex manner to achieve the goal of identification of compounds. All MS machines have three fundamental components in common, and these three are an ion source, a mass analyzer, and a detector [145]. The ion source is used for ionization of compounds, because detection is based on electrical fields where compounds need to have a charge in order to move through a tunnel with an electrical field [146]. The mass analyzer component of the MS machine is where the measurement of the mass-to-charge (m/z) ratio happens (a ratio where the mass of the compound is divided by its detected charge). Here, the ions are separated based on their m/z ratio, which makes it possible for the detector to identify each molecule separately, and the detector is the last component of the MS machine [145].

TIMS, which is part of the timsTOF technology, is a method for gas-phase separation, where ions are funneled through a tunnel by a gas flow. The tunnel has an electrical field, which together with the gas flow can control each ion that enters the tunnel. Through decreasing the electrical field in a step-wise manner over time, ions are released from the tunnel based on their charge and size [147]. Detection of the molecules is presented by a mass-to-charge ratio (m/z), and the data you get from the machine is a spectrum consisting of various peaks, where each peak is a specific molecule or component that has a unique m/z ratio. The height of the peak translates to the relative abundance of each component in the sample [148].

TOF, the abbreviation for time of flight, is a measurement where you utilize the time it takes to travel a given distance for determining properties of the compound [149]. This is also based on size of the compound and the charge.

1.11 Aim

The aim of this master project was to investigate the antibiotic resistance profiles of *P. aeruginosa* isolates, to determine their genomic antimicrobial potential through genome sequencing and finally to identify the mechanism of antimicrobial resistance through proteomics analysis.

2 Materials

2.1 Clinical Strains

Clinical strains of *P. aeruginosa* were sampled from seven patients living with an infection of the bacterium. These patients also suffer from the hereditary disease Cystic Fibrosis. The clinical strains were sampled at Ullevaal university hospital in 2020, and the seven isolates are sampled from seven different patients. The clinical strains were stored in a freezer at -80 °C throughout the entire thesis period. Clinical strains are abbreviated with PAU and a number, where PAU stands for *P. aeruginosa* Ullevaal, and the number denotes the patient the strain was sampled from. The different strains worked with during this thesis, are PAU1, PAU2, PAU3, PAU4, PAU5, PAU6, PAU7, and the laboratory strain ATCC27853.

2.2 Preparation of Antibiotics

Different antibiotics were used in this thesis, and they were used for performing minimum inhibitory concentration (MIC) analysis, growth curve experiments of bacteria exposed to antibiotics, and when performing proteomics analysis to investigate the bacterial response to being subjected to an antibiotic.

Six different antimicrobial agents were used, and all came in dry powder form. The antibiotics in powder form were stored in a dry container in a fridge at around 4 °C or in a freezer at -20 °C. After dissolving in the given solvent, antibiotics were stored in a freezer at either -20 °C or -80 °C. Total concentration varied between antibiotics (table 2.1). The following formula was used for calculating amount of solvent needed:

$$V(mL) = \frac{\mathrm{W(mg)} \times \mathrm{P}(\mu\mathrm{g/mg})}{\mathrm{C}(\mu\mathrm{g/mL})} \tag{1}$$

where V(mL) = Volume of solvent needed to dissolve the antibiotic in mL, W(mg) = Weight of antibiotic that was weighed out. P(μg/mg) = Potency, which was the concentration of the antibiotic delivered by the supplier.

After dissolving the different antibiotics completely in the solvent, all antibiotics were filter sterilized through a 0.2 μm filter inside a laminar flow cabinet (LAF) bench. Method of dissolving the antibiotics is shown in table 2.1 below.

Table 2.1. Dissolving antibiotics. The types of antibiotics used, the abbreviation for each antibiotic, the amount of antibiotic in dry powder form that was weighed out, how much dissolvant was added, and lastly the final concentration after dissolving.

Name of antibiotic	Abbreviation	Solvent	Amount weighed out	Potency	Dissolved in	Total concentration
Ceftazidime	CAZ	H_2O	1.0mg	1000 μg/mg	1.563 mL	640 μg/mL
Ciprofloxacin	CIP	HCl	1.0mg	980 μg/mg	12.25 mL	80 μg/mL
Colistin sulfate salt*	CST	H_2O	1.0mg	796 μg/mg	1.244 mL	640 μg/mL
Meropenem trihydrate	MEM	H_2O	1.0mg	860 μg/mg	1.344 mL	640 μg/mL
Piperacillin sodium salt	PIP	H_2O	1.0mg	935 μg/mg	1.461 mL	640 μg/mL
Tazobactam	TAZ	H_2O	1.0mg	792 μg/mg	3.960 mL	200 μg/mL
Tobramycin sulfate salt	TOB	H_2O	1.0mg	686 μg/mg	4.288 mL	160 μg/mL

* = has to be dissolved right before use. Cannot be stored in dissolved form over a longer period of time.

Table 2.1 shows how the antibiotics were dissolved. 1.0mg was used as a calculation example. In reality, the weights of dry powder for each aliquot was somewhere between 1.5mg and 3.0mg, and amount of solvent was then calculated by using equation 1.

Piperacillin/Tazobactam:

A mixture between piperacillin sodium salt (PIP) and Tazobactam (TAZ) was used as an antimicrobial agent. Concentration of TAZ was kept constant, while PIP was diluted in a dilution series in both the MIC experiment and growth curve experiment (see section 3.4 and 3.7.2, respectively). When weighing out, between 1 and 4mg of PIP was diluted in dH_2O to a final concentration of 640 μg/mL. For TAZ, between 1 and 3mg was weighed out, and diluted in dH_2O to a concentration of 400 μg/mL. The antibiotics were sterile filtered separately using a 0.2 μm filter before making aliquots, and the antibiotics were kept in separate eppendorf tubes for storage. Dilution of both PIP and TAZ were stored in a freezer at -20 °C.

Meropenem:

Meropenem (MEM) was prepared by dissolving around 1mg of MEM in dH_2O to a final concentration of 640 μg/mL. After MEM had completely dissolved, it was sterile filtered using a 0.2 μm filter. Aliquots were made, and eppendorf tubes containing around 1 mL of MEM was stored in a freezer at -80 °C.

Ciprofloxacin:

Ciprofloxacin (CIP) was diluted in 0.1 M HCl due to insolubility in water. Between 1 and 3mg of CIP was weighed out and dissolved in 0.1 M HCl to a final concentration of 80 μg/mL. The dissolved antibiotic was sterile filtered using a 0.2 μm filter, aliquots were made, and eppendorf tubes containing 1-1.5 mL each were stored in a freezer at -20 °C.

Colistin:

Colistin (CST) has a relatively short half-life compared to the other antibiotics, and thereby had to be freshly diluted on the day of using it. Between 1 and 3 mg of CST was dissolved in dH_2O to a final concentration of 640 μg/mL. The dry powder was stored in a refrigerator at 4 °C, and diluted right before use. After diluting, it was sterile filtered through a 0.2 μm filter before usage.

Ceftazidime:

Ceftazidime (CAZ) was prepared by dissolving around 1.0 mg of dry powder CAZ in dH_2O to a final concentration of 640 μg/mL. The dissolved antibiotic was sterile filtered using a 0.2 μm filter, aliquots were made and the eppendorf tubes containing around 1 mL of CAZ were stored at -20 °C.

Tobramycin sulfate salt:

Tobramycin sulfate salt (TOB) was prepared by dissolving around 3.0 mg of dry powder TOB in dH_2O to a final concentration of 160 μg/mL. The antibiotic was sterile filtered in a 0.2 μm filter, aliquots were made, and tubes were stored in a freezer at -20 °C.

2.3 Cultivation Media & Agar

For cultivation of bacteria, different media were used. Medium used was Lysogeny Broth (LB), which is a medium frequently used for general bacterial cultivation and growth [42]. Mueller-Hinton Broth (MHB) medium was used when doing MIC analysis and making growth curves. Mueller-Hinton Broth has historically been the number one used media for MIC analysis, and breakpoint tables for comparison of values when doing MIC still uses Mueller-Hinton Broth medium. RPMI-LB10 medium was used for MIC analysis as a nutrient poor medium.

2.3.1 Lysogeny Broth

Liquid medium:

Dry reagents were weighed out and added to a 1 L flask. Dry reagents were 10 g Bacto-tryptone, 5 g Bacto-yeast extract, and 10 g of NaCl. The flask was then filled to 1 L by adding ddH_20 while continuously shaking the flask to dissolve the dry reagents. pH was adjusted to 7.0 ± 0.1, before the medium was sterilized by autoclaving for 15 minutes at 121 °C. Autoclaved flasks containing liquid medium was stored at room temperature.

Agar plates:

Lysogeny broth (LB) medium was prepared by first weighing out the dry reagents and adding them to an empty 1 L flask. The dry reagents were 10 g of Bacto-Tryptone, 5 g of Bacto-yeast extract, 10 g of NaCl and 15 g of Agar powder. Next, ddH_20 was added to a final volume of 1 L while simultaneously shaking the flask to dissolve the dry reagents. pH was adjusted to 7.0 ± 0.1 before the LB medium was sterilized by autoclaving for 15 minutes at 121 °C. After autoclaving, the medium was poured onto sterile petri dishes inside a LAF bench, and when solidified the plates were stored at 4 °C.

2.3.2 Mueller-Hinton Broth

Mueller Hinton Broth was prepared according to the instructions given by the supplier, Sigma-Aldrich. Directions stated to suspend 22 g of Mueller Hinton Broth 2 powder in 1 L ddH_2O. Powder was dissolved completely, and pH adjusted to 7.3 ± 0.1 before it was

sterilized by autoclaving for 15 minutes at 121 °C. Autoclaved flasks were stored at room temperature.

2.3.3 RPMI medium 1640 w/10 % LB medium

RPMI medium (500 mL) flasks were kindly provided by Per Kristian Edvardsen. To the RPMI medium, 10 % LB medium was added by taking out 50 mL of the 500 mL RPMI-LB10, before transferring 50 mL LB medium to achieve a 10 % LB medium concentration. LB medium was prepared as stated in section 2.3.1.

2.4 Buffers & Other Solutions

2.4.1 0.85 % NaCl Solution

For many experiments, a solution for stopping growth was needed. 0.85 % NaCl solution was used both in 3.3 and 3.4. Generally, the solution was used for stopping the growth of the bacteria, in order to do analysis of growth on a different media or as a solution for resuspension of colonies grown on LB agar plates overnight. This ensured that growth of the bacteria seen in the different experiments was not due to a continuation of growth, but rather due to the experiment conducted. 0.85 % NaCl solution was prepared by dissolving 8.5 g of NaCl powder in 1 L of ddH_2O.

2.4.2 1 M Tris(hydroxymethyl)aminomethane hydrochloride (Tris-HCl)

1 M Tris-HCl stock solution was kindly provided by Per Kristian Edvardsen.

2.4.3 Dithiothreitol (DTT)

1 M DTT stock solution was kindly provided by Per Kristian Edvardsen.

2.4.4 Phenylmethylsulfonyl Fluoride (PMSF) Buffer

50 mM PMSF was kindly provided by Per Kristian Edvardsen.

2.4.5 0.1 M NaCl

0.1 M NaCl solution was kindly provided by Per Kristian Edvardsen.

2.4.6 100 mg/mL Lysozyme

100 mg/mL Lysozyme stock was kindly provided by Per Kristian Edvardsen.

2.4.7 Buffers & Solutions for STrap Protocol

Table 2.2 shows all buffers and solutions used during the STrap protocol (method in section 3.8.4).

Table 2.2. STrap protocol solutions and buffers. An overview showing the different solutions, their constituents, and what they are used for in the STrap protocol for protein digestion

Name	Full name	Constituents	Final concentration	Goal
IAA	Iodoacetamide solution	9.25mg C_2H_4INO 0.1 mL MQ	92.5mg/mL IAA	Alkylating agent, prevent formation of disulfide bonds between cysteines
PA	Phosphoric Acid solution	14.1 μL 85 % H_3PO_4 86 μL MQ	11.99 % PA	Create a nice protein suspension
Strapping	Strapping solution	90 % MeOH 50mM Tris-Cl pH 7.1	90 % MeOH 50mM Tris-Cl pH 7.1	Create a nice protein suspension of SDS-solubilized proteins
ABC	Ammonium Bicarbonate solution	200 μL 1M ABC 100 μL 100 % ACN 1.7 mL MQ	0.1M ABC 5 % ACN	Alkaline buffering agent, decomposes to volatile compounds which makes it useful for LC-MS
Trypsin	Trypsin solution	20 μg Trypsin 500 μL ABC solution	40ug/mL trypsin	Catalyze hydrolysis of peptide bonds. Proteins are broken down into smaller peptide fragments
Elution	Elution solution	800 μL 100 % ACN 200 μL 0.5 % TFA	80 % ACN 0.1 % TFA	Elute peptides from the stacked filters
Loading	LC-MS loading solution	200uL 10 % ACN 50uL 10 % TFA 9.75 mL MQ	2 % ACN 0.05 % TFA	Create a suitable environment for the peptides in the LC-MS

2.5 Kits Used in This Study

Various laboratory kits were used during DNA extraction and library preparation before performing whole genome sequencing of the seven genomes. These kits contain buffers and various components needed to execute the protocol they are designed for (table 2.3).

Table 2.3. Kits used throughout the study. Overview of kits used in this study, manufacturer and contents in each kit.

Kit	Manufacturer	Contents	
Nanobind CBB kit	PacBio	PBS Buffer Proteinase K CLE3 Rnase A	Buffer BL3 Nanobind disks Buffer CW1 Buffer CW2 Buffer EB
Native Barcoding Kit 24 V14 (SQK-NBD114.24)	Oxford Nanopore Technologies	Native barcodes DNA Control Sample Native Adapter Sequencing Buffer Library Beads Library Solution	Elution Buffer AMPure XP Beads Long Fragment Buffer Short Fragment Buffer EDTA Flow Cell Flush Flow Cell Tether
Native Barcode Auxiliary V14 (EXP-NBA114)	Oxford Nanopore Technologies	Native Adapter AMPure XP Beads	Long Fragment Buffer Short Fragment Buffer
Sequencing Auxiliary Vials V14 (EXP-AUX003)	Oxford Nanopore Technologies	Elution Buffer Sequencing Buffer Library Solution	Library Beads Flow Cell Flush Flow Cell Tether
Short Read Eliminator (SRE) XS	PacBio	Buffer SRE XS Buffer EB	

2.6 Software & Computer Programs Used

Many different programs were utilized throughout this thesis, from data processing and visualization in Excel, through visualizations using R, to databases used for searching after protein names and/or sequence.

2.6.1 R Programming Language

R software environment for statistical computing and graphics, version 4.2.2, was used for visualization of data. Venndiagrams, volcano plots, and heatmaps were all made in RStudio. The large venndiagram (see figure 4.6) was made primarily by Ronja M. Sandholm, and venndiagram comparing two strains (see figure 4.7) was made by me with help from Ronja M. Sandholm.

Package used for all coding was tidyverse. Packages used for making venndiagrams were ggvenn, ggVennDiagram, dplyr, and stringr. Packages used for making volcano plots were ggplot2 and geom_point where $\log_2$ Fold Change calculated by Perseus was plotted on the x-axis, and the p-value was plotted on the y-axis. Furthermore, readxl was used to open the excel-file in the R environment. Packages used for making heatmaps were ggplot2 and geom_tile. Color for the heatmaps was coded manually, and color was based on the $\log_2$ Fold Change value. Furthermore, readxl and RColorBrewer was used to load the excel-file into the R environment and for manual coding of color, respectively.

2.6.2 Microsoft 365 (Office)

Excel was used during this thesis for analysis of data. Areas of use were when making growth curves (data from the Varioskan LUX), making tables for the thesis, but also during genomics and proteomics analysis for grouping, filtering, as a search engine for genes or proteins. In addition it was used for doing various other data processing steps before loading the excel files into the R environment for visualization.

2.6.3 Databases & Online Resources

Below, all resources used during this thesis are stated with a clickable url added (table 2.4).

Table 2.4. Databases & Online Resources. Databases & Online Resources used throughout the thesis.

Databases & Online Resources	Supplier	Website
Clustal Omega	EMBL-EBI	https://www.ebi.ac.uk/Tools/msa/clustalo/
European Committee on Antimicrobial Susceptibility Testing (EUCAST) breakpoint tables, version 13.0	EUCAST	https://www.eucast.org/
MaxQuant, version 2.4.10.0	Max Planck Institute of Biochemistry	https://www.maxquant.org/maxquant/
National Library of Medicine (NCBI)	NCBI	https://www.ncbi.nlm.nih.gov/
Overleaf, Online LaTeX Editor	Overleaf	https://www.overleaf.com/
Perseus, version 2.0.10.0	Max Planck Institute of Biochemistry	https://www.maxquant.org/perseus/
Pseudomonas genome database, version 22.1	The Brinkman Lab at Simon Fraser University, and Cystic Fibrosis Foundation, Therapeutics	https://pseudomonas.com/
Search Tool for Retrieval of Interacting Genes/Proteins (STRING) analysis, version 12.0	Global Core Biodata Resource & ELIXIR Core Data Resource	**https://string-db.org/**
Uniprot, version 2023_04	European Bioinformatics Institute (EMBL-EBI), Swiss Institute of Bioinformatics (SIB), Protein Information Resource (PIR)	https://www.uniprot.org/

Table 2.4 shows the various programs, online resources, and databases used in this study. Clustal Omega was used for multiple sequence alignment (MSA) of interesting genes identified during genomics analysis, EUCAST breakpoint table was used for determining resistance in the clinical strains, MaxQuant was used for proteomics data handling along with Perseus, and NCBI was used for protein, gene and article searches. Furthermore, Overleaf was used for writing the entire thesis. The pseudomonas genome database was used for gene searches, while the STRING database was used for identifying protein networks of interesting proteins identified during the proteomics analysis, and lastly, uniprot was used for identification of protein function.

3 Method

3.1 Overview

The method section consists of determination of colony forming units (CFU/mL), determination of minimum inhibitory concentration (MIC), method for performing DNA extraction and subsequent DNA sequencing, and lastly method for proteomics experiments in two different manners.

3.2 Overnight Cultures

Materials:

- Clinical strains of *P. aeruginosa*
- LB agar plates
- Nalgene® Labtop Cooler
- Inoculation loops
- LAF bench
- Incubator at 37 °C, static
- Falcon tubes (15 or 50 mL)
- Incubator at 37 °C with shaking at 225 rpm

Method:

Overnight cultures were made by streaking out the clinical strains onto LB agar plates inside a LAF bench. The tubes containing the clinical strains stored at -80 °C, were kept in a Nalgene® Labtop Cooler while transferring colonies from the tubes and onto the agar plates. Plastic inoculation loops were used for transferring. Clinical strain tubes were put back in the -80 ° freezer, while agar plates were incubated overnight at 37 °C. The next day, one colony from the LB agar plate was transferred into LB medium inside a falcon tube using inoculation loops. Sometimes, colonies were too small to pick out one, then a few (six-seven) were transferred. Afterwards, falcon tubes were incubated at 37 °C for 18 hours with 225 rpm shaking. The following day, overnight cultures were ready for use.

Depending on how much overnight culture was needed, smaller or larger volumes of LB medium was used inside the falcon tubes. For smaller volumes, used in section 3.7, 5 mL of LB medium was enough, while for larger volumes such as in 3.8.1, 15 mL LB medium was used.

3.3 Determination of Colony Forming Units (CFU/mL)

The first experiment that was conducted in the lab was determining the number of colony forming units (CFU/mL) *P. aeruginosa* produced. This was needed for MIC analysis later. The estimation of CFU/mL for all clinical strains of *P. aeruginosa* was used both when diluting during the MIC analysis, and for comparison of MIC results with the EUCAST breakpoint tables. The EUCAST breakpoint tables carries a MIC protocol that is widely

used for testing bacterial antibiotic susceptibility, so following the same protocol was crucial for getting results that could be comparable to other research. Needed inoculum for doing MIC testing was 5x10^5 CFU/mL [150].

The estimates of concentration were achieved by using serial dilutions, streaking the 3 lowest dilutions (10^{-4}, 10^{-5}, and 10^{-6}) out on LB agar plates and then incubating them overnight. The next day the number of colonies were counted to backtrack to what the original concentration had to be. Serial dilutions and the 3 lowest dilutions were used to get colonies on the LB agar plates that were spatially separated from each other, and thereby possible to count with the naked eye. All estimates of concentration are given in CFU/mL (colony forming units per mL).

Materials:

- LB agar plates
- Nalgene® Labtop Cooler
- Inoculation loops
- 0.85 % NaCl solution
- 15 mL plastic tubes
- Eppendorf tubes for the dilution series
- 1.5 mL plastic cuvettes
- Spectrophotometer, BioPhotometer 6131

Method:

Samples of bacterial clinical strains stored at -80 °C were streaked out on LB agar plates using inoculation loops before they were incubated at 37 °C overnight. The bacterial clinical strains were kept in a Nalgene® Labtop Cooler while streaking out onto the agar plates. The following day, overnight colonies were transferred and resuspended in approximately 5 mL 0.85 % NaCl solution inside a 15 mL falcon tube, using inoculation loops to transfer the bacteria. Close to complete resuspension of colonies inside the falcon tube was achieved by using a vortex machine to mix the contents. When there were no more visible aggregations in the solution seen by the naked eye, the colonies were thought to be completely resuspended.

After resuspension, absorbance was measured by transferring 1 mL of the resuspended bacteria to plastic cuvettes and measuring OD_{600}. Samples were then diluted to $OD_{600} = 0.1$ if needed, using 0.85 % NaCl solution. For the dilution series 6x 1 mL eppendorf plastic tubes were used to achieve dilution from 10^{-1} down to 10^{-6}. To all tubes in the dilution series, 180 μL NaCl solution was added. Then, 20 μL of sample with $OD_{600} = 0.1$ was added to the first eppendorf tube to make a 10^{-1} dilution. Pipette tips were changed, and mixing was performed using a clean pipette tip before transferring 20 μL from the first eppendorf tube to the next to achieve dilution down to 10^{-2}. Steps were repeated until 10^{-6} dilution was achieved. From dilution 10^{-4}, 10^{-5}, and 10^{-6}, 100 μL was transferred and streaked onto an LB agar plate. The dilution series workflow is illustrated in figure 3.1 below.

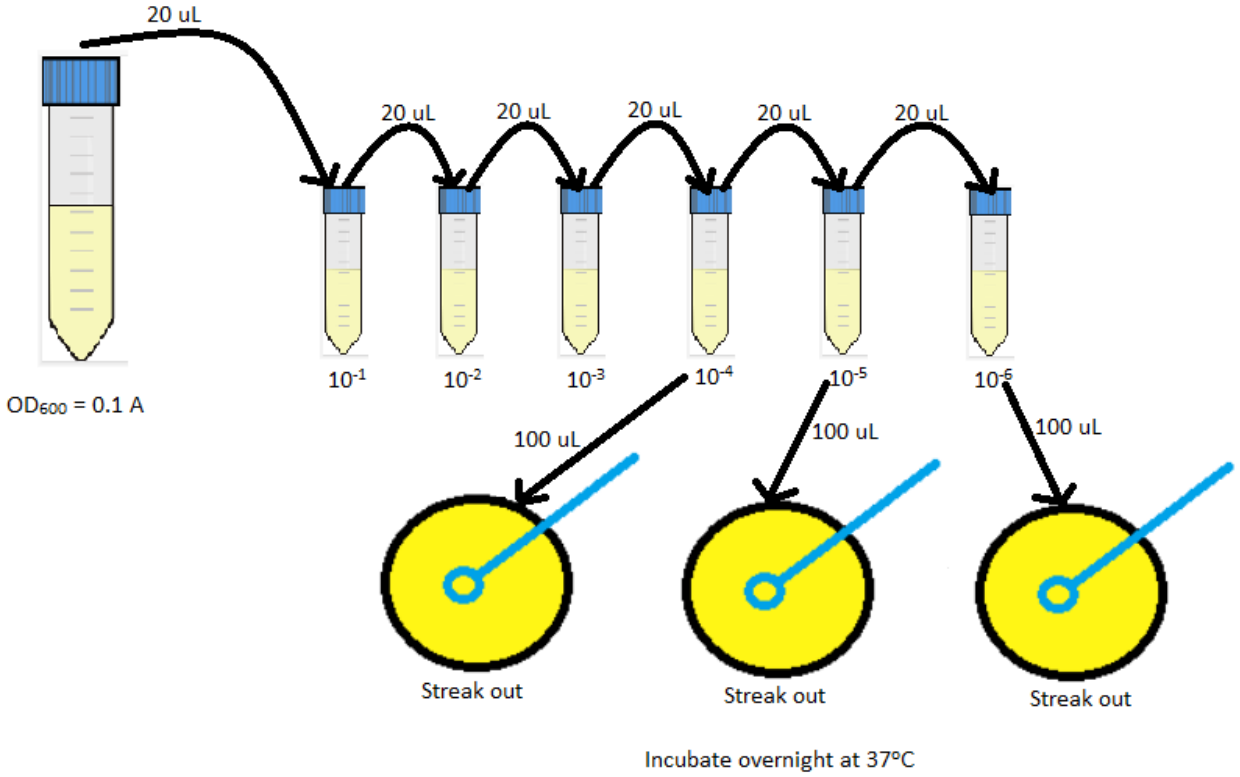

Figure 3.1. Concentration estimation of *P. aeruginosa*. The figure shows the workflow of the dilution series. All dilution tubes contained 180 μL 0.85 % NaCl solution before transferring 20 μL sample

LB agar plates were incubated overnight at 37 °C, and the next day colonies were counted. For the dilution where number of colonies were easily separable with the naked eye (preferably between 20 and 100), concentration was backtracked to give an estimate of the original concentration. Three replicates of each strain was made, and results can be seen in section 4.1.

3.4 Determination of Minimum Inhibitory Concentration (MIC)

Minimum inhibitory concentration (MIC) is a widely used method for characterizing antibiotic susceptibility of different bacterial strains. In a MIC experiment, bacteria are grown in a serial dilution of antibiotics to determine what concentration is needed for inhibition of bacterial growth to occur (if there is any inhibition happening at all). The testing was done in a sterile 96-well micro testplate, and results from the experiment were used to compare with values for resistance and susceptibility set by EUCAST. This table is called the EUCAST breakpoint table [150]. The MIC target and range values of the antimicrobial agents are given in μg/mL, and target and range depends on the antibiotics being used. Mueller-Hinton Broth is usually used as a growth medium, but for this MIC analysis both Mueller Hinton Broth and RPMI-LB10 with 10 % LB medium was used and results from the different media were compared. The explanation for testing two different media, was to test whether using a nutrient poor medium (such as RPMI) would yield different MIC-values compared to the values determined by using Mueller-Hinton Broth. RPMI more closely mimics the

nutrient-poor environment of the lung, making this an interesting analysis for the clinical strains.

Materials:

- Nalgene® Labtop Cooler
- Sterile 0.2 μm filter
- AeraSeal^{TM} BS-25 (sterile) sealing film
- Clinical isolates of *P. aeruginosa*
- LB agar plates
- Incubator set at 35 °C
- Dissolved antibiotics
- Autoclaved Mueller Hinton Broth and RPMI-LB10 with 10 % LB media
- Sterile Microtest Plate 96-Wells
- 1.5 mL Plastic Cuvettes
- Varioskan LUX
- NaCl 0.85 % solution
- 15 mL tubes
- Empty petri dishes
- Spectrophotometer, BioPhotometer 6131
- 8-channel pipette

Method:

Clinical isolates stored at -80 °C were transferred onto LB agar plates and incubated overnight at 37 °C for 16-20 hours. The next day, 100 μL of either Mueller Hinton Broth or RPMI-LB10 medium was added to 96-well microplates in columns 1 through 9. 6 rows were used (one for each antibiotic agent or combination). To the 10^{th} column, 160 μL medium and 40 μL of one antibiotic was added to each well which resulted in a total volume of 200 μL. Then, a dilution series was made starting from column 10 (table 3.1). Mixing was performed with a pipette, and 100 μL was transferred from column 10 to column 9, and this was repeated until reaching column 1. All wells had a total volume of 100 μL by the end of the dilution series. Lastly, 2 μL of Tazobactam (TAZ) was added to the row containing the Piperacillin antibiotic to achieve the combination drug.

Table 3.1. Antibiotic dilution series for MIC. Dilution series used when performing the MIC determination. All values are given in μg/mL. TZP = Piperacillin/Tazobactam, MEM = Meropenem, CIP = Ciprofloxacin, TOB = Tobramycin, CST = Colistin, CAZ = Ceftazidime.

Antibiotic	1	2	3	4	5	6	7	8	9	10
TZP	0.125/4	0.25/4	0.5/4	1/4	2/4	4/4	8/4	16/4	32/4	64/4
MEM	0.125	0.25	0.5	1	2	4	8	16	32	64
CIP	0.016	0.031	0.0625	0.125	0.25	0.5	1	2	4	8
TOB	0.031	0.062	0.125	0.25	0.5	1	2	4	8	16
CST	0.125	0.25	0.5	1	2	4	8	16	32	64
CAZ	0.125	0.25	0.5	1	2	4	8	16	32	64

After making the dilution series of the antibiotics, clinical isolates of *P. aeruginosa* incubated on LB agar plates for 16-20 hours were resuspended in 5-6 mL of either Mueller Hinton Broth or RPMI-LB10 medium in a 15 mL plastic tube. Each tube containing one clinical isolate was mixed thoroughly using a vortex until colonies inside were completely resuspended. Any residual colonies not diluted in the media were removed using a pipette. OD_{600} was measured, and bacteria were diluted to $OD_{600} = 0.1$ for all strains expect PAU1 which needed $OD_{600} = 0.02$. All dilutions had a total volume of 3 mL. The concentration of bacteria was now 1 x 10^7 CFU/mL. Bacteria were diluted one more time to a concentration of 1 x 10^6 CFU/mL before transferring 100 μL to each well in the 96-well microtiter plate using a 8-channel pipette. Lastly, 100 μL of medium and 100 μL of bacteria was added to one well to serve as positive control, and 200 μL of medium was added to another well to serve as negative control. Control of growth and correct dilution was checked by transferring 10 μL of the positive control from the microtiter plate to 9.990 mL 0.85 % NaCl solution for a total volume of 10 mL. Then, 100 μL of the NaCl suspension was transferred to an LB agar plate. Inoculation loops were used to streak out the suspension, and they were left to dry before incubating the plates either over night or for two nights at 37 °C (depending on how well and quickly colonies grew). Microtiter plates were covered with AreaSeal BS-25 (sterile) sealing film, and incubated at 35 °C for 18 h ± 2 h.

The next day, colonies were counted on the LB agar plates, where a number of colonies around 20-80 (with some discrepancy) was an acceptable number. MIC was determined doing both visual analysis as well as absorbance analysis using the Varioskan LUX to determine at what concentration of antibiotic the growth of bacteria stopped. Then, values were checked against the EUCAST table [150] to determine the minimum inhibitory concentration based on the EUCAST breakpoint table values (table 3.2).

Table 3.2. Breakpoint values provided by EUCAST. Breakpoint values provided by EUCAST [150] for the antibiotics used in this study. MIC values above the threshold value given for each antibiotic in this table, will label the clinical strain as resistant against that antibiotic. Values assume testing performed in Mueller-Hinton Broth medium.

Antibiotic	MIC breakpoint, R >	Unit
TZP	>16	μg/mL
MEM	>8	μg/mL
CIP	>0.5	μg/mL
TOB	>2	μg/mL
CST	>4	μg/mL
CAZ	>8	μg/mL

3.5 Whole Genome Sequencing

The next step in the thesis work was to investigate whether differences between clinical strains of *P. aeruginosa* in the analysis of MIC described in the results section (section 4.2), could be explained by genetic variability between clinical strains. By conducting sequencing, specifically whole-genome sequencing in this experiment, and analyzing the results, an

overview of genetic content was achieved, commonly referred to as genomics. Genomics was covered in section 1.10.2.

The genomics part consisted of DNA extraction of high molecular weight (HMW) DNA, followed by sequencing of the genetic data from each strain. Achieving HMW DNA was important because longer reads would increase the accuracy for the genome assembly after performing DNA sequencing. This is especially true when performing long-read next generation sequencing.

The work of DNA extraction was mainly conducted by Ronja Marlonsdatter Sandholm, and she taught me the practice of how to get high quality HMW DNA. Furthermore, Ronja Marlonsdatter Sandholm conducted the DNA sequencing and data processing of sequencing results before talking me through the different steps in a superficial manner. Lastly, I did the analysis of finding genes that were interesting, and together with Ronja Marlonsdatter Sandholm we made some visualizations in the form of vennndiagrams (see figure 4.6 and 4.7).

The goal was to investigate whether differences between clinical strains identified during the MIC analysis, could be explained by genetic variability. Another goal with sequencing was to use the genomic library obtained to perform proteomics analysis, and using the sequence to align the proteins present in the proteomics analysis that would be conducted later (see section 3.8 for proteomics method).

3.5.1 High-Molecular Weight (HMW) DNA Extraction

In order to do sequencing, extraction of the bacterial DNA was needed. The aim of the DNA extraction was to achieve high molecular weight (HMW) DNA. Generally, a concentration $>$30 ng/μL would be considered sufficient HMW DNA for further work [134, (21-22.02.2023)].

Performing the DNA extraction was primarily done by Ronja Marlonsdatter Sandholm, while I watched to learn and contributed when needed. The quality and quantity check was performed by me with guidance from Ronja. For strains PAU1, PAU2, PAU3, PAU4, and PAU6 extraction was performed two times. Apart from steps described below, the protocol supplied by PacBio was followed.

The kit and protocol used in this experiment was the Nanobind® HMW DNA extraction - gram-negative bacteria supplied by PacBio [151].

Materials:

Nanobind HMW DNA extraction - gram-negative bacteria kit containing all reagents (see protocol [151]). In addition to reagents supplied by the kit, several other equipment and reagents were needed:

- DynaMag-2 Magnetic Tube Rack
- HulaMixer^{TM} Sample Mixer
- Allegra X-30R Centrifuge
- Microcentrifuge, Ministar

- ThermoMixer C
- 1.5 mL Protein LoBind Microcentrifuge tubes
- Ethanol (96-100 %)
- Isopropanol (100 %)
- 1 x PBS (phosphate buffered saline)
- NanoDrop^{TM} One/OneC Microvolume UV-Vis Spectrophotometer
- Qubit 3.0 Fluorometer
- Sterile 26 g blunt end needle

Method:

Steps that were modified, or specifics in regards to practical approach in the protocol are described here. If steps are not commented here, the steps were followed as explained in the protocol.

In step 11 on page 5 of the protocol, the tubes were placed on a magnetic tube rack. The important approach for this step was to place the tubes on the magnetic rack while they were upside down. After placing the tubes on the magnetic rack, the whole rack was carefully and slowly turned around. This made it possible for the solution to move down to the bottom of the tubes, while the Nanobind disk was glued to the wall of the tube. This was an easy way to avoid touching the Nanobind disk in the step that followed (step 12), which was crucial in order for bound HMW DNA to stay bound, and without fragmentation, to the Nanobind disk. In step 18, we added the smallest amount of buffer EB (75 μL), to avoid diluting the DNA too much (which would have given a lower concentration). In step 20, it was important to try and get all the DNA out, even though it might clump together and become viscous. Step 23 on page 6 of the protocol consisted of letting the samples rest overnight. Modification to this step was that samples were stored at room temperature until the end of the day, before placing them in the refrigerator overnight.

DNA-extraction was performed twice for strains PAU1, PAU2, PAU3, PAU4, and PAU6. For the second round of extraction, another step was modified. Cell input used for the 2^{nd} round was 1.5 mL instead of 1 mL due to too low concentration after short read elimination (SRE) in the previous extraction attempt.

3.5.2 Short-Read Elimination (SRE)

For most of the strains, short-read elimination (SRE) was needed to remove contamination in the form of short fragments of DNA. Because we only needed HMW DNA for downstream analysis, removing the short fragments would not, in theory, impose any loss of genomic information. The reality was that some HMW DNA would be lost during SRE, and therefore quality/quantity check of DNA after SRE was also necessary. SRE was mainly performed by Ronja M. Sandholm, while I contributed at certain steps. In the first round, on all strains except from PAU5 and PAU7, SRE was performed. This was based on gel electrophoresis performed during qualitative and quantitative checking of DNA (section 3.6) where results revealed short fragments of DNA 4.3. After the second round of DNA-extraction, SRE was performed on strains PAU3 and PAU4.

After performing SRE, quality and quantity of DNA was checked again using Nanodrop and Qubit, in order to make sure there was enough HMW DNA for sequencing (>30 ng/μL). Protocol used when conducting short-read elimination was the Short Read Eliminator (SRE) XS kit supplied by PacBio. The part of the protocol used here was on page 11 of the original protocol, and this page can be seen in appendix C. Changes made in the protocol are commented in the method section below.

Materials:

- SRE XS kit supplied by PacBio 2.3. In addition:
- Qubit dsDNA Broad Range assay kit 2.3
- 1.5 mL DNA LoBind Microcentrifuge tubes
- 200 μL wide bore pipette tips
- Ethanol (96-100 %)
- Deionized (DI) water
- Thermo Fisher Scientific Nanodrop One Microvolume UV-Vis
- Thermo Qubit 3.0 Fluorometer
- Tabletop mini centrifuge, 7000 rpm

Method:

Table 3.3 shows how much of sample and elution buffer (EB) was added to the SRE XS buffer. Volume added was based on previous measurements made using Qubit dsDNA Broad Range assay, and the first round of doing SRE, volume modification was made from 60 μL to 55 μL. This was an attempt to retain as high concentration as possible. The second round, 60 μL as described in the protocol was used.

Table 3.3. Buffer volumes in short read elimination (SRE) protocol. Amount of each sample and elution buffer (EB) to add to the short-read elimination (SRE) XS buffer. Values given in μL.

Strain	Sample(μL)	EB(μL)	Buffer SRE XS(μL)
First round of SRE			
PAU1	21,4	33,6	55
PAU2	30,4	24,6	55
PAU3	18,4	36,6	55
PAU4	19	36	55
PAU6	14,4	40,6	55
Second round of SRE			
PAU3	45	15	60
PAU4	38	22	60

3.5.3 Library Preparation & Sequencing

The different subprotocols inside the library preparation protocol:

- DNA repair and end-prep
- Native barcode ligation
- Adapter ligation and clean-up
- Priming and loading the SpotON flow cell
- Data acquisition and basecalling

After finishing DNA-extraction, measuring quality and quantity of genomic DNA (gDNA), and performing short-read elimination (SRE) on samples where that was necessary, the next step was to do library preparation. The protocol used was the Native Barcoding Kit 24 V14 supplied by Oxford Nanopore Technologies [152]. The protocol is 32 pages long, hence is not attached in the appendix. All materials and equipment used are stated in the Native Barcoding protocol.

The protocol consisted of several "subprotocols". The first protocol in library preparation was DNA repair and end-prep. DNA repair was supposed to repair breaks in the DNA, such as nicks, gaps, blocked 3' ends and more [153]. Then, end-prep was performed, where the ends of all fragments were repaired in a fashion that would enhance the attachment of DNA barcodes that would be added in the next part of the protocol.

The next protocol was native barcode ligation. In this section, barcodes would be added on every genomic fragment end, and this was important because this library preparation consisted of multiplexing samples together downstream. To be able to separate the fragments and annotate to the correct strain later, a barcode on each fragment was therefore needed [134, (21-22.02.2023)][134, (17.03.2023)].

Next, adapter ligation and clean-up was performed, where the goal was to connect an adapter to both ends of the DNA fragments. Adapters serve as anchoring sequences, that will attach to the flow cell when performing the sequencing later [134, (22.02.2023)]. DNA clean-up was performed, where removal of all short fragments that had not bound to the high-molecular weight (HMW) DNA, such as primers, adapters, enzymes, or other things were removed. These were constituents that had been added to the samples throughout the library preparation protocol.

Steps in library preparation was performed in collaboration with Ronja Marlonsdatter Sandholm, where I contributed to certain steps but mostly watched as she performed the protocols. After performing all the preparative steps, it was time to perform the sequencing. Sequencing device used was the MinION supplied by Oxford Nanopore Technologies, and this was performed solely by Ronja Marlonsdatter Sandholm. She talked me through the steps of sequencing and raw data analysis afterwards, when the finished data was ready to be investigated.

Assembly of genomes was performed by using both Canu and Flye assembly. Flye works better for data containing fewer contigs from the sequencing, while Canu works better if there are more contigs, which means more fragmented. In this thesis, long-read de novo

assembly was performed using both Flye and Canu. Long-read assembly is defined as the method of assembling a genome from long sequencing reads (>10 kbp).

3.5.4 Investigation of Genomics

The investigation of the genomic contents were of a superficial manner, with the goal of using the genomics analysis to do proteomics analysis afterwards. Therefore, the genomics part did not do a deep-dive into what genes were present and not, but rather looked at common genes that are often present in *P. aeruginosa* which can be linked to either virulence or antibiotic resistance.

Method:

Results shown are the analytical analyses performed on annotation results, where genes present, and differences between isolates were investigated. For visualization of results, venndiagrams were made using R (see section 2.6 for more information on usage of R). Two venndiagrams were made, one with all strains (except for PAU2) showing shared and unique genes, and one venndiagram comparing only PAU3 and PAU5.

Clustal Omega was used for multiple sequence alignment of GyrA (DNA gyrase), ParC (topoisomerase IV subunit A), and AmpC. PAO1 sequence for the different genes was obtained from www.uniprot.org by searching for the protein name. Results of alignments can be seen in section 4.5.2.

Virulence factors and resistance genes were investigated, and tables were made showing presence of those (see tables 4.7 and 4.8). Files used were the protein sequence files for all strains, where one file contained all annotated genes of one strain with the translated amino acid sequence conferred from the DNA sequence. The reason for using the protein sequence file was that this made it easy to perform protein alignments if something interesting unveiled. The files containing each genomic sequence are not included in the thesis due to large file size.

3.6 DNA Quality & Quantity

For all isolates, DNA quality and quantity was checked. This was achieved by both NanoDrop^{TM} One/OneC Microvolume UV-Vis Spectrophotometer and Qubit (using the Qubit^{TM} dsDNA BR Assay Kit). The Qubit assay is accurate for sample concentration between 100 pg/μL and 1000 ng/μL [154], and wanted concentration for HMW DNA was above 30 ng/μL for reliable analysis downstream [134, (21-22.02.2023)]. In addition, Nanodrop was used for checking concentration, but this also gave values regarding purity and potential contaminants by the use of ratios between 260nm/280nm and 260nm/230nm. The 260/280 ratio reflects whether extraction was successful or if there are any protein contaminants in the sample. This value should be around 1.8 [151, p. 8]. The other ratio, 260/230, reveals potential contaminants of solvents used during the extraction, carbohydrates or phenolic components [134, (21-22.02.2023)][134, (17.03.2023)]. 260nm/230nm the ratio should be in the range of 1.2-1.8 [151, p. 8].

3.6.1 Concentration Determination using Qubit

For measuring concentration and quality of the HMW DNA extracted, both Qubit and Nanodrop was used. For Qubit measurements, the Qubit^{TM} dsDNA BR Assay kit was used.

Materials:

- Qubit^{TM} dsDNA Broad Range (BR) assay kit was used. In addition:
- Nuclease free pipette tips
- Qubit^{TM} assay tubes
- Thermo Qubit 3.0 Fluorometer

Method:

A working solution was made, where 1990 μL Qubit^{TM} dsDNA BR Buffer (Component B) was mixed with 10 μL Qubit^{TM} dsDNA BR Reagent (Component A) (supplied by the kit shown in section 2.5). To 1 μL of sample, 199 μL of the working solution was then added inside Qubit^{TM} assay tubes. The same was done for the standards, to the two standards Qubit^{TM} dsDNA BR Standard #1 (Component C) and Qubit^{TM} dsDNA BR Standard #2 (Component D) 1 μL of standard was added to 199 μL of working solution. The Thermo Qubit 3.0 Fluorometer was then standardized using the two standards prepared. Measurements were made in triplicates, and the results can be seen in section 4.3.

3.6.2 Concentration Determination using Nanodrop

Another method used, was the Nanodrop. This would ensure both quality and quantity check of HMW DNA. For measuring Nanodrop, the machine Thermo Fisher Scientific Nanodrop One Microvolume UV-Vis was used. After wiping off the pedestal with water and Kimtech paper, 1.5 μL of sample was loaded and measurements were made in triplicates. Results of these measurements can be seen in section 4.3.

3.6.3 DNA Agarose Gel Electrophoresis

To check whether samples contained high-molecular weight DNA after conducting DNA extraction, or if there was also shorter fragments present in the sample that would need to be removed, DNA agarose gel electrophoresis was performed.

Materials:

- 1 % Agarose gel:
  - 0.5 g Agarose powder
  - 50 mL TAE Buffer
  - 1 μL PeqGreen
- Loading Buffer (Gel Loading Dye, Purple)
- Running Buffer (TAE Buffer)
- DNA ladder: Quick-Load® 1kb ladder
- Gel Doc^{TM} EZ Imager System

- UV sample tray
- Mini-Sub Cell GT Horizontal Electrophoresis System
- 8-well comb
- Sub-Cell GT Gel Caster
- PowerPac^{TM} Basic Power Supply

Method:

The 1 % agarose gel was made from dissolving 0.5 g agarose powder in 50 mL TAE Buffer, inside a 250 mL erlenmeyer flask or similar. Solution was heated inside a microwave for around 90 seconds and until the powder had completely dissolved and the solution was completely transparent. Solution was either left to cool down to about 60 °C, or the flask was cooled down under cold running water. After cooling the solution down to the wanted temperature, 1 μL of PeqGreen was added, and the flask was swirled around in order to mix the DNA dye. After adding PeqGreen, the solution was poured onto a gel caster with a comb sitting inside it. The gel caster had been previously assembled and leveled. The gel was left to solidify for approximately 20 minutes before removing the combs carefully. This resulted in nice wells inside the gel. Then, the gel and the gel caster was transferred onto a Mini-Sub GT Horizontal cell. The Mini-Sub GT Horizontal cell was then filled with TAE Buffer for submersion of the gel in the TAE Buffer. Before loading samples and ladder into the wells, 1 μL Gel Loading Dye was added to 5 μL sample and 5 μL Quick-Load® 1kb ladder. Then, all samples and the ladder was loaded carefully into separate wells. After transferring, power was turned on, and the gel was run for around 30 minutes with a voltage of 100 V on the PowerPac^{TM} Basic Power Supply machine.

3.7 Growth curves

A growth curve is a graphical illustration of the amount of bacteria present in a culture as a function of time, with number of bacteria on the y-axis and time on the x-axis [155]. The curve consists of four growth phases called the lag, the exponential, the stationary, and the death phase. In the lag phase the bacteria becomes accustomed to the conditions in the new environment. Once the cell has adapted and the required cellular components have been produced, the bacterial cells enter the exponential phase [155]. This phase is recognized by rapid growth where there is a constant production rate with high levels of replication, transcription, and translation [155]. The growth in this phase is more or less exponential, hence the name. Once the cell growth plateus, the culture reaches stage three which is called the stationary phase. This happens when nutrients that were available starts to become scarce, or there is an accumulation of toxic intermediates as a result of the rapid growth in the exponential phase [155]. Many bacterial cells are still alive, but the rate of growth is decreased substantially to the point where growth rate and death rate is the same. Because of the rates of death and growth being more or less the same, the growth curve will show this stage as a plateau. The stationary phase is followed by the death phase, and this is characterized by death of cells by lysis due to severe nutrient depletion and accumulation of toxic intermediates [155]. This is shown in the growth curve as a large drop from the plateau down until the curve comes close to zero on the y-axis.

Before conducting the proteomics experiment, knowledge about when the bacterium was in exponential phase was needed. The reason was that the response to exposure of antibiotics would be most prominent in the exponential phase, due to the antibiotics used is active against actively dividing cells, and the exponential phase contains a lot of active cells that are continuously dividing. Growth curves were generated in two different ways, PAU5 both with and without antibiotic exposure, and PAU3 growth curve with antibiotic exposure.

3.7.1 Growth Curves without Antibiotic Exposure

After briefly investigating genomics on a general basis for all strains and deciding to work with strain PAU5 for antibiotic spiking proteomics (section 3.8.1), a growth curve for strain PAU5 was made. A growth curve was needed in order to do proteomics sampling later because the proteomics would be focused on looking at change in expression when adding antibiotics to the growing bacteria (in exponential phase). Hence, the time point at which the bacteria was in exponential phase was needed.

Growth curves were made by measuring absorbance at 600 nm every 20 minutes for 24 h using the kinetic loop mode on the Varioskan LUX machine. Visualization of data was achieved using Microsoft Excel from Office 16, and both growth curve for each replicate, mean, and standard deviation was visualized (see section 4.6 for results).

Materials:

- Overnight culture of *P. aeruginosa* (PAU5)
- Nalgene® Labtop Cooler
- Sterile inoculation loops
- LB agar plates
- Autoclaved Mueller Hinton Broth
- Incubator at 37 °C, both with and without shaking
- Autoclaved LB medium
- Sterile microtest plate 96 well
- Varioskan LUX
- Sterile needle
- AeraSeal^{TM} BS-25 (sterile) sealing film
- 15 mL falcon plastic tubes
- LAF bench
- Pipettes and pipette tips

Method:

Three replicates of overnight cultures were made in the same manner as explained in section 3.2, using 5 mL of LB medium for the falcon tubes. After overnight cultures had been made, the experiment of generating a growth curve could start. To a sterile microtest 96 well plate, 196 μL of Mueller-Hinton Broth and 4 μL of overnight culture was added to one well. For each overnight culture 2 technical replicates were made, and this was repeated for all 3 overnight cultures which resulted in a total of 6 replicates in the microtest 96 well plate.

Figure 3.2 below shows the workflow for this experiment. Additionally, and not depicted in figure 3.2 below, 6 x 200 μL Mueller Hinton Broth was added to another 6 wells. This would serve as a control for the growth curve.

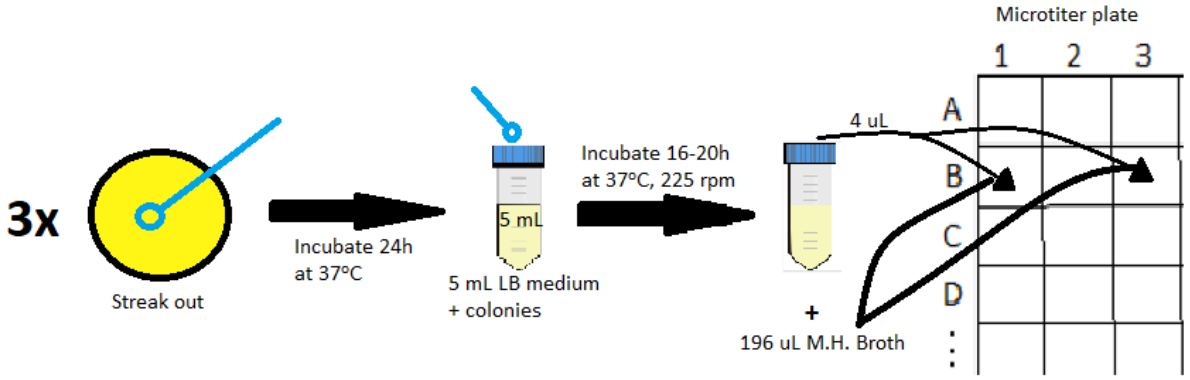

Figure 3.2. Growth curve workflow. Workflow of what the pre-measurement steps were when generating a growth curve for clinical strain PAU5.

After everything had been transferred to the microtest 96 well plate, the plate was covered with a sterile film. In order to measure absorbance while the microtest plate was in the Varioskan, a sterile needle was used to carefully nick a hole in the film above the wells where the replicates and controls were. The reason for applying a film on top was that it reduced the chance of contamination of *P. aeruginosa* in the lab drastically, while also ensuring gas exchange and aeration of the bacteria. When placed inside the Varioskan LUX, the measurement was set to kinetic loop, and measurements were taken every 20 minutes for a total of 24 h. Absorbance was measured using a specified wavelength of 600 nm (absorbance value used for detection of cells).

Data obtained after 24 h, was an excel file exported from the Varioskan LUX. The excel file contained data of all absorbance values measured at all time points for replicates and control wells. Microsoft Excel was used for all data processing and visualization. Growth curves were generated by subtracting the value of the control wells at each time-point (see results in section 4.6)

3.7.2 Growth curves with Antibiotic Exposure

A second set of growth curves was made where isolates PAU3 and PAU5 were subjected to a dilution series of Piperacillin, and constant concentration of Tazobactam (TZP). The growth curves were made with the antibiotic added from the start, because this would also be done during the proteomics analysis later. This would able determination of when isolates were in the exponential phase whilst being subjected to TZP.

Materials:

- Nalgene® Labtop Cooler
- Overnight cultures of *P. aeruginosa* (PAU3 & PAU5)
- Sterile inoculation loops

- LB agar plates
- Autoclaved Mueller Hinton Broth
- Autoclaved LB medium
- Incubator at 37 °C, both with and without shaking
- Sterile Microtest plate 96 well
- Varioskan LUX, booked in advance
- Sterile needle
- AeraSeal^{TM} BS-25 (sterile) sealing film
- 15 mL falcon plastic tubes
- LAF bench
- Piperacillin Sodium Salt
- Tazobactam

Method:

Overnight cultures were generated as explained in section 3.2. Inside a LAF bench, a dilution series of Piperacillin (PIP) in 1 mL eppendorf tubes was made, spanning from 5120 μg/mL down to 10 μg/mL (10 tubes in the dilution series). Then, 20 μL of each tube was transferred to wells in a sterile Microtest 96 wells plate where each well already contained 176 μL of Mueller-Hinton Broth. After adding PIP, 2 μL Tazobactam (TAZ) was added to each well (for a final concentration of 4 μg/mL), before transferring 4 μL of overnight culture to each well. This resulted in a 1:10 dilution of the PIP antibiotic (20 μL added to a total volume of 200 μL). The experiment was done in triplicates. In addition, both positive and negative controls were made for each replicate of each strain. To the positive control, 160 μL Mueller Hinton Broth and 40 μL of overnight culture was added, and for the negative control, 180 μL Mueller Hinton Broth and 20 μL of dH_2O was added.

After transferring everything to the sterile Microtest 96 well plate as described above, the method of placing a sterile film on top, how to measure, and how to analyze results was done in the same manner as in the previous section of growth curves (see section 3.7.1). Results from this experiment is shown in section 4.6.2.

3.8 Proteomics

In this thesis, the goal was to look at expression proteomics and hopefully decipher how the bacterium adapts to being subjected to antibiotics of various concentrations. The various concentrations would be compared as well as comparing them to a control where the bacterium was not subjected to the antibiotic. Two rounds of proteomics was performed, one round with only PAU5 spiked with three different antibiotics, and a second round with both PAU3 and PAU5 continuously subjected to different concentrations of one Piperacillin and constant concentration of Tazobactam. The choice of antibiotic and strains to use was based on results of MIC analysis performed in advance (see section 4.2 for MIC results).

3.8.1 Antibiotic Spiking with β-lactams

First round of proteomics consisted of spiking strain PAU5 with the three different antibiotics Meropenem, Ceftazidime, and Piperacillin/Tazobactam (all targeting peptidoglycan synthesis). The antibiotics were selected based on results from determination of MIC (see section 4.2). Below, an illustration of the workflow is shown (figure 3.3).

Materials:

- 4x overnight cultures of *P. aeruginosa* PAU5 in LB
- 2.8 L or 4 x 700 mL of Mueller Hinton Broth (see section 2.3.2)
- Incubator at 37 °C with shaking at 200 rpm
- 4 x 2 L erlenmeyer flasks
- 16 x 500 mL erlenmeyer flasks
- Meropenem (MEM) final concentration 0.0064 μg/mL
- Ceftazidime (CAZ) final concentration 32 μg/mL
- Piperacillin & Tazobactam (TZP) final concentration 32/4 μg/mL
- PhosSTOP (Roche)
- PMSF (Sigma)
- Complete Mini EDTA free protease inhibitors (Roche)
- Ultrasonic processor, Vibra-Cell^{TM}, VC 505
- 20 mM Tris-HCl (pH = 7.5)
- 0.1 M NaCl
- 1 mM EDTA
- Lysozyme

Method:

The workflow of this experiment followed the order shown illustratively in figure 3.3. Overnight cultures (see section 3.2 for how overnight cultures were prepared) were diluted 1:50 by adding 14 mL overnight culture to 700 mL of Mueller Hinton Broth inside 4 x 5 L autoclaved flasks, followed by incubation at 37°C and 200 rpm. Samples were grown to exponential phase (because this is the cell stage where the β-lactam antibiotics will be active) and the time-point at which the culture was in the middle of the exponential phase was after 6 hours, which was determined by the growth curve generated (results in section 4.6.1). After 6 hours, each flask culture was further divided into 4 cultures of 150 mL and the 4 cultures for each flask culture were subsequently spiked with either 1.5 mL dH_2O (negative control), 1.5 mL MEM (final concentration 0.064 μg/mL), 1.5 mL CAZ (final concentration 32 μg/mL), or 1.5 mL TZP (final concentration 32/4 μg/mL). Cultures were incubated again with the same settings of 37°C and 200 rpm for 60 minutes, with 14 mL samples being taken out after 30 minutes and 60 minutes. See figure 3.3 for illustration and explanation of workflow for sampling.

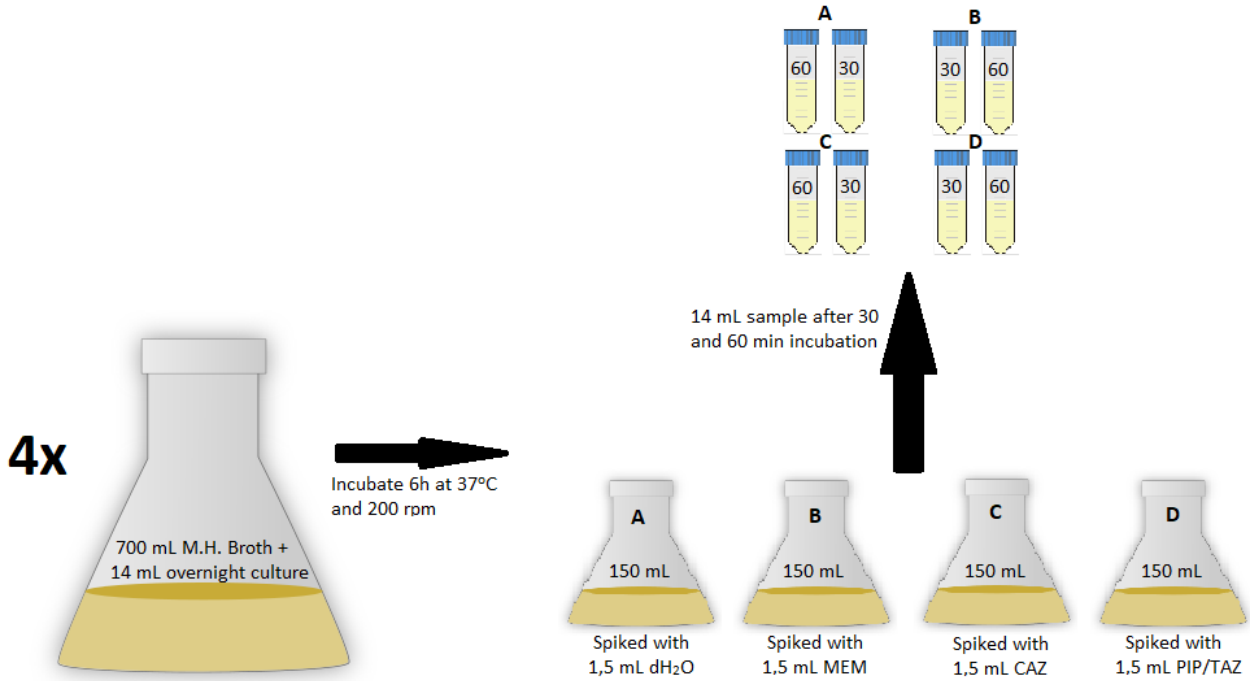

Figure 3.3. Workflow of proteomics sampling with 3 antibiotics. Workflow showing how proteomics sampling was executed, where PAU5 was subjected to MEM = Meropenem, CAZ = Ceftazidime, and TZP = Piperacillin/Tazobactam.

Immediately after taking out samples, 1x PhosSTOP (Roche), 1 mM phenylmethylsulfonyl fluoride (PMSF, Sigma), and 1 x Complete Mini EDTA (Ethylenediaminetetraacetic acid) free protease inhibitor (Roche) was added to each sample. The amount added to each sample was 0.15 mL from a 10 mL stock solution mixture containing 10x PhosSTOP + 2 PI tablets + 2 mL 50 mM phenylmethylsulfonyl fluoride (PMSF). After addition of the protease inhibitor solution, cell pellet and supernatant was separated by centrifugation (4200 xg, 10 min, 4 °C).

The bacterial cell pellet was resuspended in 1 mL of 20 mM Tris-HCl (pH 7.5), 0.1 M NaCl, 1 mM EDTA, 1x Complete Mini EDTA free protease inhibitor and lyzosyme (0.5 mg/mL). The next step was to disrupt the cells by sonication (20x, 5" pulses and 5" pauses, 27 % amplitude). After sonication, cellular debris was removed by centrifugation at 16 900 xg for 10 minutes at 4 °C.

After finishing this protocol, the next step was to perform protein precipitation (see section 3.8.3), and suspension trapping (STrap) (see section 3.8.4).

3.8.2 Continuous Exposure to Antibiotics

The second proteomics sampling performed, consisted of subjecting two strains (PAU3 and PAU5) to antibiotics continuously over a span of 3.5 h. 3.5 h was based on growth curves generated in section 3.7.2. This round had some changes to the sampling protocol, but both protein precipitation (section 3.8.3) and STrap (section 3.8.4) remained the same.

Materials:

- 3x overnight cultures of *P. aeruginosa* in LB for each strain
- LB agar plates
- Falcon tubes (15 mL and 50 mL)
- Erlenmeyer flasks, 150 mL
- Incubator at 37 °C with shaking at 180 rpm
- Centrifuge for 50 mL falcon tubes, 4 °C at 4255xg
- Piperacillin & Tazobactam (TZP) final concentration 1/4 μg/mL
- Piperacillin & Tazobactam (TZP) final concentration 512/4 μg/mL
- PhosSTOP (Roche)
- PMSF (Sigma)
- 2x Complete Mini EDTA free protease inhibitors (Roche)
- 20 mM Tris-HCl (pH = 7.5)
- 0.1 M NaCl
- 1 mM EDTA
- Ultrasonic processor, Vibra-Cell^{TM}, VC 505

Method:

Overnight cultures were made as explained in section 3.2. 600 μL of overnight cultures in LB was transferred to 30 mL of Mueller Hinton Broth (see section 2.3.2) for a dilution of 1:50 of the overnight cultures, using 150 mL Erlenmeyer flasks. Each overnight culture was added to three Erlenmeyer flasks, making it a total of 18 flasks. For each strain, three replicates of each condition was made. To three flasks for each strain, TZP was added to a final concentration of 1/4 μg/mL. Then, to another three flasks for each strain, TZP was added to a final concentration of 512/4 μg/mL. 2 dilutions of the antibiotics were made beforehand, for consistent transfer of 1 mL of PIP and 300 μL of TAZ even though there were two different concentrations. To the last 3 flasks for each strain, 1.3 mL of dH_2O was added (to add the same amount of volume in all flasks). Upon adding both the overnight cultures and the combination antibiotic to all of the 18 flasks, they were incubated at 37 °C with shaking at 180rpm.

After approximately 3.5 h, bacteria were sampled (based on growth curves made in section 4.6.2). To each sample, 300 μL of a protease inhibitor "cocktail" made beforehand was added. This "cocktail" consisted of 10 mL 10X PhosSTOP, 2x PI tablets, and 2 mL 50 mM PMSF. Afterwards, cell pellet and supernatant was separated using 50 mL falcon tubes, and centrifugation settings at 4255xg, 15 minutes, at 4 °C. Supernatant was removed, and bacterial cell pellet were resuspended in 0.5 mL of 20 mM Tris-HCl (pH = 7.5), 0.1 M NaCl, 1 mM EDTA, and 1x Complete Mini EDTA free protease inhibitors. The resuspended cell pellet was transferred to 15 mL falcon tubes, before disruption of cells by sonication using an ultrasonic processor (12x, 5" pulses and 5" pauses, 27 % amplitude). After sonication, cellular debris was removed by centrifugation at 16 900 xg, 10 minutes at 4 °C.

The samples were now ready for the protein precipitation protocol (see section 3.8.3) where the goal would be to precipitate the proteins in a wanted buffer for further use in the STrap protocol (see section 3.8.4).

3.8.3 Protein Precipitation

After proteomics sampling was done, protein precipitation was performed. The goal when performing protein precipitation was to separate the proteins from the solution as a solid (precipitate), before solubilizing in a wanted buffer for use in the STrap protocol (section 3.8.4). The protocol used for protein precipitation was the Wessel & Fluegge protein precipitation protocol (see appendix B for protocol). The protocol was followed apart from the steps described in the method section below.

Materials:

- Samples from proteomics sampling
- Chloroform
- Methanol
- 50 mM Tris-HCl (pH = 7.5)
- 10 mM Dithiothreitol (DTT)
- ddH_2O (Bidest. water)
- Allegra X-30R Centrifuge
- 15 mL Falcon Tubes

Method:

In step 1, centrifugation was done for 1 minute at 4255 xg. The centrifuge in the laboratory could not go any higher, therefore adjustments were made to the protocol. In step 2, 500 μL chloroform was added to the samples, and centrifugation was again 1 min. at 4255 xg. In step 3, 1.5 mL of ddH_2O was added, and centrifugation step was 5 min. at 4255 xg. In step 5, 1.5 mL of methanol was added before samples were centrifuged at 4255 xg for 5 minutes. Another centrifugation step was added in step 5, 10 minutes and 4255 xg settings. In the last step, step 7, the dried pellet was solubilized in 50 mM Tris-HCl (pH = 7.5) and 10 mM DTT, because these buffers would be used in the STrap protocol that followed (section 3.8.4).

3.8.4 Suspension Trapping (STrap)

After successfully completing proteomics sampling, and doing protein precipitation, the next step which was the STrap protocol could be performed. The goal of the protocol was to go from intact proteins to peptides ready for analysis on the mass spectrometry (MS) machine (timsTOF machine). The protocol was based on using a filter to trap peptides after denaturation of the proteins and protease treatment. The product of the STrap protocol would be a sample that was ready for the mass spectrometer (LC-MS/MS in this case). See section 1.10.3 and 1.10.4 for theory on the techniques.

Materials:

- 1/32" peeksil capillary
- 16 gauge needle
- 2 Empore C18 disks (filter)
- Munktell MK360 quartz filter
- 1 M DTT stock
- 20 % SDS solution
- 1 M Tris-HCl stock solution
- IAA solution
- PA solution
- Strapping solution
- ABC solution
- Trypsin solution
- ACN/TFA elution solution
- LC-MS loading solution
- ThermoMixer C
- Sonicator Bath, Bransonic® Ultrasonic 2510
- Concentrator plus - Centrifuge Concentrator
- Microcentrifuge, Heraeus^{TM} Pico^{TM} 21
- Concentrator plus - Centrifuge Concentrator
- NanoDrop^{TM} One/OneC Microvolume UV-Vis Spectrophotometer

Method:

All solutions used in this protocol, and how to prepare them, as well as what each solution does, is stated in table 2.2.

Before starting the actual protocol, the STrap tips had to be made. 2 disks of Empore C18 material were cut out by using a 16 gauge needle, and stacked firmly together in a 200 μL pipette tip using a 1/32" peeksil capillary. After stacking the 2 disks of C18 material, the same needle was used to cut out 11 disks from a Munktell MK360 quartz filter. These disks were stacked firmly on top of the C18 material, and after successfully stacking all disks, the STrap column was ready for use.

To each sample (which were now in eppendorf tubes), SDS was added to a final concentration of 5 %, Tris-HCl (pH 8) to a final concentration of 50 mM, and DTT to a final concentration of 10 mM. The tubes with the samples were heated to 100 °C for 10 minutes using a heat block in order to denature the proteins. The following step was to add 0.1 x volume of 500 mM Iodoacetamide (IAA). IAA was a solution prepared in advance (table 2.2). After adding IAA, mixing was performed by pipetting up and down a few times. Samples were then incubated in the dark for 20 minutes. After incubation, samples were acidified by adding 0.1 x volume of a phosphoric acid (PA) solution (table 2.2) and mixed by pipetting up and down a few times.

Next, the STrap tip (the tip prepared in advance with the disks inside) was mounted in a retainer tube (an eppendorf tube with the lid cut off) using an adaptor and labelling it with a marker. After setting up the system, 170 μL of strapping solution was added to the tip (assuming sample volume = 20-30 μL, and a sample-to-solution ratio between 1:6 and 1:8). Then, the sample was carefully added to the top third volume of the strapping solution. The eppendorf tube with the STrap tip was centrifuged for 10 minutes at 2500 xg, with the label facing outwards. If the solution did not flow through the filter after the first centrifugation, the centrifugation was increased to maximum 4000 xg, and inside the centrifuge the tube was rotated so that the label was now facing inwards (or opposite of what it did in the first centrifugation). Considering the centrifugation went smoothly the first time, flow-through was discarded, and another 50 μL of strapping solution was added to the tip before the sample was centrifuge again, but this time for 5 minutes at 2500 xg. This time the label was facing inwards (opposite of the previous centrifugation). After centrifugation, the flow-through was again discarded. 70 μL of ammonium bicarbonate (ABC) solution (see table 2.2) was added to the tip before the sample was placed the opposite direction as the previous time (turn 180 °) was centrifuged for 5 minutes at 2500 xg. Flow-through was again discarded.

After adding the alkaline buffering agent called ABC solution and centrifuging the sample, the tip and adaptor was transferred to a clean, labelled 1.5 mL eppendorf tube. Now, Trypsin solution could be added (since the previous buffering compounds now had been washed away), and 15 μL of trypsin solution as well as 15 μL of ABC solution was applied to the tip (table 2.2).After adding the solutions to the tip, the sample was centrifuged for 1 minute at 1000 xg. This would be sufficient to leave a few mm of liquid above the stacked filters. After centrifugation, the top of the pipette tip was covered with parafilm and the samples were incubated for 60 minutes at 47 °C.

Incubation step was followed by centrifugation for 2 minutes at 4000 xg. Then, 50 μL 0.5 % TFA was added to the flow through before the flow through with the TFA solution was transferred back into the tip. Tip and tube was again centrifuged, now for 5 minutes at 2500 xg. After this centrifugation step, flow through was discarded. Another 100 μL of TFA solution was added to the tip, but this time with a concentration of 0.1 % TFA. Tip and tube was centrifuged to run the solution through the filter, and with settings 5 minutes at 2500 xg. Flow through was discarded afterwards. Tip and adaptor was transferred to a new, clean, and labelled 1.5 mL eppendorf tube. Then, 50 μL of elution solution (see table 2.2) was added before centrifugation for 10 seconds at 1000 xg. Samples were then left to rest for 10 minutes, before they were centrifuged again for 10 minutes at 1000 xg. All eluted peptides would now be in the eppendorf tube.

In the next step, samples were evaporated to dryness using a centrifuge concentrator (temperature 30 °C for approximately 1.5 hours), before 12 μL of loading solution was used to redissolve the peptides by sonication in a Sonicator Bath for 10 minutes. Lastly, peptide concentration was measured at A_{205}nm using the NanoDrop One/One^C UV-Vis before 10 μL of the peptide solution was transferred to AS vials for use in the timsTOF Pro instrument from BRUKER (The LC-MS/MS machine).

3.8.5 LC-MS/MS

For performing identification of peptides, the LC-MS/MS machine timsTOF supplied by BRUKER was used. This part of the experiment was solely and kindly performed by Morten Skaugen. The method used was label-free proteomics quantification.

3.8.6 Preliminary Data Handling

Before being able to say anything about up-regulation, down-regulation, and differences between conditions, preliminary handling of raw data was performed. This was achieved by using both MaxQuant and Perseus, but also BRUKER Compass DataAnalysis. Preliminary data handling was performed together with Per Kristian Edvardsen, where he taught me how to do this specific analysis while I took notes and learnt the procedure. For both rounds of proteomics, the same settings were used.

First, spectral data was retrieved from the LC-MS/MS machine into MaxQuant (free download of software on www.maxquant.org. Under group-specific parameters inside the MaxQaunt software, several settings were changed and/or selected for. Under modification, oxidation (M), acetyl (protein N-terminal), deamination (NQ), and Gln -> pyro-Glu was selected. This ensured that modifications that could have happened to the samples inside the chromatography-mass spectrometry instrument were taken into account. Label-free quantification was used, therefore this needed to be selected for. Then, digestion setting used was Trypsin/p (a modified version of Trypsin, where Lysine residues have been methylated for highly active and stable Trypsin). The modified Trypsin targets Lysines (L) and Arginines (R) specifically during protein digestion. Max. missed cleavages was also ticked, and this included spectra where cleavages by Trypsin had not happened. This could have occurred if the Trypsin was not able to gain entry into the protein chain due to for example large aromatic side chains (Tryptophan, Tyrosine, Phenylalanine, or Histidine).

For annotating the peptide spectra to proteins, a reference file was needed. This was where the fasta-file from whole genome sequencing was used. The fasta-file contained the entire amino acid sequence for the specific strain, and this was loaded into the software under global parameters. Then, under description rule, the fasta-file was divided by annotation and sequence to fit into a list format. The same modifications as added under group-specific parameters above, were also added here. Additionally, match between runs was ticked, which would transfer previously matched proteins to the next sample. This would make the run go quicker as well as providing more identified protein, but it would also introduce the problem of false positives. MaxQuant also contains databases of i.e., human proteins, which would be a part of matching spectra to database. This ensured that contaminants of e.g., human proteins during laboratory work, would be identified and removed.

File obtained contained data on quantification of peptides. Some additional data tweaking was needed, such as filtering out data "only identified by site", "potential contaminants", and "reverse" matches. The filtering gave empty columns, which was removed. A lot of NaN were present, which were also removed. This means annotation had been successful, but quantification had not.

Lastly, statistical computations could be performed. Perseus contained many tools that could be used, and in this analysis t-test, two-sample test and p-value was used. This would give positive values for up-regulation of proteins, and negative values for down-regulation of proteins in a $\log_2$-fold scale. Two and two conditions were compared for each statistical test, resulting in three sets of data containing dys-regulated proteins for each strain and for each proteomics sampling. For antibiotic spiking (isolate PAU5), the different antibiotic subjected bacteria were compared to a dH_2O control, while for continuously exposed bacteria (isolates PAU3 and PAU5) comparison both between the control and the lower antibiotic concentration was performed. The results could then be exported as an excel-file, and used to make visualizations using R, as well as identifying functions of proteins using database searching on www.uniprot.org.

3.8.7 Proteomics Analysis

After performing preliminary data handling, an excel-file containing dys-regulated proteins was the result. This gave information about relative dys-regulated proteins compared to either a control or the lower antibiotic concentration. For visualization of the data, R was used to make volcano plots and heatmaps. The results can seen in section 4.7.2. For proteomics on antibiotic spiking, visualizations of dys-regulated proteins were not made.

For identification of all proteins, a combination of searches in the Uniprot database (Uniprot.org) and article search was used in order to gain knowledge about what the different proteins do. In the Uniprot database, the protein name was inserted into the search bar. All information that is not directly cited, was obtained from Uniprot. Information about the proteins obtained from somewhere else, is cited in the text.

Another analysis performed, was a STRING analysis. STRING is a web resource containing both known and predicted protein-protein interactions that can be visualized in a network. STRING analysis was performed on ampC to investigate whether ampC was involved in a network of proteins. In STRING proteins search site, AmpC protein name was inserted. An organism-specific search was used, and that was *Pseudomonas aeruginosa* PAO1. The result of the STRING analysis can be seen in section 4.7.3.

4 Results

4.1 Determination of Colony Forming Units (CFU/mL)

Before performing analysis of minimum inhibitory concentration (MIC), determination of colony forming units was performed. This is needed for MIC determination, according to ISO standard 20776-1 (info obtained from [150]). In the MIC testing, 5x10^5 CFU/mL inoculum (source material) is needed, hence the number of colony forming units for each isolate had to be determined. Estimation of concentration was done in three replicates for each strain, and estimation was based on the number of colonies in the dilution where colonies were easily distinguishable (see section 3.3). Results are shown in table 4.1 below.

Table 4.1. Concentration estimation of *P. aeruginosa*. Estimated concentration in CFU/mL for all the bacterial strains. * = Number of colony forming units for strain PAU4, replicate 2, was counted on the agar plate containing dilution 10^{-5}. All other replicates of all strains were counted using the 10^{-6} dilution.

Identification	Repl. 1	Repl. 2	Repl. 3	Mean	Unit
PAU1	12	5	9	8.67 x 10^7	CFU/mL
PAU2	8	7	9	8.00 x 10^7	CFU/mL
PAU3	2	1	4	2.33 x 10^7	CFU/mL
PAU4	6	6.3*	7	6.50 x 10^7	CFU/mL
PAU5	8	2	9	6.33 x 10^7	CFU/mL
PAU6	4	8	7	6.33 x 10^7	CFU/mL
PAU7	4	5	11	6.67 x 10^7	CFU/mL
ATCC27853	7	4	7	6.00 x 10^7	CFU/mL

As shown in table 4.1, all replicates fell within the same order of magnitude, but with slightly varying base number. Replicate 2, isolate PAU4, was counted on the agar plate containing dilution 10^{-5}. The determined CFU/mL showed that the bacteria would have to be diluted in the MIC determination experiment due to inoculum = 5 x 10^5 CFU/mL as explained above.

4.2 MIC Determination

Minimum inhibitory concentration (MIC) of the antibiotics Piperacillin/Tazobactam, Meropenem, Ciprofloxacin, Tobramycin, Colistin, and Ceftazidime was determined for seven clinical strains of *P. aeruginosa* (PAU1-7) in both Mueller-Hinton Broth (MHB) and RPMI-LB10 medium (table 4.2). The goal for this experiment was to figure out whether the clinical isolates showed resistance against the 6 types of antibiotics tested. Testing was based on the MIC determination protocol set by ISO standard 20776-1 [150]. As described in the ISO standard, Mueller-Hinton Broth was used as medium. Additionally, the same protocol was conducted in RPMI-LB10 medium to investigate whether medium was a determinant for MIC.

Table 4.2 shows the mean for 3 replicates of minimal antibiotic concentration needed for inhibiting growth of *P. aeruginosa*. Values are given in μg/mL, and values above the threshold value for being considered resistant to the antibiotic according to EUCAST breakpoint

tables [150], are marked with (R) (see table 3.2 for breakpoint values). EUCAST provides breakpoint values for bacteria grown in Mueller-Hinton Broth only (M.H.B.), hence values in RPMI-LB10 cannot be labeled as resistant (even though they might be above the EUCAST threshold).

Table 4.2. MIC determination. MIC determination in Mueller-Hinton Broth (MHB) and RPMI-LB10 medium. All values are given in μg/mL, and red values and (R) behind it signifies resistant values in Mueller-Hinton Broth based on breakpoint tables from EUCAST. TZP = Piperacillin/Tazobactam, MEM = Meropenem, CIP = Ciprofloxacin, TOB = Tobramycin, CST = Colistin, and CAZ = Ceftazidime.

Antibiotic	Antibiotic target	PAU1		PAU2		PAU3		PAU4	
		M.H. Broth	RPMI-LB10	M.H.Broth	RPMI-LB10	M.H. Broth	RPMI-LB10	M.H.Broth	RPMI-LB10
TZP	Peptidoglycan synthesis	0,5/4-1/4	2/4	2/4-4/4	2/4-4/4	>64/4 (R)	>64/4	32/4 (R)	>64/4
MEM	Peptidoglycan synthesis	<0.125	<0.125	1-2	2-4	4-8	8	0.5-1	8-16
CIP	Binds DNA gyrase	4 (R)	0.5-1	>8 (R)	4	0.5	0.5	0.5	0.5
TOB	Binds 16S rRNA	2	8	2	16	2	4-8	2	8
CST	Bacterial outer membrane	0.25	0.25	0.25-0.5	0.5	1	2-4	0.25-0.5	1
CAZ	Peptidoglycan synthesis	2	0.25-0.5	2-4	1	32 (R)	8	8	4-8

Antibiotic	Antibiotic target	PAU5		PAU6		PAU7		ATCC27853	
		M.H. Broth	RPMI-LB10	M.H.Broth	RPMI-LB10	M.H. Broth	RPMI-LB10	M.H. Broth	RPMI-LB10
TZP	Peptidoglycan synthesis	>64/4 (R)	<0.125/4	4/4	8/4-16/4	8/4	16/4	4/4-8/4	8/4-16/4
MEM	Peptidoglycan synthesis	<0.125	<0.125	0.5	1-2	0.5-1	2-4	0.25-0.5	1
CIP	Binds DNA gyrase	2 (R)	<0.016	0.125-0.25	0.125	0.25-0.5	0.125	0.5-1 (R)	0.062
TOB	Binds 16S rRNA	8 (R)	<0.031	1-2	2	1	2	0.5-1	1
CST	Bacterial outer membrane	0.25	<0.125	0.5	2	1	2	0.5	1
CAZ	Peptidoglycan synthesis	>64 (R)	<0.125	2	1	4	2	2-4	1

Figure 4.1 shows how a regular set-up and results would look like, and green color indicates bacterial growth, while clear wells indicate either empty or no growth of bacteria.

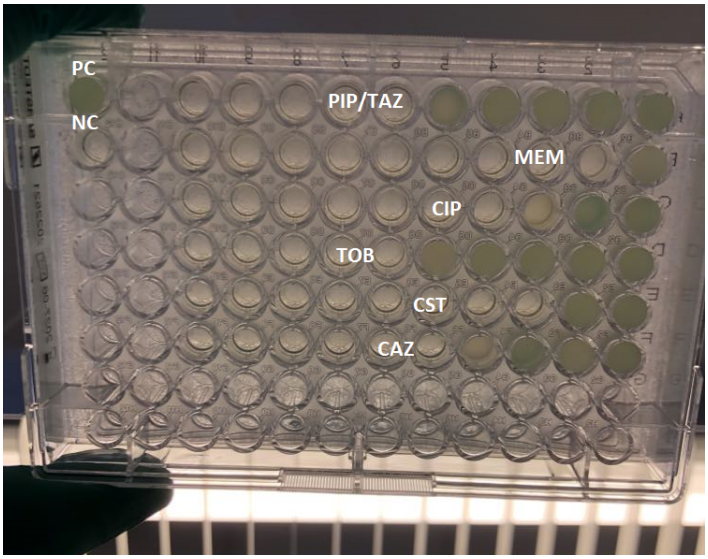

Figure 4.1. Standard MIC-result in 96-well microtiter plate. Standard MIC-result in a 96-well microtiter plate. Each row (A-I) was designated to one antibiotic and the dilution series of it. Concentration of antibiotic was lowest on the right handside of the picture, with a doubling increment of antibiotic concentration for each column (like dilution series shown in table 3.1). TZP = Piperacillin/Tazobactam, MEM = Meropenem, CIP = Ciprofloxacin, TOB = Tobramycin, CST = Colistin, CAZ = Ceftazidime, PC = positive control (bacteria in either Mueller-Hinton Broth or RPMI-LB10-medium), NC = negative control (only medium).

4.2.1 Piperacillin/Tazobactam

For the combination of Piperacillin and Tazobactam (TZP), MIC breakpoint value given by EUCAST characterizes resistance as growth of *P. aeruginosa* in medium with antibiotic concentration of >16 μg/mL (see table 3.2 for breakpoint value). Table 4.2 shows that in Mueller-Hinton Broth (M.H.B) strains PAU3, and PAU5 had a MIC 4 times higher than the breakpoint value given by EUCAST. PAU4 was also characterized as resistant, with an inhibiting antibiotic concentration 2 times higher than the breakpoint value. The other strains were not resistant against this combinatory antibiotic, according to EUCAST. In RPMI-LB10 medium, PAU1 showed growth in higher concentration, and PAU2 and PAU3 showed growth at the same concentration as they did in the M.H.B. PAU4 showed increased tolerance against the antibiotic, with an even higher value in the nutrient-poor RPMI-LB10 compared to in M.H.B. PAU5, interestingly, was not able to grow at all in the RPMI-LB10 medium, giving a large deviation in results between bacteria in the M.H.B and RPMI-LB10. PAU6 showed increased tolerance against TZP in the RPMI-LB10 medium, and so did PAU7. Lastly, the laboratory strain, ATCC27853, also showed increased tolerance against the antibiotic in the RPMI-LB10 medium.

4.2.2 Meropenem

For the carbapenem Meropenem (MEM), MIC resistance threshold for *P. aeruginosa* was growth of the bacterium in medium with antibiotic concentration of >8 μg/mL (table 3.2). None of the strains showed resistance against this antibiotic, and the drug even showed efficiency by inhibiting growth all together for both strain PAU1 and PAU5. It is noteworthy

that strain PAU3 was inhibited by antibiotic concentration of 8 μg/mL for some replicates, which is the threshold value. This was seen in the Mueller-Hinton Broth.

For bacteria grown in RPMI-LB10 medium, both PAU1 and PAU3 showed roughly the same MIC-values compared to the values in M.H.B. Strain PAU2 had a slight increase in growth in the RPMI-LB10 medium, while PAU5 did not grow at all in RPMI-LB10. The other strains had a two-fold increase, or more, in MIC-value when grown in the RPMI-LB10 medium, and PAU4 was the strain with the highest increase in inhibitory concentration, showing a four-fivefold increase (from 0.5-1 μg/mL in M.H.B. to 8-16 μg/mL in RPMI-LB10).

4.2.3 Ciprofloxacin

For the third antibiotic tested, the fluoroquinolone ciprofloxacin (CIP), breakpoint value for resistance given by EUCAST was >0.5 μg/mL (table 3.2). The data showed that ciprofloxacin was the antibiotic agent most strains showed resistance levels towards. PAU1, PAU2, PAU5, and ATCC27853 all showed resistance against the compound in MHB medium (table 4.2. Strain PAU1 was inhibited by an antibiotic concentration of 4 μg/mL, which was a 8-fold increase in antibiotic concentration compared to the breakpoint value for resistance. Strain PAU2, interestingly, showed growth in all concentrations of the drug and was not inhibited by the highest concentration of the antibiotic (8 μg/mL). For strain PAU5, resistance was also observed against the fluoroquinolone, with a concentration of 2 μg/mL needed for inhibition of growth. The last strain that showed resistance, was the laboratory strain ATCC27853. Inhibitory concentration of ATCC27853 was barely above the breakpoint value, with an inhibitory concentration being between 0.5 μg/mL and 1 μg/mL.

When grown in RPMI-LB10 medium, all strains showed either no difference (PAU3, PAU4, and PAU6) or a slight decrease in inhibitory concentration (PAU1, PAU2, PAU6, PAU7, and ATCC27853) compared to the data obtained from MHB medium. PAU5 did not show any growth in RPMI-LB10 medium and subjected to CIP.

4.2.4 Tobramycin

Tobramycin (TOB) was the fourth antibiotic tested, and the EUCAST breakpoint table characterizes a *P. aeruginosa* strain as resistant if there is growth in antibiotic concentration >2 μg/mL. PAU5 was the only strain that showed resistance against this antibiotic. Strains PAU1, PAU2, PAU3 and PAU4 were inhibited by concentration of 2 μg/mL, and therefore were not classified as resistant.The remaining strains PAU6, PAU7, and ATCC 27853 were inhibited by concentrations right below the breakpoint value, as seen in table 4.2.

In RPMI-LB10 medium, all strains except PAU5 (which did not show growth at all), showed an increase in tolerance against the antibiotic compared to in MHB medium. The inhibitory concentration was increased for all other strains in RPMI-LB10 medium, compared to the MHB medium. Some strains had a large increase in MIC value in RPMI-LB10 medium compared to MHB medium, such as PAU2, which showed an eight-fold increase when changing the medium.

4.2.5 Colistin

Colistin (CST), showed efficiency against all strains, and none of the strains were characterized as resistant. Breakpoint value for resistance against this antibiotic agent was >4 μg/mL (see table 3.2 for breakpoint values). In MHB medium, all strains except PAU3 and PAU7 showed MIC value between 0.25 and 0.5 μg/mL. Strains PAU3 and PAU7 had a slightly higher MIC value compared to the other strains, of 1 μg/mL. In RPMI-LB10 medium, strains PAU2, PAU3, PAU4, PAU6, PAU7, and ATCC27853 showed a slight increase in MIC compared to MHB medium.

4.2.6 Ceftazidime

Ceftazidime (CAZ) has a resistant threshold at >8 μg/mL (see table 3.2 for breakpoint values). Strain PAU3 and PAU5 showed resistance, with growth observed at antibiotic concentrations 4-8 times higher than the breakpoint value (32 μg/mL for PAU3, and >64 μg/mL for PAU5) (see table 4.2). PAU5 showed growth in all concentrations of the antibiotic, while PAU3 was inhibited by the second highest concentration of CAZ in the MIC testing. Strain PAU4 showed inhibition by antibiotic concentration of 8 μg/mL which is equal to the breakpoint value, while the remaining strains showed inhibition at low concentrations of the antibiotic compared to both breakpoint value and resistant strains PAU3 and PAU5. In RPMI-LB10 medium, the response was a decrease in inhibitory concentration for all strains. PAU3 had the largest decrease in MIC, going from 32 μg/mL to one fourth of that, 8 μg/mL.

4.2.7 Summary of MIC Analysis

PAU5 was the clinical isolate that showed resistance against most antibiotics in the Mueller-Hinton Broth medium. PAU5 was resistant against 4 classes of antibiotics, β-lactam Piperacillin/-Tazobactam, the fluoroquinolone Ciprofloxacin, the aminoglycoside Tobramycin, and the 3^{rd} generation cephalosporin Ceftazidime (also a β-lactam). PAU5 did, however, not show any growth at all in RPMI-LB10 medium (see table 4.2). Based on MIC values, it puts clinical isolate PAU5 in the multi-drug resistant (MDR) category [156]. An isolate is considered as MDR if there is lack of susceptibility to at least one agent in three or more antibiotic classes [18]. This was the case for PAU5 (two β-lactams, one fluoroquinolone, and one aminoglycoside). PAU3 was the clinical strain showing second most resistance, with resistant values against the β-lactams Piperacillin/Tazobactam and Ceftazidime in Mueller-Hinton Broth. PAU3 showed roughly the same values when switching to the nutrient-poor RPMI-LB10-LB10 medium, but for CAZ the concentration at which the bacterium could grow was drastically reduced from 32-8 μg/mL.

Several of the isolates showed the response of increased tolerance against the various antibiotics when bacteria were grown in the nutrient-poor medium RPMI-LB10-LB10. This was true for several of the strains when exposed to TZP, MEM, TOB, and CST (see table 4.2 for values).

4.3 DNA Extraction

After observing that antibiotic susceptibility varied substantially among the clinical isolates, as shown in determination of MIC (see results in section 4.2), it was decided to sequence the genomes. These strains are novel, therefore it would be interesting to determine their genetic potential, and especially in relation to antibiotic resistance. The first step of sequencing entails growing bacterial biomass and extracting high quality DNA for downstream processing. In this case, the goal was high-molecular weight (HMW) DNA, meaning long fragments of DNA because when using the Nanopore to perform sequencing, long fragments yields higher confidence and better sequencing results [134].

Results of DNA-extraction consisted of concentrations measured on both Nanodrop and Qubit, gel electrophoresis pictures, and new measurements of concentrations after performing short read elimination (SRE), which entails removal of short DNA-fragments present in the sample.

The first results obtained from DNA-extraction were the measured concentrations using Qubit. DNA extraction was performed in two rounds for some isolates, due to concentration of HMW DNA being too low in the first extraction round. The values can be seen in table 4.3 below.

Table 4.3. Qubit measurements post DNA-extraction. Concentration determined by Qubit post extraction of high-molecular weight DNA. DNA-extraction was performed in two rounds for some isolates due to inadequate results the first time, therefore results are divided in first and second DNA-extraction. Concentration was calculated based on a mean of three measurements

First DNA-extraction			Second DNA-extraction		
Strain	**Amount**	**Unit**	**Strain**	**Amount**	**Unit**
PAU1	386	ng/μL	**PAU1**	135	ng/μL
PAU2	271	ng/μL	**PAU2**	244	ng/μL
PAU3	449	ng/μL	**PAU3**	200	ng/μL
PAU4	435	ng/μL	**PAU4**	238	ng/μL
PAU5	161	ng/μL	**PAU6**	144	ng/μL
PAU6	571	ng/μL			
PAU7	537	ng/μL			

Afterwards, DNA was measured using Nanodrop (table 4.4). In addition to measuring concentration, Nanodrop also provided a value for assessing purity of DNA. The 260/280 ratio would reveal protein contaminants or other, and a value of 1.8 meant there were no contaminants in the sample. The 260/230 ratio would reveal potential contaminants of solvents used during the extraction of DNA, and if there were no contaminants, the ratio would be between 1.2 and 1.8.

Table 4.4. Nanodrop measurements post DNA-extraction. Concentration determined by Nanodrop post extraction of high-molecular weight DNA. DNA-extraction was performed in two rounds. First extraction was performed on all seven strains, while second extraction did not include PAU5 and PAU7.

First DNA-extraction					Second DNA-extraction				
Strain	**260/280**	**260/230**	**Concentration**	**Unit**	**Strain**	**260/280**	**260/230**	**Concentration**	**Unit**
PAU1	1,93	1,89	566,4	ng/μL	PAU1	1,92	1,50	410,4	ng/μL
PAU2	1,95	2,00	498,6	ng/μL	PAU2	1,93	1,75	302,6	ng/μL
PAU3	1,92	1,81	730,1	ng/μL	PAU3	1,90	1,82	449,8	ng/μL
PAU4	1,90	1,82	694,8	ng/μL	PAU4	1,97	1,95	521,3	ng/μL
PAU5	1,95	2,07	246,3	ng/μL	PAU6	1,95	1,98	462,6	ng/μL
PAU6	1,91	1,87	471,8	ng/μL					
PAU7	1,93	1,98	1079,9	ng/μL					

For both the first and second extraction, table 4.4 shows 260/280 ratios were consistently slightly above the wanted ratio of 1.8. 260/230 ratios were more dispersed, ranging from 1.50-2.07, indicating contaminants in some of the samples, but improvement of purity in the second DNA-extraction. Concentration ranged from 246.3 to 1079.9 ng/μL.

After performing SRE, DNA quality and quantity was assessed again to ensure there was still HMW DNA present in the sample after removing shorter DNA fragments. Then, gel electrophoresis was performed again to ensure there was HMW DNA and not fragmented DNA still present (because this would not be revealed in neither Nanodrop nor Qubit). Figure 4.2 shows gel electrophoresis results of all isolates after first round of DNA-extraction.

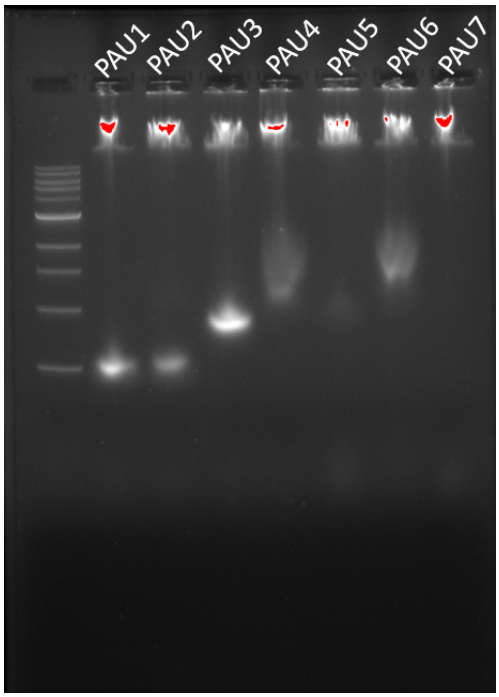

Figure 4.2. Gel electrophoresis of all isolates. Image of gel electrophoresis results on all isolates after performing the first round of DNA-extraction. PAU5 and PAU7 would be used for sequencing, while the DNA of the other isolates had to be extracted again.

PAU5 and PAU7 gave high quality DNA, with little contaminants and little to no short fragments of DNA present in the sample. These could be used directly for library preparation and subsequent sequencing. PAU1, PAU2, PAU3, PAU4, and PAU6, however, had shorter

fragments of DNA present in their sample. This was the reason for performing SRE on those isolates. Figure 4.3 shows gel electrophoresis picture after performing short-read elimination on the five isolates.

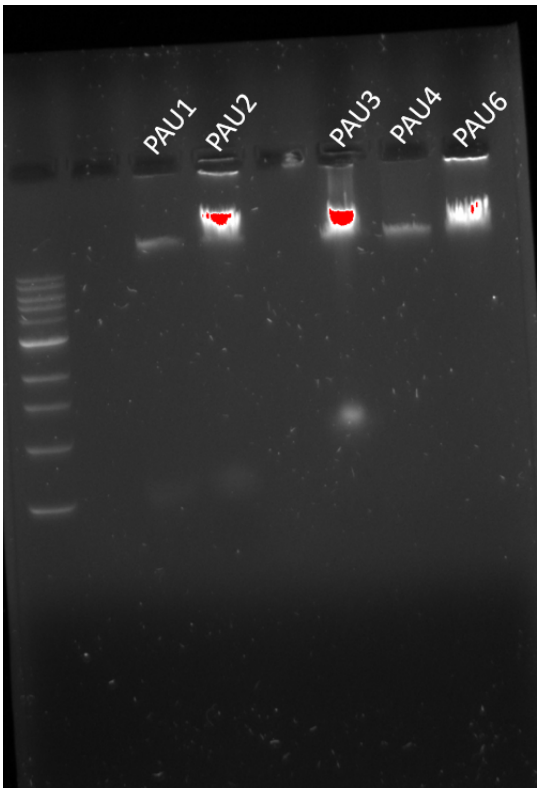

Figure 4.3. Gel Electrophoresis of five isolates post SRE. Image of gel electrophoresis results on isolates PAU1, PAU2, PAU3, PAU4, and PAU6 post performing short-read elimination (SRE) in the first round of DNA-extraction.

After performing SRE, gel electrophoresis revealed little to no contamination of short-read fragments but the SRE protocol had removed too much HMW DNA for it to be possible to use the samples in sequencing. Extraction was therefore performed once again on all isolates except PAU5 and PAU7. The results of the second DNA-extraction are shown in figure 4.4 below.

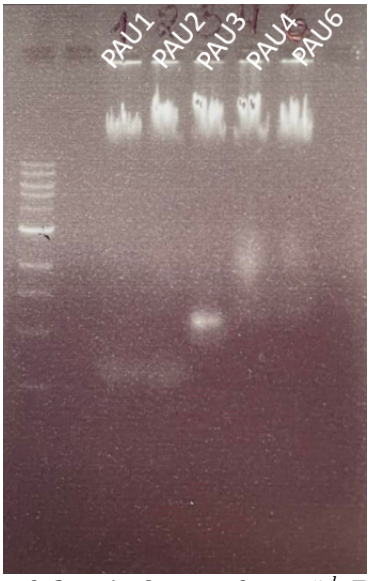

Figure 4.4. Gel Electrophoresis of five isolates after 2nd DNA-extraction. Image of gel electrophoresis results on isolates PAU1, PAU2, PAU3, PAU4, and PAU6 after second DNA-extraction. Samples PAU1, PAU2, and PAU6 were used for sequencing, while short-read elimination was performed on PAU3 and PAU4 first.

The second DNA-extraction was successful on isolates PAU1, PAU2, and PAU6, meaning these were ready for library preparation and subsequent sequencing. Gel electrophoresis revealed there were shorter fragments of DNA in PAU3 and PAU4. Short-read elimination was therefore performed on extracted DNA on these isolates one more time. Table 4.5 shows Nanodrop and Qubit results after SRE, while figure 4.5 shows gel image of PAU3 and PAU4 after performing SRE on the second DNA-extraction samples.

Table 4.5. Qubit and Nanodrop values after SRE on PAU3 and PAU4. Qubit and Nanodrop values post performing SRE on PAU3 and PAU4 on the second DNA-extraction samples.

Strain	260/280	260/230	Qubit	Nanodrop	Unit
PAU3	1,91	2,08	38,9	156,3	ng/μL
PAU4	1,77	1,83	61,7	12,3	ng/μL

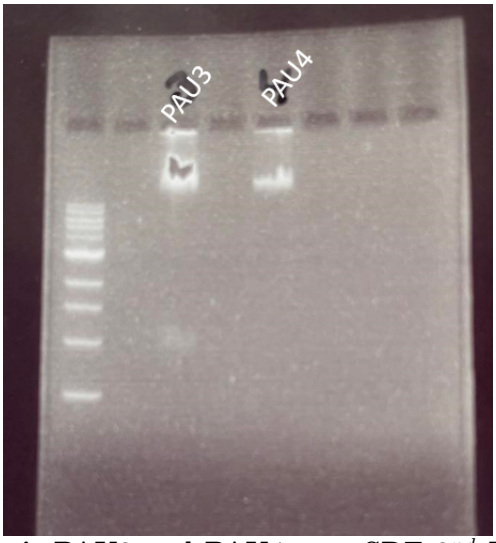

Figure 4.5. Gel electrophoresis PAU3 and PAU4 post SRE 2^{nd} DNA-extraction. Image of gel electrophoresis results on isolates PAU3 and PAU4 post performing short-read elimination (SRE) in the 2^{nd} round of DNA-extraction. These samples were used for whole genome sequencing.

Gel picture and Nanodrop as well as Qubit measurements showed successful extraction that could be used for sequencing the genome of isolates PAU3 and PAU4.

4.4 DNA Sequencing

The DNA extracted from the strains showed high enough quality to proceed with Nanopore sequencing (high molecular weight with a concentration preferably >30 ng/μL). The sequence data was obtained using the MinION device from Oxford Nanopore Technologies, and sequence was assembled using Flye and Canu assembly. Results from DNA sequencing are shown in table 4.6 below.

Table 4.6 gives an overview of results from sequencing, in the form of genome size, and various parameters used for determining the quality and confidence of the results. N50 (Mb) is a parameter for sequence length, and it is defined as the sequence length of the shortest contig at 50 % of the total assembly length, and in short the closer N50 is to the real genome size, the better. Contigs are overlapping DNA segments that when assembled together using Flye or Canu in this instance, results in a continuous genomic region, and the fewer contigs, the better because this reduces the amount of possibly missing genomic regions [134]. Mean coverage is a percentage showing the average coverage of each nucleotide in the sequence, and is also called sequencing depth [134]. This means it shows the percentage of times a nucleotide in the sequence is covered by a unique sequence read. The higher percentage, the higher the confidence due to more data about what each nucleotide might be (threshold=50 %). Benchmarking Universal Single-Copy Orthologs (BUSCO) completeness % is a way of determining how well the sequencing performed by looking for marker genes known to be a part of the *P. aeruginosa* genome [134]. Genes are species specific, and Pseudomonadales has 782 BUSCO marker genes (threshold is >95 %). Lastly, % duplication BUSCO shows the percentage of duplicated BUSCO marker genes present in each sample. Some duplication is expected, but if this value is too high (e.g., 10 %) this could entail that the assembly has not

Table 4.6. Summary of sequencing. Summary of sequencing for *P. aeruginosa*, showing genome size in Mega bases (Mb, 10^6), N50 = the sequence length of the shortest contig at 50 % of the total assembly length, contigs = overlap of DNA segments that results in a continuous genomic region (the fewer the better), mean coverage meaning the average coverage of each nucleotide in the sequence, also called sequencing depth (value between 50 and 100 gives higher confidence), % completeness (BUSCO) = percentage of BUSCOs marker genes identified during sequencing (>95 %). Pseudomonadales has 782 BUSCOs marker genes.% duplication (BUSCO) = Percentage of duplications of genes.

Sample	Genome size (Mb)	N50 (Mb)	Contigs	Mean coverage	% completeness (BUSCO)	% duplication (BUSCO)
Flye assembly						
PAU1	6,39	6,39	1	86	99,5	0,30
PAU2	6,22	0,61	18	6	77,6	0,40
PAU3	6,41	6,41	1	59	98,1	0,40
PAU4	6,46	6,46	1	29	96,8	0,40
PAU5	6,62	1,81	7	50	98,7	0,40
PAU6	7,10	7,10	1	84	99,4	0,80
PAU7	6,44	6,44	1	73	99,8	0,40
Canu assembly						
PAU2	5,78	1,79	44	6	73,3	0,40
PAU5	6,99	4,04	2	53	98,7	1,00

been able to distinguish between many different genes, equating to poor sequencing results [134].

Flye assembly was performed on all strains, while Canu assembly was performed on strain PAU2 and PAU5 after insufficient assembly results from Flye [134]. Genome size ranged from 5,78 Mb (PAU2) up to 7,10Mb (PAU6). For most strains, there was only one contig (except PAU2 and PAU5). Benchmarking Universal Single-Copy Orthologs (BUSCO) completeness showed identification of the BUSCO marker genes in a percentage above the threshold of 95 % for all strains except PAU2. PAU2 had a % completeness of 77,6 % which is lower than the threshold. % Duplication was seen in highest amount in PAU5 after performing Canu assembly. Mean coverage of bases in the genome varied from 6 for PAU2, and 29 for PAU4, up to 86 for PAU1.

N50 showed that the sequence length of the shortest contig at 50 % of the total assembly length was the entire genome size for strains PAU1, PAU3, PAU4, PAU6, and PAU7 (because there was only 1 contig). For PAU5, N50 was 4,04 for the Canu assembly and 1,81 for Flye assembly. This meant that there were several shorter fragments, but the assembler performing best was Canu. The results obtained by the Canu assembler were used for subsequent analysis of both PAU2 and PAU5.

Results of PAU2 sequencing could not be used as reliable data for downstream analysis due to low mean coverage, low identification of BUSCO marker genes, and many contigs (meaning unreliable results) [134]. Instead, PAU2 was used for showing a comparison between successful sequencing and unsuccessful sequencing, and to give direct examples of the implications poor sequencing results might have in the genomic analysis that followed.

4.5 Genomics

4.5.1 Pangenome

After getting the full sequence of each genome for the seven clinical isolates of *P. aeruginosa* (but with poor results for PAU2), these sequences were used for investigating the genomic contents, and specifically genes linked to antibiotic resistance or clearance. This part of the thesis was meant to be of a superficial manner, with the superior goal of using the genome sequences to do proteomics analysis of isolates later.

Two venndiagrams were made for visualization of genome. The first one shows core genes and accessory genes between strains PAU1, PAU3, PAU4, PAU5, PAU6, and PAU7 (see figure 4.6). Another venndiagram was made for showing shared and unique genes between PAU3 and PAU5 because this could be used later for comparison in the proteomics analysis (see figure 4.6). Isolate PAU2 was excluded from this analytical part, because including the genomic sequence of this isolate would affect the results of the venndiagrams and the number of genes present as core, shell and cloud genome. Since PAU2 sequencing results were of low quality and confidence, it did not make sense to include them in the analysis that followed.

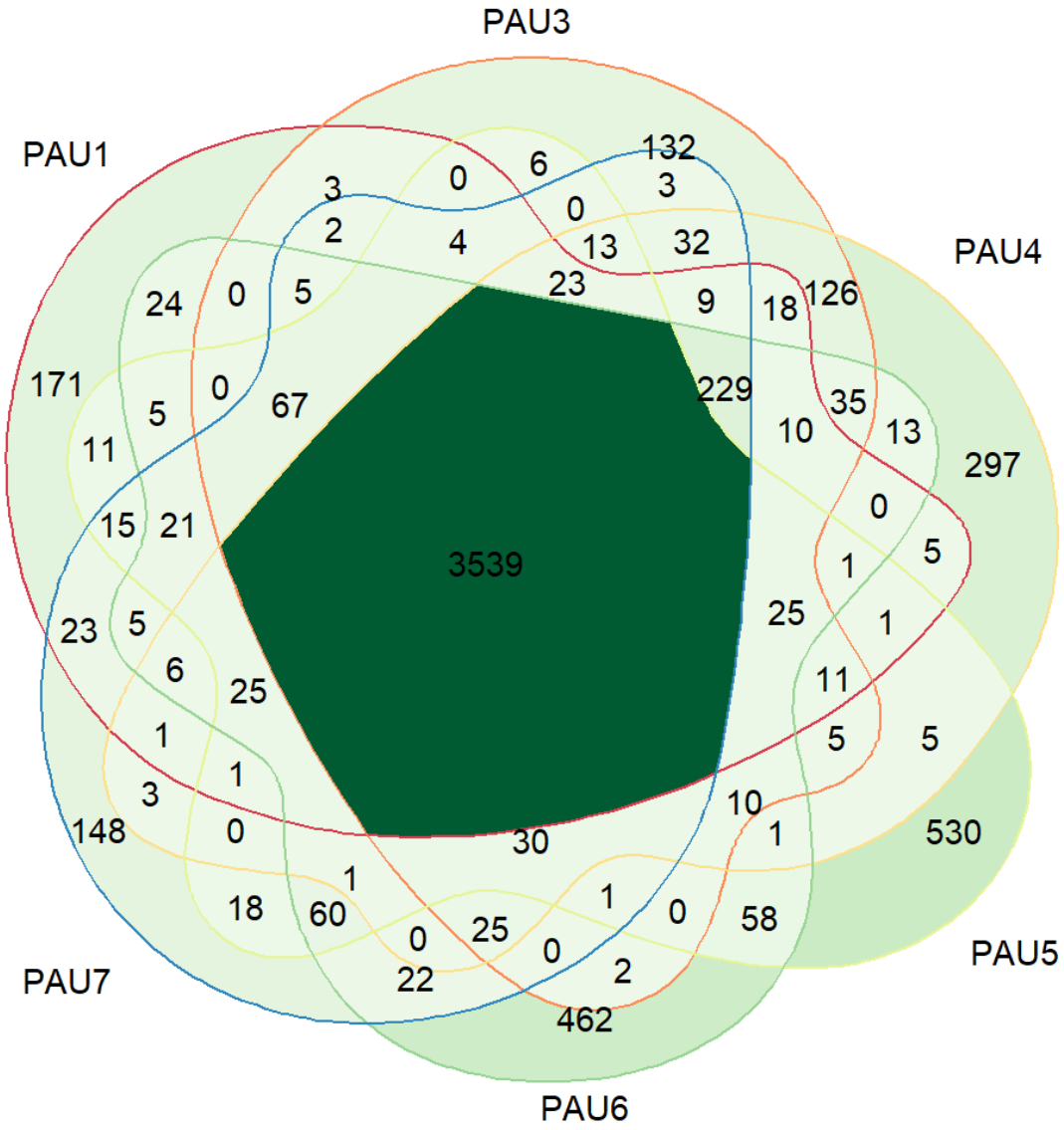

Figure 4.6. Venndiagram all isolates. Venndiagram showing all core and accessory genes identified for each isolate (except PAU2). Genes shared between all isolates are shown in the middle of the figure, while unique genes for each isolate and shared among one or more isolates are shown in the area surrounding the middle. PAU1 had 171 unique genes, PAU3 had 132 unique genes, PAU4 had 297, PAU5 had 530, PAU6 had 462 unique genes, and PAU7 had 148. Each strain has a line with a specific color, that shows how many genes overlap with the various strains. E.g., PAU3 has a orange line, while PAU4 has a yellow line, and where these overlap the number 126 is written, meaning these have 126 genes in common that they do not share with any of the other isolates.

3539 genes were identified as core genome between the 6 clinical isolates (not counting PAU2). Summarizing all genes in the venndiagram, gives a total of 6498 genes in total, meaning 54,4 % of all genes compared between the six isolates is part of the core genome (genome shared between all strains). The size of the shell genome, where shell genome is defined as genes shared between two strains or more, was 4758 (or 73,2 %). Cloud genome size, where cloud genome is genes only present in one strains, showed a total of 1740 genes (or 26,8 %).

Of the cloud genome, isolate PAU5 contributed to 530 of those genes, or 30,46 %, making it the largest contribution of unique genes.

Another venndiagram was made, this time with isolates PAU3 and PAU5 to look at the distribution of core and accessory genome (figure 4.7). This was of interest due to the proteomics analysis that would be performed on these two isolates later.

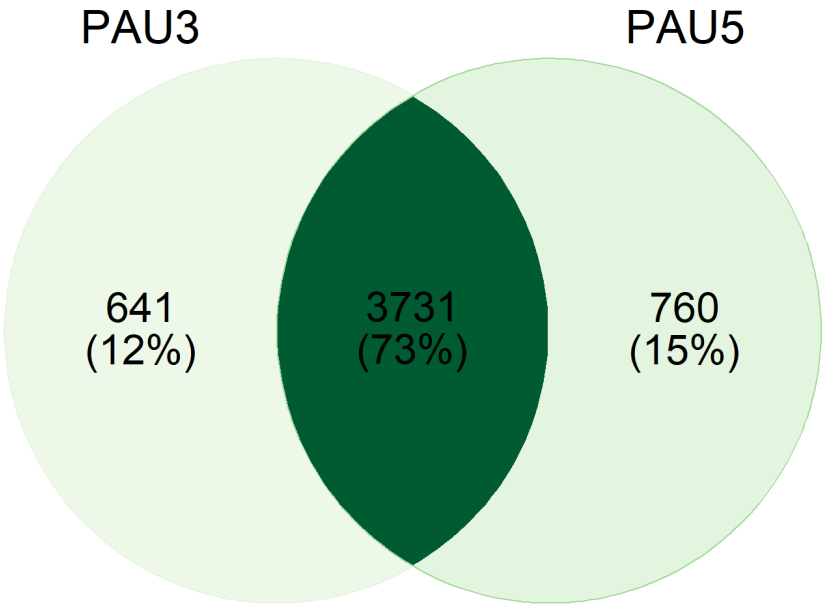

Figure 4.7. Venndiagram PAU3 and PAU5. Distribution of core and accessory genome between isolates PAU3 and PAU5, showcased using ggVennDiagram in R. PAU3 had 641 unique genes (12 % of all genes identified between the two isolates), PAU5 had 760 unique genes (constituting 15 % of all genes identified between the two isolates), and 3731 genes were shared/core genes (which equated to 73 % of all genes identified between the two isolates).

Comparison of genomic content between PAU3 and PAU5 showed that they had 3731 genes in common, which was categorized as the core genome between these two isolates. PAU5 had 760 unique genes, while PAU3 had 641, as illustrated in figure 4.7. Percentages given in the figure are calculated based on total number of genes present between the two. Cloud genome in this venndiagram was 37.6 %, while the core genome was 72.4 % showing that the core genome was larger in this venndiagram compared to the venndiagram containing the six isolates in the figure above (see figure 4.6).

4.5.2 Analysis of Genomic Content

After looking at the difference in genomic size and gene numbers between the six isolates, an analysis of genomic potential (genes present in the genome) was performed. Presence of resistance genes and virulence factors known to be a part of *P. aeruginosa* genome was investigated. Analysis of the genomic contents of the various strains are shown in table 4.7 below, where virulence factors and resistance genes present in the seven clinical isolates is shown. Isolate PAU2 was included in this part as a way of showing what the results of poor sequencing might look like.

Table 4.7. Genomic virulence factors. Genomics virulence factors and resistance genes present, and in which strains they are present. + sign signifies presence in the strain, while - in red color signifies not present in the strain. The most relevant functions of the genes are also denoted, but many of the genes have additional functions not mentioned here.

Virulence factors and other relevant genes	Most relevant functions	PAU1	PAU2	PAU3	PAU4	PAU5	PAU6	PAU7
Exopolysaccharides								
Pel	Biofilm formation, immune evasion, bacterial adhesion	+	+	+	+	+	+	+
Psl	Biofilm formation, immune evasion, bacterial adhesion	+	-	+	+	+	+	+
Alginate	Biofilm formation, immune evasion, bacterial adhesion	+	+	+	+	+	+	+
Siderophores								
Pyochelin (Pch)	Chelates iron, stimulates to growth	+	+	+	+	+	+	+
Pyoverdin	Chelates iron, stimulates to growth, regulation of other virulence factors	+	-	+	+	+	+	+
Proteases								
LasA	Degradation of proteins in host tissue, cause tissue damage	+	+	+	+	+	+	+
Protease IV	Degradation of host proteins involved in immunity against infection	+	+	+	+	+	+	+
Toxin								
Exotoxin A (ExoA/PEA)	Inhibition of protein synthesis within eukaryotic cells leading to cell death	+	+	+	+	-	+	+
Phospholipase C (PLC)	Damage of host cells by degradation of phospholipid backbone	+	+	+	+	+	+	+
Pyocin	A bacteriocin protein part of host interaction but also intraspecific competition	+	+	+	+	+	+	+
Surface structures								
Flagella	Movement, biofilm, adhesion	+	+	+	+	+	+	+
Type IV pilus	Attachment to host cells, movement, biofilm	+	+	+	+	+	+	+
LPS	Resistance against phagocytosis and serum killing, stimulation of host inflammatory response	+	+	+	+	+	+	+
One-step secretion systems								
T1SS	heme uptake, utilization of iron, secretion of proteases	+	+	+	+	+	+	+
T3SS	Injection of effectors into host cells	+	+	+	+	+	+	+
T6SS	Delivery of toxins to neighboring bacteria or host cells, biofilm formation	+	+	+	+	+	+	+
Two-step secretion system								
T2SS	Secretion of lytic enzymes (PLC, protease IV, PEA)	+	+	+	+	+	+	+
T5SS	Secretion of biofilm formation and adhesion proteins	+	+	+	+	+	+	+
Cell-to-cell interaction								
Quorum sensing (QS)	Communal regulation of many genes, i.e. movement or biofilm formation	+	+	+	+	+	+	+
Biofilm	Escape from host immune response, evade antibiotics	+	+	+	+	+	+	+
Various genes								
Putative QS regulated virulence factor	Probably virulence factor expressed upon QS "message"	+	+	+	+	+	+	+
Two-component system	Signal system for quick adaptation to changing environment	+	+	+	+	+	+	+
Porins								
OprD	Carbapenem, β-lactam antibiotics mode of entry, delivery of virulence factors, structural support in biofilm	+	+	+	+	+	+	+
OprF	Involved in QS, biofilm, stabilize OM, necessary for growth in CF sputum (anaerobic)	-	-	-	-	-	-	-
OprH	The smallest porin in *P. aeruginosa*. Involved in polymyxin resistance	-	-	-	-	-	-	-
OprO and OprP	Anion specific porin, import of phosphates	+	+	-	+	+	+	+
Efflux pumps								
MexAB-OprM	Efflux of i.e., β-lactams and fluoroquinolones, constitutively active, often involved in MDR	+	+	+	+	+	+	+
MexCD-OprJ	Efflux of fluoroquinolones and tetracycline, not normally expressed in WT	+	+	+	+	+	+	+
MexEF-OprN	Efflux of fluoroquinolones, and imipenem, regulated by MexT	+	+	+	+	+	+	+
MexXY-OprM	Efflux of aminoglycoside (i.e., TOB), regulated by MexZ	-	-	+	+	+	+	+

The analysis showed that most strains shared the various virulence factors analyzed. Genes involved in biofilm formation (Pel, Psl, and Alginate) were present in all strains, except for PAU2 which did not have any Psl genes. Genes annotated as part of pyochelin pathway or part of regulation of it was present in all strains, while pyoverdin was found in all strains except strain PAU2. Furthermore, proteases such as LasA and protease IV were present in all strains, while AprA or LasB was not present in any of the strains (not included in the table). Looking further down the table, toxins like ExoA was present in all strains except PAU5, while PLC and pyocin was present in all strains. Surface structures, one-step and two-step secretion system, as well as cell-to-cell interaction and two-component systems were present in all strains.

Regarding porins, the OprD porin, important for both entry of carbapenem and β-lactams, was present in all strains, while the OprF and OprH porins on the other hand were not present in any strains. Anion specific porins OprO and OprP were present in all strains except PAU3.

Several efflux pumps were identified, and starting with the constitutively active MexAB-OprM efflux pump that is often involved in MDR, this was seen in all strains. MexCD-OprJ, which is not normally expressed in wild-type (environmental) strains of the bacterium was also present in all strains. This efflux pump is largely involved in efflux of fluoroquinolones, which the strains were subjected to during MIC (the fluoroquinolone Ciprofloxacin). MexEF-OprN, also involved in fluoroquinolone efflux, was also present in all strains. This efflux pump is positively regulated by the gene MexT, which additionally acts as a repressor of OprD transcription, resulting in lowered carbapenem and β-lactam uptake. The last efflux pump investigated, was the MexXY-OprM. Neither strain PAU1 nor PAU2 possessed this efflux pump, but in the 5 other strains this efflux pump was identified. MexXY-OprM is important for efflux of aminoglycosides such as tobramycin, and is regulated by MexZ. The MexZ has been seen to accumulate mutations in cystic fibrosis patients, where mutations lead to loss of MexXY-OprM repression, resulting in increased resistance towards aminoglycosides (e.g., Tobramycin).

Table 4.8. Number of hits on systems/virulence factors. System and virulence factors that stood out as different in number of hits in the different strains. The numbers are number of gene hits present in each strain. T6SS = Type VI secretion system.

Systems and/or virulence factors	PAU1	PAU2	PAU3	PAU4	PAU5	PAU6	PAU7
Two-component regulatory system	110	88	108	107	99	113	109
T6SS	51	51	54	54	50	53	53
Flagella	45	43	44	44	33	44	45
Alginate	11	6	13	13	11	12	12

Table 4.8 shows that there was a difference in the number of identified genes between isolates. Genes identified as involved in two-component regulatory system (TCS) varied the most out of the four systems and virulence factors searched for. PAU2 had an overall low number of hits for all the different searches. Type VI secretion system (T6SS) in PAU2 was identical to PAU1, but both TCS, Flagella, and Alginate showed fewer hits in PAU2 than for the rest of the clinical strains. PAU6 had the highest number of TCS, but the lowest number of T6SS. PAU5 had the lowest amount of genes annotated as involved in flagellar systems.

The system out of the four listed in table 4.8 that was most homogeneous in number across all clinical strains was the T6SS, with the highest number of identified genes being 54 and the lowest being 50.

4.5.3 Sequence Alignment of Class C β-lactamase, GyrA, and ParC

After investigating the genomic potential, three genes encoding proteins often involved in resistance had been identified. This was the class C β-lactamase responsible for resistance against β-lactam antibiotics. Next, genes encoding GyrA and ParC, which are often involved in fluoroquinolone resistance was investigated. These three genes were picked based on results obtained from MIC, where differences between isolates had been identified. Results from the multiple alignment of these three genes is explained and showed below.

β-lactamase

The first multiple sequence alignment (MSA) looked at, was that of the β-lactamase class C gene which was identified in all strains. Alignment program used was ClustalL provided by EMBL-EBI [157], and sequence for PAO1 (ATCC15692) was obtained from www.uniprot.org. Alignment is shown in figure 4.8 below.

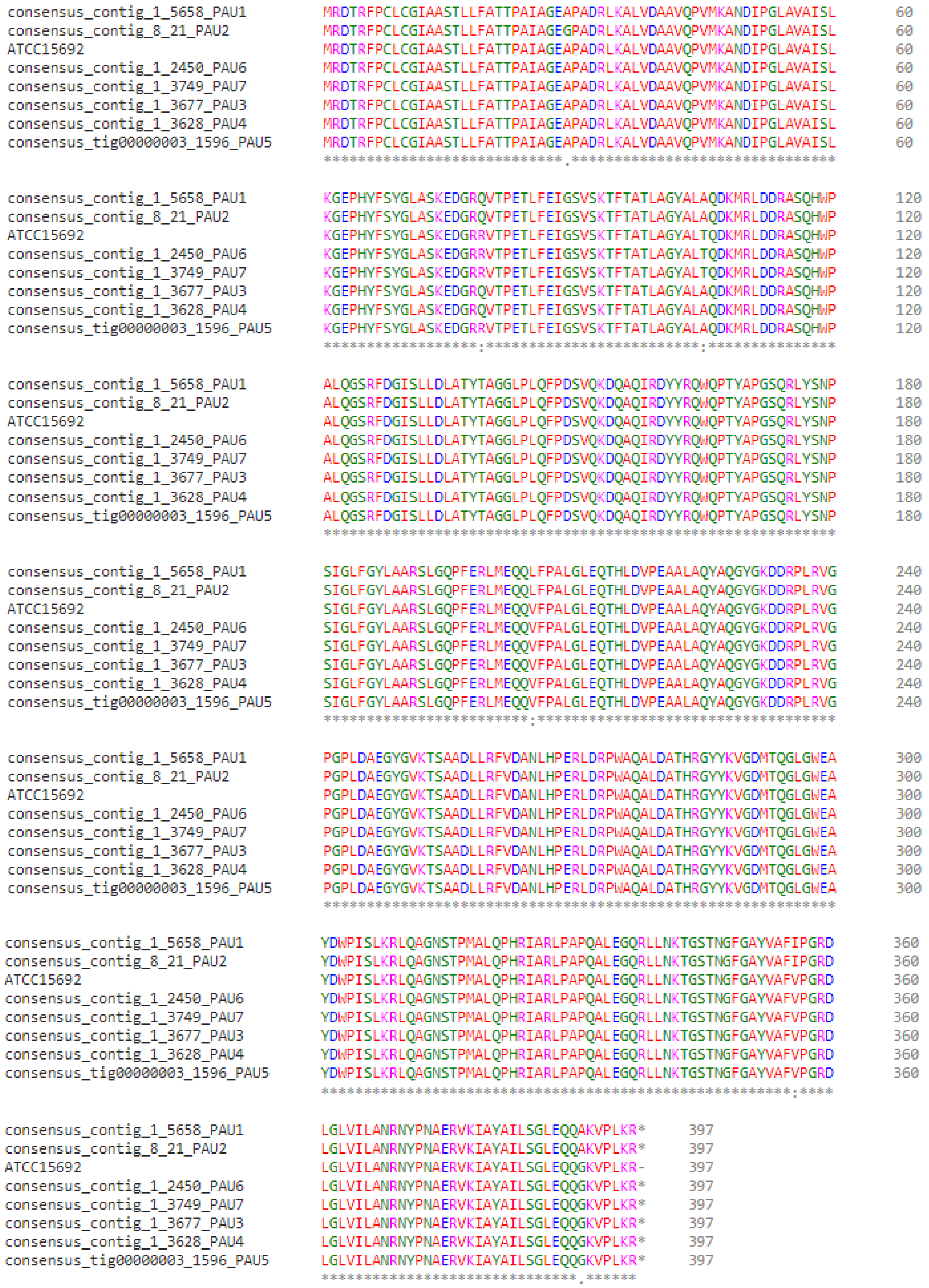

Figure 4.8. Multiple sequence alignment of β-lactamase. Multiple sequence alignment performed on the identified β-lactamase class C gene from all isolates, as well as a laboratory strain obtained from Uniprot.org. Identification of each isolate is shown on the left handside of the figure. Deviations are marked with either **.** or **:**.

Alignment method used was ClustalL 0(1.2.4). PAU2, which did not yield reliable sequencing results, had mutations at 5 positions (further underscoring its unreliability). In total, there were 6 point mutations in the alignment. β-lactamases are genes known for accumulating mutations quickly due to antibiotic exposure, so seeing 5 point mutations in this alignment makes sense based on prior knowledge about the gene [43]. The first point mutations showed PAU2 having the hydrophobic amino acid glycine (G), where the other isolates/strains had the hydrophobic acid alanine (A). The second point mutation was at position 79, which revealed half of the strains containing a positively charged arginine (R) (PAU5, PAU6, PAU7, and ATCC15692), while the other half of the strains contained the polar amino acid glutamine (Q) (PAU1, PAU2, PAU3, and PAU4). The next mutated site was the hydrophobic amino acid alanine (A) substituted for the polar amino acid threonine (T), where ATCC15692, PAU6, and PAU7 had a T instead of an A. Going from a hydrophobic amino acid to a polar could have large consequences in terms of 3-dimensional structure of the folded protein.

The next mutated site was a mutation in PAU1 and PAU2. The other strains had the hydrophobic amino acid valine (V), while PAU1 and PAU2 had another hydrophobic amino acid, leucine (L). The next position where mutation had happened was at position 356, where PAU1 and PAU2 had undergone a substitution from the hydrophobic amino acid V to another hydrophobic amino acid, isoleucine (I). Lastly, at position 391 PAU1 and PAU2 had, again, undergone a mutation from the hydrophobic amino acid glycine (G) to an A.

GyrA

The second MSA looked at, was the sequences of the GyrA gene (figure 4.5). This is a topoisomerase involved in negative supercoiling of the dsDNA, and substitutions in the sequence might lead to ciprofloxacin resistance, because this is the target of the antibiotic. GyrA often undergoes a mutation at position 83 from the polar amino acid Threonine (T), to the hydrophobic amino acid Isoleucine (I) [1]. This is the most common mutation in both CF and non-CF isolates, and it is a mutation often found in cystic fibrosis patients suffering from a *P. aeruginosa* infection after prolonged treatment of the antibiotic Ciprofloxacin [1]. The mutation was present in the GyrA gene of PAU2, but none of the other strains.

```
consensus_tig00000003_590_PAU5      MGELAKEILPVNIEDELKQSYLDYAMSVIVGRALPDARDGLKPVHRRVLYAMSELGNDWN      60
consensus_contig_17_1234_PAU2       MGELAKEILPVNIEDELKQSYLDYAMSVIVGRALPDARDGLKPVHRRVLYAMSELGNDWN      60
sp|P48372|_ATCC15692                MGELAKEILPVNIEDELKQSYLDYAMSVIVGRALPDARDGLKPVHRRVLYAMSELGNDWN      60
consensus_contig_1_4639_PAU1        MGELAKEILPVNIEDELKQSYLDYAMSVIVGRALPDARDGLKPVHRRVLYAMSELGNDWN      60
consensus_contig_1_2732_PAU3        MGELAKEILPVNIEDELKQSYLDYAMSVIVGRALPDARDGLKPVHRRVLYAMSELGNDWN      60
consensus_contig_1_4583_PAU4        MGELAKEILPVNIEDELKQSYLDYAMSVIVGRALPDARDGLKPVHRRVLYAMSELGNDWN      60
consensus_contig_1_3425_PAU6        MGELAKEILPVNIEDELKQSYLDYAMSVIVGRALPDARDGLKPVHRRVLYAMSELGNDWN      60
consensus_contig_1_2746_PAU7        MGELAKEILPVNIEDELKQSYLDYAMSVIVGRALPDARDGLKPVHRRVLYAMSELGNDWN      60
                                    ************************************************************

consensus_tig00000003_590_PAU5      KPYKKSARVVGDVIGKYHPHGDTAVYDTIVRMAQPFSLRYMLVDGQGNFGSVDGDNAAAM      120
consensus_contig_17_1234_PAU2       KPYKKSARVVGDVIGKYHPHGDIAVYDTIVRMAQPFSLRYMLVDGQGNFGSVDGDNAAAM      120
sp|P48372|_ATCC15692                KPYKKSARVVGDVIGKYHPHGDTAVYDTIVRMAQPFSLRYMLVDGQGNFGSVDGDNAAAM      120
consensus_contig_1_4639_PAU1        KPYKKSARVVGDVIGKYHPHGDTAVYDTIVRMAQPFSLRYMLVDGQGNFGSVDGDNAAAM      120
consensus_contig_1_2732_PAU3        KPYKKSARVVGDVIGKYHPHGDTAVYDTIVRMAQPFSLRYMLVDGQGNFGSVDGDNAAAM      120
consensus_contig_1_4583_PAU4        KPYKKSARVVGDVIGKYHPHGDTAVYDTIVRMAQPFSLRYMLVDGQGNFGSVDGDNAAAM      120
consensus_contig_1_3425_PAU6        KPYKKSARVVGDVIGKYHPHGDTAVYDTIVRMAQPFSLRYMLVDGQGNFGSVDGDNAAAM      120
consensus_contig_1_2746_PAU7        KPYKKSARVVGDVIGKYHPHGDTAVYDTIVRMAQPFSLRYMLVDGQGNFGSVDGDNAAAM      120
                                    ********************* ************************************

consensus_tig00000003_590_PAU5      RYTEVRMAKLAHELLADLEKETVDWVPNYDGTEQIPAVMPTKIPNLLVNGSSGIAVGMAT      180
consensus_contig_17_1234_PAU2       RYTEVRMAKLAHELLADLEKETVDWVPNYDGTEQIPAVMPTKIPNLLVNGSSGIAVGMAT      180
sp|P48372|_ATCC15692                RYTEVRMAKLAHELLADLEKETVDWVPNYDGTEQIPAVMPTKIPNLLVNGSSGIAVGMAT      180
consensus_contig_1_4639_PAU1        RYTEVRMAKLAHELLADLEKETVDWVPNYDGTEQIPAVMPTKIPNLLVNGSSGIAVGMAT      180
consensus_contig_1_2732_PAU3        RYTEVRMAKLAHELLADLEKETVDWVPNYDGTEQIPAVMPTKIPNLLVNGSSGIAVGMAT      180
consensus_contig_1_4583_PAU4        RYTEVRMAKLAHELLADLEKETVDWVPNYDGTEQIPAVMPTKIPNLLVNGSSGIAVGMAT      180
consensus_contig_1_3425_PAU6        RYTEVRMAKLAHELLADLEKETVDWVPNYDGTEQIPAVMPTKIPNLLVNGSSGIAVGMAT      180
consensus_contig_1_2746_PAU7        RYTEVRMAKLAHELLADLEKETVDWVPNYDGTEQIPAVMPTKIPNLLVNGSSGIAVGMAT      180
                                    ************************************************************

consensus_tig00000003_590_PAU5      NIPPHNLGEVIDGCLALMDNPDLTVDELMQYIPGPDFPTAGIINGRAGIIEAYRTGRGRI      240
consensus_contig_17_1234_PAU2       NIPPHNLGEVIDGCLALMDNPDLTVDELMQYIPGPDFPTAGIINGRAGIIEAYRTGRGRI      240
sp|P48372|_ATCC15692                NIPPHNLGEVIDGCLALMDNPDLTVDELMQYIPGPDFPTAGIINGRAGIIEAYRTGRGRI      240
consensus_contig_1_4639_PAU1        NIPPHNLGEVIDGCLALMDNPDLTVDELMQYIPGPDFPTAGIINGRAGIIEAYRTGRGRI      240
consensus_contig_1_2732_PAU3        NIPPHNLGEVIDGCLALMDNPDLTVDELMQYIPGPDFPTAGIINGRAGIIEAYRTGRGRI      240
consensus_contig_1_4583_PAU4        NIPPHNLGEVIDGCLALMDNPDLTVDELMQYIPGPDFPTAGIINGRAGIIEAYRTGRGRI      240
consensus_contig_1_3425_PAU6        NIPPHNLGEVIDGCLALMDNPDLTVDELMQYIPGPDFPTAGIINGRAGIIEAYRTGRGRI      240
consensus_contig_1_2746_PAU7        NIPPHNLGEVIDGCLALMDNPDLTVDELMQYIPGPDFPTAGIINGRAGIIEAYRTGRGRI      240
                                    ************************************************************

consensus_tig00000003_590_PAU5      YIRARAVVEEMEKGGGREQIIITELPYQLNKARLIEKIAELVKEKKIEGISELRDESDKD      300
consensus_contig_17_1234_PAU2       YIRARAVVEEMEKGGGREQIIITELPYQLNKARLIEKIAELVKEKKIEGISELRDESDKD      300
sp|P48372|_ATCC15692                YIRARAVVEEMEKGGGREQIIITELPYQLNKARLIEKIAELVKEKKIEGISELRDESDKD      300
consensus_contig_1_4639_PAU1        YIRARAVVEEMEKGGGREQIIITELPYQLNKARLIEKIAELVKEKKIEGISELRDESDKD      300
consensus_contig_1_2732_PAU3        YIRARAVVEEMEKGGGREQIIITELPYQLNKARLIEKIAELVKEKKIEGISELRDESDKD      300
consensus_contig_1_4583_PAU4        YIRARAVVEEMEKGGGREQIIITELPYQLNKARLIEKIAELVKEKKIEGISELRDESDKD      300
consensus_contig_1_3425_PAU6        YIRARAVVEEMEKGGGREQIIITELPYQLNKARLIEKIAELVKEKKIEGISELRDESDKD      300
consensus_contig_1_2746_PAU7        YIRARAVVEEMEKGGGREQIIITELPYQLNKARLIEKIAELVKEKKIEGISELRDESDKD      300
                                    ************************************************************

consensus_tig00000003_590_PAU5      GMRVVIELRRGEVGEVVLNNLYAQTQLQSVFGINVVALVDGQPRTLNLKDMLEVFVRHRR      360
consensus_contig_17_1234_PAU2       GMRVVIELRRGEVGEVVLNNLYAQTQLQSVFGINVVALVDGQPRTLNLKDMLEVFVRHRR      360
sp|P48372|_ATCC15692                GMRVVIELRRGEVGEVVLNNLYAQTQLQSVFGINVVALVDGQPRTLNLKDMLEVFVRHRR      360
consensus_contig_1_4639_PAU1        GMRVVIELRRGEVGEVVLNNLYAQTQLQSVFGINVVALVDGQPRTLNLKDMLEVFVRHRR      360
consensus_contig_1_2732_PAU3        GMRVVIELRRGEVGEVVLNNLYAQTQLQSVFGINVVALVDGQPRTLNLKDMLEVFVRHRR      360
consensus_contig_1_4583_PAU4        GMRVVIELRRGEVGEVVLNNLYAQTQLQSVFGINVVALVDGQPRTLNLKDMLEVFVRHRR      360
consensus_contig_1_3425_PAU6        GMRVVIELRRGEVGEVVLNNLYAQTQLQSVFGINVVALVDGQPRTLNLKDMLEVFVRHRR      360
consensus_contig_1_2746_PAU7        GMRVVIELRRGEVGEVVLNNLYAQTQLQSVFGINVVALVDGQPRTLNLKDMLEVFVRHRR      360
                                    ************************************************************

consensus_tig00000003_590_PAU5      EVVTRRTVYELRKARERGHILEGQAVALSNIDPVIELIKSSPTPAEAKERLIATAWESSA      420
consensus_contig_17_1234_PAU2       EVVTRRTVYELRKARERGHILEGQAVALSNIDPVIELIKSSPTPAEAKERLIATAWESSA      420
sp|P48372|_ATCC15692                EVVTRRTVYELRKARERGHILEGQAVALSNIDPVIELIKSSPTPAEAKERLIATAWESSA      420
consensus_contig_1_4639_PAU1        EVVTRRTVYELRKARERGHILEGQAVALSNIDPVIELIKSSPTPAEAKERLIATAWESSA      420
consensus_contig_1_2732_PAU3        EVVTRRTVYELRKARERGHILEGQAVALSNIDPVIELIKSSPTPAEAKERLIATAWESSA      420
consensus_contig_1_4583_PAU4        EVVTRRTVYELRKARERGHILEGQAVALSNIDPVIELIKSSPTPAEAKERLIATAWESSA      420
consensus_contig_1_3425_PAU6        EVVTRRTVYELRKARERGHILEGQAVALSNIDPVIELIKSSPTPAEAKERLIATAWESSA      420
consensus_contig_1_2746_PAU7        EVVTRRTVYELRKARERGHILEGQAVALSNIDPVIELIKSSPTPAEAKERLIATAWESSA      420
                                    ************************************************************

consensus_tig00000003_590_PAU5      VEAMVERAGADACRPEDLDPQYGLRDGKYYLSPEQAQAILELRLHRLTGLEHEKLLSEYQ      480
consensus_contig_17_1234_PAU2       VEAMVERAGADACRPEDLDPQYGLRDGKYYLSPEQAQAILELRLHRLTGLEHEKLLSEYQ      480
sp|P48372|_ATCC15692                VEAMVERAGADACRPEDLDPQYGLRDGKYYLSPEQAQAILELRLHRLTGLEHEKLLSEYQ      480
consensus_contig_1_4639_PAU1        VEAMVERAGADACRPEDLDPQYGLRDGKYYLSPEQAQAILELRLHRLTGLEHEKLLSEYQ      480
consensus_contig_1_2732_PAU3        VEAMVERAGADACRPEDLDPQYGLRDGKYYLSPEQAQAILELRLHRLTGLEHEKLLSEYQ      480
consensus_contig_1_4583_PAU4        VEAMVERAGADACRPEDLDPQYGLRDGKYYLSPEQAQAILELRLHRLTGLEHEKLLSEYQ      480
consensus_contig_1_3425_PAU6        VEAMVERAGADACRPEDLDPQYGLRDGKYYLSPEQAQAILELRLHRLTGLEHEKLLSEYQ      480
consensus_contig_1_2746_PAU7        VEAMVERAGADACRPEDLDPQYGLRDGKYYLSPEQAQAILELRLHRLTGLEHEKLLSEYQ      480
                                    ************************************************************
```

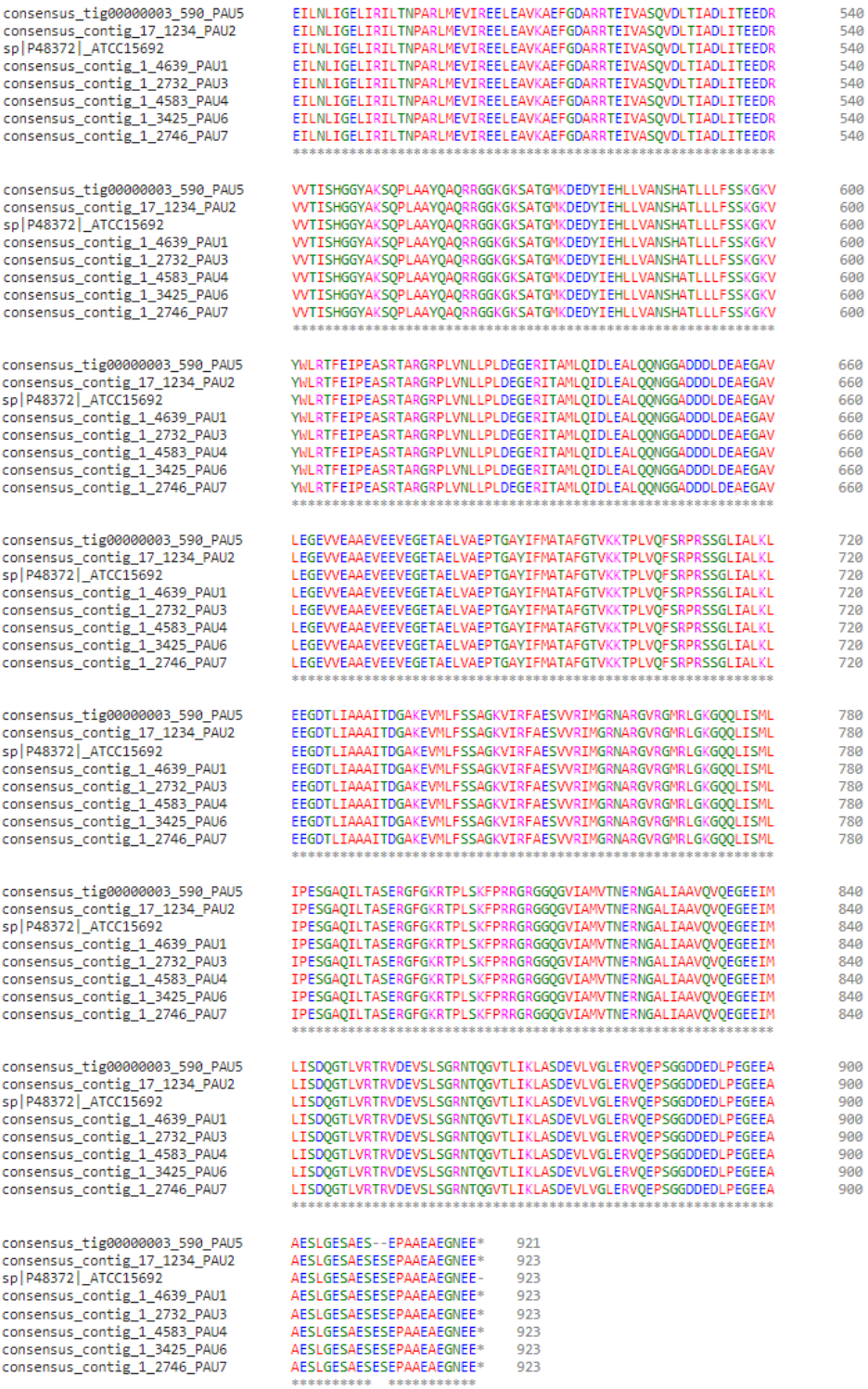

Figure 4.5. Alignment of GyrA sequences. Alignment of the sequence of DNA gyrase subunit A (GyrA), where a Thr83Ile substitution is common in resistant strains. Only PAU2 showed the common mutation in position 83 from a Threonine (T) to an Isoleucine (I). Strains are aligned against the laboratory strain ATCC15692, where sequence was obtained from uniprot.org by searching "GyrA AND pseudomonas aeruginosa".

Figure 4.5 shows the entire sequence alignment of DNA gyrase subunit A, a gene that often undergoes mutational changes in order to increase tolerability of DNA gyrase-acting antibiotics, or even facilitate resistance against them. The DNA gyrase-acting antibiotic used in this thesis was Ciprofloxacin (CIP). Thr83Ile substitution has been shown to be the primary mechanism of CIP resistance [158]. This substitution is important for the binding of Ciprofloxacin to DNA gyrase, with the substitution leading to drastically lowered affinity between DNA gyrase and the antibiotic [1]. When this mutation is combined with a mutation in the ParC, which is also the target of CIP, resistance levels are increased even more compared to only having mutations at one of the two genes. ParC alignment is discussed below.

ParC

The last MSA that was performed, was that of the topoisomerase IV subunit A (ParC) gene (figure 4.6) which is a gene encoding a protein involved in transcription, and specifically chromosome segregation of DNA strands by relaxing supercoiled DNA. Substitutions in the sequence is often involved fluoroquinolone resistance, and fluoroquinolones target both GyrA and ParC proteins.

```
consensus_contig_7_312_PAU2          MSESLDLSLEGVERRSLAEFTEQAYLNYSMYVIMDRALPHIGDGLKPVQRRIVYAMSELG   60
consensus_contig_1_2081_PAU4         MSESLDLSLEGVERRSLAEFTEQAYLNYSMYVIMDRALPHIGDGLKPVQRRIVYAMSELG   60
consensus_contig_1_5218_PAU3         MSESLDLSLEGVERRSLAEFTEQAYLNYSMYVIMDRALPHIGDGLKPVQRRIVYAMSELG   60
consensus_tig00000003_1821_PAU5      MSESLDLSLEGVERRSLAEFTEQAYLNYSMYVIMDRALPHIGDGLKPVQRRIVYAMSELG   60
consensus_contig_1_5220_PAU7         MSESLDLSLEGVERRSLAEFTEQAYLNYSMYVIMDRALPHIGDGLKPVQRRIVYAMSELG   60
sp|Q9HUK1_ATCC15692                  MSESLDLSLEGVERRSLAEFTEQAYLNYSMYVIMDRALPHIGDGLKPVQRRIVYAMSELG   60
consensus_contig_1_1280_PAU1         MSESLDLSLEGVERRSLAEFTEQAYLNYSMYVIMDRALPHIGDGLKPVQRRIVYAMSELG   60
consensus_contig_1_828_PAU6          MSESLDLSLEGVERRSLAEFTEQAYLNYSMYVIMDRALPHIGDGLKPVQRRIVYAMSELG   60
                                     ************************************************************

consensus_contig_7_312_PAU2          LDADSKHKKSARTVGDVLGKFHPHGDSACYEAMVLMAQPFSYRYPLVDGQGNWGAPDDPK   120
consensus_contig_1_2081_PAU4         LDADSKHKKSARTVGDVLGKFHPHGDSACYEAMVLMAQPFSYRYPLVDGQGNWGAPDDPK   120
consensus_contig_1_5218_PAU3         LDADSKHKKSARTVGDVLGKFHPHGDSACYEAMVLMAQPFSYRYPLVDGQGNWGAPDDPK   120
consensus_tig00000003_1821_PAU5      LDADSKHKKSARTVGDVLGKFHPHGDSACYEAMVLMAQPFSYRYPLVDGQGNWGAPDDPK   120
consensus_contig_1_5220_PAU7         LDADSKHKKSARTVGDVLGKFHPHGDSACYEAMVLMAQPFSYRYPLVDGQGNWGAPDDPK   120
sp|Q9HUK1_ATCC15692                  LDADSKHKKSARTVGDVLGKFHPHGDSACYEAMVLMAQPFSYRYPLVDGQGNWGAPDDPK   120
consensus_contig_1_1280_PAU1         LDADSKHKKSARTVGDVLGKFHPHGDSACYEAMVLMAQPFSYRYPLVDGQGNWGAPDDPK   120
consensus_contig_1_828_PAU6          LDADSKHKKSARTVGDVLGKFHPHGDSACYEAMVLMAQPFSYRYPLVDGQGNWGAPDDPK   120
                                     ************************************************************

consensus_contig_7_312_PAU2          SFAAMRYTEARLSRYSEVLLSELGQGTVDWVPNFDGTLDEPAVLPARLPNLLLNGTTGIA   180
consensus_contig_1_2081_PAU4         SFAAMRYTEARLSRYSEVLLSELGQGTVDWVPNFDGTLDEPAVLPARLPNLLLNGTTGIA   180
consensus_contig_1_5218_PAU3         SFAAMRYTEARLSRYSEVLLSELGQGTVDWVPNFDGTLDEPAVLPARLPNLLLNGTTGIA   180
consensus_tig00000003_1821_PAU5      SFAAMRYTEARLSRYSEVLLSELGQGTVDWVPNFDGTLDEPAVLPARLPNLLLNGTTGIA   180
consensus_contig_1_5220_PAU7         SFAAMRYTEARLSRYSEVLLSELGQGTVDWVPNFDGTLDEPAVLPARLPNLLLNGTTGIA   180
sp|Q9HUK1_ATCC15692                  SFAAMRYTEARLSRYSEVLLSELGQGTVDWVPNFDGTLDEPAVLPARLPNLLLNGTTGIA   180
consensus_contig_1_1280_PAU1         SFAAMRYTEARLSRYSEVLLSELGQGTVDWVPNFDGTLDEPAVLPARLPNLLLNGTTGIA   180
consensus_contig_1_828_PAU6          SFAAMRYTEARLSRYSEVLLSELGQGTVDWVPNFDGTLDEPAVLPARLPNLLLNGTTGIA   180
                                     ************************************************************

consensus_contig_7_312_PAU2          VGMATDVPPHNLREVASACVRLLDQPGATVAELCEHVPGPDFPTEAEIITPRADLQKVYE   240
consensus_contig_1_2081_PAU4         VGMATDVPPHNLREVASACVRLLDQPGATVAELCEHVPGPDFPTEAEIITPRADLQKVYE   240
consensus_contig_1_5218_PAU3         VGMATDVPPHNLREVASACVRLLDQPGATVAELCEHVPGPDFPTEAEIITPRADLQKVYE   240
consensus_tig00000003_1821_PAU5      VGMATDVPPHNLREVASACVRLLDQPGATVAELCEHVPGPDFPTEAEIITPRADLQKVYE   240
consensus_contig_1_5220_PAU7         VGMATDVPPHNLREVASACVRLLDQPGATVAELCEHVPGPDFPTEAEIITPRADLQKVYE   240
sp|Q9HUK1_ATCC15692                  VGMATDVPPHNLREVASACVRLLDQPGATVAELCEHVPGPDFPTEAEIITPRADLQKVYE   240
consensus_contig_1_1280_PAU1         VGMATDVPPHNLREVASACVRLLDQPGATVAELCEHVPGPDFPTEAEIITPRADLQKVYE   240
consensus_contig_1_828_PAU6          VGMATDVPPHNLREVASACVRLLDQPGATVAELCEHVPGPDFPTEAEIITPRADLQKVYE   240
                                     ************************************************************

consensus_contig_7_312_PAU2          TGRGSVRMRAVYRVEDGDIVIHALPHQVSGSKVLEQIAGQMQAKKLPMVADLRDESDHEN   300
consensus_contig_1_2081_PAU4         TGRGSVRMRAVYRVEDGDIVIQALPHQVSGSKVLEQIAGQMQAKKLPMVADLRDESDHEN   300
consensus_contig_1_5218_PAU3         TGRGSVRMRAVYRVEDGDIVIQALPHQVSGSKVLEQIAGQMQAKKLPMVADLRDESDHEN   300
consensus_tig00000003_1821_PAU5      TGRGSVRMRAVYRVEDGDIVIQALPHQVSGSKVLEQIAGQMQAKKLPMVADLRDESDHEN   300
consensus_contig_1_5220_PAU7         TGRGSVRMRAVYRVEDGDIVIHALPHQVSGSKVLEQIAGQMQAKKLPMVADLRDESDHEN   300
sp|Q9HUK1_ATCC15692                  TGRGSVRMRAVYRVEDGDIVIHALPHQVSGSKVLEQIAGQMQAKKLPMVADLRDESDHEN   300
consensus_contig_1_1280_PAU1         TGRGSVRMRAVYRVEDGDIVIHALPHQVSGSKVLEQIAGQMQAKKLPMVADLRDESDHEN   300
consensus_contig_1_828_PAU6          TGRGSVRMRAVYRVEDGDIVIHALPHQVSGSKVLEQIAGQMQAKKLPMVADLRDESDHEN   300
                                     ********************:***************************************

consensus_contig_7_312_PAU2          PTRIVIIPRSNRVDVEELMTHLFATTDLETSYRVNLNIIGLDGKPQVKDLRQLLSEWLQF   360
consensus_contig_1_2081_PAU4         PTRIVIIPRSNRVDVEELMTHLFATTDLETSYRVNLNIIGLDGKPQVKDLRQLLSEWLQF   360
consensus_contig_1_5218_PAU3         PTRIVIIPRSNRVDVEELMTHLFATTDLETSYRVNLNIIGLDGKPQVKDLRQLLSEWLQF   360
consensus_tig00000003_1821_PAU5      PTRIVIIPRSNRVDVEELMTHLFATTDLETSYRVNLNIIGLDGKPQVKDLRQLLSEWLQF   360
consensus_contig_1_5220_PAU7         PTRIVIIPRSNRVDVEELMTHLFATTDLETSYRVNLNIIGLDGKPQVKDLRQLLSEWLQF   360
sp|Q9HUK1_ATCC15692                  PTRIVIIPRSNRVDVEELMTHLFATTDLETSYRVNLNIIGLDGKPQVKDLRQLLSEWLQF   360
consensus_contig_1_1280_PAU1         PTRIVIIPRSNRVDVEELMTHLFATTDLETSYRVNLNIIGLDGKPQVKDLRQLLSEWLQF   360
consensus_contig_1_828_PAU6          PTRIVIIPRSNRVDVEELMTHLFATTDLETSYRVNLNIIGLDGKPQVKDLRQLLSEWLQF   360
                                     ************************************************************

consensus_contig_7_312_PAU2          RIGTVRRRLQFRLDKVERRLHLLDGLLIAFLNLDEVIHIIRTEDQPKAVLMERFELSEVQ   420
consensus_contig_1_2081_PAU4         RIGTVRRRLQFRLDKVERRLHLLDGLLIAFLNLDEVIHIIRTEDQPKAVLMERFELSEVQ   420
consensus_contig_1_5218_PAU3         RIGTVRRRLQFRLDKVERRLHLLDGLLIAFLNLDEVIHIIRTEDQPKAVLMERFELSEVQ   420
consensus_tig00000003_1821_PAU5      RIGTVRRRLQFRLDKVERRLHLLDGLLIAFLNLDEVIHIIRTEDQPKAVLMERFELSEVQ   420
consensus_contig_1_5220_PAU7         RIGTVRRRLQFRLDKVERRLHLLDGLLIAFLNLDEVIHIIRTEDQPKAVLMERFELSEVQ   420
sp|Q9HUK1_ATCC15692                  RIGTVRRRLQFRLDKVERRLHLLDGLLIAFLNLDEVIHIIRTEDQPKAVLMERFELSEVQ   420
consensus_contig_1_1280_PAU1         RIGTVRRRLQFRLDKVERRLHLLDGLLIAFLNLDEVIHIIRTEDQPKAVLMERFELSEVQ   420
consensus_contig_1_828_PAU6          RIGTVRRRLQFRLDKVERRLHLLDGLLIAFLNLDEVIHIIRTEDQPKAVLMERFELSEVQ   420
                                     ************************************************************

consensus_contig_7_312_PAU2          ADYILDTRLRQLARLEEMKIRGEQEELLKEQKRLQTLLGSEAKLKKLVREELIKDAETYG   480
consensus_contig_1_2081_PAU4         ADYILDTRLRQLARLEEMKIRGEQEELLKEQKRLQTLLGSEAKLKKLVREELIKDAETYG   480
consensus_contig_1_5218_PAU3         ADYILDTRLRQLARLEEMKIRGEQEELLKEQKRLQTLLGSEAKLKKLVREELIKDAETYG   480
consensus_tig00000003_1821_PAU5      ADYILDTRLRQLARLEEMKIRGEQEELLKEQKRLQTLLGSEAKLKKLVREELIKDAETYG   480
consensus_contig_1_5220_PAU7         ADYILDTRLRQLARLEEMKIRGEQEELLKEQKRLQTLLGSEAKLKKLVREELIKDAETYG   480
sp|Q9HUK1_ATCC15692                  ADYILDTRLRQLARLEEMKIRGEQEELLKEQKRLQTLLGSEAKLKKLVREELIKDAETYG   480
consensus_contig_1_1280_PAU1         ADYILDTRLRQLARLEEMKIRGEQEELLKEQKRLQTLLGSEAKLKKLVREELIKDAETYG   480
consensus_contig_1_828_PAU6          ADYILDTRLRQLARLEEMKIRGEQEELLKEQKRLQTLLGSEAKLKKLVREELIKDAETYG   480
                                     ************************************************************
```

```
consensus_contig_7_312_PAU2        DDRRSPIVARAEARALSETELMPTEPVTVVLSEKGWVRCAKGHDIDAAGLSYKAGDGFKA   540
consensus_contig_1_2081_PAU4       DDRRSPIVARAEARALSETELMPTEPVTVVLSEKGWVRCAKGHDIDAAGLSYKAGDGFKA   540
consensus_contig_1_5218_PAU3       DDRRSPIVARAEARALSETELMPTEPVTVVLSEKGWVRCAKGHDIDAAGLSYKAGDGFKA   540
consensus_tig00000003_1821_PAU5    DDRRSPIVARAEARALSETELMPTEPVTVVLSEKGWVRCAKGHDIDAAGLSYKAGDGFKA   540
consensus_contig_1_5220_PAU7       DDRRSPIVARAEARALSETELMPTEPVTVVLSEKGWVRCAKGHDIDAAGLSYKAGDGFKA   540
sp|Q9HUK1_ATCC15692                DDRRSPIVARAEARALSETELMPTEPVTVVLSEKGWVRCAKGHDIDAAGLSYKAGDGFKA   540
consensus_contig_1_1280_PAU1       DDRRSPIVARAEARALSETELMPTEPVTVVLSEKGWVRCAKGHDIDAAGLSYKAGDGFKA   540
consensus_contig_1_828_PAU6        DDRRSPIVARAEARALSETELMPTEPVTVVLSEKGWVRCAKGHDIDAAGLSYKAGDGFKA   540
                                   ************************************************************

consensus_contig_7_312_PAU2        AAPGRSNQYAVFIDSTGRSYSLPAHSLPSARGQGEPLSGRLTPPPGASFECVLLPDDDAL   600
consensus_contig_1_2081_PAU4       AAPGRSNQYAVFIDSTGRSYSLPAHSLPSARGQGEPLSGRLTPPPGAASNACCCRTTMHC   600
consensus_contig_1_5218_PAU3       AAPGRSNQYAVFIDSTGRSYSLPAHSLPSARGQGEPLSGRLTPPPGASFECVLLPDDDAL   600
consensus_tig00000003_1821_PAU5    AAPGRSNQYAVFIDSTGRSYSLPAHSLPSARGQGEPLSGRLTPPPGASFECVLLPDDDAL   600
consensus_contig_1_5220_PAU7       AAPGRSNQYAVFIDSTGRSYSLPAHSLPSARGQGEPLSGRLTPPPGASFECVLLPDDDAL   600
sp|Q9HUK1_ATCC15692                AAPGRSNQYAVFIDSTGRSYSLPAHSLPSARGQGEPLSGRLTPPPGASFECVLLPDDDAL   600
consensus_contig_1_1280_PAU1       AAPGRSNQYAVFIDSTGRSYSLPAHSLPSARGQGEPLSGRLTPPPGASFECVLLPDDDAL   600
consensus_contig_1_828_PAU6        AAPGRSNQYAVFIDSTGRSYSLPAHSLPSARGQGEPLSGRLTPPPGASFECVLLPDDDAL   600
                                   ***********************************************: :.

consensus_contig_7_312_PAU2        FVIASDAGYGFVVKGEDLQAKNKAGKALLSLPNGSAVVAPRPVRDVEQDWLAAVTTEGRL   660
consensus_contig_1_2081_PAU4       S*----------------------------------------------------------   601
consensus_contig_1_5218_PAU3       FVIASDAGYGFVVKGEDLQAKNKAGKALLSLPNGSAVVAPRPVRDVEQDWLAAVTTEGRL   660
consensus_tig00000003_1821_PAU5    FVIASDAGYGFVVKGEDLQAKNKAGKALLSLPNGSAVVAPRPVRDVEQDWLAAVTTEGRL   660
consensus_contig_1_5220_PAU7       FVIASDAGYGFVVKGEDLQAKNKAGKALLSLPSGSAVVAPRPVRDVEQDWLAAVTTEGRL   660
sp|Q9HUK1_ATCC15692                FVIASDAGYGFVVKGEDLQAKNKAGKALLSLPNGSAVVAPRPVRDVEQDWLAAVTTEGRL   660
consensus_contig_1_1280_PAU1       FVIASDAGYGFVVKGEDLQAKNKAGKALLSLPNGSAVVAPRPVRDVEQDWLAAVTTEGRL   660
consensus_contig_1_828_PAU6        FVIASDAGYGFVVKGEDLQAKNKAGKALLSLPNGSAVVAPRPVRDVEQDWLAAVTTEGRL   660

consensus_contig_7_312_PAU2        LLFKVSDLPQLGKGKGNKIIGIPGERVASREEYLTDLAVLPAGATLVLQAGKRTLSLKGD   720
consensus_contig_1_2081_PAU4       ------------------------------------------------------------   601
consensus_contig_1_5218_PAU3       LLFKVSDLPQLGKGKGNKIIGIPGERVASREEYLTDLAVLPAGATLVLQAGKRTLSLKGD   720
consensus_tig00000003_1821_PAU5    LLFKVSDLPQLGKGKGNKIIGIPGERVASREEYLTDLAVLPAGATLVLQAGKRTLSLKGD   720
consensus_contig_1_5220_PAU7       LLFKVSDLPQLGKGKGNKIIGIPGERVASREEYLTDLAVLPAGATLVLQAGKRTLSLKGD   720
sp|Q9HUK1_ATCC15692                LLFKVSDLPQLGKGKGNKIIGIPGERVASREEYLTDLAVLPAGATLVLQAGKRTLSLKGD   720
consensus_contig_1_1280_PAU1       LLFKVSDLPQLGKGKGNKIIGIPGERVASREEYLTDLAVLPAGATLVLQAGKRTLSLKGD   720
consensus_contig_1_828_PAU6        LLFKVSDLPQLGKGKGNKIIGIPGERVASREEYLTDLAVLPAGATLVLQAGKRTLSLKGD   720

consensus_contig_7_312_PAU2        DLEHYKGERGRRGTSCRAVSSASTACWWIFRHRIEMSRYRSPISRISAREWRKRPLPRPA   780
consensus_contig_1_2081_PAU4       ------------------------------------------------------------   601
consensus_contig_1_5218_PAU3       DLEHYKGERGRRGNKLPRGFQRVDSL----------------LVDIPPQD*---------   754
consensus_tig00000003_1821_PAU5    DLEHYKGERGRRGNKLPRGFQRVDSL----------------LVDIPPQD*---------   754
consensus_contig_1_5220_PAU7       DLEHYKGERGRRGNKLPRGFQRVDSL----------------LVDIPPQD*---------   754
sp|Q9HUK1_ATCC15692                DLEHYKGERGRRGNKLPRGFQRVDSL----------------LVDIPPQD----------   754
consensus_contig_1_1280_PAU1       DLEHYKGERGRRGNKLPRGFQRVDSL----------------LVDIPPQD*---------   754
consensus_contig_1_828_PAU6        DLEHYKGERGRRGNKLPRGFQRVDSL----------------LVDIPPQD*---------   754

consensus_contig_7_312_PAU2        FRGNVVSLAGSAGFSPDAGGPKPVSEYALPLELWRWLGDDTPLRPPFPMAGGQ*   833
consensus_contig_1_2081_PAU4       ------------------------------------------------------   601
consensus_contig_1_5218_PAU3       ------------------------------------------------------   754
consensus_tig00000003_1821_PAU5    ------------------------------------------------------   754
consensus_contig_1_5220_PAU7       ------------------------------------------------------   754
sp|Q9HUK1_ATCC15692                ------------------------------------------------------   754
consensus_contig_1_1280_PAU1       ------------------------------------------------------   754
consensus_contig_1_828_PAU6        ------------------------------------------------------   754
```

Figure 4.6. Alignment of ParC sequences. Multiple sequence alignment of topoisomerase IV subunit A (ParC), where a Ser87Leu substitution specifically is a common mutation in Ciprofloxacin resistant strains, as well as Ser80Leu and Glu84Lys [1][159]. Strains are aligned against the laboratory strain ATCC15692, where sequence was obtained from www.uniprot.org by searching "ParC AND pseudomonas aeruginosa".

An often detected mutation in this gene happens at position 87, where mutations from the polar amino acid serine (S), to the hydrophobic amino acid leucine (L) has been seen as a common mutation in. The mutation has been seen in strains being exposed to prolonged treatment of the fluoroquinolone Ciprofloxacin [1]. This mutation was not detected in either of the strains, and all of them had S at position 87. In a study performed by Nakano et al. (1997), it was found that a substitution from a glutamine (E) to a lysine (K) in position 84 conferred higher resistance against Ciprofloxacin when in combination with a substitution in the DNA gyrase (GyrA) [159]. At this position in the sequence alignment,

the amino acid present was histidine (H), which is a positively charged amino acid (like lysine). It can, based on this knowledge, be interpreted as an adaptive mutation for increased ciprofloxacin resistance, but with a slightly different amino acid that still has a lot of the same characteristics. Another mutation found by Nakano et al. (1997) in their study, was a substitution from serine (S) to a leucine (L) at position 80 [159]. This substitution also contributes to increased resistance against fluoroquinolones (e.g., ciprofloxacin) [159].

In PAU4, the gene was identified as a DNA gyrase/topoisomerase IV, subunit A with a rank D, while for the other isolates the gene was identified as topoisomerase IV subunit A with a rank C. Based on the sequence, it indicates that base calling of this gene was insufficient for the PAU4 isolate. PAU4 showed large difference in sequence from the other sequences from the other strains. The sequence of PAU4 was a lot shorter than the rest, only 601 amino acids long, compared to 754 a.a. sequences for the other strains (except PAU2). Furthermore, PAU4 showed mutations at positions when approaching the end of the sequence (positions 587-601 were totally different from the other strains, while the other strains were homogeneous in these positions). PAU2 also differed largely from the remaining strains in regards to length (833 amino acids long compared to 754 for the remaining sequences). From position 734-754, almost all amino acids of PAU2 was different from those of the other strains. PAU3, PAU4, and PAU5 all showed a mutated 262 position, where the positively charged histidine (H) (in all the other strains) was the polar uncharged glutamine (Q) in these three strains.

In summary, there were 6 substitutions identified in the β-lactamase class C gene, where 1 substitution was present in PAU2 alone, while 3 were present in both PAU1 and PAU2. 2 positions showed substitutions in the other isolates as well, and substitutions were seen in PAU3, PAU4, PAU6, PAU7, and ATCC15692. This meant that there was subsitutions present in PAU3, but not PAU5 which might show relevant in the upcoming proteomics analysis. The gyrA gene did not contain the common substitution often linked with antibiotic resistance in 6 out of 7 genes (PAU2 had this substitution). Lastly, the parC gene showed to be very different for PAU2 and PAU4, with longer stretches of amino acid sequence either missing or additional stretches inserted into the sequence of these two isolates. The mutation commonly seen in ciprofloxacin resistant strains was not present in any of the strains, but another substitution also linked to resistance was seen (Glu84His).

4.5.4 Other Relevant Genes Identified

In addition to the genes identified above, there were genes found that are still involved in antimicrobial resistance (AMR), but not necessarily against the antibiotic tested in this thesis. Still, they are worth mentioning.

Tetracycline resistance genes were identified in all strains. This is another class of broad-spectrum antibiotics, that target the protein synthesis machinery [160]. Bacitracin resistance genes were also found in the strains, and this is another cyclic polypeptide (in the same class as Colistin). Bacitracin is an antibiotic usually active against gram-positive bacteria, where it inhibits cell wall synthesis [161].

Another gene present in all strains was the Lantibiotic resistance gene. Lantibiotics are bacteriocins, and bacteriocins are proteinaceous compounds that has the ability to kill other bacteria, and often closely related ones [162]. This might give a form of competitive advantage, e.g., inside the CF lung microbiome.

4.6 Growth Curves

After investigating the genomic potential of all isolates, and with interesting genes identified such as the β-lactamase gene, it was decided to perform proteomics on two of the isolates. Proteomics served as a suitable method for identifying response to antibiotic exposure in PAU3 and PAU5. This could maybe tell us more about what mechanisms a bacterium utilizes to confer resistance against the antibiotics tested. Two different sampling methods were used, one where isolate PAU5 was spiked with three β-lactams after growing for 6 h, and another sampling method where isolates PAU3 and PAU5 was grown continuously exposed to the TZP.

Growth curves for PAU3 and PAU5 were generated to determine how the bacterium grows, and when it would be in exponential phase. This would tell us when to add the antibiotic to the isolate (for spiking) and for knowing when to do sampling of the proteome.

4.6.1 Growth Curves for Antibiotic Spiking with β-lactams

Based on results from MIC, where PAU5 showed resistance levels against four out of six tested antibiotics, and not seeing distinct genes that could explain the multidrug resistance, it was decided to perform proteomics on this strain. Before conducting proteomics sampling with antibiotic spiking, a growth curve was needed to determine at which time point the bacterium was in exponential phase. The mid-exponential phase would be the point at which the bacterium would be spiked with the three antibiotics.

In the experiment described in section 3.7, growth curves based on six replicates of PAU5 were generated. The results from the growth curve measurements are shown in figures 4.7 and 4.8.

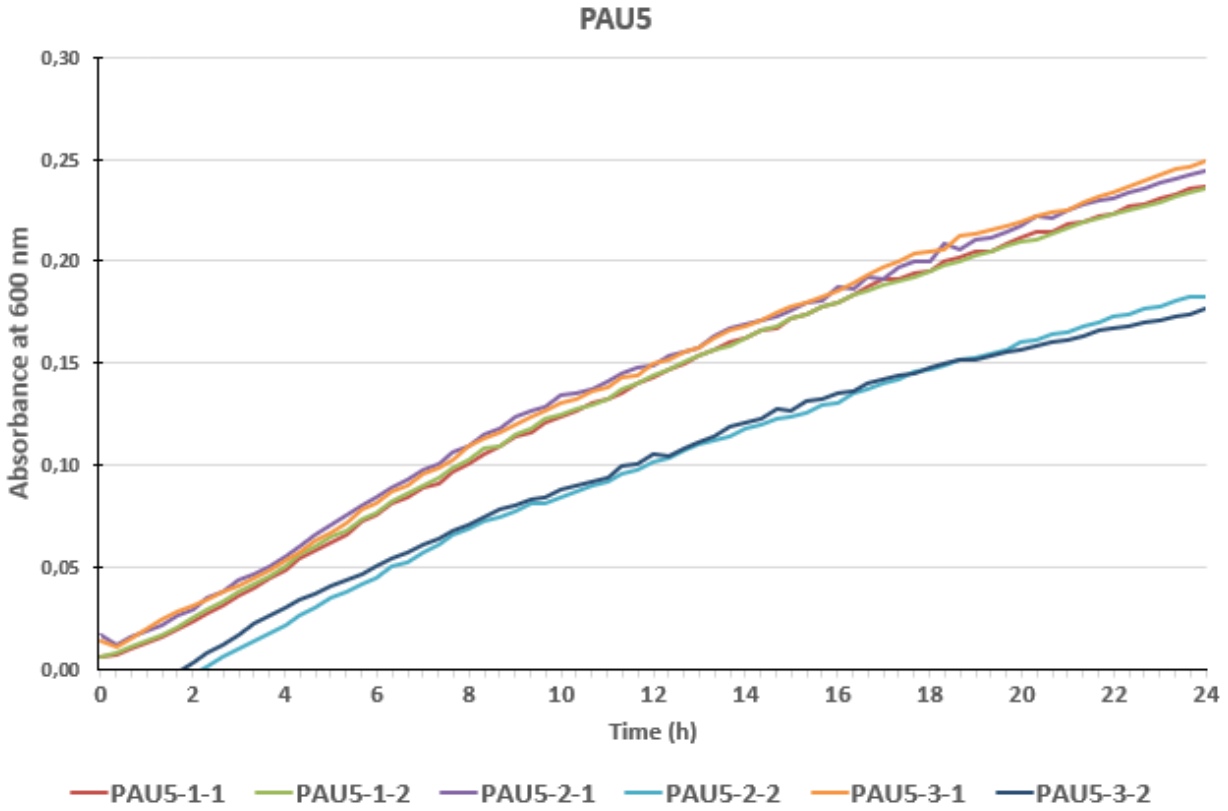

Figure 4.7. Growth curves for all replicates of PAU5. Growth curve for each replicate of PAU5, both biological and technical replicates. Medium used was Mueller-Hinton Broth. Identification of each line is shown underneath the graph. The graph was generated in Excel.

Figure 4.7 illustrates differences in growth curves between replicates. Replicates PAU5-1-1, PAU5-1-2, PAU5-2-1, and PAU5-3-1 are all clustered together with more or less the same shape as well as the same values of absorbance. Graphs for replicates PAU5-2-2 and PAU5-3-2 illustrates a shorter exponential phase, and an earlier shift towards the stationary phase. At the same time, absorbance values are lower for these two than for the other 4 replicates. The two deviating replicates also showed a lag phase with negative values in the beginning of the sampling. This can be seen by the lines for PAU5-2-2 and PAU5-3-2 appearing first after approximately 2 hours, indicating there could be some error when measurements were performed on these replicates.

In order to achieve a more coherent view of the growth curve for PAU5, a mean was calculated for all absorbance values and deviations from the mean was illustrated using standard deviation calculation in Excel. Figure 4.8 below shows the illustrated results of this data processing.

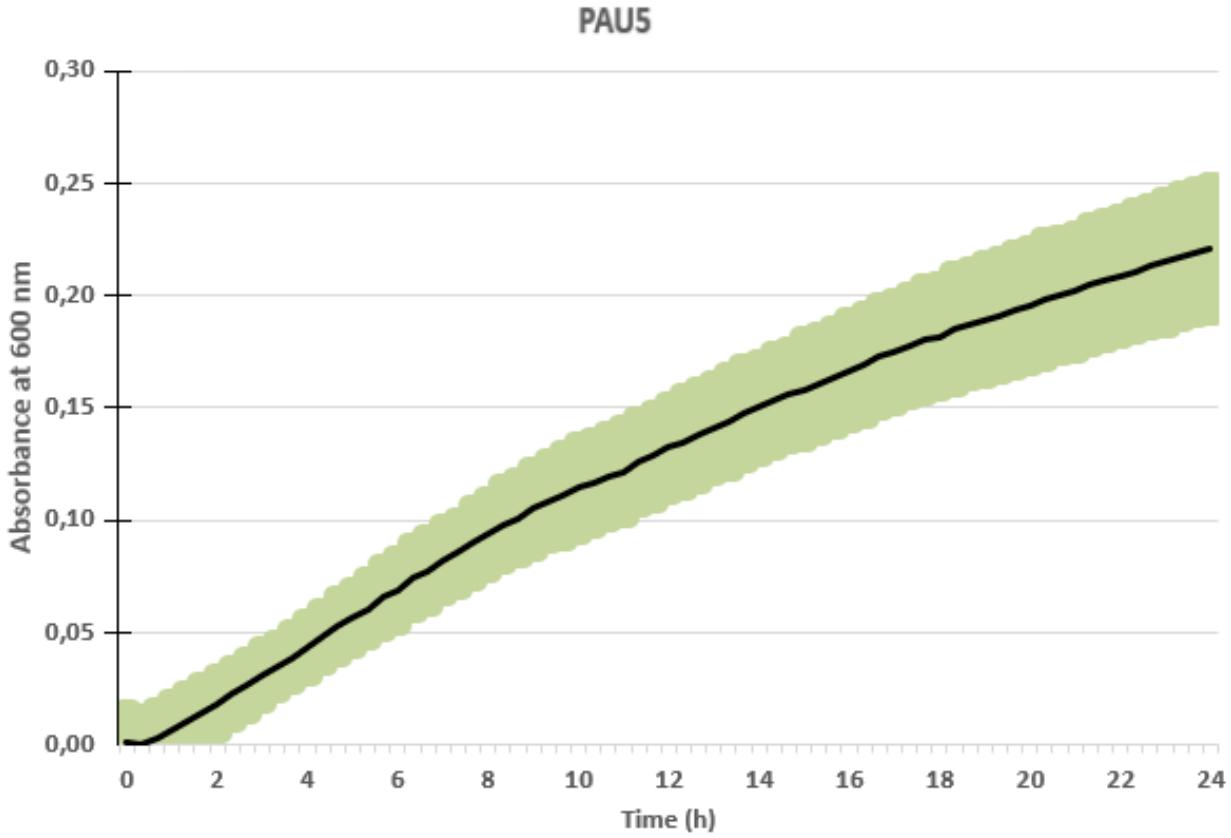

Figure 4.8. Growth curve mean and standard deviation. This figure shows the growth curve mean for all replicates of PAU5 illustrated by the black line, and the standard deviation illustrated by the green area surrounding the black line. The graph and standard deviation was generated in Excel.

Figure 4.8 shows that the exponential phase starts after approximately 1 h, and lasts approximately until time point 10 h where it curves off. At this time point, the curve of the graph changes from a relatively straight line in the exponential phase to a curved line that is characteristic for the stationary phase. The death phase was not showed in the figure, but the black line flattens out more and more leading up to the end of the experiment (and the end was set to 24 h).

In conclusion, the exponential phase was determined to be in the 1-10 h time range. It was therefore decided that after 6 h, which would mean mid-exponential phase, the isolate would be spiked with the three β-lactam antibiotic in the proteomics sampling.

4.6.2 Growth Curves for continuous exposure to antibiotics

Another proteomics sampling method was tested, where the two isolates PAU3 and PAU5 would be exposed to Piperacillin/Tazobactam (TZP) continuously before sampling in the exponential phase. This required a growth curve for the isolates while exposed to TZP in order to know when the isolates were in exponential phase. Compared to the previous growth curves generated for PAU5, it was thought that growth curves for this isolate when exposed to antibiotics would be slightly different, hence it was necessary to do it again. Growth curves were made for bacteria in six different antibiotic concentrations, as well as a control.

In the experiment described in section 3.7.2, growth curves were generated. The results from that experiment is shown in figures 4.9 and 4.10 below.

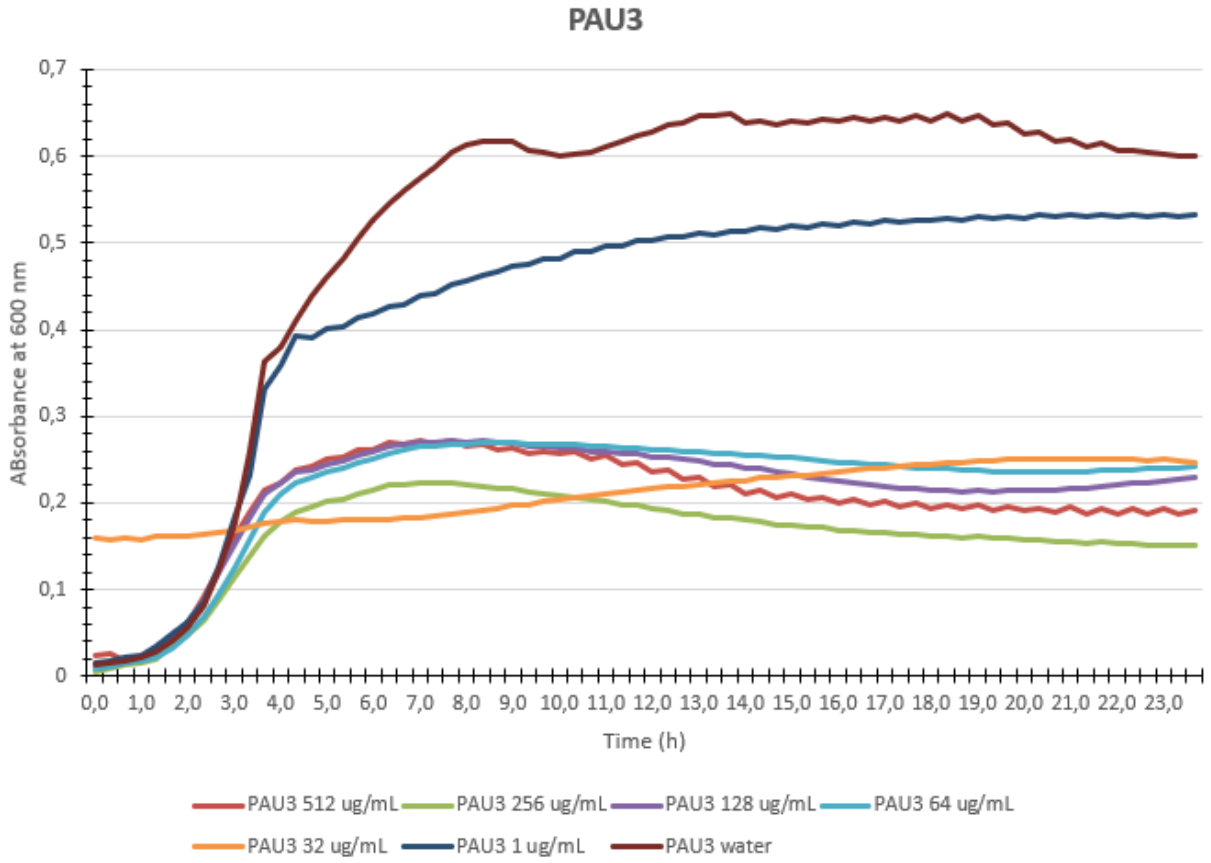

Figure 4.9. Growth curve for PAU3 in different TZP concentrations. Growth curve of strain PAU3 exposed to various concentrations of the antibiotic Piperacillin. In all replicates where Piperacillin was present, there was a constant 4 μg/mL of Tazobactam. Medium used was Mueller-Hinton Broth. The graph was generated in Excel.

Growth curves for PAU3 were varying depending on antibiotic concentration (figure 4.9). Replicate PAU3 32 μg/mL gave a growth curve that resembled some noise or contaminants being present in the sample since it started measuring at around 0.16 A. The absorbance for this replicate did not show the same growth that all the other replicates did. PAU3 replicates 64-128-256-512 μg/mL were clustered together, showing more or less the same growth. The replicate that grew to the lowest level was not the PAU3 in the highest concentration, as would be expected, but rather PAU3 in the second highest concentration of antibiotic. Replicate PAU3 1 μg/mL deviated from the others, giving a growth curve more alike the control replicate with water. Based on all growth curves, it was decided that at the 3-4 h time point replicates both in the lowest and in the highest concentration of antibiotic were in the exponential phase.

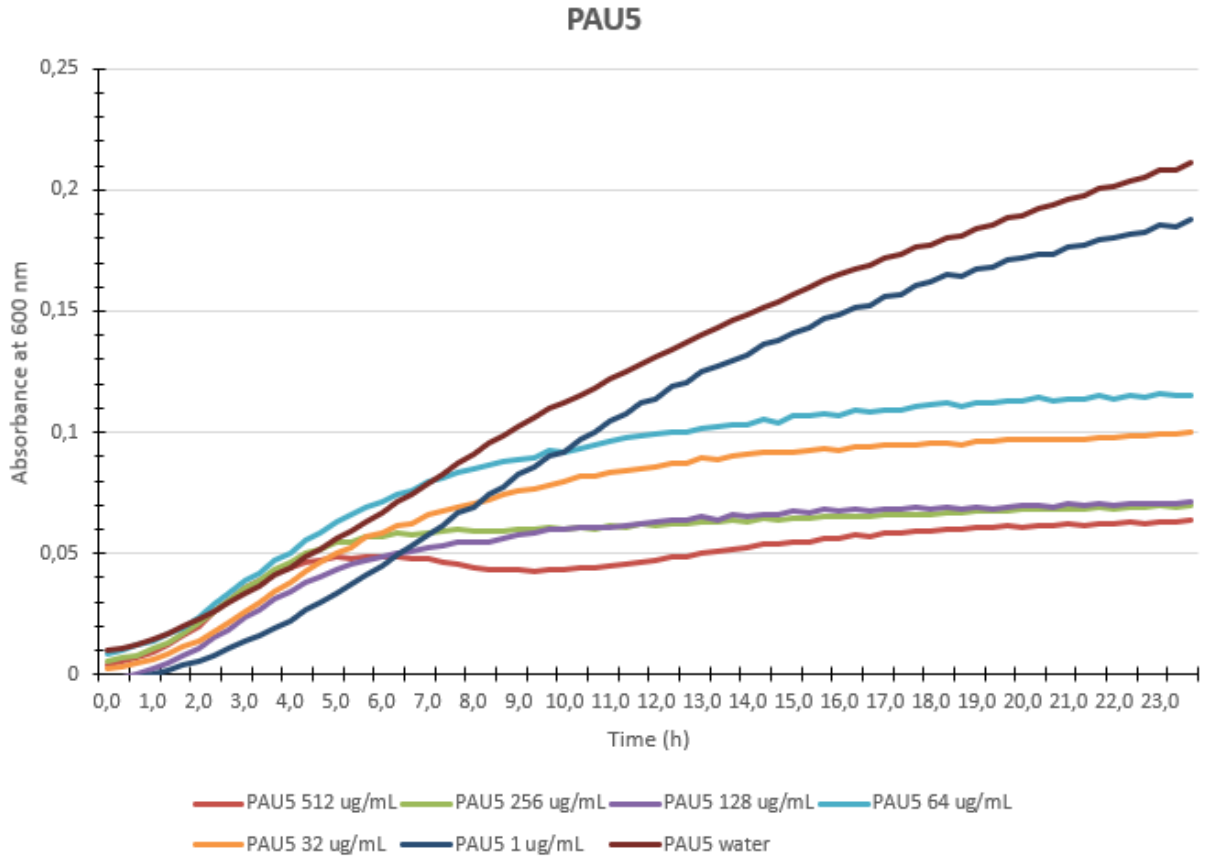

Figure 4.10. Growth curve for PAU5 in different TZP concentrations. Growth curve of strain PAU5 exposed to various concentrations of the antibiotic Piperacillin. In all replicates where Piperacillin was present, there was also a constant 4 μg/mL of Tazobactam. Medium used was Mueller-Hinton Broth. The graph was generated in Excel.

For PAU5, growth curves also showed to be different depending on the antibiotic concentration, which was also expected due to the nature of exposing a bacterium to an antibiotic (which often affects rate of growth, particularly) [42]. The water control replicate was the one that grew the most, followed by the bacterium in the lowest concentration of Piperacillin, as expected. The highest level of growth was slightly above 0.2 A, which is considerably lower than the highest level of growth in PAU3 (grew to around 0.75 A). Replicate PAU5 512 μg/mL showed a slight dip after entering the stationary phase (around 7 h-10 h), before growth rate again increased (around 10 - 14 h) until it reached the previous stationary phase level of absorbance value. PAU5 32-64 μg/mL growth curves showed similar growth, as did PAU5 128-256 μg/mL. Growth curves for all replicates showed a steady decrease in level of growth as the antibiotic concentration was increased.

In conclusion, all replicates showed to be in the mid-exponential phase at hour 3-4. Since both PAU3 and PAU5 showed to be in the mid-exponential phase at this time-point, the time-point to perform proteomic sampling on, was determined to be at 3.5 h.

4.7 Proteomics

At this point, determination of MIC had been performed, where strain PAU5 showed to be multidrug resistant (MDR) in Mueller-Hinton Broth (MHB) medium, followed PAU3 which was resistant against 2 antibiotics in MHB medium. Four more strains showed resistance levels against 1 antibiotic in the MHB medium. The two most interesting isolates were therefore PAU3 and PAU5, but when performing whole-genome sequencing and investigating the genomic potential, these did not stand out as having particularly unique genes involved in antibiotic resistance. PAU5 did, however, have the highest number of unique genes. Now, it would be interesting to see whether the proteome was the cause for the high resistance levels, and whether PAU3 and PAU5 would respond differently when exposed to the cell-wall acting antibiotic Piperacillin/Tazobactam (TZP). In proteomics sampling, lysates were used for analysis, which came with limitations in regards to identifying potential dys-regulation of membrane-associated proteins (such as efflux pumps for increased resistance). However, lysates would give information about the proteome in both the cytoplasm and the periplasm of the cell, and the periplasm would be the place where a potential β-lactamase would be present (and investigating this was of interest).

Proteomics data obtained was of dys-regulated proteins identified in cell lysates, which were annotated with both protein and gene name as well as degree of dys-regulation given in a $\log_2$ fold change value with a p-value (all dys-regulated proteins are shown in appendix D for PAU3, appendix E for PAU5 and appendix F and G for PAU5 spiked with β-lactams).

4.7.1 Proteomics of PAU5 with Antibiotic Spiking of β-lactams

PAU5 showed to be the most interesting isolate to perform proteomics analysis on, based on the MIC determination where it showed MDR in MHB medium, but was unable to grow at all when switching to RPMI medium. In the spiking proteomics experiment, the bacterium was exposed to the three different β-lactam antibiotics Ceftazidime (CAZ), Meropenem (MEM), and Piperacillin/Tazobactam (TZP). PAU5 showed resistance values against both TZP and CAZ, but not against MEM. In MEM, PAU5 was not able to grow at all, therefore it would be interesting to see whether different antibiotics (with the same target) elicit a different proteome response in the bacterial cells. Table of all dys-regulated proteins is shown in appendix F and G.

Visualizations of proteomic response exposed to the different antibiotics was not made for this experiment due to poor response when investigating the data. Instead, a summary text was made for the response with reference to the appendix where all dys-regulated proteins are shown (see appendix F and G). It was thought that the reason for the poor response was either too short incubation time (30 minutes) or too low concentration of antibiotic to provoke a shift in expression levels of proteins involved in either resistance or stress tolerance. Additionally, the class C β-lactamase identified in the genome of all strains, was not identified as up-regulated in either of the conditions in this experiment when comparing with a water control.

PAU5 exposed to CAZ:

Starting with the response PAU5 showed when exposed to 32 μg/mL CAZ, there was only 25 dys-regulated proteins in total when compared to the control (see table in appendix F). Up-regulated proteins included 2 type IV pilus proteins, acyclic terpene utilization (Atu proteins), where acyclic terpenes can be used as carbon and energy source, ribosome maturation factor (RimP), while down-regulated proteins included transcriptional regulators, protease (PfpI), peptidoglycan metabolic process (rlpA), and iron-binding periplasmic protein. The protease PfpI is involved both in stress toleration, and DNA protection under non-stress conditions [163]. The response did not show any proteins directly involved in resistance against CAZ, nor did it reveal any stress-tolerance proteins often seen when a bacterium is in a stressed environment (and being exposed to an antibiotic would be expected to be stressful). Seeing as only 25 proteins were dys-regulated (8 proteins up-regulated) compared to the control, it seemed as if the isolate did not elicit a response against being subjected to the antibiotic. The antibiotic concentration in this experiment was lower than the determined MIC value. PAU5 was able to grow in all concentrations of CAZ when performing analysis of MIC, and combining that with the poor response on a proteomic level, it indicates that the MIC value might be substantially higher. Additionally, it indicates that resistance against this antibiotic might be either constitutively expressed, or mediated by membrane-associated proteins not detected in the lysate fraction used for identification of proteome.

PAU5 exposed to MEM:

Proteomic analysis revealed that when the strain was exposed to 0.0064 μg/mL MEM, a total of 91 proteins were dys-regulated, and 41 up-regulated proteins (see appendix F). The response was up-regulation of various regulatory proteins (e.g., CatR, and PA1309), cell division proteins (e.g., ZipA), and transferases involved in various cellular pathways. Down-regulated proteins consisted of heat-shock proteins (e.g., PA5195, ibpA), DNA pol. III γ/τ (dnaX), stress proteins (e.g., PA3017), elongation factors (involved in protein synthesis), and DNA repair proteins (e.g., RadA). The down-regulation of various proteins involved in stress-tolerance indicates that the bacterium did not experience the environment as stressful. There can be several reasons for why this was the response, but two possible explanations is that the concentration of antibiotic was too low for the bacterium to consider it stressful, or genes conferring resistance are constitutively expressed, resulting in not seeing these as dys-regulated when comparing expression with the control. Another explanation might also here be that response was happening in changed expression of membrane-associated proteins, which was not possible to detect due to the nature of sampling (sampling the lysate fraction).

PAU5 exposed to TZP:

The last antibiotic tested, was the combination drug of TZP, at a final concentration of 32/4 μg/mL. The response of PAU5 to this drug was substantially larger than the response to CAZ, with over 350 dysregulated proteins identified, with 46 of them being up-regulated (see table in appendix G). Up-regulated proteins included flagellar protein (e.g., PA3352), several stress-response proteins that for example protect the cell against reactive oxygen species (ROS) (e.g., PA0653 and grpE), proteins involved in iron uptake (e.g., bfrA), ribosomal protein (RpsO), as well as proteins involved in various metabolism pathways (e.g., ATP synthase

protein atpF). Down-regulation consisted of proteins involved in replication, transcription, other stress-response proteins (e.g., SspA), metallo-β-lactamase (PA2915), various metabolic pathways, type IV pilus, and a class D β-lactamase (OXA-50) (poxB). Down-regulation of a β-lactamase when being exposed to a β-lactam might entail that either annotation is wrong, or another protein is responsible for the clearance of the antibiotic from the inside of the bacterial cell (such as membrane-associated proteins that were not detected here). Many more proteins were down-regulated than up-regulated, with 46 being up-regulated compared to 304 down-regulated proteins. Down-regulation may often be a way of evading a drug, such as down-regulating proteins involved in synthesis of peptidoglycan when being subjected to TZP, which acts on the cell wall, but a protein involved in peptidoglycan synthesis (ftsI), was actually seen up-regulated.

Interpreting the data obtained, which showed up-regulation of virulence factors such as flagellar proteins, with down-regulation of proteins such as metallo-β-lactamase, the class D β-lactamase and stress-induced proteins, reveals that PAU5 might not indeed have been stressed at all.

In conclusion, these results did not show PAU5 eliciting a particular response towards any of the antibiotics it was being subjected to. The anticipated class C β-lactamase was not identified as dysregulated either, which resulted in a decision of attempting another proteomics sampling with a different setup. The poor and non-conclusive data was the reason for not including visualizations of the data obtained from this experiment.

4.7.2 Proteomics of PAU3 & PAU5 with Continuous Antibiotic Exposure

After performing proteomics on PAU5 with spiking of the three β-lactam antibiotics which gave poor results, it was decided to perform proteomics on this isolate once more. In addition, it was thought that if including one more isolate, this would give another dimension to the data obtained. If the proteomes of two isolates were investigated, a comparative analysis tied together with the determined MIC-values could be performed. It was therefore decided to perform proteomics sampling on isolates PAU3 and PAU5, which both showed to be resistant towards Piperacillin/Tazobactam (TZP), but also were the two isolates showing resistance against most antibiotics (PAU3 resistant against TZP and CAZ, and PAU5 resistant against TZP, CIP, TOB, and CAZ). Additionally, during genomic analysis, PAU3 and PAU5 were different in terms of number of genes associated with two-component regulatory systems, type VI secretion systems, and flagellar proteins. Furthermore, when comparing the genome of the two isolates (see figure 4.7), it revealed that many genes were only present in one of the isolates (there was a large portion of cloud genome in the pangenome shared between PAU3 and PAU5). All these differences combined, could maybe be observed by the difference in proteome of these two strains. TZP was decided to be used as an antibiotic, with constant concentration of Tazobactam (4 μg/mL) and varying concentration of Piperacillin (1 & 512 μg/mL) to investigate adaptations to lower and higher levels of environmental stress imposed by the antibiotic.

Results from performing proteomics analysis on clinical strains PAU3 and PAU5 continuously exposed to the combinatory antibiotic drug TZP, includes tables of all dys-regulated proteins

for each strain as well as volcano plots and heatmaps for visualization (see appendix D for all dys-regulated proteins in strain PAU3, and appendix E for all dys-regulated proteins in strain PAU5). Furthermore, results include investigation of interesting proteins found during this analysis. All visualizations made in this section are based on the tables of all dys-regulated proteins shown in appendix D and E.

In the volcano plots, only top 20 up and down-regulated proteins are annotated (for a total of 40 annotated proteins). This was due to aesthetic limitations set by R when annotating points in the volcano plot with their respective protein name. For achieving informative figures and for the sake of homogeneity across all plots, it was not possible to include more than 40 annotated proteins per plot. Heatmaps was another representation of the data, which also showed the top 20 up-regulated and bottom 20 down-regulated proteins, due to size and aesthetic limitations and considerations. Volcano plots were made from all identified proteins (as identified by perseus), where some proteins did not have an identification/were not mapped to a gene. These proteins, if part of top 40 dys-regulated proteins, does therefore not have an annotation in volcano plots. Some proteins in the heatmaps were not successfully annotated either, and are labelled with an "Unknown" label.

For clinical strain PAU3, a total of 1900 proteins were identified, and for PAU5 the number of all identified proteins was 2093 (the same number for each isolates in all conditions).

PAU3 1 μg/mL Piperacillin compared to control:

In this first comparison, isolate PAU3 exposed to 1 μg/mL Piperacillin and 4 μg/mL of Tazobactam was compared to the control where only water was added. This was of interest because there could have been a response happening even though the antibiotic concentration was low. This could also serve as a comparison of identified dys-regulated proteins between PAU3 being exposed to the low and to the high antibiotic concentration. Such data could reveal specific adaptations of PAU3 to lower and higher levels of environmental stress. Figure 4.11 below shows a volcano plot of the top 20 and bottom 20 dys-regulated proteins.

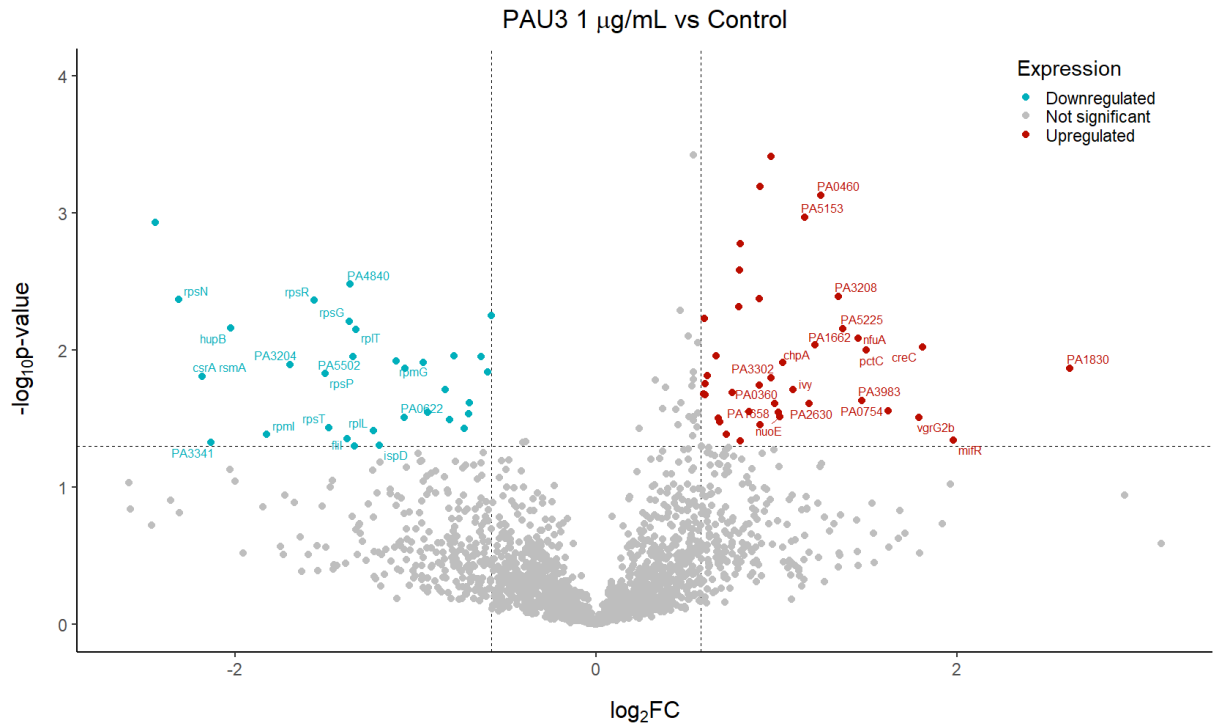

Figure 4.11. Volcano plot of PAU3 in 1 μg/mL Piperacillin vs. control. Volcano plot of PAU3 exposed to 1 μg/mL Piperacillin (and 4 μg/mL Tazobactam) compared to the water control. Up-regulated proteins are colored red, and down-regulated proteins are colored blue. Not significantly dys-regulated proteins, meaning a -$\log_{10}$p-value below 1.3 and a Log_2 Fold Change = -0.58<Log_2FC>0.58, are colored grey. There are 18 down-regulated proteins due to 2 of them not being annotated (the protein is unknown). Dashed lines shows threshold for being significantly dys-regulated. Graph was generated in RStudio.

When comparing PAU3 exposed to antibiotic concentration of 1 μg/mL Piperacillin and 4 μg/mL Tazobactam and the control replicate, the protein that was most up-regulated was the PA1830 gene (see volcano plot in figure 4.11 and heatmap in figure 4.14). In the Uniprot database it was identified as a SCP2 domain-containing protein (SCP2 = Sterol Carrier Protein 2), and in Interpro this protein family is involved in binding sterols [164]. In other species, such as humans, this protein is part of lipid metabolism [165]. The up-regulation was quite clear when inspecting both the volcano plot and the heatmap.

Other up-regulated proteins were mifR (involved in transcriptional regulation of an α-ketoglutarate transporter), CreC (part of the two-component system CreBC which plays an important part in β-lactam response)[166], and VgrG2b (protein involved in the H2 Type VI secretion system) [167]. Checking STRING protein interaction between CreBC-system and AmpC, revealed that these were in co-expression network with the inner membrane protein CreD creating the network between the AmpC and CreBC (results of STRING analysis will be covered in the next section, see section 4.7.3. One research has shown that deletion of the mifR gene increased survival time of mice injected with *P. aeruginosa* mediated pneumonia and sepsis, as well as reduced lung injury when the *mifR* gene was knocked out [168].

NfuA, Ivy, chpA/MazF, nuoE, and pctC were all up-regulated proteins. NfuA is a required factor for maturation of Fe/S containing proteins, especially under oxidative stress and/or

iron starvation [169][170]. Ivy is a strong inhibitor of vertebrate lysozyme C [171], while chpA/MazF is an endoribonuclease involved in the toxin-antitoxin system by inhibiting protein synthesis through cleavage of mRNA [172]. nuoE is a protein involved in shuttling of electrons in the respiratory chain, and lastly, pctC is a signal-transducer for regulation of i.e., gene expression or DNA replication based on the milieu [173].

When looking at down-regulated proteins in both the volcano plot (figure 4.11), and the heatmap (figure 4.14), algP/algR3 was the least down-regulated protein among the bottom 20 down-regulated proteins (not annotated in the volcano plot). AlgP/AlgR3 is a promoter for another gene, the alginate biosynthetic gene AlgD. The regulation of this promoter is reduced compared to the control, but not largely ($\log_2$FC = -0.96). Other proteins significantly down-regulated were rpmB, rpmG, rplL, rplT, rpsG, rpsT, rpsR, rpmI, CsrA/rsmA, and rpsN. All these proteins have in common that they in one way or another either regulate or is directly involved in protein synthesis (translation). Some of them are translational regulators, such as CsrA, while others are important in assembly of the translational machinery, such as rpsN that binds 16S rRNA and is required for the assembly of 30S subunit of the ribosome performing translation. A protein that stood out from the rest of the down-regulated proteins was the fliI protein. This is a flagellum-specific ATP synthase, meaning it is involved in movement of the flagellum and energy expenditure. Another protein worth noting when it came to down-regulation compared to the control was the ispD. This is a protein involved in the MEP pathway, which is thought to be important in virulence. Research also points towards this protein being important in combating oxidative stress by reactive oxygen species (ROS) [174]. Lastly, the hupB and csrA/rsmA were among the most down-regulated proteins. hupB is a histon-like DNA-binding protein that contributes to packing of DNA and it has been shown to protect DNA by shielding it from reactive oxygen species, but also from denaturation [175]. csrA/rsmA is also involved in translation, but by regulating translation initiation as well as mRNA stability. This protein has more functions, and that is positive control of swarming motility, mediation of global changes in gene expression and it does so by creating a link between stress on the cellular envelope from the outside, the stringent response and catabolite repression. This ensures quick adaptation to changes in nutrient availability [176].

Down-regulation of translation can be interpreted as a stress-response where the cell is trying to minimize potential damage imposed by e.g., an antibiotic or the immune system. It can serve as a way of evasion, where the cell will move into a more dormant state and wait for "better times". This could be what is happening in this condition. Why then, does the PAU3 strain make these adaptations at such low antibiotic concentrations? It might be that the strain is familiar with this antibiotic compound (the Piperacillin/Tazobactam combination), and upon identification it immediately makes expressional changes due to previous exposure.

The other proteins that were labelled with PA followed by four digits, were uncharacterized proteins. Since the function of these proteins are largely unknown, the focus was directed towards the proteins that were characterized and that could tell us something specific about the response.

PAU3 512 μg/mL compared to control:

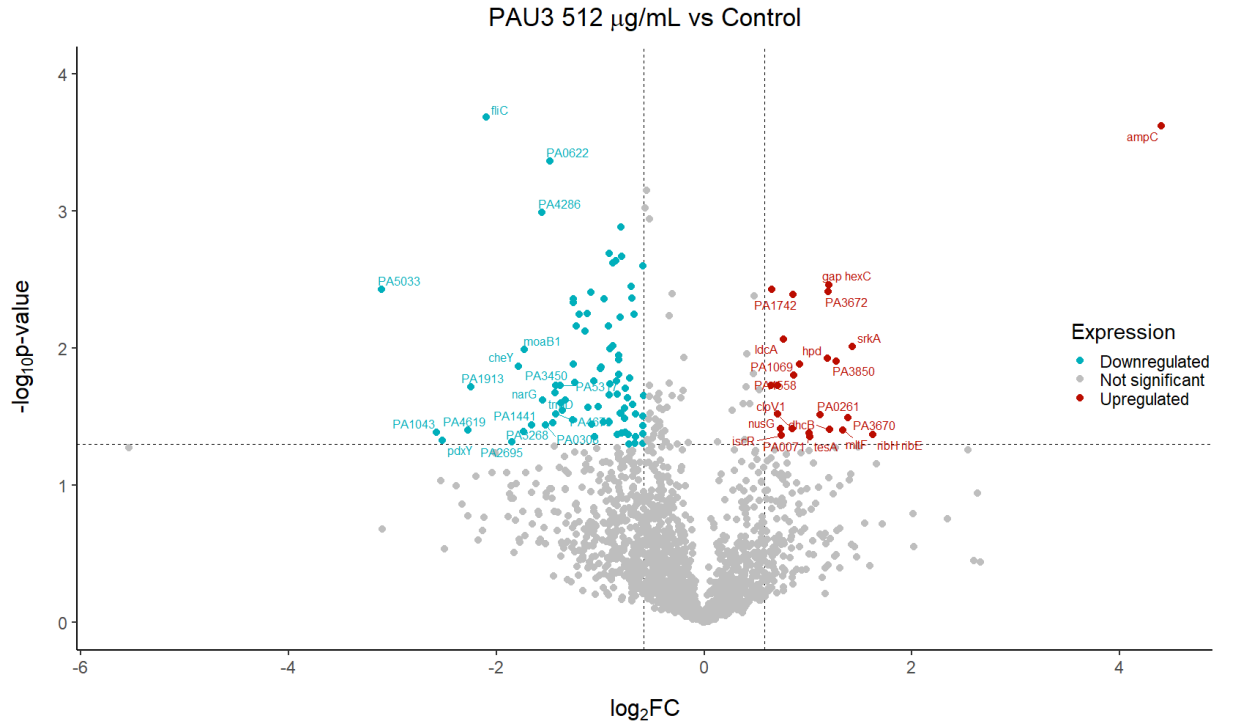

Figure 4.12. Volcano plot of PAU3 in 512 μg/mL Piperacillin vs. control. Volcano plot of PAU3 exposed to 512 μg/mL Piperacillin (and 4 μg/mL Tazobactam) compared to the water control. Up-regulated proteins are colored red, and down-regulated proteins are colored blue. Not significantly dys-regulated proteins, meaning a -$\log_{10}$p-value below 1.3 and a Log_2 Fold Change= -0.58<Log_2FC>0.58, are colored grey. Dashed lines shows threshold for being significantly dys-regulated. Graph was generated in RStudio.

When exposing strain PAU3 to 512 μg/mL PIP and 4 μg/mL TAZ, a different response happened compared to the previous condition (figure 4.12). The most up-regulated protein in this condition was the AmpC ($\log_2$FC=4.4) protein (see volcano plot in figure 4.12 and heatmap in figure 4.14). This protein is characterized as a β-lactamase responsible for the cleavage of the β-lactam ring in β-lactam antibiotics (e.g., PIP) thereby inactivating it. The response and up-regulation of this protein was large compared to the up-regulation of the other proteins (the second highest up-regulated protein was ribH, with $\log_2$FC=1.63). AmpC is a protein present in the periplasmic space, and this is also where the β-lactam antibiotic is present. The β-lactam is able to enter the periplasmic space through porins situated in the outer membrane of the bacterium, which upon entering the periplasm inactivates the penicillin-binding proteins (PBPs). Up-regulation of the porins could not be detected by this method of proteomics because these are situated in the membrane and analysis was performed on lysate. Therefore, no membrane-associated proteins are seen in the proteome.

Other proteins that were up-regulated was ribH/ribE, which are proteins involved in riboflavin synthesis. Riboflavin biosynthesis genes have been suggested as important for virulence and pathogenesis, maybe because it can produce reactive oxygen species (ROS) and nitric oxide (NO) to perform oxidative damage on tissues or to inhibit growth of other pathogens present [177]. The third protein that was up-regulated in this condition, was the

srkA, formerly known as yihE, which is a stress response kinase. This protein tries to suppress the effects of stress performed on the cell linked to ROS. It protects the cells from stress by working against the MazE-MazF TA module, inhibiting the TA system from performing the cell death pathway [178]. When looking further down the heatmap, there were several more up-regulated proteins, such as mltF (involved in cell wall recycling, and a signaling molecule for AmpC production) [179], dhcB (involved in metabolism of aromatic compounds for usage as carbon source) [180], hexC (involved in carbohydrate degradation), hpd (part of tyrosine degradation pathway, possibly linked to pyomelanin biosynthesis, a pigment for oxidative stress resistance) [181], and tesA (multifunctional enzyme, thioesterase, lysophospholipase, and maybe a protease) [182]. dhcB might be involved in degradation of the aromatic part of Piperacillin, due to its involvement in aromatic compound degradation (Piperacillin has an aromatic ring in its structure, see figure 1.5). Investigation of potential network between dhcB and hexC showed no interaction between the two proteins, but dhcB might still be used for degradation of various aromatic compounds for usage as carbon source. This is only an hypothesis, but changes to the structure of proteins (amino acid substitutions) are known to sometimes result in subsequent changes of substrate.

Proteins that were still up-regulated, but the $\log_2$FC-value was less than 1, were clpV1, ldcA, iscR, and nusG. ClpV1 is an ATPase, and a component of the H1 type VI secretion system. It plays a role in targeting both eukaryotic and prokaryotic species by releasing toxins into the cells [183]. LdcA is a protein present in the cytoplasm, involved in cell wall recycling by release of the terminal amino acid alanine on the tetrapeptide chain attached to the NAM subunit of the peptidoglycan chain (structure explained in section 1.3). IscR is a helix-turn-helix transcriptional regulator (binds DNA), and this protein regulates transcription of several operones and genes, especially those involved in production of Fe-S containing proteins. Under oxidative stress or iron deprivation it acts as an activator for genes involved in generating Fe-S clusters. The last up-regulated protein in the heatmap was nusG. This protein is, among other things, involved in rRNA transcription and is a termination/antitermination protein, supporting rapid transcription of rRNA operons when needed.

When it came to down-regulated proteins, several of the proteins identified have not yet been characterized. One of the proteins where function is known was the trmD protein ($\log_2$FC=-1.44). This protein is involved in methylation on tRNA as a part of post-transcriptional modification of tRNAs [184]. Methylation is important for regulation of mRNA stability and translation of mRNA. narG, which was also down-regulated, is a nitrate reductase enzyme complex which, in the bacterium *Escherichia coli*, has been shown to be important for using nitrate as an electron acceptor during anaerobic growth (work together with moaB1, another protein present under anaerobic conditions which uses nitrogen compounds as an electron source) [185]. MoaB1 was also identified as down-regulated compared to the control, and moaB1 stands for molybdenum cofactor biosynthesis protein B. Molybdenum is a chemical element that *P. aeruginosa* uses for respiration in anaerobic and microaerophilic environments (like the environment in a cystic fibrosis lung) [185]. This protein may be involved in the biosynthesis of molybdopterin which is a metal-binding ligand.

MoaB1 and narG are important for *P. aeruginosa* when considering it is a facultative aerobe, which in the absence of oxygen can respire by using nitrate or nitrite as a final electron acceptor. This makes it possible for the bacterium to survive even in the mucus filled milieu of the CF lung where oxygen is not always readily available.

The chemotaxis protein cheY was also down-regulated (Log_2FC=-1.79), and it is involved in transmission of sensory signals from chemoreceptors to the flagellar motors. The cheY proteins job, specifically, is to aid in changing rotation of the flagellum from counterclockwise to clockwise rotation [186]. fliC, is a protein called flagellin, and this is the subunit protein within the flagellum that polymerizes in order to form the filaments of the bacterial flagellum. pdxY, pyridoxal kinase, is a protein involved in the salvage pathway to generate the active form of vitamin B_6. This is performed by the cell because it makes any non-phosphorylated B_6 vitamer available to the cell as co-factors [187][188]. The active form of vitamin B_6 is essential for the cell as it serves as a co-factor for many reactions. It is active in metabolism of substrate, but also in cellular signaling.

PAU3 512 μg/mL compared to 1 μg/mL:

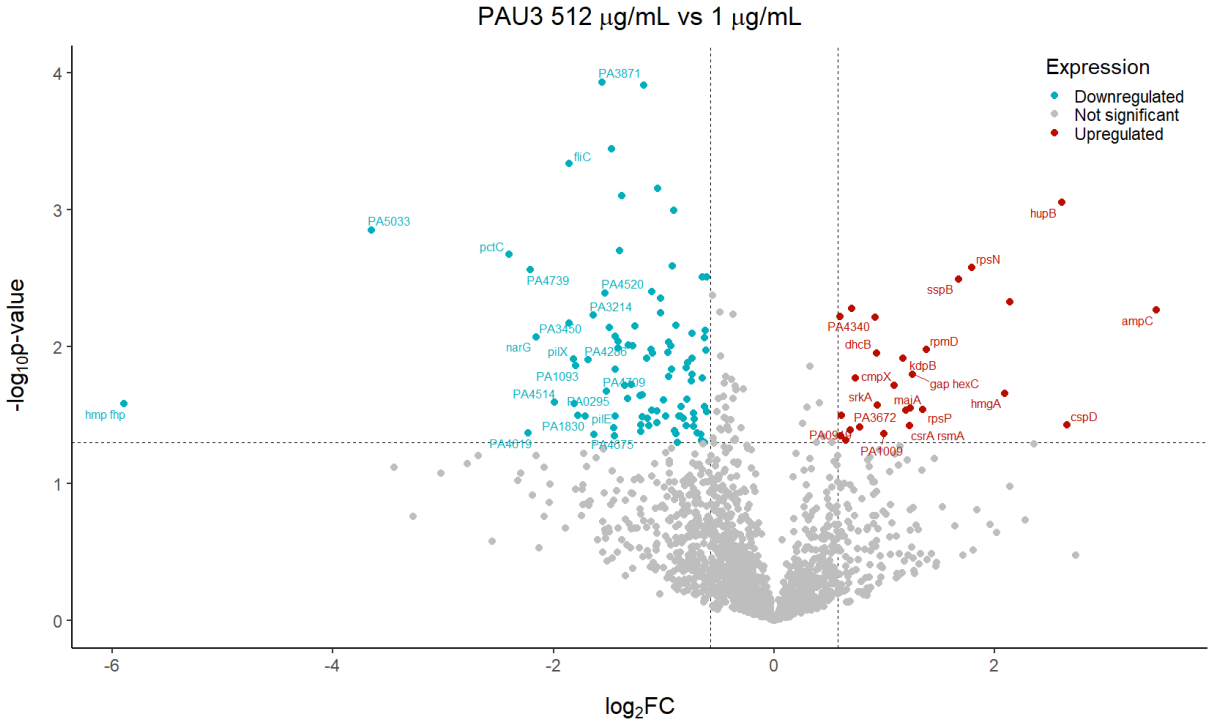

Figure 4.13. Volcano plot of PAU3 in 512 μg/mL vs. 1 μg/mL Piperacillin. Volcano plot of PAU3 512 μg/mL Piperacillin compared to 1 μg/mL (and constant 4 μg/mL Tazobactam). Up-regulated proteins are colored red, and down-regulated proteins are colored blue. Not significantly dysregulated proteins, meaning a -$\log_{10}$p-value below 1.3 and a Log_2 Fold Change= -0.58<Log_2FC>0.58, are colored grey. Dashed lines shows threshold for being significantly dys-regulated. Graph was generated in RStudio.

The last comparison was that of PAU3 exposed to 512 μg/mL and 1 μg/mL Piperacillin (PIP) (figure 4.13). Comparing these two was of interest firstly because the lowest concentration of PIP was below the resistance level determined during MIC analysis, while the other one was far above the determined MIC value (see results for determined MIC in table 4.2). For

PAU3, the determined MIC value was >64/4 μg/mL, meaning the true MIC value might in reality be much higher. For this reason, the highest concentration was chosen to see what would happen to the bacterial cells. Additionally, growth curves shown in figure 4.9 showed that the bacterium grew differently at different levels of antibiotic concentration, with a trend of decreased growth as antibiotic concentration increased. All of the results explained above, was the justification for doing this comparison.

When running a comparison of the proteome between bacteria subjected to the highest concentration and the lowest concentration of the antibiotic, several relevant proteins were identified (see figure 4.13). These include the highest up-regulated protein ampC ($\log_2$ Fold Change = 3.46), followed by an arsenal of proteins involved in translation (rpsN, rpmD, rpsP, and csrA/rsmA). Other proteins include cspD, hupB, hmgA, gap/hexC, maiA, kdpB, and cmpX. SrkA and dhcB had a Log_2 Fold Change value of <1 along with two other proteins that were not annotated when searching in the uniprot database (see heatmap in figure 4.14). The fourth highest up-regulated protein was of unknown character, meaning it was not successfully annotated to any protein when matching proteome to the sequenced genome of strain PAU3.

The cspD protein is involved in inhibition of DNA replication at both initiation and elongation steps. At the same time, it is involved in persister cell formation, but overproduction of this protein is toxic to the cell. This protein is found to be induced during stationary phase (which we know the bacteria was not in since we sampled in the exponential phase), glucose starvation and oxidative stress. It localizes to the nucleoid and inhibits DNA rep [189]. It could be that this protein was induced due to oxidative stress.

hupB was the third highest up-regulated protein ($\log_2$Fold Change = 2.61). For comparison, this was the fifth most down-regulated protein in the 1 μg/mL condition compared to the water control (see the heatmap on left side of figure 4.14). HupB is a protein that serves in binding of DNA for both protection against reactive oxygen species (ROS), and denaturation [175].

hmgA (Homogentisate 1,2-dioxygenase), part of the homogentisate pathway, which had a $\log_2$ Fold Change = 2.09, is a protein involved in degradation of phenylalanine and tyrosine, and it catalyzes oxidative cleavage of the aromatic ring of these amino acids [190]. It is not an impossibility that the isolate can adapt various pathways to be used on other structures e.g., as a carbon source [43]. An hypothesis for the up-regulation of this protein could be an adaptation to catabolizing other compounds consisting of an aromatic ring, such as the antibiotic it is being subjected to, Piperacillin.

SspB (a stringent starvation protein, involved in degradation of stalled peptides during translation), gap/hexC (part of the carbohydrate degradation pathway), and maiA (involved in amino acid degradation) were also up-regulated proteins. MaiA has been shown to be one of the most abundantly present proteins in a bloodstream isolate of *P. aeruginosa* compared to a peripheral isolate cultured from the same patient [191]. Due to this discrepancy between peripheral isolated and isolated from the bloodstream, there might be unknown but important functions for the bacterial cell of this enzyme in the bloodstream milieu. Additionally, kdpB, cmpX, srkA, and dhcB were also up-regulated proteins. KdpB is a part of the

high-affinity, ATP-driven potassium (K) transport system for transportation of K into the cytoplasm. CmpX is a mechanosensitive channel which participates in regulation of osmotic pressure within the cell. A knockout mutant of cmpX has been found to have increased sensitivity towards membrane detergents and antibiotics such as Tobramycin [192]. SrkA is a stress-response kinase, which acts by phosphorylating serine and threonine residues, and acts to suppress the effect of stress linked to accumulation of ROS. The last protein among the 20 top up-regulated ones that had a known function, dhcB, we know already is involved in aromatic compound metabolism, and an hypothesis is that PAU3 uses this protein for degradation of the antibiotic Piperacillin which contains an aromatic ring [180].

Down-regulated proteins included pilE and pilX, which are essential components in the type IV pilus (aiding in adhesion, colonization, biofilm maturation, virulence, and twitching motility) (see section 1.7.2). FliC, another down-regulated protein, is involved in filament formation of the bacterial flagellum. NarG was seen down-regulated here, just like in the 512 μg/mL Piperacillin vs Control comparison, and this protein is important for nitrate reduction in absence of oxygen, meaning it uses nitrate as a final electron acceptor [185]. PctC and hmp/fhp were two out of the three most down-regulated proteins in this comparison. PctC had a $\log_2$ Fold Change = -2.4, while hmp/fhp had a $\log_2$ Fold Change = -5.9. PctC is a chemotaxis protein, i.e., a receptor that responds to changes in the environment and forwards a signal for adaptation of methylation level of DNA. This, in turn regulates both DNA replication and gene expression, where higher methylation levels inhibit proteins from accessing the genes, while lower methylation levels leave the genes accessible [193]. Lastly, hmp/fhp, is involved in oxidation of NO to NO_{3-}, which is important in reducing nitrosative stress (i.e., there might be less nitrosative stress present in the highest concentration of antibiotic PIP compared to the lowest concentration of the antibiotic PIP).

Along with the characterized proteins described above, there were 14 proteins not annotated. To visualize the data in a more clear manner and to easily compare the different dys-regulated proteins identified, a heatmap was made. Figure 4.14 below shows the three heatmaps made for strain PAU3.

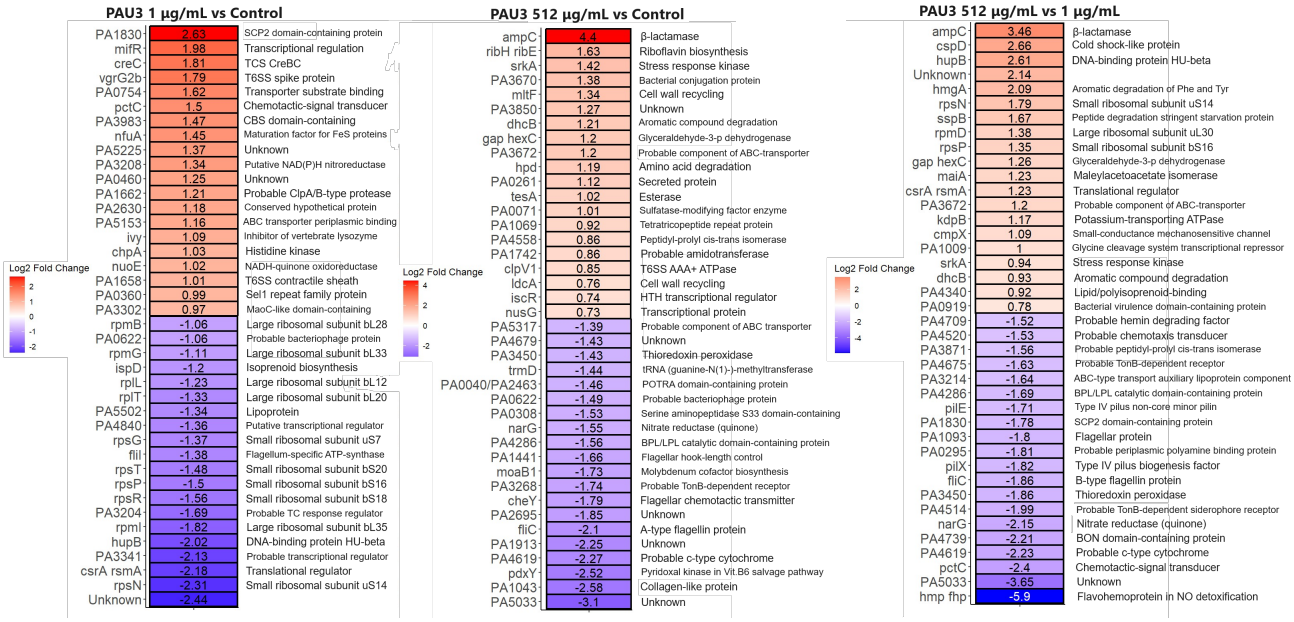

Figure 4.14. Heatmaps of top dys-regulated proteins PAU3. Heatmap showing the top 20 most up and down-regulated proteins and their function in PAU3 for all three comparisons. Up-regulated proteins are colored with a red color palette, and down-regulated proteins are colored with a blue color palette. Values inside each box is the Log_2 Fold Change value, which translates to relative abundance of each protein compared to the either the control or the 1 μg/mL Piperacillin condition. Title above each heatmap shows which comparison the heatmap applies to. Heatmaps were generated in RStudio.

The heatmaps in figure 4.14 visualizes the different proteins identified as dys-regulated in the three comparisons, as well as each proteins identified or probable function. AmpC, which was the highest up-regulated protein in both 512 μg/mL compared to control and 512 compared to 1 μg/mL, was not among top 20 up-regulated proteins in 1 μg/mL Piperacillin compared to the water control. In this comparison, ampC was not among the dys-regulated proteins at all (see table in appendix D). This shows that there is adaptation happening to the environment, and even at different antibiotic levels there is dys-regulation happening, where the most relevant resistance gene ampC is significantly up-regulated when comparing the highest antibiotic concentration both to the lowest one and to the water control.

PAU5 1 μg/mL Piperacillin compared to control:

Next, the proteome of isolate PAU5 was investigated. This was done in the same manner as for PAU3, and in this investigation of up-regulation the isolate exposed to the lowest piperacillin concentration (1 μg/mL) and 4 μg/mL Tazobactam, was compared to the water control. In figure 4.15 below, the resulting volcano plot for this comparison is shown. Additionally, a heatmap of the 11 up-regulated and 20 down-regulated proteins is shown on the left side of figure 4.18.

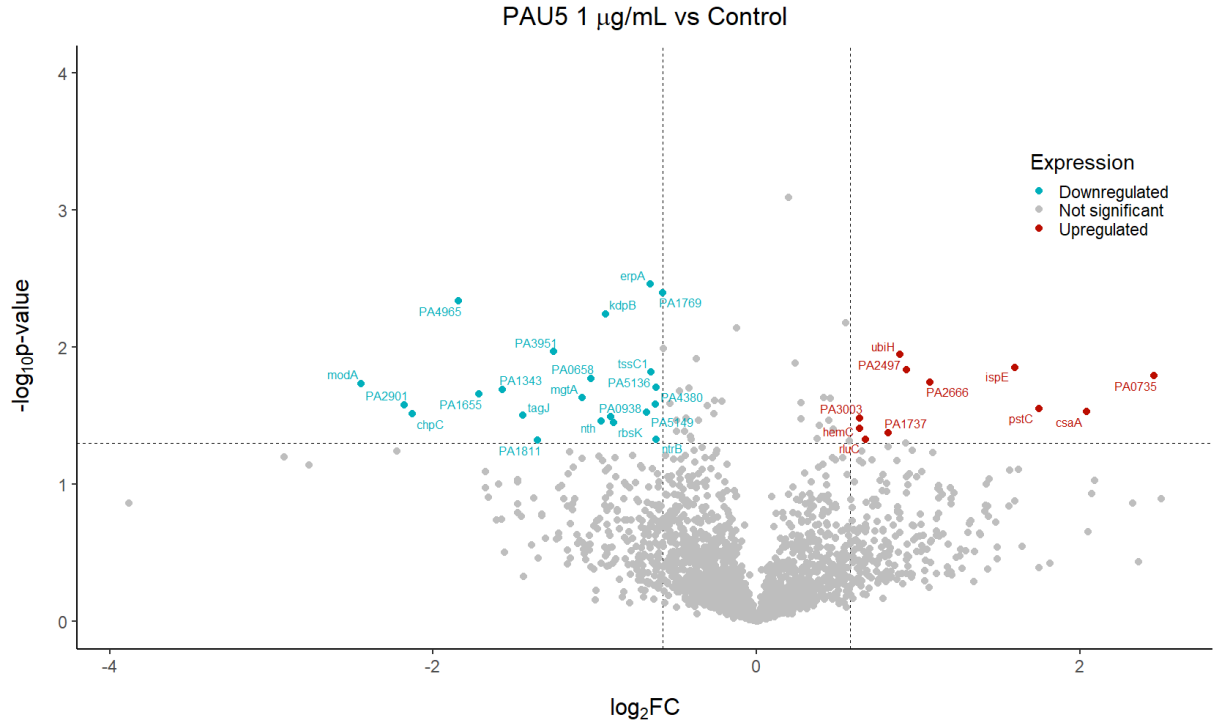

Figure 4.15. Volcano plot of PAU5 in 1 μg/mL Piperacillin vs. control. Volcano plot of PAU5 1 μg/mL Piperacillin (and constant 4 μg/mL Tazobactam) compared to the water control. 11 up-regulated proteins, and 20 down-regulated proteins are annotated in the plot. Up-regulated proteins are colored red, down-regulated proteins are colored blue. Not significantly dysregulated proteins, meaning a -$\log_{10}$p-value below 1.3 and a Log_2 Fold Change= -0.58<Log_2FC>0.58, are colored grey. Dashed lines shows threshold for being significantly dys-regulated. Graph was generated in RStudio.

There was a total of only 11 up-regulated proteins when comparing the two proteomes. Number of down-regulated proteins was 22, making it a total of 33 dys-regulated proteins. The most up-regulated protein, PA0735 ($\log_2$FC = 2.46), was not an annotated protein in the Uniprot database, but the second most up-regulated protein, csaA ($\log_2$FC = 2.04) was annotated. This is a protein secretion chaperone, involved in sec-dependent translocation of proteins in B. subtilis. It aids in folding of the proteins, and this chaperone is abundant in bacteria [194]. An hypothesis is that there might be a mechanism happening that is preventing proteins from folding correctly, which leads to up-regulation of this chaperone compared to the control. pH stress, temperature stress, salt stress and pressure stress all contribute to folding stability or instability and denaturation, which might be what is happening here [195]. Furthermore, in the article written by Devi et al. (2022), they talk about freezing/thawing and mechanical stress, heavy metals generating free radicals, generating ROS which leads to even more cellular stress and potentially cellular death [195]. PstC is the third up-regulated protein, and it is part of the phosphate transport system, and is involved in translocation of phosphate across the membrane. pstC forms the membrane channel together with pstA [196], and transports inorganic phosphate (Pi) from periplasm into the cytosol. IspE is a kinase involved in isoprenoid biosynthesis. Isoprenoids are involved in many vital biological functions, and the MEP pathway has been implicated in the virulence of other pathogens [174]. ubiH, another protein that was up-regulated ($\log_2$FC = 0.89) is an oxygenase part of ubiquinone biosynthesis, which is important in the electron transfer chain. Ubiquinone is

one essential coenzyme in the respiratory chain which is partly made up of isoprenoid units [197]. RluC ($\log_2$FC = 0.67) is a part of the ribosomal large subunit 50S, responsible for synthesis of pseudouridine from uracil in 23S rRNA. Pseudouridine is a modification made to the uracil which offers stability and aids in ribosome assembly. HemC ($\log_2$FC = 0.64), was the lowest up-regulated protein out of the annotated proteins. It is a porphobilinogen deaminase, part of the *hemCD* operon, and it is part of the heme biosynthesis pathway [198]. Heme is essential for both aerobic and anaerobic respiration, and some types of hemes function as transporter of oxygen while others transport nitrite or sulfite [199].

Down-regulated proteins consisted of the two proteins tssC1 ($\log_2$FC = -0.65) and tagJ ($\log_2$FC = -1.45), involved in type VI secretion system (T6SS). TssC1 plays a role in release of toxins targeting both eukaryotic and prokaryotic species via the T6SS, while tagJ is an accessory component in the T6SS. ErpA, another down-regulated protein is an iron-sulfur cluster insertion protein, which is thought to be involved in insertion of Fe-S cluster into apoproteins (where the prosthetic group of Fe-S will be placed). RbsK, ($\log_2$FC = -0.88), is a ribokinase which catalyzes the phosphorylation of ribose. The resulting product can be utilized in nucleotide, histidine, tryptophan synthesis, or as a component of the pentose phosphate pathway. KdpB ($\log_2$FC = -0.93) is a potassium-transporting ATPase, part of the ATP-driven potassium transport (Kdp) system, which transports K into the cytoplasm, while nth ($\log_2$FC = -0.96) is a DNA repair enzyme which releases damaged pyrimidines from the DNA. MgtA is a magnesium-transporting ATPase, and aids in magnesium influx into the cytosol. The third most down-regulated protein was the chpC ($\log_2$FC = -2.13), which is a protein that controls twitching motility-mediated expansion of the biofilm. It is part of a chemosensory system that affects the type IV pili. This protein is involved in response to host-derived signals like serum albumin, mucin (first line of defense for the lungs, lines the epithelium) and oligopeptides [200]. The most down-regulated protein was modA ($\log_2$FC = -2.45), and modA is a tungstate/molybdate/chromate-binding protein. It is involved in transport of molybdenum into the cell. Molybdate (MoO_4^{2-}) is important for nitrate reduction (metal ion binding). T6SS secretes molybdate-binding protein (ModA), and this system provides *P. aeruginosa* with both a growth advantage in bacterial competition under anaerobic conditions, as well as being important in virulence [201]. ModA uses another outer membrane protein (IcmP) to deliver the molybdate back into the cell.

PAU5 512 μg/mL Piperacillin compared to control:

The next comparison made, was that of PAU5 exposed to 512 μ/mL of Piperacillin (and 4 μg/mL of Tazobactam) and the water control. This resulted in a volcano plot, shown in figure 4.16 below, and a heatmap, shown in the middle of figure 4.18.

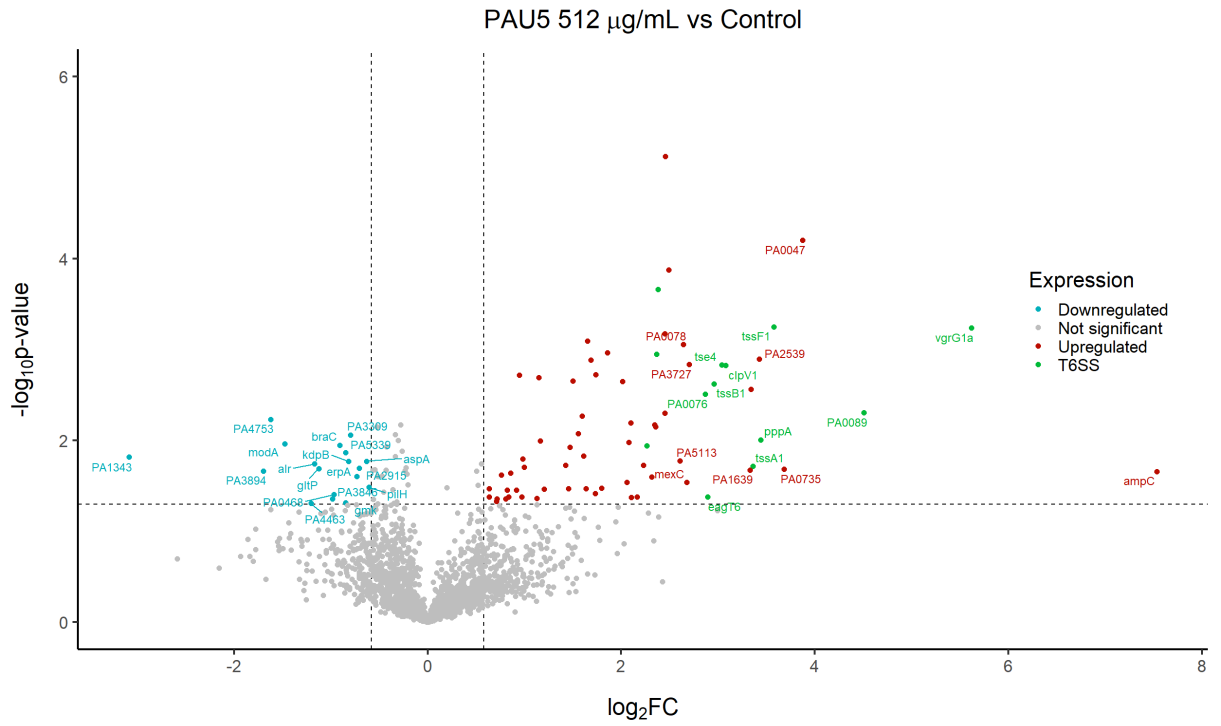

Figure 4.16. Volcano plot of PAU5 in 512 μg/mL Piperacillin vs. control. Volcano plot of PAU5 512 μg/mL Piperacillin (and constant 4 μg/mL Tazobactam) compared to the water control. Up-regulated proteins are colored red, down-regulated proteins are colored blue. Proteins known to be involved in the type VI secretion system (T6SS) are colored green. Not significantly dys-regulated proteins, meaning a -$\log_{10}$p-value below 1.3 and a Log_2 Fold Change= -0.58<Log_2FC>0.58, are colored grey. Dashed lines shows threshold for being significantly dys-regulated. Graph was generated in RStudio.

Figure 4.16 shows a lot more up-regulated proteins than down-regulated ones. In this comparison between the bacteria subjected to high concentration of antibiotic and the water control, there are only a total of 18 down-regulated proteins, while there were 70 significantly up-regulated proteins (see appendix E). The highest up-regulated protein was the β-lactamase ampC ($\log_2\text{FC} = 7.53$). Next, various proteins involved in the type VI secretion system (T6SS) was up-regulated. These included vgrG1a (a spike protein that allows delivery of tse6 toxin to target cells) [202], tssF1 (important in release of toxins), pppA (prepilin peptidase, identified as a regulator for the T6SS [203], tssA1 (a dodecameric ring-shaped structure at one end of the T6SS sheath), clpV1 (disassembly of the contracted sheath), tse4 (one of the toxins secreted by T6SS), tssB1 (work together with tssC1 by assembling and stacking which makes up the sheath around the tube proteins), and lastly eagT6 (essential in delivery of tse6 toxin by T6SS).

Furthermore, the volcano plot (4.16) shows other proteins not annotated but with green color that are also defined as a part of the T6SS. These proteins are tssC1, tagJ, tssM1, and tssK1 (tssK1 is not shown in the volcano plot due to p-value = 8.64795). Volcano plot was not made larger due to unfortunate clustering and of points closely situated in the plot when changing the range for the y-axis.

Down-regulated proteins included several uncharacterized proteins, and the proteins that have been characterized were pilH, aspA, erpA, kdpB, gmk, braC, gltP, alr, and modA.

pilH, is inferred from homology to be a part of signal-transduction system in regards to twitching motility, specifically extension and retraction of the pilus for twitching motility on a surface to happen. ErpA was also down-regulated in this comparison, just like in the previous comparison. ErpA was the protein involved in inserting Fe-S clusters into proteins. KdpB ($\log_2$FC = -0.82) was also seen as down-regulated in the previous comparison, and this protein was involved in transport of potassium. Gmk ($\log_2$FC = -0.85) is a guanylate kinase, aiding in recycling of GMP. BraC is a hydrophobic amino acid binding protein, as well as Threonine (T). It transports amino acids, and is present in the periplasm [204]. GltP ($\log_2$FC = -1.12), is a probable proton and glutamate/aspartate symporter, but this is an unreviewed annotation by Uniprot. Alr ($\log_2$FC = -1.17) is an alanine racemase that provides D-alanine by interconversion from L-alanine, for usage in cell wall synthesis (the only protein indicating that cell wall synthesis is down-regulated). modA was the most down-regulated protein in the previous comparison, and here it is one of the most down-regulated ones. ModA is, as described earlier, a molybdate-binding protein. The most down-regulated protein, PA1343 ($\log_2$ Fold Change = -3.08), is a protein that has been inferred from homology to be a Sn-glycerol-3-phosphate transporter (Uniprot database), and on pseudomonas.com it has been seen in expression of various isolates, both pathogenic and nonpathogenic strains [205]. Function or pathway of this protein is unknown.

PAU5 512 μg/mL compared to 1 μg/mL:

The last comparison made was that of the isolate exposed to the highest concentration of the antibiotic Piperacillin, and the lowest antibiotic concentration. This was investigated because the hypothesis was that the bacterium elicits a different response when subjected to different antibiotic concentrations. Different growth when performing the growth curve experiment was seen in the isolate exposed to different antibiotic concentrations, therefore it was thought that there would be a different proteomic response too (see figure 4.10). Figure 4.17 below shows the volcano plot of all proteins identified, with dys-regulated proteins colored red or blue, and with proteins involved in the type VI secretion system colored green. Lastly, the heatmap on the right handside of figure 4.18 showed the top 20 and bottom 20 dys-regulated proteins in this last comparison.

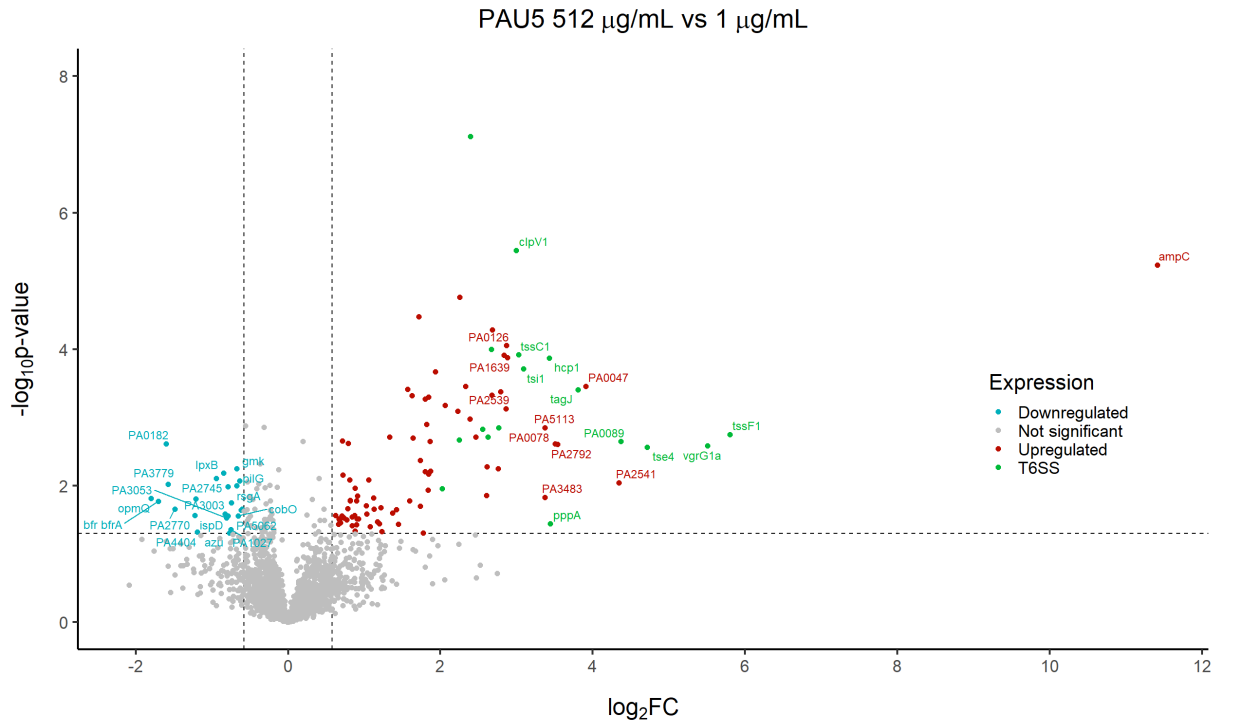

Figure 4.17. Volcano plot of PAU5 in 512 μg/mL vs. 1 μg/mL Piperacillin. Volcano plot of PAU5 512 μg/mL Piperacillin compared to 1 μg/mL (and constant 4 μg/mL Tazobactam). Up-regulated proteins are colored red, down-regulated proteins are colored blue. Proteins known to be involved in the type VI secretion system (T6SS) are colored green. Not significantly dys-regulated proteins, meaning a -$\log_{10}$p-value below 1.3 and a Log_2 Fold Change= -0.58<Log_2FC>0.58, are colored grey. Dashed lines shows threshold for being significantly dys-regulated. Graph was generated in RStudio.

Figure 4.17 shows a large response in the form of up-regulation. Number of dys-regulated proteins are skewed towards up-regulation, with 23 proteins being down-regulated, and 97 proteins being up-regulated (see appendix E for all dys-regulated proteins). The most up-regulated protein, with a $\log_2$fold change value of 11.41 was the β-lactamase ampC. Next, many of the proteins involved in the type VI secretion system (T6SS) were up-regulated (tssF1, vgrG1a, tse4, tagJ, pppA, hcp1, tsi1, tssC1, and clpV1). Their specific function is explained in the previous section, under PAU5 512 μg/mL Piperacillin compared to the control, apart from hcp1 (which was not identified as dys-regulated in the previous comparison). Hcp1 is a protein required for the assembly of the secretion apparatus HSI-I (which is one of the three type VI secretion loci identified in *P. aeruginosa*, with HSI being an abbreviation for Hcp secretion island) [206]. Various genes encoded in HSI-I has been found to be important in identifying target mammalian lung tissue, as well as being important for chronic *P. aeruginosa* infections of rat lungs [206].

All the remaining up-regulated proteins that are annotated in the figure, are proteins not annotated in the uniprot database, and they are denoted with PA followed by four digits. Down-regulated proteins include cobO, gmk, pilG, rsgA, azu, lpxB, ispD, bfr/bfrA, and opmQ. CobO, Corrinoid adenosyltransferase, is a part of corrin ring synthesis, e.g., for usage of corrinoid, which is a group of cobalt-containing compounds, in vitamin B12 [207]. Vitamin B_{12} is important in many metabolic processes, but also gene regulation. Gmk, guanylate ki-

nase, is responsible of recycling of GMP, while pilG aids in regulation of the twitching motility of type IV pilus. PilG is coupled to the chemosensory system chp, but it also regulates cyaB, and cyaB is a protein serving as a critical control point for virulence gene regulation [208]. RsgA, is part of the 30S ribosomal subunit, while azu is important for transfer of electrons in the denitrification process in *P. aeruginosa*, where nitrate (NO_3^-) is reduced to molecular nitrogen (N_2). LpxB, is part of the biosynthesis of the lipopolysaccharide (LPS) moiety lipid A. From the introduction (section 1.7.2), we know that LPS is important for virulence and here it is down-regulated ($\log_2$FC = -0.85). IspD ($\log_2$FC=-1.22), is a protein which, along with ispE (up-regulated in the first comparison), is involved in the MEP pathway. Research points towards this protein being important in combating oxidative stress by reactive oxygen species (ROS) [174]. Bfr ($\log_2$FC = -1.70), is a bacterioferritin, or an iron-storage protein. A ferroxidase center binds Fe^{2+} ions, oxidizes them then participates in mineral core formation. OpmQ ($\log_2$FC = -1.80) was the most down-regulated protein, and this is a probable outer membrane protein, involved in secretion of newly synthesized pyoverdine (PVD) but also release of PVD after it has delivered iron into the cell (serving as a part of the iron uptake pathway) [209].

Figure 4.18 below shows the three heatmaps generated for the three conditions compared.

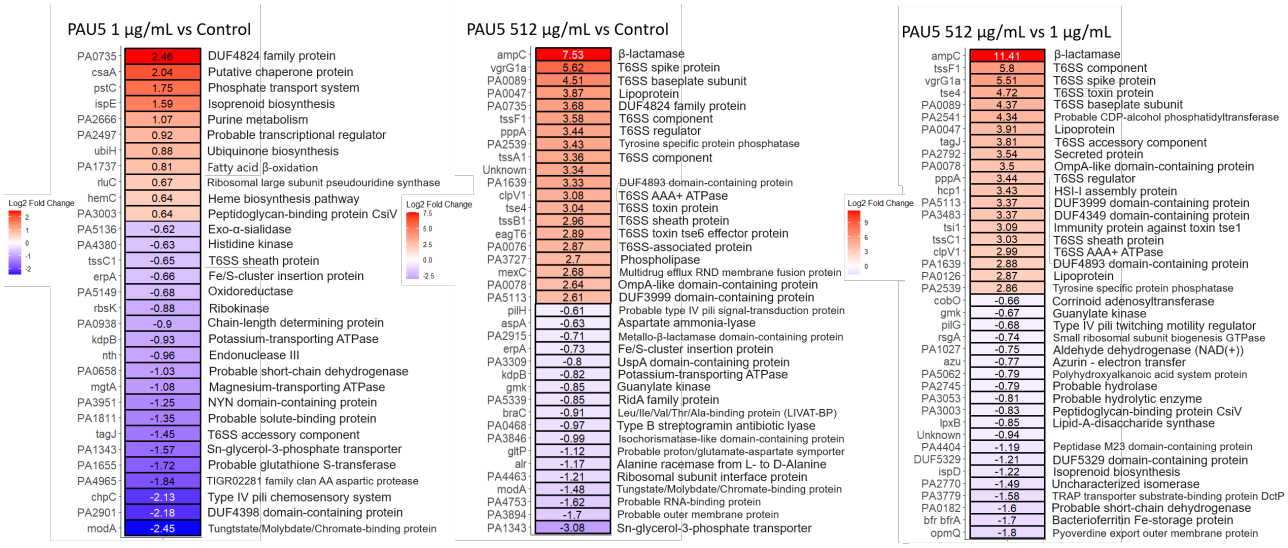

Figure 4.18. Heatmaps of top dys-regulated proteins PAU5. Heatmap of PAU5 showing top up and down-regulated proteins and function for each protein. Up-regulated proteins are visualized with red colored boxes, while down-regulated proteins are visualized with blue colored boxes. The values inside each box is the Log_2 fold change value for the specific protein. The first heatmap on the left side showcases 11 up-regulated proteins because that was the total up-regulated proteins. The second heatmap shows 18 down-regulated proteins because that was the total number of down-regulated proteins. The rest shows 20 up-regulated and 20 down-regulated proteins. Heatmaps were generated in RStudio.

The heatmap illustrates that there is diversity in which types of proteins are most dys-regulated. In the first heatmap on the left, there are 11 up-regulated proteins in total, while in the second and third there is a large up-regulation of proteins. In both the second and third heatmap, the largest up-regulated protein is ampC, followed by several type VI secretion system involved proteins (neither of which are up-regulated in the first heatmap). Up-regulation of ampC is largest when comparing PAU5 subjected to 512 μg/mL of Piperacillin

with PAU5 subjected to 1 μg/mL of Piperacillin.

4.7.3 STRING Analysis of AmpC

After conducting a thorough research on the proteins identified as dys-regulated in each condition (both low and high antibiotic concentration), the data showed that the ampC β-lactamase was highly expressed in both the high and low concentration of antibiotic compared to the control. It was therefore of interest to investigate what proteins this lactamase has been shown to be in a network with. To do this, STRING analysis was performed. First, multiple protein STRING analysis was performed between the various type VI secretion system (T6SS) proteins and the β-lactamase to see whether these were either genomically closely situated, whether they have been shown previously to be co-expressed, or if there were any interaction at all between the T6SS and ampC. STRING showed that T6SS and ampC were not in network with each other, meaning they have neither been seen as co-expressed, in genomic neighborhood (closely situated in the genome), nor in co-occurrence (gene families where occurrence patterns across various genomes show similarities) with each other.

Next, STRING analysis network search of ampC alone, revealed the enzyme being in a protein network with many different proteins. This is shown in figure 4.19 below.

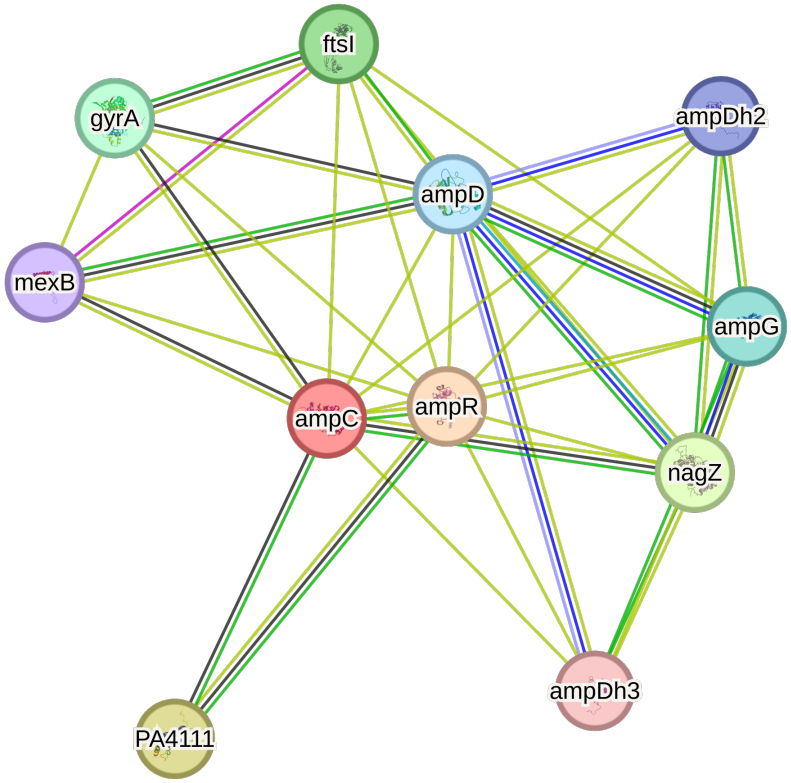

Figure 4.19. STRING analysis of AmpC. Using STRING, version 12 for visualization of protein network ampC is involved in. Dark green line signifies gene neighborhood = Genes that are frequently observed in each others genomic neighborhood. Dark blue line shows gene co-occurence = gene families where occurrence pattern across genomes show similarities. Black line signifies co-expression = across many experiments, the proteins for the genes have been observed to be correlated in expression. Light green line shows textmining = proteins that are frequently mentioned together in scientific articles. Light blue line shows protein homology = meaning common ancestry between two proteins. Purple colored line shows experimental determination = the proteins have been experimentally determined.

STRING analysis showed that ampC is in a network with ampC transriptional regulator AmpR, gyrA protein which is the DNA gyrase subunit A that is involved in DNA replication, transcription, recombination and repair (GyrA was investigated in regards to sequence in section 4.5.3). AmpC is in a textmining network with all proteins except PA4111. PA4111 is a protein of unknown function, and when investigating homologs to this protein among STRING organisms, it shows other proteins that are also not annotated or unknown in regards to function. AmpC and AmpR furthermore shows being in a genomic neighborhood, and having an intergenic distance of 148 bp (score = 0.524). Intergenic distance are the stretches of DNA between two genes, and in this case the distance between ampC and ampR. The score is a score given by STRING, which are scores of confidence, i.e., how likely STRING judges an interaction to be accurate or true [210]. AmpC is also in network nagZ, which is a protein involved in peptidoglycan recycling. This network makes sense, considering ampC is involved in inhibiting a β-lactam from binding the penicillin-binding proteins that perform the transpeptidation step in cell wall synthesis. Neighborhood in

genome has not been seen in these two proteins, but in two homologous genes (score = 0.066). Co-expression is not seen in these two proteins, but in homologs of these proteins, co-expression has been identified (confidence score = 0.146). Other proteins AmpC is in co-expression network with, is mexB (score = 0.084), gyrA (score = 0.042) but this has only been seen in homologs. MexB is a part of the MexAB-oprM efflux system (the efflux system is explained in section 1.9.2).

When searching for the proteins shown to be in network with ampC, neither of them were found to be dys-regulated among any of the conditions. Slight up-regulation of ftsZ was found (in strain PAU3, 512 μg/mL condition compared to control), which again is shown in network with ftsI (one of the proteins shown to be in network with ampC in figure 4.19). The up-regulation was, however, not significant. Tables used for searching were the excel-files of all proteins identified. These tables are not included in this thesis, due to size limitations.

5 Discussion

5.1 Overview

P. aeruginosa is an opportunistic pathogen often seen as multi-drug resistant (MDR), and it is one of the most common causes of respiratory infections in hospitalized patients [16][39]. It is a widespread issue that affects immunocompromized patients in all areas of the world. In this thesis, seven clinical isolates of the opportunistic pathogen has been sampled from patients suffering with the genetic disease cystic fibrosis. Sampling was done at Ullevaal University Hospital in 2020, and the clinical isolates have been investigated with antibiotic resistance in mind. In this discussion section, results obtained from both determination of MIC, whole genome sequencing, and proteomics will be discussed for each isolate. Proteomics results for isolates PAU3 and PAU5 will be discussed in a separate section below.

5.2 PAU1

Minimum inhibitory concentration (MIC) analysis on PAU1 revealed it was difficult to obtain reliable results in the control agar plate (plate was overgrown by colonies in one spot, or there were too many colonies in the control plate). MIC analysis was performed in several rounds on this isolate, before changing one step in the protocol (dilution of bacteria from $OD_{600} = 0.1$ to $OD_{600} = 0.02$) (see section 3.4 for the protocol). This gave good results, which might be due to lower bacterial input. This isolate might have a higher growth rate, or there might have been an error in the experiment leading to overgrowth (see section 3.3). Some problems that may occur is production of biofilm, which will complicate counting of individual bacteria, or that the bacteria adhere to each other [42].

The MIC analysis showed PAU1 was resistant against the DNA gyrase-acting antibiotic ciprofloxacin, and large discrepancy was seen when testing in Mueller-Hinton Broth compared to RPMI-LB10 (MIC reduced in RPMI-LB10 medium). Changing the medium had a large effect on the bacterium's ability to resist damage performed by the antibiotic. With Tobramycin, on the other hand, MIC was increased when testing in RPMI-LB10 medium. The effect of media on MIC values has been tested before, by Heithoff et al. (2023), and they saw that when changing from the standard nutrient-rich medium MHB, to a mammalian cell-culture medium (DMEM), around 15 % of the MIC values predicted a change in susceptibility so large that it could cross a clinical breakpoint, going from susceptible (S) to resistant (R) [211]. Furthermore, they saw an increase in diagnostic accuracy when antibiotic susceptibility testing was carried out in the cell-culture medium rather than MHB medium. This could be due to the cell-culture medium more closely mimicking a host-pathogen environment than the nutrient-rich MHB medium [211].

Whole-genome sequencing revealed PAU1 did not have the efflux pump MexXY-OprM (see figure 1.4). This pump is important in aminoglycoside (e.g., Tobramycin) efflux which might be an explanation for the low MIC value in the MHB medium. In MHB medium, growth is expected to be high, which also means high influx of various components present in the medium (e.g., nutrients, but also antibiotics). If efflux of the antibiotic again is not possible because the strain does not possess the correct efflux pump, this would explain the low MIC

value in the MHB medium (especially when compared to the nutrient-poor RPMI-LB10 medium). The other efflux pumps MexAB-OprM, MexCD-OprJ, and MexEF-OprN were present, and these three pumps all help in efflux of fluoroquinolones such as ciprofloxacin [1], which the isolate showed resistance towards in the MHB medium.

The number of genes involved in the two-component regulatory system found in PAU1 was the second highest of all strains (see table 4.8). These included both genes encoding proteins directly involved in the system, but also genes serving as regulators for expression of various two-component systems. The two-component system is known to be important for persisting in tough or ever-changing environments, which is a niche *P. aeruginosa* is well adapted to (see section 1.3 for more theory on the two-component system). The type VI secretion system (T6SS) was another virulence factor with varying number of hits in the different genomes. The number of genes present for each system did not stand out from the other clinical isolates, which was also the conclusion from investigating presence of virulence factors and resistance genes. Analysis of the genomic content could not explain the Ciprofloxacin resistance.

Multiple sequence alignment (MSA) of GyrA and ParC was of interest for this isolate because GyrA and ParC is the target for Ciprofloxacin (figure 4.5. The common mutation in the GyrA sequence mentioned in the results section 4.5.3 (Threonine (T) to an Isoleucine (I)) often seen in resistant strains, was not identified in PAU1. This further indicated that there might be another mechanism important for resistance present in PAU1, such as an efflux pump, and considering no other substitutions were identified in the MSA, it is most likely another mechanism resulting in resistance, such as the efflux pump MexAB-OprM or MexCD-OprJ. Both of these efflux pumps are responsible for efflux of both β-lactams, fluoroquinolones, and tetracyclines [1], and both of these pumps were present in PAU1 (see table 4.7). In the ParC sequence, a substitution was found, but this gene had a D rank. This means that poor base calling might be the reason for the substitution, and not because it was factual. All isolates, however, showed the Gln84His substitution, indicating that base calling at this position was correct, but also that this was likely not the reason for resistance in PAU1 (considering not all isolates were resistant against CIP).

5.3 PAU2

PAU2 showed resistance against the fluoroquinolone Ciprofloxacin at the highest concentration tested during determination of MIC. When subjecting the isolate to the antibiotic in RPMI-LB10 medium, the inhibitory concentration was reduced to half of that in the Mueller-Hinton Broth (see table 4.2). However, when testing Tobramycin, the bacterium was able to grow at a 8-fold higher concentration of the antibiotic in the nutrient-poor medium RPMI-LB10 (compared to MHB medium), which is the opposite of what is happening when subjected to Ciprofloxacin.

An explanation for reduced inhibitory concentration towards ciprofloxacin in RPMI-LB10 medium might be because the isolate will be naturally more resistant in a nutrient-rich environment. PAU2 might be able to sustain a high level of efflux pump expression (due to carbon and energy sources being abundantly available) [212], and relevant for this antibiotic are

the efflux pumps MexAB-OprM and MexCD-OprJ (which can pump out fluoroquinolones). Changing to a nutrient-poor environment might have resulted in reduced levels of efflux pump expression which will not be efficient enough for efflux of the antibiotic, which there will still be high influx of into the bacterial cell. Tobramycin is taken up by diffusion across the outer membrane [1]. In PAU2 the efflux pump responsible for efflux of aminoglycosides, MexXY-OprM, was not identified. Therefore, it might be that in the MHB medium the MIC-value is low because the bacterium has a high growth rate due to nutrients being abundantly available. Increased growth, however, leads to increased presence of the antibiotic target, ribosomal RNA (rRNA), which makes the bacterium more susceptible towards the antibiotic. In the nutrient-poor medium, however, there is not as much nutrients present for the cell to use in metabolic processes. This may lead to a lowered metabolic level and lowered growth rate [99, p.230], and in turn possibly lowered abundance of the antibiotic target giving increased MIC-value. It might also be that the isolate has been previously exposed to Tobramycin in the nutrient-poor environment of the lung, giving the bacterium an adaptive advantage by e.g., hyperexpression of efflux pumps. Adaptivity comes with disadvantages, and the phenomenon of reduced fitness when antibiotic resistance appears is known to be a mechanism that happens. This might be an explanation for the low MIC value against TOB in MHB medium, where PAU2 has developed resistance in a nutrient-poor milieu, leading to reduced fitness when exposed to a different milieu. The work of Rajer et al. (2022) found this to be true for plasmid-borne resistance, but also that the larger the resistance range (the higher the number of antibiotics a bacterium is resistant to), the larger the fitness cost [213]. Even though this was tested for plasmid-borne resistance, it might also be true for resistance conferred through the genome.

Ojkic et al. (2022) has looked at the phenomenon of different media and the effect of a translation-acting antibiotic, and they found that in nutrient-rich media (i.e., Mueller-Hinton Broth), cells became smaller to increase the surface-to-volume ratio (S/V) [214]. In the study they explained that this resulted in importing more nutrients per volume to counter the antibiotics' attempt to inhibit growth. Cells grown in nutrient-poor media (e.g., RPMI-LB10) became larger, which gave smaller S/V ratio. A reduction of S/V reduced antibiotic influx per volume, which also reduced the damage that the antibiotic was able to confer [214]. Morphology of cells was not investigated in this thesis, but this might very well be a characteristic also affecting resistance levels.

Flye assembly of genome after sequencing was not successful (probably due to the many contigs), but when using Canu assembly which is better with samples that has many contigs, assembly was slightly improved. Still many contigs remained, and mean coverage was far below the threshold of 50 % (see table 4.6). Analysis of genomic content further revealed several genes present in all other isolates were not detected in PAU2 as shown in table 4.7. PAU2 was highly viscous when performing DNA extraction, which might explain the poor sequencing results. It is possible that viscous DNA led to clogging of the Nanopore when performing sequencing [134]. Another problem could be too fragmented DNA due to too harsh treatment when attempting to solubilize the viscous DNA [134]. When mean coverage in addition was as low as 6 %, templates were probably too low in concentration for there to be enough signal intensity the computer software could detect [134]. Due to poor sequencing results of this isolate, PAU2 was not included in the venndiagram in figure 4.6. Including

PAU2 in the venndiagram could have given skewed results due to wrong annotations or genes not found in PAU2 due to the fragmented DNA.

In regards to multiple sequence alignment (MSA) of the β-lactamase, GyrA, and ParC, PAU2 was included both in order to visualize what the result of poor sequencing might look like, and including it would not affect the results of the other isolates like it would have if it was included in the venndiagram. PAU2 was the isolate with the most mutations, and also with the sequences that varied the most from the other sequences that were aligned (in all MSA). A gyrA mutation was of interest, because it is often seen in cystic fibrosis patients that has undergone prolonged treatment of Ciprofloxacin (see figure 4.5 for alignment). This antibiotic was also the only antibiotic that PAU2 showed resistance values against. Considering this fact, it is not impossible that the base calling at this position was correct. ParC, the last alignment, showed the sequence of PAU2 being much longer compared to the other sequences of the other isolates. This further underscored the point of poor base calling and unreliable results. Indeed, genes obtain mutations and bacteria can increase mutation rates in stressed environments, but an addition of 79 amino acids in the ParC sequence seems unlikely in all thinkable scenarios.

5.4 PAU3

PAU3 showed resistance values against Piperacillin/Tazobactam (TZP) and Ceftazidime (CAZ). The isolate was able to withstand high concentrations of peptidoglycan-acting antibiotics except for Meropenem, which inhibited growth at much lower concentrations making it more effective than both TZP and CAZ. MEM, which is a carbapenem, has shown to be stable against many different β-lactamases, including extended-spectrum β-lactamases and AmpC-enzymes. This is of particular interest for this isolate, because overexpression of an ampC enzyme was identified in the proteomics analysis of this isolate (see section 5.10 below). If that is the only β-lactamase in its arsenal, it will indeed work better against TZP and CAZ, but not against MEM, considering a class D β-lactamase, with its highly hydrophobic active site is needed for cleaving the carbapenem β-lactam ring (see section 1.9.5 for theory on the β-lactamases).

Venndiagram in figure 4.6, showed PAU3 and PAU5 did not share any genes that were not also shared with the other strains. When looking at the venndiagram made between PAU3 and PAU5, there was a substantial amount of genes characterized as cloud genome (see figure 4.7). This might be an explanation for the different MIC values seen between the two isolates, and furthermore the difference in response during the proteomics analysis. Genomic differences between the two isolates were not found in virulence factors and various resistance genes, but regulatory genetic differences might still have happened leading to different proteomic responses.

PAU3 growth curve in 32 μg/mL Piperacillin (section 4.6) did not yield a nice growth curve like in the other antibiotic concentrations, and the suspicion was that there was some error performed during the experiment such as an error during pipetting. In the highest concentration of the antibiotic, PAU3 was not totally inhibited from growing, and gave a nice growth curve. A study performed by Tomaselli et al. (2003), showed that in infected

lung tissue, the maximal tissue concentration (C_{max}) of Piperacillin was 176 ± 105 μg/mL [215]. When comparing the concentration in Tomaselli et al.'s study to the concentration PAU3 was subjected to in the growth curve experiment and proteomics experiment (which at lowest difference was 231 μg/mL higher than what Tomaselli et al. found), it is safe to say that this isolate is highly resistant against this antibiotic. One explanation for the high resistance might be that the substitutions detected in the ampC sequence of PAU3 in the multiple sequence alignment (see figure 4.8), somehow conferred increased affinity between the β-lactamase and the β-lactam antibiotic, making the lactamase highly effective against the antibiotic. Another explanation might be that simultaneous hyper-expression of the various efflux pumps could have contributed to the very high resistance level, which is a response that has been seen before [1]. This would further explain the high resistance value against Ceftazidime, which is also a β-lactam.

Proteomics analysis revealed many different proteins, and the discussion for this part of the thesis will be covered in the proteomics discussion section (section 5.10).

5.5 PAU4

PAU4 showed increased MIC value in RPMI-LB10 medium for TZP, MEM, TOB, and CST compared to in the MHB medium. The MIC value when exposed to MEM in RPMI-LB10 medium would classify this isolate as resistant against the antibiotic if the medium was Mueller-Hinton Broth because it is above the breakpoint value set by EUCAST (see table 3.2), and this underscores the importance of knowing how the medium affects antibiotic susceptibility (but also that this might be a flawed method for susceptibility testing, and that such testing in nature is difficult). RPMI-LB10 medium more closely mimics the condition in the cystic fibrosis (CF) lung, therefore seeing such high MIC values could mean that this isolate might actually be resistant towards this antibiotic even though it would not be detected since all resistance testing is done in MHB medium. In RPMI-LB10, slow growth and thereby down-regulation of transcription, translation, and replication might be preferred. Down-regulation not only removes a lot of antibiotic targets, it also helps in evasion of the immune system present. Lastly, it preserves the few nutrients that are available, and being present in the mucus-filled CF lung means needing to preserve energy, focus on essential pathways, and through that achieve at least persistence (and through that be characterized as resistant).

An overall problem with the DNA extraction was that the high-molecular weight DNA was highly viscous (as explained in section 5.3). This could also have affected PAU4, and in this case the confidence of the nucleotides at each position was lower (poor base calling).

Alignment revealed the problem with base calling. The ParC gene in PAU4 was highly different from the other isolates, both in regards to length and amino acids at each position. The β-lactamase gene was, however, not different from the other isolates, and this shows that even though base calling might have been less certain there is still a lot of correct base calling happening. Virulence factors, resistance genes, and number of genes involved in specific systems identified in this isolate did not deviate from the other strains (like PAU1, PAU2, and even PAU3 did) (see table 4.7. Therefore, the MIC values seen in PAU4 is

thought to be conferred by expressional changes (e.g., hyperexpression of ampC), and not by its genomic potential. Lastly, PAU4 was the isolate with the highest MIC value against MEM, pointing to a potential different β-lactamase than ampC being present in this isolate.

5.6 PAU5

PAU5 earned the label multi-drug resistant (MDR) through MIC testing. To be given the label MDR, the strain or isolate must have a resistant value against 3 or more antimicrobial categories, which is shown in table 4.2 (TZP, CIP, TOB, and CAZ) [18]. In the MEM antibiotic, which is another β-lactam, it was not able to grow at all. Proteomics revealed PAU5 produced large amounts of the β-lactamase AmpC as a response, which might explain the high susceptibility towards MEM. MEM has been shown to be stable, meaning not be degraded when subjected to the ampC lactamase (see theory in section 1.9.5). If ampC is the only lactamase produced by PAU5, this could explain why it is not able to confer resistance against the third β-lactam antibiotic.

The largest differences in growth between media was seen in the PAU5 isolate. When exposing the isolate to any of the antibiotics in RPMI-LB10 medium, the isolate was not able to grow at all (see table 4.2). This could mean that the isolate is adapted to living in a nutrient-rich environment, and when nutrients are removed, the bacterial cells are not able to persist in the presence of antibiotics. One adaptation that can happen in nutrient-rich media, is that of increasing uptake of nutrients to counter the antibiotics attempt to inhibit growth [214]. An adaptation seen in Ojkic et al. (2022) study, was that bacteria in nutrient-rich media became smaller in order to increase the surface-to-volume ratio (S/V) [214]. This resulted in increased uptake of nutrients by keeping the cells as small as possible (maybe to limit the damage an antibiotic was able to impose on the cell). This observation can be translated into this experiment, because when switching to the nutrient-poor RPMI-LB10 medium, uptake of antibiotics continued to be large, but now there was low nutrient influx due to nutrient scarcity. The antibiotics actually becomes even more effective in the nutrient-poor medium, and this might be the reason for the low susceptibility seen in PAU5 in the RPMI-LB10 medium. PAU5 stands out from the other isolates, which makes it natural to think that PAU5 has been present in another environment than the other isolates. Furthermore, a fitness cost might have happened in this isolate to confer antimicrobial resistance against that many antibiotics in the MHB medium, and this is based on the study that Rajer et al. (2022) performed [213]. None of the isolates did, however, show any presence of plasmids, but seeing as the Flye assembly had issues with this isolate due to too many contigs, there might be plasmids and even plasmid-borne resistance genes present in this isolate that was not identified.

Sequencing showed that the genome size for PAU5 varied between the two different assemblies that were used. It is well-known that when using different genome assemblies, variables such as genome size will vary with the softwares used [134]. This will again affect gene number predictions. For genome analysis, Canu assembly results were used for PAU5. Flye assembly resulted in many contigs, and this might be because Flye is optimalized for circularization of prokaryotic genomes where there is one contig and the result is a software that yields the fewest sequencing errors [216]. The down-side of Flye assembler is that it is not good when

your sample has many contigs (like PAU5 did) [134]. The circularization problem is a known issue, and Canu (which performs better at genomes with more contigs), does not do as good a job with the circularization issue as Flye does. Therefore, there are pros and cons to any software used. When using Canu, number of contigs were reduced, and mean coverage was slightly increased. This is why Canu assembly results were used for the genomics part [134]. Since the sequenced genome would be used for gene search as well as mapping of proteins during proteomics, primarily, the problem with relatively low mean coverage and the two contigs would most likely not impose a large problem (but rather during MSA due to poor base calling). Gene duplication, which was the highest out of all isolates, could however affect the downstream analyses performed (e.g., counting number of hits for systems and virulence factors like in table 4.8). The high gene duplication number and the genome size might be accurate, but it might also be because a different assembler software was used.

PAU5 was the isolate with the most unique genes present in its genome, and this might explain the high resistance values seen in four out of the six antibiotics tested during MIC analysis. It had the most unique genes in common with PAU6, but responses were not alike when investigating MIC. PAU5 was the only isolate resistant against Tobramycin (TOB) in MHB medium, and this might be explained by the high number of unique genes in the isolate. PAU5 and PAU3 compared in the venndiagram in figure 4.7, showed that PAU5 had a lot of cloud genome. The discrepancy between number of unique genes in PAU5 compared to the other isolates might be why it has the ability to persist in such high antibiotic concentrations across many different antibiotic classes. Investigation of resistance genes and virulence factors did, however, not reveal any genes that were only present in PAU5 or abundantly present, hence it is likely that genes involved in other pathways might be what is seen in the cloud genome. It is furthermore a possibility that substitutions in regulators for resistance genes is the reason for the high resistance level. Other explanations might be modifications to the outer membrane structures such as lipopolysaccharide (LPS) structure [217]. The LPS is known to be important in resistance against cationic antimicrobial peptides, which are short peptides secreted by both immune cells and epithelial cells in a host, polymyxins, but also membrane permeability (which is relevant for antibiotics taken up by diffusion [1] [217]. If modifications such as lowered net negative charge has happened to the LPS, this could reduce uptake of other antibiotics as well as polymyxins (e.g., the positively charged Tobramycin, uptake by diffusion) [57]. Another important factor is the amount of porins in the outer membrane, or substitution mutations in the sequence of the porin gene [1]. β-lactams and quinolones are dependent on porins for uptake, hence introducing mutations to porins might reduce, or theoretically completely inhibit interaction between the antibiotic and the porin for influx [1].

Multiple sequence alignment of class C β-lactamase, GyrA, and ParC gave no results that could explain the MDR phenotype (see section 4.5.3 for results). Table 4.7 showed that PAU5 did not have the gene for Exotoxin A (ExoA), which is a toxin released by the type III secretion system (T3SS). It did contain the T3SS, meaning either there are other effectors present that serve the same job as ExoA, such as the ones depicted in figure 1.4, or there has occurred an error while assembling the genome back together resulting in either loss of the gene encoding the toxin or wrong annotation. Table 4.8 showed that PAU5 had fewer genes involved in various systems, which might be due to poor sequencing results, but it might

also be correct and an adaptation (a fitness cost in order to confer large resistance range[5]) [213]. The isolate has been shown to grow at higher concentrations of all antibiotics when grown in a nutrient-rich medium (except for Meropenem MIC testing), and when coupling this to lower number of hits for various systems in this isolate (e.g., flagella genes), what might be happening is gene loss by deletion. Gabrielaite et al. (2020) showed in a study that *P. aeruginosa* tends to loose genes, especially those associated with virulence during chronic infection [218]. It might therefore be an adaptation for evasion of immune system while at the same time minimizing genome size which has implications for metabolic rate as well as growth rate. Furthermore, as explained in section 1.3, what can happen over time, is a shift towards auxotrophy where an isolate becomes more dependent on the environment for delivery of nutrients. Over time, genes are deemed as superfluous, and through natural selection and evolution through bacterial generations, the genes that are not essential for survival will by chance be deleted, but still yield viable progeny, and over time auxotrophic isolates.

The various growth curves generated showed that at the highest concentration, the curve showed a slight dip which might translate to a briefly higher level of cellular death than cellular growth before the cellular growth was increased again (figure 4.10). This might be due to the degradation of the antibiotic, that over time results in lowered concentration which enables bacterial growth more than when the antibiotic concentration was higher. An attempt to explain this is given below.

The half-life of Piperacillin and Tazobactam has been extensively studied, but the estimates vary a lot. According to drugbank, the half-life of Piperacillin is between 36 and 72 minutes, and the half-life of Tazobactam is between 0.7 h and 1.2 hours (but depends on what β-lactam it is given in combination with) [219][220]. Other sources claim that when used in treatment, half-life was 4.3 $\pm$ 1.2 h. The half-life of Tazobactam was 5.6 h $\pm$ 1.3 h [221]. NCBI states that 94-97 % of a drug will be eliminated after 4-5 half-lives when given to a patient, in this case meaning somewhere between 162 to 324 minutes (or 2.7 h to 5.4 h) [222].

What this theory entails, is that the half-life of the antibiotic might have inhibited the isolate in the highest antibiotic concentration until all TZP was eliminated. The stability of the antibiotic is likely higher in a growth medium compared to the in-vivo measurements stated above, therefore this might explain the dip in the growth curve showing up at around 9 hours instead of earlier. It might also be that the isolate was able to use the inactive antibiotic as a carbon source, making the increase after the dip even more visible. A study done by Ranjan et al. (2021) showed that pandrug-resistant *Pseudomonas* sp. were able to utilize ampicillin as a sole carbon source, showing that this happens within the *Pseudomonas* genus [223].

The other growth curves at lower Piperacillin concentration were able to grow progressively more as the concentration of antibiotic was lowered. Lastly, the lowest concentration showed bacteria growing in similar fashion as the control, underscoring the low effect this antibiotic concentration had on the growth rate of the isolate. When comparing all growth curves made for PAU5, the growth maximum usually stopped at an absorbance level substantially lower than PAU3 (see figure 4.9 for PAU3, and figures 4.7, 4.8, and 4.10 for PAU5). This

[5]Resistance range means the various antibiotics an isolate or a bacterial species is resistant against.

might be due to either genomic differences (as was detected during genome sequencing), or it might be due to expressional differences between the isolates as was seen during proteomics analysis. Proteomics analysis revealed many different proteins, and the discussion for this part of the thesis is covered in the proteomics discussion section (section 5.10).

5.7 PAU6

PAU6 did not show resistance against any of the antibiotics, but it did show largely increased MIC value in the RPMI-LB10 medium when exposed to TZP (see table 4.2). It seemed as if the isolate was adapted to living in the nutrient-poor medium, as has been seen with several of the other isolates. The largest increase in MIC value when changing to RPMI-LB10 medium,was seen in CST and TZP (4-fold increase in both). When investigating the genomic potential of this isolate, it showed to have many unique genes as well as the largest genome size (see figure 4.6 and table 4.6), but this did not result in the isolate being highly resistant (e.g., like PAU5). No unique virulence factors or resistance genes were identified in PAU6. PAU6 had the most TCSs genes (table 4.8), and usually the number of TCS genes indicates ability to quickly adapt and persist in rapidly changing milieus 1.3. This could be the case for PAU6, because it is able to persist in both the nutrient-rich MHB medium, and the nutrient-poor RPMI-LB10 medium. The differences in the milieus are large, but the MIC values for this isolate does not change drastically (as it does for PAU5). PAU6 might be able to make use of its many TCS genes to quickly adapt.

In regards to alignment of the β-lactamase, both PAU6, PAU7, and the ATCC27853 showed roughly the same MIC value against TZP in MHB medium. This might be explained by the fact that these isolates inhabit the same substitutions in their β-lactamase gene, as shown by the alignment (section 4.5.3). They also responded by an increase in MIC value when switching to RPMI-LB10 medium, but this is likely not explained by the β-lactamase sequence, but rather explained by a change in efflux pump expression, reduced uptake of the β-lactam through the OprD porin (which was present in all isolates, see table 4.7), or other adaptations made possible by the TCS.

5.8 PAU7

PAU7, showed overall increased MIC values when exposed to the antibiotic in the RPMI-LB10 medium, and proved to be an isolate better adapted to persist in antibiotic exposure when nutrients were scarce. It did not, however, show any values above the threshold for being considered resistant. This might be explained by no previous exposure to the antibiotics, which again will not elicit a cellular response (e.g., by the help of TCS). In regards to MSA and genomic potential, it was not identified any specific adaptations that deviated from the other isolates, apart from having the same substitutions in the β-lactamase gene as both PAU6 and ATCC15692 (explained in section 5.7 above). This substitution might have helped it when exposed to the β-lactam, with the lactamase having either improved efficacy or affinity towards binding with the β-lactam Piperacillin.

5.9 Summary

According to the e-handbook provided by Oslo University hospital [77], the first drug that is utilized during treatment of *P. aeruginosa* infection in patients with cystic fibrosis, is Ciprofloxacin (CIP), in addition to either Colistin (CST) or Tobramycin (TOB). CIP was the antibiotic that isolates in this thesis showed most resistance towards (4 out of 7 isolates showed resistance). If patients have been treated firstly with CIP, it makes sense that so many of the isolates confer resistance against it. There are several reasons why CIP resistance is so prevalent in these isolates. One reason could be mutations in the porin responsible for quinolone influx leading to reduced influx of the antibiotic. This can delay, or even inhibit, the antibiotic from reaching its target (DNA gyrase) inside the bacterial cell. Another hypothesis for the prevalence of resistance could be due to hyperexpression of efflux pumps that effectively pump the antibiotic out of the bacterial cell. The most obvious reason is that of substitutions happening to the target, gyrA or ParC, but substitutions identified in previous studies in *P. aeruginosa* isolates showing resistance, was only identified in PAU2.

Antibiotics often utilized for treatment of chronic *P. aeruginosa* infection in patients with cystic fibrosis, are aminoglycosides (e.g., Tobramycin) and various β-lactams. Several different β-lactams are used, such as Ceftazidime (CAZ) and Piperacillin/Tazobactam (TZP). TZP resistance, especially, was prevalent in the MIC analysis and the reason for this might be the class C β-lactamase identified during sequencing. There might be hyperexpression of the ampC enzyme going on, which was proven to happen in the proteomics analysis of PAU3 and PAU5. This further proves that mutations in the sequence of the resistance gene is not the only way to achieve resistance; hyperexpression might be just as effective, and it is indeed a common response seen in *P. aeruginosa* isolates, as explained in the review by Langendonk et al. (2021) [1].

It seems as if many of the isolates (PAU2, PAU3, PAU4, PAU6, and PAU7) are adapted to living in an environment where nutrients are scarce. This coincides well with the milieu of the cystic fibrosis lung. An adaptation might be to down-regulate metabolic processes, leading to slow and steady cellular growth. This aids the bacterium both in evading host immune responses by not expressing the arsenal of virulence factors it has in its genome, but also by reducing the amount of antibiotic target. A bacterial cell being in a dormant state can be very difficult to remove by the help of antibiotics, because most antibiotics are dependent on the cells actively dividing. The most common antibiotic is that of the β-lactams, but if the cells are not synthesizing cell wall at all, the antibiotic will have no penicillin-binding protein to bind to. A dormant state is something that is known to happen in chronic infection isolates of *P. aeruginosa*. The bacterium will down-regulate both virulence factors and other genes to avoid being detected or attacked, but also for shifting towards a more sessile state of growth (as shown in figure 1.3 and explained in section 1.6.2). Substitutions might also happen to the PBP, which can reduce affinity between the β-lactams and the protein, or even make the antibiotic completely ineffective (depending on the substitution).

During the MIC analysis, both improvements and declines of the MIC value was seen when switching from the nutrient-rich medium Mueller-Hinton Broth which is commonly used, to the more nutrient-poor medium RPMI-LB10. PAU5, which was considered to be MDR

based on testing protocols set by EUCAST, was not able to grow at all in the nutrient-poor medium at any concentrations in the dilution series. Would the label of MDR in the MHB medium have resulted in harsh antibiotic treatment (e.g., Colistin)? Harsh antibiotic treatment is known to also come with a lot of serious side effects. When adding the fact that bacteria causing chronic infection often are in a more sessile and less active state, it might not make sense to subject a patient to the harsh treatment that would probably not eradicate the bacterium anyway. The treatment might even induce adaptivity which would lead to even higher resistance, rather than eradicating the bacterium. The differences seen between media are thought provoking, and reveals that the method of determining susceptibility is flawed. High MIC value might not equate to antibiotic resistance, as isolate PAU5 clearly demonstrated.

5.10 Proteomics

5.10.1 Antibiotic Spiking

For a short recap of method, antibiotic spiking was performed on isolate PAU5, and the strain was exposed to either 32 μg/mL Ceftazidime, 0.0064 μg/mL Meropenem or 32/4 μg/mL Piperacillin/Tazobactam (see appendix F and G for all dys-regulated proteins).

Discussion of MEM proteomics:

The conclusion of this experiment was that the concentration of antibiotic was too low to trigger a particular response, in addition to the incubation time being too short. The concentration was set to approximately one half of the minimum inhibitory concentration determined in MIC, which was thought to give some indications, because adding concentration higher than the MIC value would result in the bacterium not being able to grow at all. A class D β-lactamase and a metallo-β-lactamase identified in the whole-genome sequencing was expected to be up-regulated in the MEM-exposed condition compared to the control. This is because these lactamases are carbapenemases, meaning able to inhibit carbapenems such as Meropenem (see section 1.9.5 for more theory). These lactamase was not identified as up-regulated.

Discussion of CAZ proteomics:

If the data seen from this experiment was a response triggered by being subjected to a cell-wall acting antibiotic, we might have seen some up-regulation of stress responses, and maybe up-regulation of cell-wall turnover as well as a β-lactamase. This was not the case, and only 25 proteins were dys-regulated in total compared to the control. One interesting finding was the down-regulation of iron-binding periplasmic protein, which might be a sign that the strain is down-regulating an adaptation to the cystic fibrosis lung where iron is scarcely available. In the proteomics experiment, there was iron available in the medium, hence it did not need as much iron-binding proteins for scavenging of the element. PAU5 showed high resistance against CAZ when performing MIC analysis. The strain was able to grow at all concentrations tested, therefore the second highest concentration used in the MIC analysis was chosen for proteomics. The same conclusion as in the MEM proteomics above seems highly likely, where the concentration of antibiotic was too low and incubation

time was too short for a clear response to happen. High intrinsic resistance in this isolate is also plausible, which might be why there is little to no difference in response between the CAZ subjected PAU5 and the control (more on intrinsic resistance in section 1.9.2).

Discussion of TZP proteomics:

In the antibiotic-exposed bacterium compared to the control, a down-regulation of a protein identified as a metallo-β-lactamase was seen (PA2915, see appendix G). This was the opposite response compared to what was expected, seeing as the antibiotic PAU5 is being subjected to is a β-lactam. Either the concentration was too low and incubation time too short to elicit a response, or there is intrinsic resistance present in the isolate. Another explanation might be wrong annotation of the protein during processing of proteomics data. The discrepancy between up and down-regulated proteins is large, and this might be interpreted as a reduction in cellular metabolism. If that is the case, PAU5 might actually have a response to the antibiotic. When comparing this hypothesis with the proteomics results from continuous antibiotic exposure of TZP, the response is quite different (which can be explained by the low antibiotic concentration of TZP in this experiment). It is possible that PAU5 performs down-regulation of metabolic pathways which might be enough for persistence in the low antibiotic concentration, while in the continuous exposure this response is not enough for the bacterial cells to survive.

5.10.2 Continuous Antibiotic Exposure

Proteomics with continuous antibiotic exposure was performed on isolates PAU3 and PAU5, with antibiotic concentration of Piperacillin/Tazobactam at either 1/4 μg/mL or 512/4 μg/mL.

In PAU3, the first comparison (lowest antibiotic concentration of Piperacillin, compared to control) showed triggering of CreC (two-component system (TCS) that responds to beta-lactams), Ivy (inhibitor of lysozyme) and some response to oxidative stress (nfuA), while down-regulation consisted of many different proteins involved in protein synthesis. At the same time, there was down-regulation of proteins involved in reacting to reactive oxygen species (ROS). The response seen in PAU3 shows that even though the antibiotic concentration was low (1/4 μg/mL), the isolate was already making adaptations and responding to it, but at the same time it was responding as if it was exposed to the immune system of a human host (Ivy, and nfuA). The two-component system CreBC was not seen up-regulated in PAU5, and this might be the reason why PAU3 was making adaptations already while PAU5, on the other hand, did not seem to make a lot of adaptations when being exposed to only 1 μg/mL Piperacillin and 4 μg/mL Tazobactam. It could be that PAU3 has been previously exposed to the antibiotic, and with the up-regulated CreBC system, it is able to recognize the antibiotic and elicit an immediate response.

In the two next conditions, the ampC β-lactamase was up-regulated in both PAU3 and PAU5 exposed to Piperacillin/Tazobactam (TZP). TZP is usually a weak inducer of ampC hyperproduction [224], but both PAU3 and PAU5 was seen producing large amounts of the protein in the 512/4 μg/mL condition compared to the other condition and control. It might be that ampC is the most efficient β-lactamase against TZP, because there is also

a β-lactamase inhibitor present in the antibiotic combination. The bacterium does not only have to inhibit the β-lactam, it also has to be either unaffected by the β-lactamase inhibitor, or it must produce such high amounts of the β-lactamase that the inhibitor is out-competed. There are many factors involved, both regarding the specific lactamase gene, but also regarding its regulators which highly contributes to the response (based on the large up-regulation of ampC).

Along with the ampC enzyme, PAU5 also showed large up-regulation of type VI secretion system (T6SS) proteins, while PAU3 did not. This is one of the virulence factors discussed in section 1.7, used for initiating infection and causing damage to surrounding bacteria. It might be that PAU5's two-component system is identifying the presence of the antibiotic as a competing bacterium secreting toxins to kill surrounding bacteria, hence up-regulation of T6SS happens. PAU3 in the second comparison (see heatmap in the middle of figure 4.14), also shows several proteins involved in protection against ROS, but also riboflavin synthesis which could be linked to host tissue damage by production of ROS/NO and cell wall recycling proteins. The response seems quick, specific, and successful, considering it also grew to drastically higher absorbance values than PAU5 when they were exposed to the same antibiotic concentration (see growth curves, in section 3.7.2). In the third condition of PAU3, there was a protein involved in persister cell formation significantly up-regulated (the second most up-regulated after ampC). This indicates that PAU3 might be trying to enter a dormant persister cell state where the antibiotic will not be able to impose any harm on the bacterial cells. PAU3 also diminishes expression of virulence factors such as flagellum, which is probably done for allocation of energy and further evasion of the antibiotic and immune system. This is probably also why the T6SS is not seen up-regulated in PAU3 (see acute to chronic infection section 1.6.2, and figure 1.3). Its action plan seems to be evasion and becoming a persister cell to wait for "better times", while for PAU5 it seems as if the plan is to fight off competition or to impose tissue damage on host cells as a way of either escaping the antibiotic or bacterial competition.

Isolates PAU3 and PAU5's ability to persist in the high concentrations of TZP during proteomics, shows that the dilution series for the MIC analysis should probably have been larger to find the true inhibitory concentration (but this also comes with antibiotic solubility troubles) [42]. The dilution series was based on a standard MIC protocol, which is why the exact dilution series was used [42]. The two isolates have slightly different paths to conferring resistance, but with the hyper-expression of ampC being the most significant response for both, which is likely very important in conferring resistance. Another aspect not investigated in this master project is the proteomic analysis of the membrane fraction. There might be significant up-regulation of efflux pumps in both isolates, and especially the β-lactam efflux pump MexAB-OprM which is positively regulated by reactive oxygen species (ROS) [1]. Considering there was up-regulation of proteins involved in protection against ROS, it seems likely that proteomics on the membrane fraction might reveal up-regulation of the efflux pump.

6 Conclusion & Future Studies

6.1 Conclusion

This study consisted of determining minimum inhibitory concentration (MIC) of six antimicrobial agents on 7 clinical isolates of *P. aeruginosa* sampled from patients suffering from the recessive hereditary genetic disease cystic fibrosis. Several of the isolates showed resistance values against the antibiotics tested, and isolate PAU5 got the label of being multi-drug resistant (MDR) by showing resistance against TZP, CIP, TOB, and CAZ in Mueller-Hinton Broth (MHB) medium. MIC determination was also performed in another growth medium, the cell culture medium RPMI-LB10, where PAU5 showed to be unable to grow in presence of antibiotic, even at the lowest concentration. The medium used for MIC analysis proved to have large impact on MIC value. Some isolates in certain antibiotics showed increased MIC-value in RPMI-LB10 medium compared to MHB medium, while other isolates showed the opposite to be true. The data obtained showed that the protocol which is widely used in the medical world might be flawed, and when considering MIC determination might be the key factor for determination of treatment against e.g., a chronic infection in the cystic fibrosis lung, the data by which the decision is based upon must be correct and accurate.

After determining MIC, whole-genome sequencing was performed to investigate the genomic potential of each isolate, before performing proteomics analysis on two isolates, PAU3 and PAU5. In the proteomics analysis these isolates were subjected to two concentrations (1 μg/mL and 512 μg/mL) of Piperacillin and constant concentration of Tazobactam (4 μg/mL). Proteomics analysis showed the β-lactamase ampC being the most up-regulated protein in both strains when comparing both to the water control and to the highest concentration of Piperacillin with the lowest concentration. In regards to genomic content, PAU3 showed to have the exotoxin A ExoA (eukaryotic cell toxin), which PAU5 did not have. Other virulence factors and resistance genes were all present, showing that the differences in gene numbers and unique genes between the strains were not within the group of genes important for conferring antimicrobial resistance (AMR). In the proteomics analysis, data unveiled showing that the genomic potential was not the large difference, but rather what genes were being expressed and at what rate.

The isolates performed proteomics analysis on showed different proteomic responses. PAU5 showed to up-regulate the type VI secretion system, which PAU3 did not up-regulate. The hypothesis is that PAU5 likely saw the antibiotic as competition, while PAU3 might have been previously exposed to the antibiotic, and showed a specific response (reactive oxygen species protection proteins, and a persister cell formation protein). The study concludes with other research done on the area, which is that the hyperproduction of AmpC is the main mechanism driving β-lactam resistance in *P. aeruginosa* [225], but membrane-associated proteins which were not investigated in this thesis might also be a large part of the response.

6.2 Future studies

There is still a lot to be investigated in the clinical isolates of *P. aeruginosa*. One interesting start would be to do proteomic examination of the effect medium has on the response. Therefore, a repetition of the proteomics experiment, but in RPMI-LB10 medium would be of interest. This might disclose what is happening with PAU5 that makes it unable to survive in the medium when exposed to an antibiotic. For clinical isolate PAU3, it might reveal what makes it more resistant against some antibiotics in the RPMI-LB10 medium, and less resistance against others. When testing why increased or decreased resistance is seen when changing the medium, it might also be interesting to test a strain that did not show resistance values against TZP to see whether hyperexpression of ampC is still happening there or not (to investigate whether this response is crucial for conferring resistance).

Another mechanism that might be interesting to look at, would be how inhibition of the β-lactam by the β-lactamase happens. Furthermore, it would be interesting to see whether there is a large difference in structure of the lactamases between isolates. Alphafold might be a useful tool for predicting the structure based on the sequences from the whole genome sequencing. The β-lactamase could also be produced for testing of various kinetic parameters. Is it for example true for these isolates that ampC is not as efficient against TZP? And, is Tazobactam able to inhibit any ampC at all, or is it superfluous as an antimicrobial agent?

Another investigation that would be interesting, is proteomics on the membrane fraction to look for the presence of efflux pumps and porins. These are essential for uptake and efflux of various antibiotics, such as β-lactams. Maybe the porin for influx of β-lactams has substitutions that yields lower influx of antibiotic? Or maybe there is hyperexpression of various efflux pumps that is continuously pumping the antibiotic out of the periplasm? Lastly, the type VI secretion system and ampC has neither been found co-expressed in previous research (which it was for isolate PAU5), nor to be in genomic neighborhood with each other. Could it be that the T6SS and ampC is in genomic proximity in PAU5, or that they are regulated by the same regulator? This would then explain why the T6SS is co-expressed with ampC in the PAU5 isolate.

References

[1] J.L. Fothergill R.F. Langendonk D.R. Neill. "The Building Blocks of Antimicrobial Resistance in *Pseudomonas aeruginosa*: Implications for Current Resistance-Breaking Therapies". In: *Frontiers in Cellular and Infection Microbiology* 11 (Apr. 2021). ISSN: 2235-2988. DOI: 10.3389/fcimb.2021.665759.

[2] D. Gerhard. *Antimicrobial Resistance: The Silent Pandemic*. URL: https://www.the-scientist.com/news-opinion/antimicrobial-resistance-the-silent-pandemic-71196. [updated 30.06.2023; accessed 27.09.2023].

[3] K. Brown. *Alexander Fleming*. URL: https://www.britannica.com/biography/Alexander-Fleming. [updated 08.09.2023; accessed 27.09.2023].

[4] F. Sharara C.L.J. Murray K.S. Ikuta et al. "Global burden of bacterial antimicrobial resistance in 2019: a systematic analysis". In: *The Lancet* 399 (Jan. 2022), pp. 629–655. ISSN: 0140-6736. DOI: 10.1016/S0140-6736(21)02724-0.

[5] N. Indrawattana S. Santajit. "Mechanisms of Antimicrobial Resistance in ESKAPE Pathogens". In: *BioMed research international* 2016 (May 2016). DOI: 10.1155/2016/2475067.

[6] J.Gergen P. Joi. *The silent pandemic: how drug-resistant superbugs risk becoming the world's number one killer*. URL: https://www.gavi.org/vaccineswork/silent-pandemic-how-drug-resistant-superbugs-risk-becoming-worlds-number-one-killer. [updated 21.11.2022; accessed 28.09.2023].

[7] R.A. Rayan. "Flare of the silent pandemic in the era of the COVID-19 pandemic: Obstacles and opportunities". In: *World journal of clinical cases* 11(6) (Feb. 2023), pp. 1267–1274. ISSN: 2307-8960. DOI: 10.12998/wjcc.v11.i6.1267.

[8] A. Lund. *Antibiotic resistance – the silent pandemic*. URL: https://news.ki.se/antibiotic-resistance-the-silent-pandemic. [updated 15.06.2022; accessed 28.09.2023].

[9] MedlinePlus. *Cystic fibrosis*. URL: https://medlineplus.gov/ency/article/000107.htm. [updated 15.06.2022; accessed 28.09.2023].

[10] M.L. Flaws N.M. Moore. *Introduction: Pseudomonas aeruginosa*. URL: http://clsjournal.ascls.org/content/24/1/41. [updated January 2011; accessed September 29. 2023].

[11] M. Whiteley S.P. Diggle. "Microbe Profile: *Pseudomonas aeruginosa*: opportunistic pathogen and lab rat". In: *Microbiology (Reading, England)* 166(1) (Jan. 2020). ISSN: 1350-0872. DOI: 10.1099/mic.0.000860.

[12] A. Hewlett MD P.W. Smith MD K.Watkins MBA. "Infection control through the ages". In: *American Journal of Infection Control* 40(1) (July 2012), pp. 35–42. ISSN: 0196-6553. DOI: 10.1016/j.ajic.2011.02.019.

[13] E. Larson. "A retrospective on infection control. Part 1: Nineteenth century-Consumed by fire". In: *American Journal of Infection Control* 25(3) (June 1997), pp. 236–241. ISSN: 0196-6553. DOI: 10.1016/s0196-6553(97)90010-9.

[14] N.D. Hanson P.D. Lister D.J. Wolter. "Antibacterial-Resistant *Pseudomonas aeruginosa*: Clinical Impact and Complex Regulation of Chromosomally Encoded Resistance Mechanisms". In: *American Journal of Infection Control* 22(4) (Oct. 2009), pp. 582–610. ISSN: 0893-8512. DOI: 10.1128/CMR.00040-09.

[15] J. Bodilis S. Chevalier E. Bouffartigues et al. "Structure, function and regulation of *Pseudomonas aeruginosa* porins". In: *FEMS Microbiology Reviews* 41(5) (Sept. 2017), pp. 698–722. ISSN: 0168-6445. DOI: 10.1093/femsre/fux020.

[16] Shaan L. Gellatly and Robert E.W. Hancock. "*Pseudomonas aeruginosa*: new insights into pathogenesis and host defenses". In: *Pathogens and Disease* 67(3) (Apr. 2013), pp. 159–173. ISSN: 2049-632X. DOI: 10.1111/2049-632X.12033.

[17] M. Fata Moradali, Shirin Ghods, and Bernd H. A. Rehm. "*Pseudomonas aeruginosa* Lifestyle: A Paradigm for Adaptation, Survival, and Persistence". In: *Frontiers in Cellular and Infection Microbiology* 7 (2017). ISSN: 2235-2988. DOI: 10.3389/fcimb.2017.00039.

[18] REVIVE. *Multidrug-resistant (MDR)*. URL: https://revive.gardp.org/resource/multidrug-resistant-mdr/?cf=encyclopaedia. [accessed: 10.12.2023].

[19] A. Ervin C. Stover X. Pham et al. "Complete genome sequence of *Pseudomonas aeruginosa* PAO1, an opportunistic pathogen". In: *Nature* 406 (Aug. 2000), pp. 959–964. ISSN: 6799. DOI: 10.1038/35023079.

[20] A. Shiroma K. Nakano Y. Terabayashi et al. "First Complete Genome Sequence of *Pseudomonas aeruginosa* (Schroeter 1872) Migula 1900 (DSM 50071T), Determined Using PacBio Single-Molecule Real-Time Technology". In: *Genome announcements* 3(4) (Aug. 2015). ISSN: e00932-15. DOI: 10.1128/genomeA.00932-15.

[21] P.D.Giacomo A.R.Losito F.Raffaelli et al. "New Drugs for the Treatment of *Pseudomonas aeruginosa* Infections with Limited Treatment Options: A Narrative Review". In: *Antibiotics* 11(5) (Apr. 2022). ISSN: 2079-6382. DOI: 10.3390/antibiotics11050579.

[22] R. MacLaren M.D. Obritsch D.N. Fish et al. "Nosocomial infections due to multidrug-resistant *Pseudomonas aeruginosa*: epidemiology and treatment options". In: *Pharmacotherapy* 25,10 (Oct. 2005). ISSN: 0277-0008. DOI: 10.1592/phco.2005.25.10.1353.

[23] Y. Bourigault M. Bouteiller C. Dupont et al. "*Pseudomonas* Flagella: Generalities and Specificities". In: *International journal of molecular sciences* 2(7) (Mar. 2021). ISSN: 1422-0067. DOI: 10.3390/ijms22073337.

[24] M. Kollef D. Reynolds. "The Epidemiology and Pathogenesis and Treatment of *Pseudomonas aeruginosa* Infections: An Update." In: *Drugs* 81,18 (Dec. 2021). ISSN: 0012-6667. DOI: 10.1007/s40265-021-01635-6.

[25] M. Trottier A. Besse M-C. Groleau et al. "*Pseudomonas aeruginosa* Strains from Both Clinical and Environmental Origins Readily Adopt a Stable Small-Colony-Variant Phenotype Resulting from Single Mutations in c-di-GMP Pathways". In: *Journal of bacteriology* 204(10) (Oct. 2022). ISSN: 0021-9193. DOI: 10.1128/jb.00185-22.

[26] M.A. De Pedro W.Vollmer D.Blanot. "Peptidoglycan structure and architecture". In: *FEMS Microbiology Reviews* 32(2) (Mar. 2008), pp. 149–167. ISSN: 0168-6445. DOI: 10.1111/j.1574-6976.2007.00094.x.

[27] T. Vernet A. Zapun C. Contreras-Martel. "Penicillin-binding proteins and β-lactam resistance". In: *FEMS Microbiology Reviews* 32(2) (Feb. 2008), pp. 361–385. ISSN: 0168-6445. DOI: 10.1111/j.1574-6976.2007.00095.x.

[28] W. Vollmer C. Otten M. Brilli et al. "Peptidoglycan in obligate intracellular bacteria". In: *Molecular microbiology* 107(2) (Jan. 2018), pp. 142–163. ISSN: 0950-382X. DOI: 10.1111/mmi.13880.

[29] J.D.Shirley S. Sharifzadeh N.W. Brown et al. "Chemical tools for selective activity profiling of bacterial penicillin-binding proteins." In: *Methods of enzymology* 638 (Apr. 2020), pp. 27–55. ISSN: 0076-6879. DOI: 10.1016/bs.mie.2020.02.015.

[30] M. Kjos. *Bacterial cell structure and cell biology*. PowerPoint. 02_BIO230_2023 _bacterial_cell_biology_part_1.pptx, Slides 38-39, 48-58. Jan. 2023.

[31] S.L. Michell A. Kovacs-Simon R.W: Titball. "Lipoproteins of bacterial pathogens". In: *Infection and immunity* 79(2) (Feb. 2011), pp. 548–561. ISSN: 0019-9567. DOI: 10.1128/IAI.00682-10.

[32] B.L. Lee H. Nakayama K. Kurokawa. "Lipoproteins in bacteria: structures and biosynthetic pathways". In: *The FEBS Journal* 279(23) (Oct. 2012), pp. 4247–4268. DOI: 10.1111/febs.12041.

[33] T.L. Pitt R.F. Taylor M.E. Hodson. "Adult cystic fibrosis: association of acute pulmonary exacerbations and increasing severity of lung disease with auxotrophic mutants of *Pseudomonas aeruginosa*". In: *Thorax* 48(10) (Oct. 1993), pp. 1002–1005. ISSN: 0040-6376. DOI: 10.1136/thx.48.10.1002.

[34] Genetic Enegineering & Biotechnology News. *Antibiotic-Snacking Bacteria Could Help Tackle Environmental Contamination*. URL: https://www.genengnews.com/news/antibiotic-snacking-bacteria-could-help-tackle-environmental-contamination/. [updated: 30.04.2023; accessed: 25.09.2023].

[35] C.S. Harwood C. Alvarez-Ortega. "Responses of *Pseudomonas aeruginosa* to low oxygen indicate that growth in the cystic fibrosis lung is by aerobic respiration". In: *Molecular microbiology* 65(1) (July 2007), pp. 153–165. ISSN: 0950-382X. DOI: 10.1111/j.1365-2958.2007.05772.x.

[36] Vedantu. *Questions & Answers*. URL: https://www.vedantu.com/question-answer/the-number-of-moles-of-oxygen-in-1-l-of-air-class-11-chemistry-cbse-5f87c1c39e3c7e14a8636326. (accessed: 15.10.2023).

[37] Westfield. *The ideal gas Law*. URL: https://www.westfield.ma.edu/personalpages/cmasi/%20gen_chem1/Gases/ideal%20gas%20law/pvnrt.htm. (accessed: 15.10.2023).

[38] I. Ventre M. Sivaneson H. Mikkelsen et al. "Two-component regulatory systems in *Pseudomonas aeruginosa*: an intricate network mediating fimbrial and efflux pump gene expression". In: *Molecular microbiology* 79(5) (Jan. 2011), pp. 1353–1366. ISSN: 0950-382X. DOI: 10.1111/j.1365-2958.2010.07527.x.

[39] C. Zhou S. Qin W. Xiao et al. "*Pseudomonas aeruginosa*: pathogenesis, virulence factors, antibiotic resistance, interaction with host, technology advances and emerging therapeutics." In: *Frontiers in Cellular and Infection Microbiology* 7 (June 2022). ISSN: 2059-3635. DOI: 10.1038/s41392-022-01056-1.

[40] T. Oguri A. Tsuji I. Kobayashi et al. "An epidemiological study of the susceptibility and frequency of multiple-drug-resistant strains of *Pseudomonas aeruginosa* isolated at medical institutes nationwide in Japan". In: *J Infect Chemother* 11(2) (Apr. 2005), pp. 64–70. ISSN: 1437-7780. DOI: 10.1007/s10156-005-0377-z.

[41] D.J. Wozniak S. Malhotra D. Hayes Jr. "Cystic Fibrosis and *Pseudomonas aeruginosa*: the Host-Microbe Interface". In: *Clinical Microbiology Reviews* 32(3) (May 2019). DOI: 10.1128/cmr.00138-18.

[42] P.K. Edvardsen. *Communication throughout the year*. Personal communication. Jan. 2023.

[43] G. Vaaje-Kolstad. *Communication throughout the year*. Personal communication. Jan. 2023.

[44] MedicalNewsToday. *How common is cystic fibrosis in adults and children?* URL: https://www.medicalnewstoday.com/articles/how-common-is-cystic-fibrosis#worldwide-cases. [updated: 20.09.2023; accessed: 29.10.2023].

[45] C. Elston S. Antoniou. "Cystic fibrosis". In: *Medicine* 44,5 (Apr. 2016), pp. 321–325. ISSN: 1357-3039. DOI: 10.1016/j.mpmed.2016.02.016.

[46] Cystic Fibrosis Foundation. *Understanding Changes in Life Expectancy*. URL: https://www.cff.org/managing-cf/understanding-changes-life-expectancy. accessed: 10.03.2023.

[47] H. Ritchie M. Roser E. Ortiz-Ospina. *Life Expectancy*. URL: https://ourworldindata.org/life-expectancy. [updated: 10.2023; accessed: 15.02.2023].

[48] C.d.l. Fuente-Núñez E.B.M. Breidenstein and R.E.W. Hancock. "*Pseudomonas aeruginosa*: all roads lead to resistance". In: *Trends in Microbiology* 19(8) (Aug. 2011), pp. 419–426. ISSN: 0966-842X. DOI: 10.1016/j.tim.2011.04.005.

[49] William B. Coleman and Gregory J. Tsongalis. "Chapter 12 - Understanding molecular pathogenesis: the biological basis of human disease and implications for improved treatment of human disease". In: *Essential Concepts in Molecular Pathology (Second Edition)*. Ed. by G.J. Tsongalis W.B. Coleman. Second Edition. Academic Press, 2020, pp. 191–200. ISBN: 978-0-12-813257-9. DOI: 10.1016/B978-0-12-813257-9.00012-7. URL: https://www.sciencedirect.com/science/article/pii/B9780128132579000127.

[50] The Pancreas Center Columbia Surgery. *The Pancreas and Its Functions*. URL: https://columbiasurgery.org/pancreas/pancreas-and-its-functions. [updated: 30.04.2023; accessed: 25.09.2023].

[51] H. Groninger J. Estrada-Veras. "Palliative Care for Patients with Cystic Fibrosis 265". In: *Journal of palliative medicine* 16(4) (Apr. 2013), pp. 446–447. ISSN: 1557-7740. DOI: 10.1089/jpm.2013.9515.

[52] L. van Dorp F. Balloux. "Q&A: What are pathogens, and what have they done to and for us?" In: *BMC biology* 15,1 (Oct. 2017). ISSN: 1741-7007. DOI: 10.1186/s12915-017-0433-z.

[53] A.K. Sharma et al. "Bacterial Virulence Factors: Secreted for Survival". In: *Indian journal of microbiology* 57(1) (Mar. 2017). ISSN: 0046-8991. DOI: 10.1007/s12088-016-0625-1.

[54] D. Nguyen E. Faure K. Kwong. "*Pseudomonas aeruginosa* in Chronic Lung Infections: How to Adapt Within the Host?" In: *Frontiers in Immunology* 9 (Oct. 2018). ISSN: 1664-3224. DOI: 10.3389/fimmu.2018.02416.

[55] M.P. Marco L. Vilaplana. "Phenazines as potential biomarkers of *Pseudomonas aeruginosa* infections: synthesis regulation, pathogenesis and analytical methods for their detection". In: *Analytical and Bioanalytical Chemistry* 412 (May 2020), pp. 5897–5912. ISSN: 1618-2650. DOI: 10.1007/s00216-020-02696-4.

[56] S. McClean I. Jurado-Martin M. Sainz-Mejias. "*Pseudomonas aeruginosa*: An Audacious Pathogen with an Adaptable Arsenal of Virulence Factors". In: *International Journal of Molecular Sciences* 22(6) (Mar. 2021), p. 3128. ISSN: 1422-0067. DOI: 10.3390/ijms22063128.

[57] E. Jordana-Luch M. Fernández-Billón A.E. Llambías-Cabot et al. "Mechanisms of antibiotic resistance in *Pseudomonas aeruginosa* biofilms". In: *Biofilm* 5 (Dec. 2023), p. 100129. ISSN: 2590-2075. DOI: 10.1016/j.bioflm.2023.100129.

[58] D.D. Whitt B.A. Wilson A.A Salyers et al. *Bacterial Pathogenesis A Molecular Approach*. 3rd ed. 1752 N St. NW, Washington DC 20036-2904, USA: ASM Press, 2011.

[59] G. Kaiser. *5: Virulence Factors that Promote Colonization*. URL: https://bio.libretexts.org/Bookshelves/Microbiology/Microbiology_(Kaiser)/Unit_3%3A_Bacterial_Pathogenesis/5%3A_Virulence_Factors_that_Promote_Colonization. 01.11.2023.

[60] Q. Wang C. Liao X. Huang et al. "Virulence Factors of *Pseudomonas aeruginosa* and Antivirulence Strategies to Combat Its Drug Resistance". In: *Frontiers in Cellular and Infection Microbiology* 12 (July 2022). ISSN: 2235-2988. DOI: 10.3389/fcimb.2022.926758.

[61] G. Waksman A. Toste Rego V. Chandran. "Two-step and one-step secretion mechanisms in Gram-negative bacteria: contrasting the type IV secretion system and the chaperone-usher pathway of pilus biogenesis". In: *Biochemical Journal* 425(3) (Jan. 2010), pp. 475–488. ISSN: 1470-8728. DOI: 10.1042/BJ20091518.

[62] J. Ruiz G. Horna. "Type 3 secretion system of *Pseudomonas aeruginosa*". In: *Microbiological Research* 246 (May 2021), p. 126719. ISSN: 0944-5013. DOI: 10.1016/j.micres.2021.126719.

[63] U.A. Ramagopal P.G. Leiman M. Basler et al. "Type VI secretion apparatus and phage tail-associated protein complexes share a common evolutionary origin". In: *Proceedings of the National Academy of Sciences* 106(11) (Mar. 2009), pp. 4154–4159. DOI: 10.1073/pnas.0813360106.

[64] UniProt. *tse3 - Peptidoglycan muramidase*. URL: https://www.uniprot.org/uniprotkb/Q9HYC5/entry. [updated: 13.09.2023; accessed: 01.11.2023].

[65] A. Ambora R. Trastoy Pena L. Blasco et al. "Relationship Between Quorum Sensing and Secretion Systems". In: *Frontiers in Microbiology* 10 (June 2019). ISSN: 1664-302X. DOI: 10.3389/fmicb.2019.01100.

[66] J. Mecsas E.R. Green. "Bacterial Secretion Systems – An overview". In: *Microbiology spectrum* 4(1) (Feb. 2016), Microbiology spectrum. ISSN: 2165-0497. DOI: 10.1128/microbiolspec.VMBF-0012-2015.

[67] A.R. Caballero L.S. Engel J.M. Hill et al. "Protease IV, a unique extracellular protease and virulence factor from *Pseudomonas aeruginosa*". In: *The Journal of biological chemistry* 273(27) (June 1998), pp. 16792–7. ISSN: 0021-9258. DOI: 10.1074/jbc.273.27.16792.

[68] N. Ruiz B. Bertani. "Function and biogenesis of lipopolysaccharides". In: *EcoSal Plus* 8(1) (Aug. 2019). ISSN: 2324-6200. DOI: 10.1128/ecosalplus.ESP-0001-2018.

[69] Y.S. Khan A. Farhana. *Biochemistry, Lipopolysaccharide*. URL: https://www.ncbi.nlm.nih.gov/books/NBK554414/. [updated: 17.04.2023; accessed: 11.10.2023].

[70] J.T. Weadge M.J. Franklin D.E. Nivens et al. "Biosynthesis of the *Pseudomonas aeruginosa* extracellular polysaccharides, alginate, Pel, and Psl". In: *Frontiers in Microbiology* 2 (Aug. 2011). ISSN: 1664-302X. DOI: 10.3389/fmicb.2011.00167.

[71] V. Deretic J.R.W. Govan. "Microbial Pathogenesis in Cystic Fibrosis: Mucoid *Pseudomonas aeruginosa* and *Burkholderia cepacia*". In: *Microbiological Reviews* 60(3) (Sept. 1996), pp. 539–574. ISSN: 0146-0749. DOI: 10.1128/mr.60.3.539-574.1996.

[72] Z. Ezzeddine G. Ghssein. "A Review of *Pseudomonas aeruginosa* Metallophores: Pyoverdine, Pyochelin and Pseudopaline". In: *Biology (Basel)* 11(12) (Nov. 2022). ISSN: 2079-7737. DOI: 10.339/Fbiology11121711.

[73] W.A.Adedeji. "THE TREASURE CALLED ANTIBIOTICS". In: *Annals of Ibadan postgraduate medicine* 14(2) (Dec. 2016), pp. 56–57. ISSN: 1597-1627.

[74] Worldometer. *Life Expectancy of the World Population*. URL: https://www.worldometers.info/demographics/life-expectancy/. [updated: 2023; accessed: 23.02.2023].

[75] MedicalNewsToday. *Why is it important to take antibiotics when needed?* URL: https://www.medicalnewstoday.com/articles/10278#when-to-take. [updated: 09.08.2023; accessed: 02.11.2023].

[76] Microbiology Society. *ANTIBIOTICS*. URL: https://microbiologysociety.org/why-microbiology-matters/what-is-microbiology/microbes-and-the-human-body/antibiotics.html. accessed: 02.11.2023.

[77] Oslo Universitetssykehus. *Cystisk fibrose - Antibiotikabehandling*. URL: https://ehandboken.ous-hf.no/document/133683#Pseudomonas. accessed: 10.04.2023.

[78] National Library of Medicine. *Fortaz*. URL: https://pubchem.ncbi.nlm.nih.gov/compound/Fortaz. [updated: 28.10.2023; accessed: 03.11.2023].

[79] National Library of Medicine. *Meropenem*. URL: https://pubchem.ncbi.nlm.nih.gov/compound/441130#section=2D-Structure. [updated: 28.10.2023; accessed: 03.11.2023].

[80] National Library of Medicine. *Piperacillin*. URL: https://pubchem.ncbi.nlm.nih.gov/compound/43672#section=2D-Structure. [updated: 28.10.2023; accessed: 03.11.2023].

[81] National Library of Medicine. *Tazobactam*. URL: https://pubchem.ncbi.nlm.nih.gov/compound/123630#section=Structures. [updated: 28.10.2023; accessed: 03.11.2023].

[82] National Library of Medicine. *Ciprofloxacin*. URL: https://pubchem.ncbi.nlm.nih.gov/compound/2764#section=2D-Structure. [updated: 28.10.2023; accessed: 03.11.2023].

[83] National Library of Medicine. *Tobramycin*. URL: https://pubchem.ncbi.nlm.nih.gov/compound/36294#section=2D-Structure. [updated: 28.10.2023; accessed: 03.11.2023].

[84] Chem Spider. *Colistin*. URL: https://www.chemspider.com/Chemical-Structure.4470591.html. accessed: 03.11.2023.

[85] P.A. Bradford K. Bush. "β-Lactams and β-Lactamase Inhibitors: An Overview". In: *Cold Spring Harbor perspectives in medicine* 6(8) (Aug. 2016). ISSN: 2157-1422. DOI: 10.1101/cshperspect.a025247.

[86] Y. Kwon D. Kim S. Kim et al. "Structural Insights for β-Lactam Antibiotics". In: *Biomolecules & Therapeutics* 31(2) (Feb. 2023), pp. 141–147. ISSN: 2005-4483. DOI: 10.4062/biomolther.2023.008.

[87] M. Cascella V.B Arumugham R. Gujarathi. *Third-Generation Cephalosporins*. URL: https://www.ncbi.nlm.nih.gov/books/NBK549881/. [updated: 04.06.2023; accessed: 03.11.2023].

[88] National Library of Medicine. *Cephalosporins*. URL: https://www.ncbi.nlm.nih.gov/books/NBK551517/. [updated: 23.04.2023; accessed: 03.11.2023].

[89] S . Baker L.N. Telano. *Physiology, Cerebral Spinal Fluid*. URL: https://www.ncbi.nlm.nih.gov/books/NBK519007/. [updated: 04.07.2023; accessed: 03.11.2023].

[90] MEL Science. *Features and significance of hydration in chemistry*. URL: https://melscience.com/HK-en/articles/features-and-significance-hydration-chemistry/. accessed: 03.11.2023.

[91] N.M. Lechner A.W. Buning C.J. Hodiamont et al. "Population Pharmacokinetics and Probability of Target Attainment of Different Dosing Regimens of Ceftazidime in Critically Ill Patients with a Proven or Suspected *Pseudomonas aeruginosa* Infection". In: *Antibiotics (Basel)* 10(6) (June 2021). ISSN: 2079-6382. DOI: 10.3390/antibiotics10060612.

[92] R.T. Scheife. "Protein binding: what does it mean?" In: *DICP : the annals of pharmacotherapy* 23(7-8) (July 1989), pp. 27–31. ISSN: 1042-9611. DOI: 10.1177/106002808902300706.

[93] D.M. Livermore. "Antibiotic uptake and transport by bacteria". In: *Scandinavian journal of infectious diseases. Supplementum* 74 (Jan. 1990), pp. 15–22. ISSN: 0300-8878.

[94] S. Adnan G. Wong S. Briscoe et al. "Protein Binding of β-Lactam Antibiotics in Critically Ill Patients: Can We Successfully Predict Unbound Concentrations?" In: *Antimicrobial Agents and Chemotherapy* 57(12) (Nov. 2013), pp. 6165–6170. DOI: 10.1128/aac.00951-13.

[95] Pfizer. *TAZOCIN Piperacillin Sodium/Tazobactam Sodium*. URL: https://labeling.pfizer.com/ShowLabeling.aspx?id=13994. accessed: 03.10.2023.

[96] C. Bethel P. Hinchliffe C. Tooke et al. "Penicillanic Acid Sulfones Inactivate the Extended-Spectrum β-Lactamase CTX-M-15 through Formation of a Serine-Lysine Cross-Link: an Alternative Mechanism of β-Lactamase Inhibition". In: *mBio* 13(3) (May 2022), p. 10. DOI: 10.1128/mbio.01793-21.

[97] emc. *Piperacillin/Tazobactam 4g/0.5g Powder for Solution for Infusion*. URL: https://www.medicines.org.uk/emc/product/6526/smpc#gref. [updated: 20.07.2023; accessed: 03.11.2023].

[98] A. Maxwell R.J. Reece. "DNA gyrase: structure and function". In: *Critical reviews in biochemistry and molecular biology* 26(3-4) (Jan. 1991), pp. 335–75. ISSN: 1040-9238. DOI: 10.3109/10409239109114072.

[99] S.T. Kilpatrick J.E. Krebs E.S. Goldstein. *Lewin's Genes XII*. 12th ed. 5 Wall Street, Burlington, MA 01803, USA: Jones & Bartlett Learning, 2018.

[100] National Library of Medicine. *Piperazine*. URL: https://pubchem.ncbi.nlm.nih.gov/compound/Piperazine. [updated: 03.11.2023; accessed: 03.11.2023].

[101] C.V. Preuss S. Grogan. *Pharmacokinetics*. URL: https://www.ncbi.nlm.nih.gov/books/NBK557744/. [updated: 30.07.2023; accessed: 03.11.2023].

[102] D.C. Hooper J.S. Wolfson. "MINIREVIEW The Fluoroquinolones: Structures, Mechanisms of Action and Resistance, and Spectra of Activity In Vitro". In: *Antimicrobal agents and chemotherapy* 28(4) (Oct. 1985), pp. 581–586.

[103] S.H. Lilley D.E. King R. Malone. "New Classification and Update on the Quinolone Antibiotics". In: *American family physician* 61(9) (May 2000), pp. 2741–8. ISSN: 0002-838X.

[104] M. Grudzień E. Kłosińska-Szmurło F.A. Pluciński et al. "Experimental and theoretical studies on the molecular properties of ciprofloxacin, norfloxacin, pefloxacin, sparfloxacin, and gatifloxacin in determining bioavailability". In: *Journal of biological physics* 40(4) (Sept. 2014), pp. 335–345. ISSN: 0092-0606. DOI: 10.1007/s10867-014-9354-z.

[105] D.A. Saunders E.J. Begg R.A. Robson et al. "The pharmacokinetics of oral fleroxacin and ciprofloxacin in plasma and sputum during acute and chronic dosing". In: *British journal of clinical pharmacology* 49(1) (Jan. 2000), pp. 32–38. ISSN: 0306-5251. DOI: 10.1046/j.1365-2125.2000.00105.x.

[106] T.R. Kane K.M. Krause A.W. Serio et al. "Aminoglycosides: An Overview". In: *Cold Spring Harbor perspectives in medicine* 6(6) (June 2016). ISSN: 2157-1422. DOI: 10.1101/cshperspect.a027029.

[107] fisher scientific. *Thermo Scientific Chemicals Colistin sulfate salt*. URL: https://www.fishersci.no/shop/products/colistin-sulfate-salt-4/15575146. accessed: 03.11.2023.

[108] L.D. Saravolatz M.E. Falagas S.K. Kasiakou. "Colistin: The Revival of Polymyxins for the Management of Multidrug-Resistant Gram-Negative Bacterial Infections". In: *Clinical Infectious Diseases* 40(9) (May 2005), pp. 1333–1341. ISSN: 1058-4838. DOI: 10.1086/429323.

[109] A. Rodrigues F.F. Andrade D. Silva et al. "Colistin Update on Its Mechanism of Action and Resistance, Present and Future Challenges". In: *Microorganisms* 8(11) (Nov. 2020). ISSN: 2076-2607. DOI: 10.3390/microorganisms8111716.

[110] Centers for Disease Control and Prevention. *Antimicrobial Resistance*. URL: cdc.gov/drugresistance/about.html. [updated: 05.10.2022; accessed: 15.02.2023].

[111] ReAct Group. *Antibiotic resistance claims more than 1,2 million lives a year, says new large study*. URL: https://www.reactgroup.org/news-and-views/news-and-opinions/year-2022/antibiotic-resistance-claims-more-than-1-2-million-lives-a-year-says-new-large-study/. [updated: 20.01.2022; accessed: 16.02.2023].

[112] ReAct Group. *7.7 million people die from bacterial infections every year*. URL: https://www.reactgroup.org/news-and-views/news-and-opinions/year-2022/7-7-million-people-die-from-bacterial-infections-every-year/. [updated: 15.12.2022; accessed: 15.03.2023].

[113] GOV.UK. *Taking antibiotics when you don't need them puts you at risk*. URL: https://www.gov.uk/government/news/taking-antibiotics-when-you-dont-need-them-puts-you-at-risk. [updated: 24.10.2017; accessed: 17.02.2023].

[114] National Library of Medicine. *Nosocomial Infections*. URL: https://www.ncbi.nlm.nih.gov/books/NBK559312/. [updated: 27.04.2023; accessed: 20.02.2023].

[115] J.R. Edwards D.M. Sievert P. Ricks et al. "Antimicrobial-resistant pathogens associated with healthcare-associated infections: summary of data reported to the National Healthcare Safety Network at the Centers for Disease Control and Prevention, 2009-2010". In: *Infection control and hospital epidemiology* 34(1) (Jan. 2013), pp. 1–14. ISSN: 0899-823X. DOI: 10.1086/668770.

[116] A.K. Webbm B. Limbago L.M. Weiner et al. "Antimicrobial-Resistant Pathogens Associated With Healthcare-Associated Infections: Summary of Data Reported to the National Healthcare Safety Network at the Centers for Disease Control and Prevention, 2011-2014". In: *Infection control and hospital epidemiology* 37(11) (Nov. 2016), pp. 1288–1301. ISSN: 0899-823X. DOI: 10.1017/ice.2016.174.

[117] B.R. Glick Z. Pang R. Raudonis et al. "Antibiotic resistance in *Pseudomonas aeruginosa*: mechanisms and alternative therapeutic strategies". In: *Biotechnology Advances* 37(1) (Feb. 2019), pp. 177–192. ISSN: 0734-9750. DOI: 10.1016/j.biotechadv.2018.11.013.

[118] W.C. Reygaert. "An overview of the antimicrobial resistance mechanisms of bacteria". In: *AIMS microbiology* 4(3) (June 2018), pp. 482–501. ISSN: 2471-1888. DOI: 10.3934/microbiol.2018.3.482.

[119] M.A.T. Blaskovich T.D.M. Pham Z.M. Ziora. "Quinolone antibiotics". In: *Medicinal Chemistry Communications* 10(10) (June 2019), pp. 1719–1739. ISSN: 2040-2503. DOI: 10.1039/c9md00120d.

[120] S. Lory L.R. Mulcahy J.L. Burns et al. "Emergence of *Pseudomonas aeruginosa* Strains Producing HighLevels of Persister Cells in Patients with Cystic Fibrosis". In: *Journal of bacteriology* 192(23) (Dec. 2010), pp. 6191–6199. DOI: 10.1128/JB.01651-09.

[121] M.N. Seleem H.I. Hussain A.I. Aqib et al. "Genetic Basis of Molecular Mechanisms in β-lactam Resistant Gram-negative Bacteria". In: *Microbial pathogenesis* 158 (June 2021), p. 105040. ISSN: 0882-4010. DOI: 10.1016/j.micpath.2021.105040.

[122] S. Mobashery J.F. Fisher. "Three Decades of the Class A β-Lactamase Acyl-Enzyme". In: *Current protein & peptide science* 10(5) (Oct. 2009), pp. 401–407. ISSN: 1389-2037. DOI: 10.2174/138920309789351967.

[123] V. Gerriets N.R. Khanna. *Beta-Lactamase Inhibitors*. URL: https://www.ncbi.nlm.nih.gov/books/NBK557592/. [updated: 26.09.2023; accessed: 21.09.2023].

[124] V. Kumar O.A. Pemberton R.E. Noor et al. "Mechanism of proton transfer in class A β-lactamase catalysis and inhibition by avibactam". In: *Proceedings of the National Academy of Sciences* 117(11) (Mar. 2020), pp. 5818–5825. DOI: 10.1073/pnas.1922203117.

[125] T. Palzkill. "Structural and Mechanistic Basis for Extended-Spectrum Drug-Resistance Mutations in Altering the Specificity of TEM, CTX-M, and KPC β-lactamases". In: *Frontiers in Molecular Biosciences* 5 (Feb. 2018). ISSN: 2296-889X. DOI: 10.3389/fmolb.2018.00016.

[126] E.C. Bragginton C.L. Tooke P. Hinchliffe et al. "β-Lactamases and β-Lactamase Inhibitors in the 21st Century". In: *Journal of molecular biology* 431(18) (Aug. 2023), pp. 3472–3500. ISSN: 0022-2836. DOI: 10.1016/j.jmb.2019.04.002.

[127] R. Labia A. Philippon G. Arlet et al. "Class C β-Lactamases: Molecular Characteristics". In: *Clinical microbiology reviews* 35(3) (Apr. 2022), e0015021. ISSN: 0893-8512. DOI: 10.1128/cmr.00150-21.

[128] B.-G. Jeong A.W. Bae Y.E Jung et al. "Novel inhibition mechanism of carbapenems on the ACC-1 class C β-lactamase". In: *Archives of Biochemistry and Biophysics* 693 (Oct. 2023), p. 108570. ISSN: 0003-9861. DOI: 10.1016/j.abb.2020.108570.

[129] R.A. Powers D.A. Leonard R.A. Bonomo. "CLASS D β-LACTAMASES: A RE-APPRAISAL AFTER FIVE DECADES". In: *Accounts of chemical research* 46(11) (July 2013), p. 24072415. ISSN: 0001-4842. DOI: 10.1021/ar300327a.

[130] S.H. Jeong E -J. Yoon. "Class D β-lactamases". In: *Journal of Antimicrobial Chemotherapy* 76(4) (Dec. 2020), pp. 836–864. ISSN: 0305-7453. DOI: 10.1093/jac/dkaa513.

[131] K. Rogers. *omics*. URL: https://www.britannica.com/science/omics. [updated: 27.09.2023; accessed: 23.08.2023].

[132] A.J.F. Griffiths. *genomics*. URL: https://www.britannica.com/science/genomics. [updated: 19.10.2023; accessed: 05.11.2023].

[133] A. Bollas Y. Wang Z. Zhao et al. "Nanopore sequencing technology, bioinformatics and applications". In: *Nature Biotechnology* 39 (Nov. 2021), pp. 1348–1365. ISSN: 1546-1696. DOI: 10.1038/s41587-021-01108-x.

[134] R.M. Sandholm. *Communication throughout the year*. Personal communication. 2023.

[135] A. Al-Zaabi S. Al-Amrani Z. Al-Jabra et al. "Proteomics: Concepts and applications in human medicine". In: *World journal of biological chemistry* 12(5) (Sept. 2021), pp. 57–59. ISSN: 1949-8454. DOI: 10.4331/wjbc.v12.i5.57.

[136] EMBL-EBI. *What is proteomics?* URL: https://www.ebi.ac.uk/training/online/courses/proteomics-an-introduction/what-is-proteomics/. accessed: 23.08.2023.

[137] S. Tamang. *Proteomics: Types, Methods, Steps, Applications*. URL: https://microbenotes.com/proteomics/. [updated: 03.08.2023; accessed: 23.08.2023].

[138] Drug Discovery World. *Functional proteomics in drug discovery*. URL: https://www.ddw-online.com/functional-proteomics-in-drug-discovery-813-200304/. accessed: 24.08.2023.

[139] A-C. Gingras G. Kustatscher T. Collins et al. "Understudied proteins: opportunities and challenges for functional proteomics". In: *Nature Methods* 19 (May 2022), pp. 774–779. ISSN: 1548-7105. DOI: 0.1038/s41592-022-01454-x.

[140] G. Gouda S. Sabarinathan M.K. Gupta et al. "Chapter 2 - Structural Proteomics". In: *Bioinformatics in Rice Research*. Ed. by L. Behera M.K. Gupta. Springer, Singapore, 2021, pp. 239–256. ISBN: 978-981-16-3993-7. DOI: 10.1007/978-981-16-3993-7_11. URL: https://link.springer.com/chapter/10.1007/978-981-16-3993-7_11#citeas.

[141] Bruker. *timsTOF Pro 2*. URL: https://www.bruker.com/en/products-and-solutions/mass-spectrometry/timstof/timstof-pro-2.html. accessed: 06.11.2023.

[142] Bruker Daltonics. *Bruker's timsTOF - Flexibility to empower your ideas*. URL: https://www.youtube.com/watch?v=cWjz32wky2A&t=1s&ab_channel=BrukerDaltonics. [updated: 06.06.2016; accessed: 21.09.2023].

[143] Thermo Fisher Scientific. *Liquid Chromatography Mass Spectrometry (LC-MS) Information*. URL: https://www.thermofisher.com/no/en/home/industrial/mass-spectrometry/mass-spectrometry-learning-center/liquid-chromatography-mass-spectrometry-lc-ms-information.html. accessed: 13.11.2023.

[144] P.M. Mrozek. *Communication in the lab*. Personal communication. July 2023.

[145] M. Mann A. Sinham. "A beginner's guide to mass spectrometry–based proteomics". In: *The Biochemist* 42(5) (Oct. 2022), pp. 64–69. ISSN: 0954-982X. DOI: 10.1042/BIO20200057.

[146] G. McMahon. *How a Mass Spectrometer Works, Types of Instrumentation and Interpreting Mass Spectral Data*. URL: https://www.technologynetworks.com/analysis/articles/how-a-mass-spectrometer-works-types-of-instrumentation-and-interpreting-mass-spectral-data-347878. [updated: 04.05.2021; accessed: 21.09.2023].

[147] Bruker. *Trapped Ion Mobility Spectrometry (TIMS)*. URL: https://www.bruker.com/fr/products-and-solutions/mass-spectrometry/timstof.html. accessed: 21.09.2023.

[148] Broad Institute. *What is Mass Spectrometry?* URL: https://www.broadinstitute.org/technology-areas/what-mass-spectrometry. accessed: 21.09.2023.

[149] Analog Devices. *Time of Flight*. URL: https://www.analog.com/en/design-center/glossary/time-of-flight.html. accessed: 07.11.2023.

[150] European Committee on Antimicrobial Susceptibility Testing. *Breakpoint tables for interpretation of MICs and zone diameters, Version 13.0*. URL: http://www.eucast.org. [updated: 01.01.2023; accessed: 28.08.2023].

[151] *Nanobind® HMW DNA extraction - gram-negative bacteria*. PN 102-573-800. Rev. 01. PacBio. July 2022.

[152] *Native Barcoding Kit 24 V14 protocol*. SQK-NBD114.24. Version NBE_9169_V114_REVE_15SEP2022. Oxford Nanopore Technologies. Jan. 2023.

[153] C. Elgert J. Sims G. Sestini et al. *DNA repair and end-prep*. URL: https://bio-protocol.org/exchange/minidetail?id=8763932&type=30. accessed: 30.10.2023.

[154] SelectScience. *Qubit™ dsDNA BR Assay Kit by Thermo Fisher Scientific*. URL: https://www.selectscience.net/products/qubit-dsdna-br-assay-kit/?prodID=214403. accessed: 28.10.2023.

[155] JoVE. *Growth Curves: Generating Growth Curves Using Colony Forming Units and Optical Density Measurements*. URL: https://www.jove.com/v/10511/growth-curves-cfu-and-optical-density-measurements. accessed: 26.10.2023.

[156] MSD Manuals. *Penicillins*. URL: https://www.msdmanuals.com/home/infections/antibiotics/penicillins. [updated: 09.2022; accessed: 26.09.2023].

[157] EMBL-EBI. *Clustal Omega*. URL: https://www.ebi.ac.uk/Tools/msa/clustalo/. accessed: 22.11.2023.

[158] D. Milatovic P.G. Higgins A.C. Fluit et al. "Mutations in GyrA, ParC, MexR and NfxB in clinical isolates of *Pseudomonas aeruginosa*". In: *International Journal of Antimicrobial Agents* 21(5) (May 2003), pp. 409–413. ISSN: 0924-8579. DOI: 10.1016/S0924-8579(03)00009-8.

[159] T. Kawamura M. Nakano T. Deguchi et al. "Mutations in thegyrAandparCGenes in Fluoroquinolone-Resistant Clinical Isolates of *Pseudomonas aeruginosa*". In: *Antimicrobial Agents and Chemotherapy* 41(10) (Oct. 1997), pp. 2289–2291. ISSN: 0066-4804. DOI: 10.1128/aac.41.10.2289.

[160] National Library of Medicine. *Tetracycline*. URL: https://www.ncbi.nlm.nih.gov/books/NBK549905/. [updated: 23.04.2023; accessed: 08.11.2023].

[161] MSD Manuals. *Polypeptide Antibiotics: Bacitracin, Colistin, Polymyxin B*. URL: https://www.msdmanuals.com/professional/infectious-diseases/bacteria-and-antibacterial-drugs/polypeptide-antibiotics-bacitracin,-colistin,-polymyxin-b. [updated: 09.2022; accessed: 08.11.2023].

[162] L.W. Wannamaker J.R. Tagg A.S. Dajani. "Bacteriocins of Gram-Positive Bacteria". In: *Bacteriological Reviews* 40(3) (Sept. 1976), pp. 722–756.

[163] J. Blázquez A. Rodríguez-Rojas. "The *Pseudomonas aeruginosa* pfpI Gene Plays an Antimutator Role and Provides General Stress Protection". In: *Journal of Bacteriology* 191(3) (Nov. 2000), pp. 844–850. ISSN: 0021-9193. DOI: 10.1128/JB.01081-08.

[164] InterPro. *SCP2 sterol-binding domain superfamily*. URL: https://www.ebi.ac.uk/interpro/entry/InterPro/IPR036527/. accessed: 09.11.2023.

[165] UniProt. *P22307 SCP2_HUMAN*. URL: https://www.uniprot.org/uniprotkb/P22307/entry. accessed: 09.11.2023.

[166] C. Juan L. Zamorano B. Moyà et al. "The *Pseudomonas aeruginosa* CreBC two-component system plays a major role in the response to β-lactams, fitness, biofilm growth, and global regulation". In: *Antimicrobial agents and chemotherapy* 58(9) (Sept. 2014). ISSN: 0066-4804. DOI: 10.1128/AAC.02556-14.

[167] S. Djermoun B. Berni C. Soscia et al. "A Type VI Secretion System Trans-Kingdom Effector Is Required for the Delivery of a Novel Antibacterial Toxin in *Pseudomonas aeruginosa*". In: *Frontiers in microbiology* 10 (June 2019). ISSN: 1664-302X. DOI: 10.3389/fmicb.2019.01218.

[168] I.B. Jacob W. Xiong A. PErna et al. "The Enhancer-Binding Protein MifR, an Essential Regulator of α-Ketoglutarate Transport, Is Required for Full Virulence of *Pseudomonas aeruginosa* PAO1 in a Mouse Model of Pneumonia". In: *Infection and immunity* 90(10) (Oct. 2022). ISSN: 0019-9567. DOI: 10.1128/iai.00136-22.

[169] K. Saninjuk A. Romsang J. Duang-Nkern et al. "*Pseudomonas aeruginosa* nfuA: Gene regulation and its physiological roles in sustaining growth under stress and anaerobic conditions and maintaining bacterial virulence". In: *PloS one* 13(8) (Aug. 2018). ISSN: 1932-6203. DOI: 10.1371/journal.pone.0202151.

[170] S. Ollagnier-de Choudens S. Angelini C. Gerez et al. "NfuA, a new factor required for maturing Fe/S proteins in Escherichia coli under oxidative stress and iron starvation conditions". In: *J Biol Chem* 283(20) (May 2008), pp. 14084–91. ISSN: 0021-9258. DOI: 10.1074/jbc.M709405200.

[171] B. Catacchio Z. Liu B. García-Díaz et al. "Protecting Gram-negative bacterial cell envelopes from human lysozyme: Interactions with Ivy inhibitor proteins from Escherichia coli and *Pseudomonas aeruginosa*". In: *Biochimica et Biophysica Acta (BBA) - Biomembranes* 1848(11) (Nov. 2015), pp. 3032–3046. ISSN: 0005-2736. DOI: 10.1016/j.bbamem.2015.03.024.

[172] F. Goormaghtigh D. Jurénas N. Fraikin et al. "Biology and evolution of bacterial toxin–antitoxin systems". In: *Nature Reviews Microbiology* 20 (June 2022), pp. 335–350. ISSN: 1740-1534. DOI: 10.1038/s41579-021-00661-1.

[173] D. Low J. Casadesús. "Epigenetic Gene Regulation in the Bacterial World". In: *Microbiology and molecular biology reviews* 70(3) (Sept. 2006), pp. 830–856. ISSN: 1092-2172. DOI: 10.1128/MMBR.00016-06.

[174] C.G.M. Gahan S. Heuston M. Begley et al. "Isoprenoid biosynthesis in bacterial pathogens". In: *Microbiology Society* 158(6) (June 2012), pp. 1389–1401. ISSN: 1465-2080. DOI: 10.1099/mic.0.051599-0.

[175] R.J. Maier G. Wang. "Bacterial histone-like proteins: roles in stress resistance". In: *Current Genetics* 61 (Nov. 2015), pp. 489–492. ISSN: 1432-0983. DOI: 10.1007/s00294-015-0478-x.

[176] S. Crosson C.C. Boutte. "Bacterial lifestyle shapes stringent response activation". In: *Trends in microbiology* 21(4) (Apr. 2013), pp. 174–180. ISSN: 0966-842X. DOI: 10.1016/j.tim.2013.01.002.

[177] P.P. Chong N. Farah V.K. Chin et al. "Riboflavin as a promising antimicrobial agent? A multi-perspective review". In: *Current research in microbial sciences* 3 (Feb. 2022). ISSN: 2666-5174. DOI: 10.1016/j.crmicr.2022.100111.

[178] M. Mosel A. Dorsey-Oresto T. Lou et al. "YihE kinase is a central regulator of programmed cell death in bacteria". In: *Cell reports* 3(2) (Feb. 2013), pp. 528–537. ISSN: 2211-1247. DOI: 10.1016/j.celrep.2013.01.026.

[179] D. Wu Y. Zhang W. Chen et al. "Molecular basis for cell-wall recycling regulation by transcriptional repressor MurR in Escherichia coli". In: *Nucleic Acids Research* 50(10) (May 2022), pp. 5948–5960. ISSN: 0305-1048. DOI: 10.1093/nar/gkac442.

[180] E. Schmidt M. Göbel K. Kassel-Cati et al. "Degradation of aromatics and chloroaromatics by *Pseudomonas* sp. strain B13: cloning, characterization, and analysis of sequences encoding 3-oxoadipate:succinyl-coenzyme A (CoA) transferase and 3-oxoadipyl-CoA thiolase". In: *Journal of bacteriology* 184(1) (Jan. 2002), pp. 216–223. ISSN: 0021-9193. DOI: 10.1128/JB.184.1.216-223.2002.

[181] E. Caruso F. Bolognese C. Scanferla et al. "Bacterial melanin production by heterologous expression of 4-hydroxyphenylpyruvate dioxygenase from *Pseudomonas aeruginosa*". In: *International Journal of Biological Macromolecules* 133 (Jan. 2019), pp. 1072–1080. ISSN: 0141-8130. DOI: 10.1016/j.ijbiomac.2019.04.061.

[182] S. Wilhelm F. Kovačić J. Granzin et al. "Structural and functional characterisation of TesA - a novel lysophospholipase A from *Pseudomonas aeruginosa*". In: *PloS one* 8(7) (July 2013). ISSN: 1932-6203. DOI: 10.1371/journal.pone.0069125.

[183] S. Spinelli B. Douzi Y.R. Brunet et al. "Structure and specificity of the Type VI secretion system ClpV-TssC interaction in enteroaggregative Escherichia coli". In: *Scientific reports* 6(1) (Oct. 2016). ISSN: 2045-2322. DOI: 10.1038/srep34405.

[184] R. Takase Y.M. Hou R. Matsybara et al. "TrmD: A Methyl Transferase for tRNA Methylation With m1G37". In: *The Enzymes* 41 (July 2017), pp. 89–115. ISSN: 1874-6047. DOI: 10.1016/bs.enz.2017.03.003.

[185] K. Ganio E.A. Maunders D.H.Y. Ngu et al. "The Impact of Chromate on *Pseudomonas aeruginosa* Molybdenum Homeostasis". In: *Frontiers in Microbiology* 13 (May 2022). ISSN: 1664-302X. DOI: 10.3389/fmicb.2022.903146.

[186] D. Blair M.K. Sarkar K. Paul. "Chemotaxis signaling protein CheY binds to the rotor protein FliN to control the direction of flagellar rotation in Escherichia coli". In: *Proceedings of the National Academy of Sciences of the United States of America* 107(20) (May 2010), pp. 9370–9375. ISSN: 0027-8424. DOI: 10.1073/pnas.1000935107.

[187] T.W. Man Y. Yang H.C.T. Tsui et al. "Identification and Function of the pdxY Gene, Which Encodes a Novel Pyridoxal Kinase Involved in the Salvage Pathway of Pyridoxal 5-Phosphate Biosynthesis in Escherichia coli K-12". In: *Journal of bacteriology* 180(7) (Apr. 1998), pp. 1814–1821. ISSN: 0021-9193. DOI: 10.1128/jb.180.7.1814-1821.1998.

[188] H. Hellmann M. Parra S. Stahl. "Vitamin B6 and Its Role in Cell Metabolism and Physiology". In: *Cells* 7(7) (July 2018), p. 84. DOI: 10.3390/cells7070084.

[189] T.K. Wood Y. Kim. "Toxins Hha and CspD and Small RNA Regulator Hfq Are Involved in Persister Cell Formation Through MqsR in Escherichia coli". In: *Biochemical and biophysical research communications* 391(1) (Nov. 2009), pp. 209–213. ISSN: 0006-291X. DOI: 10.1016/j.bbrc.2009.11.033.

[190] J.M. Luengo E. Arias-Berrau E.R. Olivera et al. "The Homogentisate Pathway: a Central Catabolic Pathway Involved in the Degradation of l-Phenylalanine, l-Tyrosine, and 3-Hydroxyphenylacetate in *Pseudomonas putida*". In: *Journal of bacteriology* 186(15) (Aug. 2004), pp. 5062–5077. ISSN: 0021-9193. DOI: 10.1128/JB.186.15.5062-5077.2004.

[191] S. Nguyen C. Hickey B. Schaible et al. "Increased Virulence of Bloodstream Over Peripheral Isolates of P. aeruginosa Identified Through Post-transcriptional Regulation of Virulence Factors". In: *Frontiers in cellular and infection microbiology* 9 (Oct. 2018), p. 357. ISSN: 2235-2988. DOI: 10.3389/fcimb.2018.00357.

[192] Y. Li A.Y Bhagirath D. Somayajula et al. "CmpX Affects Virulence in *Pseudomonas aeruginosa* Through the Gac/Rsm Signaling Pathway and by Modulating c-di-GMP Levels". In: *The Journal of membrane biology* 251(1) (Feb. 2018), pp. 35–49. ISSN: 0022-2631. DOI: 10.1007/s00232-017-9994-6.

[193] A. Roujeinikove A.I.M Salah Ud-Din. "Methyl-accepting chemotaxis proteins: a core sensing element in prokaryotes and archaea". In: *Cellular and Molecular Life Sciences* 74(18) (Apr. 2017), pp. 3293–3303. ISSN: 1420-9071. DOI: 10.1007/s00018-017-2514-0.

[194] M. Goel A. Sharma S. Kumari. "Uncovering the structure-function aspects of an archaeal CsaA protein". In: *Biochimica et Biophysica Acta (BBA) - Proteins and Proteomics* 1869(5) (May 2021), p. 140615. ISSN: 1570-9639. DOI: 10.1016/j.bbapap.2021.140615.

[195] S. Fatima S. Devi M. Chaturvedi et al. "Environmental factors modulating protein conformations and their role in protein aggregation diseases". In: *Toxicology* 465(15) (Jan. 2022), p. 153049. ISSN: 0300-483X. DOI: 10.1016/j.tox.2021.153049.

[196] W.A.J. Webster L. Hudek D. Premachandra et al. "Role of Phosphate Transport System Component PstB1 in Phosphate Internalization by Nostoc punctiforme". In: *Applied and Environmental Microbiology* 82(21) (Aug. 2016), pp. 6344–6356. DOI: 10.1128/AEM.01336-16.

[197] C. Vragniau S.S. Abby K. Kazemzadeh et al. "Advances in bacterial pathways for the biosynthesis of ubiquinone". In: *Biochimica et Biophysica Acta (BBA) - Bioenergetics* 1861(11) (Nov. 2020), p. 148259. ISSN: 0005-2728. DOI: 10.1016/j.bbabio.2020.148259.

[198] S. Darie P.M. McNicholas G. Javor et al. "Expression of the heme biosynthetic pathway genes hemCD, hemH, hemM and hemA of Escherichia coli". In: *FEMS Microbiology Letters* 146(1) (Jan. 1997), pp. 143–148. ISSN: 0378-1097. DOI: 10.1111/j.1574-6968.1997.tb10184.x.

[199] G. Layer. "Heme biosynthesis in prokaryotes". In: *Biochimica et Biophysica Acta (BBA) - Molecular Cell Research* 1868(1) (Jan. 2021), p. 11861. ISSN: 0167-4889. DOI: 10.1016/j.bbamcr.2020.118861.

[200] J. Merjane L.M. Nolan L.C. McCaughey et al. "ChpC controls twitching motility-mediated expansion of *Pseudomonas aeruginosa* biofilms in response to serum albumin, mucin and oligopeptides". In: *Microbiology (Reading, England)* 166(7) (July 2020), pp. 669–678. ISSN: 1350-0872. DOI: 10.1099/mic.0.000911.

[201] L. Ji T. Wang X. Du et al. "*Pseudomonas aeruginosa* T6SS-mediated molybdate transport contributes to bacterial competition during anaerobiosis". In: *Cell reports* 35(2) (Apr. 2021), p. 108957. ISSN: 2211-1247. DOI: 10.1016/j.celrep.2021.108957.

[202] P. Shantamoorthy D. Quentin S. Ahmad et al. "Mechanism of loading and translocation of type VI secretion system effector Tse6". In: *Nature microbiology* 3(10) (Oct. 2018), pp. 1142–1152. ISSN: 2058-5276. DOI: 10.1038/s41564-018-0238-z.

[203] S. Liu Y. Wu J. Gong et al. "Crystal structure of PppA from *Pseudomonas aeruginosa*, a key regulatory component of type VI secretion systems". In: *Biochemical and Biophysical Research Communications* 516(1) (Aug. 2019), pp. 196–201. ISSN: 0006-291X. DOI: 10.1016/j.bbrc.2019.06.020.

[204] K. Sato T. Hoshino K. Kose-Terai. "Solubilization and reconstitution of the *Pseudomonas aeruginosa* high affinity branched-chain amino acid transport system". In: *The Journal of biological chemistry* 267(30) (Oct. 1992), pp. 21313–8. ISSN: 0021-9258. DOI: 10.1016/s0021-9258(19)36610-4.

[205] Cystic Fibrosis Foundation. *Pseudomonas aeruginosa PAO1, PA1343*. URL: https://www.pseudomonas.com/. [updated: 06.10.2023; accessed: 09.11.2023].

[206] J. He B. Lesic M. Starkey et al. "Quorum sensing differentially regulates *Pseudomonas aeruginosa* type VI secretion locus I and homologous loci II and III, which are required for pathogenesis". In: *Microbiology (Reading, England)* 155(9) (Sept. 2009), pp. 2845–2855. ISSN: 1350-0872. DOI: 10.1099/mic.0.029082-0.

[207] K.Y. Cho S.R. Koyyalamudi S-C. Jeong et al. "Vitamin B_{12} Is the Active Corrinoid Produced in Cultivated White Button Mushrooms (Agaricus bisporus)". In: *Journal of Agricultural and Food Chemistry* 57(14) (June 2009), pp. 6327–6333. DOI: 10.1021/jf9010966.

[208] E. Klem N.B.Fulcher P.M. Holliday et al. "The *Pseudomonas aeruginosa* Chp chemosensory system regulates intracellular cAMP levels by modulating adenylate cyclase activity". In: *Molecular microbiology* 76(4) (May 2010), pp. 889–904. ISSN: 0950-382X. DOI: 10.1111/j.1365-2958.2010.07135.x.

[209] F. Hoegy M. Hannauer A. Braud et al. "The PvdRT-OpmQ efflux pump controls the metal selectivity of the iron uptake pathway mediated by the siderophore pyoverdine in *Pseudomonas aeruginosa*". In: *Environmental microbiology* 14(7) (July 2012), pp. 1696–708. ISSN: 1462-2912. DOI: 0.1111/j.1462-2920.2011.02674.x.

[210] STRING Consortium. *Interaction Scores*. URL: https://string-db.org/cgi/info. accessed: 13.11.2023.

[211] S.P. Mahan D.M. Heithoff L. Barnes V et al. "Re-evaluation of FDA-approved antibiotics with increased diagnostic accuracy for assessment of antimicrobial resistance". In: *CellPress* 4(5) (May 2023), p. 101023. ISSN: 2666-3791. DOI: 10.1016/j.xcrm.2023.101023.

[212] P.A. Levin J.D: Wang. "Metabolism, cell growth and the bacterial cell cycle". In: *Nature Reviews Microbiology* 7(11) (Nov. 2009), pp. 822–827. ISSN: 1740-1526. DOI: 10.1038/nrmicro2202.

[213] L. Sandegren F. Rajer. "The Role of Antibiotic Resistance Genes in the Fitness Cost of Multiresistance Plasmids". In: *mBio* 13(1) (Jan. 2022), e03552–21. DOI: 10.1128/mbio.03552-21.

[214] S. Banerjee N. Ojkic D. Serbanescu. "Antibiotic Resistance via Bacterial Cell Shape-Shifting". In: *mBio* 13(3) (May 2022). ISSN: 2150-7511. DOI: 10.1128/mbio.00659-22.

[215] A. Maier F. Tomaselli P. Dittrich et al. "Penetration of piperacillin and tazobactam into pneumonic human lung tissue measured by in vivo microdialysis". In: *British journal of clinical pharmacology* 55(6) (June 2003), pp. 620–624. ISSN: 0306-5251. DOI: 10.1046/j.1365-2125.2003.01797.x.

[216] L.T. Cerdeira R.R. Wick L.M. Judd et al. "Trycycler: consensus long-read assemblies for bacterial genomes". In: *Genome Biology* 22(1) (Sept. 2021). ISSN: 1474-760X. DOI: 10.1186/s13059-021-02483-z.

[217] M.S. Trent B.W. Simpson. "Pushing the envelope: LPS modifications and their consequences". In: *Nature Reviews. Microbiology* 17(7) (July 2019), pp. 403–416. ISSN: 1740-1526. DOI: 10.1038/s41579-019-0201-x.

[218] S. Molin M. Gabrielaite H.K. Johansen et al. "Gene Loss and Acquisition in Lineages of *Pseudomonas aeruginosa* Evolving in Cystic Fibrosis Patient Airways". In: *mBio* 11(5) (Oct. 2020). ISSN: 2150-7511. DOI: 10.1128/mBio.02359-20.

[219] DrugBank. *Piperacillin*. URL: https://go.drugbank.com/drugs/DB00319. [updated: 28.11.2023; accessed: 21.11.2023].

[220] DrugBank. *Tazobactam*. URL: https://go.drugbank.com/drugs/DB01606. [updated: 28.11.2023; accessed: 21.11.2023].

[221] H. Hickstein S.C. Mueller J. Majcher-Peszynska et al. "Pharmacokinetics of Piperacillin-Tazobactam in Anuric Intensive Care Patients during Continuous Venovenous Hemodialysis". In: *Antimicrobial agents and chemotherapy* 46(5) (May 2002), pp. 1557–1560. ISSN: 0066-4804. DOI: 10.1128/AAC.46.5.1557-1560.2002.

[222] V. Gerriets J. Hallare. *Half Life*. URL: https://www.ncbi.nlm.nih.gov/books/NBK554498/. [updated: 20.06.2023; accessed: 21.11.2023].

[223] S. Thakur V.K. Ranjan S. Mukherjee et al. "Pandrug-resistant *Pseudomonas* sp. expresses New Delhi metallo-β-lactamase-1 and consumes ampicillin as sole carbon source". In: *Clinical Microbiology and Infection* 27(3) (Mar. 2021), 472.e1–472.e5. ISSN: 1198-743X. DOI: 10.1016/j.cmi.2020.10.032.

[224] R.A. Bonomo P.D. Tamma Y. Doi et al. "A Primer on AmpC β-Lactamases: Necessary Knowledge for an Increasingly Multidrug-resistant World". In: *Clinical infectious diseases : an official publication of the Infectious Diseases Society of America* 69(8) (Mar. 2019), pp. 1446–1455. ISSN: 1058-4838. DOI: 10.1093/cid/ciz173.

[225] J.A. Ayala G. Torrens S.B. Hernández et al. "Regulation of AmpC-Driven β-Lactam Resistance in *Pseudomonas aeruginosa*: Different Pathways, Different Signaling". In: *mSystems* 4(6) (Dec. 2019). DOI: 10.1128/msystems.00524-19.

A Laboratory Equipment & Chemicals

Laboratory Equipment & Materials

Table A.1. Equipment & materials used in this study, as well as supplier

Category	Name	Supplier
Appliances	Certoclav Sterilizer, A-4050	CertoClav
	Freezer, -20 ° C	Bosch
	Freezer, -80 ° C	SANYO
	Incubator 37° C, B 9025	Termaks
	Incubator 37 ° C, New Brunswick TM Scientific Innova 44	Eppendorf
	Laminar Flow Workbench (LAF) SAFE 2020	VWR
	Microwave Oven MD142	Whirlpool
	Milli-Q® Direct 16 Water Purification System	Merck
	Minitron Shaker Incubator	Infors HT
	Refrigerator 4 ° C	Bosch
	Uranos Fume Hood	Netavent
Centrifuges	Allegra X-30R Centrifuge	Beckmann Coulter
	Concentrator plus - Centrifuge Concentrator	Eppendorf
	Microcentrifuge, Heraeus^{TM} Pico^{TM} 21	Thermo Fisher Scientific
	Microcentrifuge, MiniStar	VWR®
	Tabletop Mini Centrifuge, 7000 rpm	3B Scientific
Disposables	1.5 and 2 mL Safe-Lock Tubes	Eppendorf
	1.5 mL Protein LoBind Microcentrifuge Tubes	Eppendorf
	BD Microlance^{TM} 3 Sterile Needle	BD Microlance^{TM} 3
	Breathe Eazy Gas Permeable Sealing Membrane for Microtiter Plates	Sigma-Aldrich
	Extraction Disks C18	CDS Empore^{TM}
	Falcon Tubes (15 and 50 mL)	Greiner
	Petri Dishes, 90 mm	Heger
	Pipette Refill Tips	Axygen
	Plastic Cuvettes	Brand GMBH
	Quartz Filter MK360	Munktell Filtrak^{TM}
	QubitTM Assay Tubes	Thermo Fisher Scientific
	Rnase-free Pipette Tips	Thermo Fisher Scientific
	Sterile 0.2 μm Syringe Filter	Sarstedt
	Sterile 26 g blunt end needle	SAI Infusion Technologies
	Sterile 30 mL Syringe	BD Plastipak
	Sterile Inoculation Loops, 10 μL, blue	Sarstedt
	Sterile Microtest Plate 96-Wells	Sarstedt
	Wide Bore Pipette Tips 200 μL	VWR®
Equipment	8-Well Comb	Bio-Rad
	DynaMag-2 Magnetic Tube Rack	Thermo Fisher Scientific

Table A.1. Equipment & materials used in this study, as well as supplier

Category	Name	Supplier
	Gel Doc^{TM} EZ Imager System	Bio-Rad
	HulaMixerTM Sample Mixer	Thermo Fisher Scientific
	Mini-Sub Cell GT Horizontal Electrophoresis System	Bio-Rad
	PowerPac^{TM} Basic Power Supply	Bio-Rad
	Qubit 3.0 Fluorometer	Thermo Fisher Scientific
	Sonicator Bath, Bransonic® Ultrasonic 3510	Branson
	Sub-Cell GT Gel Caster	Bio-Rad
	ThermoMixer C	Eppendorf
	Ultrasonic processor, Vibra-Cell^{TM}, VC 505	Sonics & Materials, Inc.
	UV sample tray	Bio-Rad
	Vortex Mixer MS3 basic	IKA®
Instruments	Mass spectrometer, timsTOF Pro 2	BRUKER
	NanoDrop^{TM} One/OneC Microvolume UV-Vis Spectrophotometer	Thermo Fisher Scientific
	pH Meter 913	Metrohm
	Sartorius Weighing Scale	VWR
	Spectrophotometer, BioPhotometer 6131	Eppendorf
	VarioskanTM LUX multimode microplate reader	Thermo Fisher Scientific
Miscellaneous equipment	100-1000 μL Ultra-High Performance Automated Pipette	VWR®
	16 Gauge Needle	-
	Automated pipettes	Thermo Fisher Scientific
	Finnpipette^{TM} F1 Multichannel Pipette	Thermo Fisher Scientific
	Miscellaneous glassware	Duran®
	Nalgene® Labtop Cooler	Thermo Fisher Scientific
	Peeksil Capillary 1/32”	-
	PTFE Magnetic Stir Bar	Fisherbrand^{TM}
	Transferpette® S 100-1000 μL	Brand GMBH

Chemicals:

Table A.2. Chemicals used in this study and the supplier of the chemicals.

Chemical	Supplier
Acetonitrile (ACN)	VWR
Agar Powder	VWR
Ammonium Bicarbonate (ABC)	Sigma-Aldrich
Bacto Tryptone	Gibco
Bacto Yeast Extract	Gibco
BL3 Buffer	PacBio
Ceftazidime	Sigma-Aldrich
Ciprofloxacin	Sigma-Aldrich
CLE3 Buffer	PacBio
Colistin	Sigma-Aldrich
Complete Mini EDTA Free Protease Inhibitor	Roche
CW1 Buffer	PacBio
CW1 Buffer	PacBio
Dithiothreitol (DTT)	Thermo Fisher Scientific
DNA Control Sample	Oxford Nanopore Technologies
EB Buffer	PacBio
EDTA	Oxford Nanopore Technologies
Elution Buffer	Oxford Nanopore Technologies
Ethanol (96-100 %)	VWR
Gel Loading Dye Buffer	Thermo Fisher Scientific
Hydrochloric acid	VWR
Iodoacetamide (IAA)	Sigma-Aldrich
Isopropanol	VWR
Library Beads	Oxford Nanopore Technologies
Library Solution	Oxford Nanopore Technologies
Long Fragment Buffer	Oxford Nanopore Technologies
Lysozyme	Thermo Fisher Scientific
Meropenem trihydrate	Sigma-Aldrich
Mueller-Hinton Broth	Sigma-Aldrich
Native Adapter	Oxford Nanopore Technologies
Native Barcodes (NB01-24)	Oxford Nanopore Technologies
NEB Blunt/TA Ligase Master Mix (NEB, Cat #M0367)	New England BioLabs
NEBNext FFPE DNA Repair Buffer	New England BioLabs
NEBNext FFPE DNA Repair Mix (M6630)	New England BioLabs
NEBNext Ultra II End Repair / dA-tailing Module (E7546)	New England BioLabs
NEBNext® Quick Ligation Reaction Buffer (NEB B6058)	New England BioLabs
Nuclease Free Water	Invitrogen

Table A.2. Chemicals used in this study and the supplier of the chemicals.

Chemical	Supplier
PBS Buffer	PacBio
PeqGreen	Peqlab
Phenylmethylsulfonyl Fluoride (PMSF)	Sigma-Aldrich
Phosphatase Inhibitor Cocktail Tablets (PhosSTOP)	Roche
Phosphoric acid	Sigma-Aldrich
Piperacillin Sodium Salt	Sigma-Aldrich
Proteinase K	PacBio
Qubit dsDNA BR buffer (component A)	Thermo Fisher Scientific
Qubit dsDNA BR reagent (component B)	Thermo Fisher Scientific
Qubit dsDNA BR standard #1	Thermo Fisher Scientific
Qubit dsDNA BR Standard #2	Thermo Fisher Scientific
Quick T4 DNA Ligase in NEBNext® Quick Ligation Module (NEB E6056)	New England BioLabs
Quick-Load® 1kb Ladder	Thermo Fisher Scientific
Rnase A	PacBio
RPMI	Gibco
Sequencing Buffer	Oxford Nanopore Technologies
Short Fragment Buffer	Oxford Nanopore Technologies
Sodium Chloride	VWR
Sodium Dodecyl Sulfate (SDS)	Thermo Fisher Scientific
SRE XS Buffer	PacBio
TAE Buffer	Bio-Rad
TAE Running Buffer	Bio-Rad
Tazobactam	Cayman Chemical Company
Tobramycin	Sigma-Aldrich
Trifluoroacetic Acid (TFA) Solution	Sigma-Aldrich/Merck
Tris base	Fisher Bioreagents
Trypsin	Thermo Fisher Scientific
Ultra II End-prep Enzyme Mix	Oxford Nanopore Technologies
Ultra II End-prep Reaction Buffer	Oxford Nanopore Technologies

B Wessel & Fluegge Protein Precipitation

Wessel & Fluegge (1) protein precipitation

Material:

- 1.5 ml microtubes (chloroform-resistant ➔ PE or PP) / 15 ml Falcon
- Methanol p.A. or better
- Chloroform p.A. or better
- H20 bidest.
- Centrifuge equipped with a rotor for microtubes/Falcons (9000 g needed).

Method:

1. To 100 µl /1 ml sample in a microtube/Falcon add 400 µl/4 ml methanol, mix thoroughly and centrifuge for 10 s at 9000 g.
2. Add 100 µl / 1 ml chloroform, mix and centrifuge for 10 s at 9000g. For samples containing a high amount of lipids (e.g. liposomes) use 200 µl /2 ml of chloroform instead.
3. Add 300 µl / 3 ml H2O bidest, mix thoroughly and centrifuge at 9000 g for 1 min to separate phases. Three phases will become visible. An upper H2O-methanol phase, a protein interphase and a lower chloroform phase.
4. Remove the upper phase carefully without disturbing or touching the protein interphase.
5. Add another 300 µl / 3 ml of methanol to the remaining phases, mix thoroughly and centrifuge for 2 min at 9000 g. This pellets the protein.
6. Remove the supernatant carefully and dry the pellet (Until no chloroform smell is detectable anymore.).
7. The dried pellet can now be solubilized in an appropriate buffer for further processing e.g., Laemmli buffer for SDS-PAGE separation or 8 M Urea buffer for in-solution protein digestion.

References:

1. Wessel, D, and Flügge, UI A method for the quantitative recovery of protein in dilute solution in the presence of detergents and lipids. *Analytical Biochemistry* **138**, 141 143

C Short-Read Elimination (SRE) protocol

Size selection protocol for SRE XS

The following protocol details size selection of HMW gDNA or fragmented DNA. **For HiFi sequencing, size selection should be performed on gDNA prior to shearing and library preparation.** The Qubit DNA concentration should be >25 ng/µL.

HMW gDNA or sheared/fragmented DNA

1. Adjust the DNA sample to a total volume of 60 µL and a Qubit DNA concentration of between 25–150 ng/µL. Pipette the sample into a 1.5 mL Eppendorf DNA LoBind tube.
   - This concentration MUST be measured using a Qubit dsDNA Broad Range Assay or equivalent.
   - Dilute the sample using TE buffer (pH 8), Buffer EB, or water.
2. Add 60 µL of Buffer SRE XS to the sample. Mix thoroughly by gently tapping the tube or by gently pipetting up and down.
3. Load the tube into the centrifuge with the hinge facing toward the outside of the rotor.
4. Centrifuge at 10,000 x *g* for 30 mins at room temperature.
   - If using a centrifuge with temperature control (i.e., cooling function), turn this function off by setting the temperature to 29°C.
5. Carefully remove the supernatant from tube without disturbing the DNA pellet. Place the pipette tip on the thumb lip side of the tube (see Figure 7).
   - The DNA pellet will have formed on the bottom of the tube under the hinge region.
6. Add 200 µL of the 70% EtOH wash solution to tube and centrifuge at 10,000 x *g* for 2 mins at RT.
   - Do not tap or mix after adding 70% EtOH. Place tube directly into the centrifuge.
7. Carefully remove the wash solution from the tube without disturbing the DNA pellet. Place the pipette tip on the thumb lip side of the tube (see Figure 7).
8. Add 50–100 µL of Buffer EB to the tube and incubate at room temperature for 20 minutes. The buffer volume may be adjusted to achieve desired concentration.
9. After incubation, gently tap the tube to ensure that the DNA is properly re-suspended and mixed.
10. Analyze the recovery and purity of the DNA by using a NanoDrop and Qubit system.

Quick tip

Using concentrations derived from UV-Vis measurements without accounting for RNA concentrations will adversely affect yields.

Quick tip

The DNA pellet may not be visible. Placing the tube and pipetting in the directed orientations will prevent accidentally aspirating the DNA pellet.

Quick tip

Longer DNA can take more time to re-suspend. Heating to 50°C or eluting for more time can help increase recoveries.

102-582-400 REV 03 MAR2023

PacBio

D Significantly Dys-regulated Proteins in PAU3

Appendix D includes all dysregulated proteins identified in strain PAU3 continuously exposed to the β-lactam Piperacillin of varying concentrations and the β-lactamase inhibitor Tazobactam at 4 μg/mL.

Table D.1. Dys-regulated proteins PAU3. All dys-regulated proteins in strain PAU3 continuously exposed to TZP.

-$\log_{10}$ (p-value)	$\log_2$FC	Gene names	-$\log_{10}$ (p-value)	$\log_2$FC	Gene names	-$\log_{10}$ (p-value)	$\log_2$FC	Gene names
1 μg/mL vs Control			512 μg/mL vs Control			512 μg/mL vs 1 μg/mL		
1.86675	2.62726	PA1830	3.6193	4.3997	ampC	2.26655	3.4643	ampC
1.34281	1.98007	mifR	1.3675	1.6267	ribH ribE	1.42607	2.65908	cspD
2.02127	1.80891	creC	2.0119	1.4239	srkA	3.05244	2.60933	hupB
1.50878	1.78893	vgrG2b	1.4906	1.3816	PA3670	2.32809	2.14034	Unknown
1.55757	1.62022	PA0754	1.399	1.3375	mltF	1.65976	2.08915	hmgA
2.00022	1.49638	pctC	1.9042	1.2732	PA3850	2.57622	1.79027	rpsN
1.63205	1.47223	PA3983	1.4042	1.206	dhcB	2.49384	1.6709	sspB
2.08435	1.45396	nfuA	2.4611	1.2021	gap hexC	1.97712	1.38407	rpmD
2.15266	1.36722	PA5225	2.4093	1.198	PA3672	1.54281	1.35003	rpsP
2.39259	1.34236	PA3208	1.9266	1.1859	hpd	1.79952	1.2574	gap hexC
3.12955	1.24461	PA0460	1.5116	1.1174	PA0261	1.54929	1.23442	maiA
2.04012	1.21252	PA1662	1.3545	1.0165	tesA	1.42394	1.23203	csrA rsmA
1.60845	1.17997	PA2630	1.3784	1.0142	PA0071	1.5333	1.19566	PA3672
2.96872	1.15638	PA5153	1.884	0.9201	PA1069	1.91664	1.17027	kdpB
1.70969	1.0932	ivy	1.8036	0.8618	PA4558	1.71757	1.09143	cmpX
1.90994	1.03496	chpA	2.3889	0.8563	PA1742	1.36189	0.9991	PA1009
1.51451	1.01951	nuoE	1.4116	0.8473	clpV1	1.57307	0.936617	srkA
1.54789	1.01023	PA1658	2.063	0.7614	ldcA	1.95397	0.92887	dhcB
1.60915	0.989517	PA0360	1.3618	0.74	iscR	2.2159	0.917137	PA4340
1.79627	0.970675	PA3302	1.4109	0.7332	nusG	1.41189	0.778834	PA0919
3.41348	0.969336	hflX	1.7271	0.7107	PA1052	1.77065	0.737299	rpsR
1.45565	0.911108	clpV1	1.5182	0.7101	rnhA	2.28025	0.704804	PA4223
3.19201	0.910014	PA3779	2.4287	0.6489	ftsZ	1.39195	0.689529	rpmG
1.74568	0.904971	slyD	1.7255	0.6451	rplY ctc	1.31754	0.653795	algP algR3
2.37381	0.90422	rapA hepA	1.6503	-0.583	PA1521	1.4951	0.614631	rpmE
1.55014	0.851031	aph	1.3042	-0.588	PA3286	1.34662	0.604306	metZ
2.7756	0.800341	PA0399	1.4332	-0.59	mnmG gidA	2.2205	0.601453	mucD
1.33519	0.798629	nusA	1.5027	-0.591	ssb	1.52708	-0.607424	nuoE
2.58442	0.798134	PA3715	2.5989	-0.591	gmk	2.50731	-0.6115	smc
2.3136	0.793634	fliD	1.3745	-0.592	PA5343	1.97119	-0.618139	mnmE trmE
1.68895	0.755431	PA3836	1.5171	-0.658	speC	2.11559	-0.623491	cobW
1.47685	0.685301	mtnC	1.3553	-0.66	PA4400	1.30195	-0.629803	ispF
1.50136	0.678285	dsbA	1.3067	-0.666	betB	1.56338	-0.630615	Unknown
1.95615	0.664735	PA0459	2.2438	-0.675	wbpE	2.0663	-0.631528	Unknown
1.8137	0.616358	fimX	1.5865	-0.69	gatB	2.50582	-0.650375	apeB
1.7529	0.607084	fha1	2.3631	-0.695	map	1.76815	-0.652614	dapE
1.67411	0.603769	PA4880	2.4476	-0.701	pntAA	1.31534	-0.654607	arcC
2.22807	0.600992	narG	1.7815	-0.715	hisC2	1.36111	-0.666132	Unknown
1.68205	0.598805	PA2318	1.3011	-0.726	soj	1.36829	-0.695609	PA3302
2.24901	-0.580283	upp	1.3688	-0.732	ohr	1.47091	-0.722522	PA0356
1.84179	-0.600998	map	1.6352	-0.739	pilY1	1.51217	-0.728886	pdxH
1,95088	-0.635225	dapD	1.3876	-0.758	pyrR	1.41982	-0.732646	PA2462
1.61644	-0.701144	thiE	1.706	-0.758	PA0840	1.79916	-0.742465	aer tlpC
1.53494	-0.706291	PA2455	1.5628	-0.763	fabY	1.91326	-0.743883	PA4474
1.42941	-0.726894	rplM	1.4851	-0.767	lexA	2.09473	-0.744022	hslO
1.95843	-0.785435	PA1205	2.6676	-0.792	rpsG	1.74964	-0.746588	PA1458
1.49082	-0.808167	alr	1.3822	-0.796	rnhB	1.88172	-0.780259	selD
1.71038	-0.835186	rpsO	2.8811	-0.798	leuD	1.61279	-0.786099	mupP
1.54419	-0.932279	PA0937	1.5268	-0.801	fmt	1.84765	-0.794048	rlmJ
1.9103	-0.956436	algP algR3	1.5225	-0.806	murD	1.42332	-0.7983	apaG
1.865	-1.05926	rpmB	2.2243	-0.809	PA4991	1.47464	-0.819752	ccoP2
1.50799	-1.06296	PA0622	1.9469	-0.82	PA5139	1.55963	-0.843524	vgrG1a
1.91837	-1.10785	rpmG	1.9121	-0.825	PA0020	1.49291	-0.849092	PA3981
1.30755	-1.19972	ispD	1.8058	-0.825	PA3798	1.49469	-0.859451	chpA

Table D.1. continued from previous page

-log$_{10}$ (p-value)	log$_2$FC	Gene names	-log$_{10}$ (p-value)	log$_2$FC	Gene names	-log$_{10}$ (p-value)	log$_2$FC	Gene names
1 μg/mL vs Control			512 μg/mL vs Control			512 μg/mL vs 1 μg/mL		
1.41186	-1.23351	rplL	1.6637	-0.836	PA4948	1.30146	-0.873263	PA3678
2.1516	-1.33013	rplT	1.368	-0.836	flgD	1.36613	-0.888371	PA1662
1.95391	-1.34548	PA5502	1.7587	-0.844	glyA1/glyA2	2.15321	-0.888376	gcvH1
2.47965	-1.36166	PA4840	2.6354	-0.847	rsmH mraW	1.38578	-0.89915	apaH
2.21075	-1.36643	rpsG	2.6217	-0.878	PA3726	2.99645	-0.91125	kdsB
1.35431	-1.37736	fliI	2.0148	-0.879	pilM	2.58692	-0.919935	pilM
1.43573	-1.48099	rpsT	1.7391	-0.903	pctC	1.83335	-0.930025	PA3819
1.83076	-1.49962	rpsP	1.9966	-0.905	queF	2.00727	-0.9344	PA1832
2.36276	-1.55871	rpsR	1.6559	-0.913	ispD	1.78303	-0.956274	PA0041
1.89507	-1.69313	PA3204	1.4579	-0.915	ubiV	2.03349	-0.958543	PA2352
1.38792	-1.82278	rpmI	2.6926	-0.916	osmC	1.95769	-0.963358	trpA
2.15804	-2.02235	hupB	2.1583	-0.921	PA2458	1.49372	-0.980181	PA2867
1.32517	-2.13411	PA3341	2.3575	-0.96	tlpQ	1.60819	-0.998801	PA3349
1.81005	-2.18129	csrA rsmA	1.4618	-0.97	pctB	2.35045	-1.02852	PA0840
2.36825	-2.31076	rpsN	1.8628	-0.99	ctpM	2.24455	-1.03026	cysA
2.9315	-2.43897	Unknown	1.8525	-0.999	PA2116	3.15499	-1.05667	hisF1
			1.5711	-1.019	PA5109	1.44283	-1.05849	sdaA
			1.3558	-1.051	PA5440	1.53144	-1.06248	vgrG2b
			1.7601	-1.06	ptpA	1.95157	-1.10189	PA0502
			1.4448	-1.08	PA1090	2.40019	-1.1057	PA2458
			2.4088	-1.092	PA3349	1.53607	-1.1079	PA1228
			1.5697	-1.116	nirF	1.97965	-1.11582	fliD
			2.2515	-1.123	PA2352	1.42514	-1.13426	PA2528
			2.1215	-1.143	folC	1.47687	-1.14836	PA1658
			2.2452	-1.204	PA4633	1.91653	-1.1547	flgD
			2.1627	-1.227	PA0502	3.90805	-1.18253	fliF
			1.7466	-1.243	queC	1.64954	-1.19534	PA0020
			1.8826	-1.256	PA2567	1.48789	-1.1954	PA4812*
			2.3572	-1.256	dnr	1.38063	-1.20432	PA3618
			2.3338	-1.261	trpA	1.42687	-1.20499	PA5475
			1.478	-1.267	cheR1	1.64122	-1.21525	trpB
			1.6199	-1.337	trpB	2.15149	-1.25761	fliG
			1.5437	-1.361	phnC1	2.00331	-1.28217	ctpM
			1.6017	-1.375	cobT cobU	1.72472	-1.29284	cheR1
			1.7296	-1.387	PA5317	2.00921	-1.32222	pilN
			1.5209	-1.426	PA4679	1.61898	-1.32899	PA5109
			1.7253	-1.428	PA3450	1.71737	-1.35226	tlpQ
			1.6722	-1.437	trmD	3.09973	-1.37907	rapA hepA
			1.4547	-1.459	PA0040/PA2463	2.70044	-1.40271	PA4633
			3.3612	-1.486	PA0622	1.99208	-1.41132	slyD
			1.4386	-1.528	PA0308	2.03597	-1.41531	PA5139
			1.6185	-1.553	narG	1.8347	-1.43816	PA0562
			2.9882	-1.561	PA4286	1.48998	-1.4407	PA0040/PA2463
			1.4402	-1.659	PA1441	2.07432	-1.44209	PA4543
			1.9888	-1.731	moaB1	1.35064	-1.44631	nirF
			1.3915	-1.741	PA3268	1.40501	-1.45236	moaB1
			1.8677	-1.79	cheY	3.44267	-1.47069	PA4812*
			1.3142	-1.849	PA2695	2.13975	-1.49236	pctB
			3.6849	-2.095	fliC	1.67628	-1.52194	PA4709
			1.7172	-2.249	PA1913	2.39165	-1.53505	PA4520
			1.4001	-2.272	PA4619	3.93274	-1.56055	PA3871
			1.3279	-2.522	pdxY	1.36073	-1.63246	PA4675
			1.3834	-2.578	PA1043	2.22898	-1.64016	PA3214
			2.4282	-3.104	PA5033	1.90357	-1.68707	PA4286
						1.49345	-1.71276	pilE
						1.49732	-1.77633	PA1830
						1.85992	-1.80162	PA1093
						1.58108	-1.81414	PA0295
						1.91156	-1.81555	pilX
						3.33807	-1.85715	fliC
						2.1718	-1.85998	PA3450
						1.59374	-1.99011	PA4514
						2.06948	-2.15479	narG
						2.56079	-2.21251	PA4739

Table D.1. continued from previous page

-log$_{10}$ (p-value)	log$_2$FC	Gene names	-log$_{10}$ (p-value)	log$_2$FC	Gene names	-log$_{10}$ (p-value)	log$_2$FC	Gene names
1 μg/mL vs Control			**512 μg/mL vs Control**			**512 μg/mL vs 1 μg/mL**		
						1.36684	-2.2271	PA4619
						2.67135	-2.40015	pctC
						2.85244	-3.65051	PA5033
						1.58099	-5.89557	hmp fhp

E Significantly Dys-regulated Proteins in PAU5

Appendix E includes all dysregulated proteins identified in strain PAU5 continuously exposed to the β-lactam Piperacillin of varying concentrations and the β-lactamase inhibitor Tazobactam at 4 μg/mL.

Table E.1. Dys-regulated proteins PAU5. All dys-regulated proteins in strain PAU5 continuously exposed to TZP.

-log$_{10}$ (p-value)	log$_2$FC	Gene names	-log$_{10}$ (p-value)	log$_2$FC	Gene names	-log$_{10}$ (p-value)	log$_2$FC	Gene names
1 μg/mL vs Control			512 μg/mL vs Control			512 μg/mL vs 1 μg/mL		
1.79184	2.46	PA0735	1.65878	7.53	ampC	5.23425	11.41	ampC
1.52822	2.04	csaA	3.23738	5.62	vgrG1a	2.74822	5.80	tssF1
1.5513	1.74	pstC	2.30417	4.51	PA0089	2.58418	5.51	vgrG1a
1.85247	1.60	ispE	4.2016	3.87	PA0047	2.56354	4.72	tse4
1.74489	1.07	PA2666	1.68141	3.68	PA0735	2.64727	4.37	PA0089
1.83697	0.92	PA2497	3.24895	3.58	tssF1	2.04142	4.34	PA2541
1.94439	0.89	ubiH	2.00723	3.44	pppA	3.45522	3.91	PA0047
1.37707	0.81	PA1737	2.89232	3.43	PA2539	3.40844	3.81	tagJ
1.32489	0.67	rluC	1.71328	3.36	tssA1	2.6096	3.54	PA2792
1.4092	0.64	hemC	2.56341	3.34	Uknown	2.61013	3.50	PA0078
1.48258	0.63	PA3003	1.67532	3.33	PA1639	1.44099	3.44	pppA
2.3978	-0.58	PA1769	2.82485	3.08	clpV1	3.87205	3.43	hcp1
1.32518	-0.62	ntrB	2.8283	3.04	tse4	2.84926	3.37	PA5113
1.70541	-0.62	PA5136	2.62198	2.96	tssB1	1.82669	3.37	PA3483
1.58144	-0.63	PA4380	1.37697	2.89	eagT6	3.71422	3.09	tsi1
1.81736	-0.65	tssC1	2.5096	2.87	PA0076	3.91839	3.03	tssC1
2.45968	-0.66	erpA	2.83464	2.70	PA3727	5.44946	2.99	clpV1
1.52488	-0.68	PA5149	1.53837	2.68	mexC	3.87836	2.88	PA1639
1.45193	-0.88	rbsK	3.05217	2.64	PA0078	4.05169	2.86	PA0126
1.49208	-0.90	PA0938	1.7721	2.61	PA5113	3.12985	2.86	PA2539
2.24257	-0.93	kdpB	3.87215	2.49	PA0126	3.91277	2.84	PA0071
1.46169	-0.96	nth	5.1208	2.46	PA2540	3.37807	2.79	PA0277
1.77175	-1.03	PA0658	2.30089	2.45	PA5412	2.84791	2.77	PA0076
1.6292	-1.08	mgtA	3.1743	2.45	ppkA	2.24959	2.76	PA1068
1.96643	-1.25	PA3951	3.66079	2.38	tssC1	4.28194	2.68	PA2540
1.31965	-1.35	PA1811	2.94848	2.36	tagJ	3.32542	2.67	PA3727
1.50294	-1.45	tagJ	2.15022	2.35	hcp1	3.99475	2.67	tssM1
1.68957	-1.57	PA1343	2.17015	2.35	PA0071	2.71424	2.62	tssB1
1.65707	-1.72	PA1655	1.5951	2.31	csaA	2.27811	2.61	Unknown
2.33762	-1.84	PA4965	8.64795	2.27	tssK1	1.85902	2.60	mexC
1.51245	-2.13	chpC	1.94108	2.27	tssM1	2.82741	2.56	tssA1
1.57912	-2.18	PA2901	1.72759	2.23	arnT	2.71152	2.46	ppkA
1.73338	-2.45	modA	1.3764	2.17	PA3284	7.11638	2.40	tssK1
			1.37132	2.10	PA3483	2.98086	2.39	PA2793
			2.19185	2.10	PA4320	3.45867	2.33	PA5412
			1.97717	2.08	PA0277	4.76149	2.25	PA1069
			1.54031	2.06	PA2631	2.66752	2.24	eagT6
			2.64673	2.01	PA1069	3.09374	2.23	PA3021
			2.96258	1.86	PA1068	3.17411	2.06	PA4487
			1.47688	1.80	PA3021	1.96044	2.02	PA1669
			2.72444	1.73	PA3716	3.66803	1.93	PA1791
			1.41703	1.73	rtcA	2.21488	1.87	PA0045
			2.88305	1.68	PA1791	2.64882	1.86	PA0070
			3.08992	1.65	PA0070	3.29987	1.85	PA3716
			1.46763	1.64	PA2815	2.17302	1.84	PA4491
			1.82923	1.61	PA3730	1.93715	1.84	arnT
			2.26833	1.59	PA4489	2.9023	1.82	PA0938
			2.07231	1.56	PA2581	2.20655	1.80	PA4320
			2.65147	1.50	PA5441	3.2714	1.80	PA2581
			1.92574	1.47	PA2496	1.3065	1.77	PA1645
			1.47176	1.45	PA2793	2.37424	1.74	PA0659
			1.72629	1.42	Unknown	1.70187	1.73	PA3317
			1.46355	1.20	PA2666	4.47323	1.72	PA4489
			1.99298	1.16	PA3728	2.69733	1.64	PA4965
			2.69034	1.15	PA4322	3.31951	1.63	PA5441

Table E.1. continued from previous page

-log$_{10}$ (p-value)	log$_2$FC	Gene names	-log$_{10}$ (p-value)	log$_2$FC	Gene names	-log$_{10}$ (p-value)	log$_2$FC	Gene names
1 μg/mL vs Control			512 μg/mL vs Control			512 μg/mL vs 1 μg/mL		
			1.36057	1.13	pstC	1.7761	1.59	PA0065
			1.70492	1.00	lpdV	3.4113	1.57	PA5136
			1.79809	0.98	PA3729	1.43351	1.45	pncB1
			1.37739	0.97	PA0461	1.6502	1.42	PA5248
			2.71738	0.95	PA5136	1.64705	1.42	PA2503
			1.45085	0.92	PA0938	1.59972	1.37	nhaB
			1.64313	0.86	PA5178	2.71603	1.33	PA3728
			1.37917	0.84	bifA	1.33109	1.23	PA4955
			1.45501	0.82	phhA	1.67555	1.21	PA3228
			1.35605	0.80	rluC	1.44414	1.20	PA2631
			1.62125	0.76	PA1509	1.47143	1.17	gntR
			1.35906	0.71	PA5509	1.6556	1.13	PA2815
			1.32716	0.71	PA2592	1.81925	1.12	PA0418
			1.47081	0.64	PA5525	1.39902	1.08	PA3730
			1.37865	0.63	PA3238	2.08384	1.06	PA1171
			1.48678	-0.61	pilH	1.58666	1.03	PA3729
			1.77133	-0.63	aspA	1.70811	1.02	PA3267
			1.69487	-0.71	PA2915	1.51786	0.92	Unknown
			1.60128	-0.73	erpA	1.85047	0.91	atpB
			2.05883	-0.80	PA3309	1.51648	0.90	cat catB7
			1.76947	-0.82	kdpB	1.42716	0.90	PA1324
			1.31537	-0.85	gmk	1.77671	0.90	PA5178
			1.86308	-0.85	PA5339	1.96337	0.88	PA2537
			1.94832	-0.91	braC	1.33804	0.88	PA2271
			1.40556	-0.97	PA0468	1.56279	0.87	phaF
			1.35599	-0.99	PA3846	1.41284	0.84	wbpM
			1.69007	-1.12	gltP	1.54289	0.84	Unknown
			1.73973	-1.17	alr	1.78176	0.82	PA4625
			1.30765	-1.21	PA4463	1.78248	0.81	phoU
			1.96332	-1.48	modA	2.08617	0.81	pelD
			2.23198	-1.62	PA4753	2.62341	0.79	PA4430
			1.66253	-1.70	PA3894	1.66401	0.78	dtd
			1.8148	-3.08	PA1343	1.49903	0.77	PA4583
						1.52837	0.73	PA4972
						2.15742	0.72	PA4624
						2.65985	0.71	PA2378
						1.55983	0.70	PA4322
						1.45462	0.68	PA4717
						1.50044	0.68	cntL zrmB
						1.51643	0.67	moaC
						1.43884	0.66	PA4715
						1.56423	0.62	PA2592
						1.66022	-0.60	Unknown
						1.64495	-0.62	ribC
						2.0687	-0.63	Unknown
						1.55622	-0.66	cobO
						2.24626	-0.67	gmk
						2.00021	-0.68	pilG
						1.74919	-0.74	rsgA
						1.35889	-0.75	PA1027
						1.30516	-0.77	azu
						1.98591	-0.79	PA2745
						1.55427	-0.79	PA5062
						1.52705	-0.81	PA3053
						1.58539	-0.83	PA3003
						2.18342	-0.85	lpxB
						2.10632	-0.95	Unknown
						1.32202	-1.19	PA4404
						1.80518	-1.21	DUF5329
						1.56389	-1.22	ispD
						1.659	-1.49	PA2770
						2.02349	-1.58	PA3779
						2.61065	-1.60	PA0182
						1.7722	-1.70	bfr bfrA

Table E.1. continued from previous page

-$\log_{10}$ (p-value)	$\log_2$FC	Gene names	-$\log_{10}$ (p-value)	$\log_2$FC	Gene names	-$\log_{10}$ (p-value)	$\log_2$FC	Gene names
1 μg/mL vs Control			**512 μg/mL vs Control**			**512 μg/mL vs 1 μg/mL**		
						1.81095	-1.80	opmQ

F Dys-regulated Proteins in PAU5 Spiked with MEM & CAZ

Appendix F includes all dys-regulated proteins identified in strain PAU5 spiked with the β-lactams Meropenem for a final concentration of 0.0064 μg/mL on the left hand side, and Ceftazidime for a final concentration of 32 μg/mL on the right hand side of the table.

Table F.1. Dys-regulated proteins in PAU5. Overview over all dys-regulated proteins in isolate PAU5 when spiked with the β-lactams Meropenem and Ceftazidime.

$-\log_{10}$(p-value)	$\log_2$FC	Gene names	$-\log_{10}$(p-value)	$\log_2$FC	Gene names
Meropenem 0.0064 μg/mL vs Control			**Ceftazidime 32 μg/mL vs Control**		
2,57777	1,54818	PA0436	1,33897	2,30262	nirN PA0509
2,39084	1,40873	rlpA PA4000	2,10573	2,09738	PA0880
2,02732	1,69008	PA1039	1,31346	1,74397	PA1021
1,90205	1,45125	PA1737	1,34018	1,47823	PA1791
1,76906	2,37096	pcnB PA4727	2,07125	1,47242	PA2546
1,60689	1,85647	PA3697	1,44832	1,16261	atuF PA2891
1,41549	1,42143	PA2541	1,36561	1,09196	pilP PA5041
1,37526	1,47143	ldhA PA0927	1,60594	1,04069	pilP
1,28956	1,32692	PA4583	1,80495	0,74802	rimP PA4746
1,20772	2,84081	zipA PA1528	1,63211	-0,63803	PA1624
1,20500	1,90004	PA1315	2,23507	-0,65942	PA0578
1,08244	1,47804	grpE PA4762	1,342	-0,76079	bioD PA0504
1,06698	2,06839	rsaL PA1431	1,47913	-0,81831	creB PA0463
1,05829	1,81114	sfsA PA4721	1,34845	-0,86018	pfpI PA0355
1,04897	2,29091	tpiA PA4748	1,89823	-1,19832	PA1200
1,02314	1,48145	hisA PA5141	1,75165	-1,19982	algW PA4446
1,00947	1,57660	PA1752	1,46616	-1,22414	rlpA PA4000
0,97692	2,10013	cobP PA1278	2,31208	-1,26602	PA4923
0,96171	1,44980	rnc PA0770	1,95467	-1,44335	PA3199
0,91629	1,49062	PA3046	1,54406	-1,46413	PA1226
0,91029	1,44153	catR PA2510	2,33996	-1,48933	hitA PA4687
0,89523	1,38849	hslO PA5193	1,30731	-1,49486	PA3282
0,87675	1,48870	PA3965	1,474	-1,76413	betI PA5374
0,87674	1,84284	PA5523	1,70133	-2,17811	PA3277
0,87671	1,61150	PA3962	1,30962	-3,04169	PA3087
0,86936	1,69985	mtnB PA1683			
0,84500	1,47317	PA3190			
0,84187	2,52449	PA4576			
0,82610	1,37569	PA1309			
0,81462	1,36918	PA0227			
0,76704	2,25540	PA4395			
0,75344	1,48745	fdhE PA4809			
0,73660	2,51409	PA1062			
0,73607	2,00475	PA5188			
0,71119	1,78032	lexA PA3007			
0,69349	1,39635	PA0653			
0,67850	1,84562	accC fabG PA4848			
0,63381	1,55776	PA5028			
0,62240	1,33088	PA5020			
0,60354	1,46363	pyrR PA0403			
0,59925	1,77134	speA PA4389			
-0,61652	1,39178	PA3481			
-0,63312	1,56278	dnaX PA1532			
-0,65144	1,52825	hitA PA4687			
-0,65357	1,47409	PA2613			
-0,66020	2,28059	ibpA PA3126			
-0,67159	1,34562	ubiG PA3171			
-0,70317	1,92343	PA0571			
-0,73085	1,45137	pheA PA3166			
-0,74702	1,52829	queE PA0975			
-0,79419	1,36811	PA3762			
-0,84465	1,45209	aroE PA0025			
-0,86274	1,44810	earP PA2852			

Table F.1. continued from previous page

-log$_{10}$(p-value)	log$_2$FC	Gene names	-log$_{10}$(p-value)	log$_2$FC	Gene names
Meropenem 0.0064 μg/mL vs Control			**Ceftazidime 32 μg/mL vs Control**		
-0,86755	1,67770	gloB PA1813			
-0,88695	1,62831	PA5187			
-0,96232	1,40768	PA3295			
-0,96489	1,95765	PA1501			
-0,96681	1,40273	dauB PA3862			
-0,97930	1,70049	soj PA5563			
-1,02904	1,84640	PA3017			
-1,05258	1,49381	trpD PA0650			
-1,07579	1,35900	surE PA3625			
-1,12587	1,67757	pslD PA2234			
-1,17562	1,31685	PA5471			
-1,27945	1,33304	tsf PA3655			
-1,29177	1,37420	gmhB PA0006			
-1,30239	1,30183	ahpC PA0139			
-1,31028	1,93467	PA0250			
-1,32156	1,31651	pbpG PA0869			
-1,45000	1,50239	PA5209			
-1,46636	1,39481	mutM fpg PA0357			
-1,47349	1,43834	PA3859			
-1,48486	1,30215	PA5176			
-1,50695	1,45304	nirN PA0509			
-1,50786	1,69813	PA5195			
-1,56001	1,87986	PA2567			
-1,58942	1,40187	PA2631			
-1,75517	2,18337	PA4465			
-1,97662	1,89143	cysA PA0280			
-2,15546	1,37561	radA PA4609			
-2,15688	1,30422	iscS PA3814			
-2,17275	1,33104	rplU PA4568			
-2,28880	1,37592	gpsA PA1614			
-2,46286	1,68807	gacA PA2586			
-2,50745	1,65817	PA0494			
-2,70335	1,72018	PA2528			
-2,72047	1,77548	PA3895			
-2,75636	1,73785	PA5498			
-2,75759	1,69692	gmhA PA4425			
-2,80752	1,37335	PA1755			
-2,97166	2,24399	fabZ PA3645			

G Dys-regulated Proteins in PAU5 Spiked with TZP

Appendix G includes all dys-regulated proteins identified in strain PAU5 spiked with the β-lactam Piperacillin for a final concentration of 32 μg/mL and Tazobactam for a final concentration for 4 μg/mL.

Table G.1. Dys-regulated proteins in PAU5. Overview over all dys-regulated proteins in isolate PAU5 when spiked with Piperacillin/Tazobactam (TZP).

-log$_{10}$(p-value)	log$_2$FC	Gene names		-log$_{10}$(p-value)	log$_2$FC	Gene names
Piperacillin/Tazobactam 32/4 μg/mL vs Control				**Piperacillin/Tazobactam 32/4 μg/mL vs Control**		
1,45904	4,17599	PA4456		1,35711	-0,91791	PA4796
1,40565	4,11020	narH PA3874		1,69415	-0,92367	nusA PA4745
3,05400	3,94907	PA3822		1,97546	-0,93289	cysS PA1795
1,81034	3,71376	PA3026		1,45320	-0,97322	PA4322
1,35218	3,41740	PA0537		1,38985	-0,99565	rhdA PA4956
1,39036	3,36103	PA1832		1,50175	-1,00242	bioD PA0504
2,19113	3,07508	nirN PA0509		1,63010	-1,04457	spoOJ PA5562
1,43200	3,00912	narG PA3875		4,26417	-1,08945	PA4841
1,39581	3,00397	atpF PA5558		1,66093	-1,11564	PA0756
1,44759	2,97784	ccmH PA1482		1,43968	-1,12050	PA1205
2,25353	2,88371	PA2815		1,49314	-1,15326	queA PA3824
1,39154	2,75258	PA1767		1,76603	-1,15875	PA4923
1,37560	2,72035	PA1791		1,52768	-1,16680	recQ PA3344
1,31338	2,60073	cmpX PA1775		1,67236	-1,18003	rdgC PA3263
1,55412	2,32322	cspD PA2622		1,47843	-1,18397	cobO PA1272
1,34607	2,30802	fimV PA3115		1,41441	-1,19493	rsmJ PA3680
1,42565	2,18204	osmE PA4876		1,35945	-1,20478	dnaQ PA1816
1,43116	2,17718	PA3689		1,53527	-1,22432	lon PA1803
1,53377	1,97411	lnt cutE PA3984		1,46003	-1,23597	PA3717
1,30452	1,94797	PA4431		1,67660	-1,23919	dadA1 dadA PA5304
1,42405	1,93038	ftsI pbpB PA4418		1,87553	-1,24208	tufA PA4265; tufB PA4277
1,74565	1,87224	PA3352		1,50237	-1,24799	PA0487
1,30260	1,86502	PA1601		1,74021	-1,26365	nrdA PA1156
1,37921	1,83472	PA3281		2,21463	-1,27458	PA0962
1,98633	1,82062	PA5494		1,46437	-1,28237	PA4686
1,36104	1,73804	rpsO PA4741		1,33089	-1,29523	gpmI pgm PA5131
1,43628	1,64986	metN2 PA5503		1,87894	-1,32293	cca PA0584
1,74853	1,57591	PA2608		1,78064	-1,35990	PA3685
1,32283	1,54893	PA4429		1,38037	-1,38698	aroQ PA5184
1,69010	1,53149	PA0126		1,59146	-1,38781	folA PA0350
1,39541	1,52636	PA3690		1,35257	-1,39614	glyA3 PA4602
1,77323	1,51363	secF PA3820		1,65578	-1,40308	prfA prf1 PA4665/5470
1,34143	1,49931	PA3205		3,38495	-1,41768	PA4388
1,39854	1,36801	bfr bfrA PA4235		1,40227	-1,45028	PA4991
1,83543	1,35214	arcB PA5172		2,03550	-1,45426	gmhB PA0006
1,32988	1,31561	pyrB PA0402		1,83726	-1,46125	PA3225
1,44015	1,31283	pyrC' pyrX PA0401		1,54776	-1,49116	PA5435
2,01004	1,14022	PA0653		2,89675	-1,49654	PA3732
1,41858	1,07788	grpE PA4762		1,57532	-1,50726	purD PA4855
1,77536	1,07566	PA3046		1,90307	-1,51406	nadE PA4920
1,59115	0,99505	PA0991		1,75822	-1,51575	liuE PA2011
1,99726	0,99415	phnW PA1310		1,72132	-1,52608	msrA PA5018
1,55256	0,88834	lpdG PA1587		2,39394	-1,53936	PA1995
1,83109	0,78106	PA4453		1,33980	-1,54620	PA2798
2,00324	0,72610	katA PA4236		3,55977	-1,55017	potD PA3610
1,40552	0,59345	tssC1 PA0084		1,44728	-1,55209	phhB PA0871
1,57394	-0,58656	thiC PA4973		1,83841	-1,55759	minC PA3243
2,19134	-0,61857	rlmN PA3806		1,53554	-1,55896	PA0317
1,39056	-0,62956	rplR PA4247		1,91072	-1,57149	PA3539
1,75059	-0,69682	PA1746		1,56069	-1,57359	accC fabG PA4848
1,68424	-0,75584	PA5229		2,02645	-1,58252	PA0759
1,44004	-0,77594	msrP PA4692		2,19069	-1,58697	bioB PA0500
1,35708	-0,80277	PA2854		1,72925	-1,62537	PA5313
1,73456	-0,81897	argJ PA4402		1,45042	-1,63851	tolB PA0972
1,43655	-0,83790	nusG PA4275		2,23585	-1,63937	fimL PA1822
1,45650	-0,84175	PA0629		1,46686	-1,65775	fabD PA2968

Table G.1. continued from previous page

-log$_{10}$(p-value)	log$_2$FC	Gene names	-log$_{10}$(p-value)	log$_2$FC	Gene names
Piperacillin/Tazobactam 32/4 μg/mL vs Control			Piperacillin/Tazobactam 32/4 μg/mL vs Control		
1,62002	-0,86273	sseA PA1292	1,77776	-1,67346	rpiA PA0330
1,75668	-0,87452	ybeY PA3982	1,83362	-1,68001	queE PA0975
1,32675	-0,90480	PA1673	1,33023	-1,68341	PA5312
1,56332	-0,90774	PA3967	1,39762	-1,68831	crc PA5332
1,43789	-1,69723	astB aruB PA0899	1,61938	-2,17134	glnS PA1794
1,64693	-1,69940	glmS PA5549	1,47124	-2,17210	PA0367
1,97868	-1,70480	acnB PA1787	1,72204	-2,17376	PA4615
2,11206	-1,71212	truB orp PA4742	2,16636	-2,17800	mnmA trmU PA2626
1,40252	-1,72208	ttcA PA1192	1,49956	-2,18239	dadX PA5302
1,34117	-1,73741	tpiA PA4748	1,43987	-2,18917	argR PA0893
2,43133	-1,75885	PA1624	1,73242	-2,19298	PA2251
1,60470	-1,76483	PA0891	1,49059	-2,20624	ppsA PA1770
2,26560	-1,77304	proC PA0393	1,66426	-2,22554	PA3889
1,48392	-1,78291	pdxH PA1049	1,51018	-2,23202	PA5441
1,49426	-1,78720	PA4769	1,70376	-2,23399	gatB PA4484
1,57491	-1,80302	PA1440	1,30524	-2,23497	murC PA4411
2,26723	-1,80928	PA0571	1,47265	-2,25721	proA PA4007
2,01139	-1,81786	PA3787	1,54313	-2,27140	PA5236
1,32602	-1,81819	PA1737	1,40785	-2,27565	dxs PA4044
1,33716	-1,82214	PA1234	1,39380	-2,28594	PA2530
1,37922	-1,82415	argG PA3525	1,36252	-2,32257	PA5176
1,37549	-1,82733	carB PA4756	1,63677	-2,32260	hemH PA4655
1,60638	-1,83599	pyrE PA5331	1,64624	-2,32304	pilT PA0395
1,33162	-1,84619	epd PA0551	3,50650	-2,34030	xpt PA5298
1,66562	-1,86393	serS PA2612	1,37893	-2,34208	PA0122
1,77332	-1,87699	smc PA1527	1,51329	-2,34817	serA PA0316
1,66440	-1,88824	atuR PA2885	1,71776	-2,34818	PA0369
1,53793	-1,89480	aspA PA5429	3,24733	-2,35069	trpG PA0649
2,57764	-1,89613	mtnC PA1685	1,32902	-2,35233	fdhE PA4809
1,42924	-1,89902	PA1067	2,30230	-2,36107	PA0533
4,04880	-1,90801	hitA PA4687	3,26707	-2,36346	earP PA2852
1,54397	-1,91650	PA5217	1,34775	-2,36710	PA3895
1,33531	-1,92701	PA3076	2,03903	-2,37313	PA2915
1,84728	-1,96405	PA2547	1,32100	-2,37614	PA1573
1,33831	-1,96514	aruH PA4976	1,49245	-2,37615	astA aruF PA0896
1,62807	-1,96772	trpI PA0037	1,69953	-2,38419	trhO PA0858
1,68442	-1,97546	gshA PA5203	1,55115	-2,40640	amgK PA0596
2,18289	-1,98141	PA0840	2,08652	-2,41028	PA4349
2,09536	-1,98481	queF PA2806	1,53149	-2,41514	pqsC PA0998
1,41873	-1,98730	rnc PA0770	1,45810	-2,44111	PA1296
1,94150	-1,98955	PA5506	1,77234	-2,44253	dtd PA5079
1,73343	-1,99623	aruG PA0897	1,94719	-2,44590	prlC PA0067
1,30904	-2,00714	fumC2 PA4470	1,70511	-2,44932	PA2813
1,64495	-2,01135	sucA PA1585	1,79595	-2,45213	PA1616
1,75482	-2,02590	murF PA4416	2,15107	-2,45393	murA PA4450
1,53980	-2,02762	proS PA0956	1,36004	-2,47475	PA1576
1,38311	-2,02841	PA2554	1,32082	-2,48168	gmk PA5336
1,34372	-2,03593	PA0387	1,80237	-2,48185	PA2613
1,38677	-2,04005	rlmL PA3048	1,60828	-2,49700	pykA PA4329
2,18610	-2,04472	betI PA5374	1,38663	-2,49966	trpD PA0650
1,54725	-2,04984	PA5436	1,36775	-2,50604	dauB PA3862
1,43506	-2,05734	cysI PA1838	1,36128	-2,50937	xenB PA4356
1,54505	-2,05997	tktA PA0548	1,81834	-2,51405	leuS PA3987
1,32341	-2,06655	nfxB PA4600	1,33826	-2,52159	PA2990
2,11167	-2,06677	rnhB PA3642	1,41686	-2,52502	PA3459
1,52899	-2,07592	pgk PA0552	1,68542	-2,52917	PA0399
1,60419	-2,11820	galU PA2023	1,44084	-2,53805	trpS PA4439
1,36117	-2,11967	PA3919	1,55507	-2,56007	thrS PA2744
1,69631	-2,12248	PA4709	2,00041	-2,56402	cysG PA2611
1,32348	-2,12435	PA5190	1,74499	-2,58612	glyS PA0008
2,26481	-2,12767	rlmG PA4617	1,64407	-2,58932	priA PA5050
1,39194	-2,14286	truD PA3626	1,44547	-2,59534	PA0902
1,41016	-2,14485	PA5309	2,43589	-2,60898	thiI PA5118
1,57941	-2,15803	thrC PA3735	2,03179	-2,61383	PA2380
1,63063	-2,61438	gatA PA4483	2,76413	-3,25689	psrA PA3006

Table G.1. continued from previous page

-log$_{10}$(p-value)	log$_2$FC	Gene names		-log$_{10}$(p-value)	log$_2$FC	Gene names
Piperacillin/Tazobactam 32/4 μg/mL vs Control				**Piperacillin/Tazobactam 32/4 μg/mL vs Control**		
1,41242	-2,62543	fabV PA2950		3,01170	-3,26462	rsgA PA4952
1,52920	-2,62704	nudC PA1823		1,44664	-3,27410	PA4434
1,36555	-2,63995	pepP PA5224		1,46677	-3,29201	mutY PA5147
1,74838	-2,64344	tyrS2 PA0668		1,30947	-3,32699	PA5391
2,57839	-2,66000	hutI PA5092		1,46647	-3,33641	PA1027
1,61587	-2,66326	glmR PA5550		1,36277	-3,35424	PA1181
1,33637	-2,67201	PA4475		1,32976	-3,38864	PA1752
1,46683	-2,68488	PA1304		1,33525	-3,42075	PA3255
2,22673	-2,68998	pheA PA3166		1,47055	-3,43102	PA1623
3,34161	-2,70232	PA2871		1,49552	-3,43570	hudA PA0254
1,76057	-2,70791	mnmE trmE PA5567		1,48647	-3,44198	PA3613
1,87077	-2,70997	cobL PA2907		1,65859	-3,53075	dhcB PA2000
1,83483	-2,73187	pmrA PA4776/PA2479		1,31124	-3,54161	anmK PA0666
1,63277	-2,75585	PA5187		1,37143	-3,57805	PA0419
2,45820	-2,75825	phaJ2		1,45331	-3,58672	PA3356
1,54083	-2,76349	ung PA0750		1,58642	-3,58704	PA4068
1,43819	-2,76708	glcB PA0482		1,45315	-3,59428	hmgA PA2009
1,40884	-2,76829	speE1 speE PA1687		1,78496	-3,60595	gltD PA5035
1,55296	-2,77348	PA5509		2,04642	-3,61377	PA5007
1,91294	-2,78204	morB PA2932		1,63651	-3,61796	PA5508
1,41038	-2,79129	davD PA0265		1,74857	-3,64547	coaX coaA PA4279
1,41995	-2,80404	PA1024		2,25566	-3,66306	prpC PA0795
1,39589	-2,81635	purL PA3763		1,73426	-3,67035	gloB PA1813
2,16313	-2,82822	PA1069		1,44402	-3,68178	PA5104
1,39169	-2,83484	PA3454		1,52039	-3,71005	PA0335
1,64823	-2,84305	argS PA5051		1,40786	-3,73112	PA0159
1,43511	-2,85501	metF PA0430		1,36732	-3,73335	fmt PA0018
1,94427	-2,85560	PA2196		1,30982	-3,75067	acsA2 acsB PA4733
1,44278	-2,87113	trmA PA4720		2,36618	-3,77506	pslB PA2232
1,37325	-2,88347	pckA PA5192		1,87110	-4,01710	PA5433
1,58295	-2,88610	PA3106		1,59860	-4,06892	PA4968
1,55704	-2,89682	glk PA3193		1,34936	-4,10153	PA0478
1,85367	-2,90809	PA1039		2,04190	-4,14027	prfC PA3903
1,36490	-2,91768	valS PA3834		1,64361	-4,23860	rlmD rumA PA0933
1,68395	-2,92694	phhC PA0870		1,95205	-4,33627	ansA PA2253
1,82438	-2,93670	PA4955		1,48793	-4,35609	hpcC PA4123
1,87100	-2,93859	pheS PA2740		1,79031	-4,42593	PA2592
1,52817	-2,93919	rnd PA1294		1,31192	-4,43770	PA2831
1,53008	-2,94021	surE PA3625		1,84965	-4,46352	PA0418
1,99848	-2,94878	astE aruE PA0901		1,60466	-4,50882	trkA PA0016
1,76120	-2,95952	thyA PA0342		1,75554	-4,57528	zwf PA5439
1,75624	-2,99342	PA1859		1,47589	-4,61816	PA3896
1,89114	-3,03418	pheT PA2739		1,72182	-4,92383	PA3615
1,98438	-3,05440	glyQ PA0009		2,64023	-4,93472	PA1221
1,46772	-3,05750	PA3128		1,41660	-5,00091	PA5422
1,59169	-3,06083	gltB PA5036		1,46734	-5,09770	dhcA PA1999
2,52215	-3,08790	PA3087		2,97069	-5,21301	sspA PA4428
1,86144	-3,09791	PA0148		1,34046	-5,26536	PA0794
1,31435	-3,12013	trmB PA0382		1,33867	-5,31383	rlmH PA4004
1,48464	-3,12916	mpl PA4020		1,96130	-5,31497	PA3924
2,64226	-3,13279	tesB PA3942		1,77600	-6,72460	cti PA1846
1,73015	-3,14377	usg PA3116				
1,58899	-3,15660	gcvT PA5215				
1,35354	-3,16897	purH PA4854				
1,39283	-3,17764	nadK PA3088				
1,42541	-3,21660	rsmH mraW PA4420				
1,51061	-3,23152	PA2497				
1,56814	-3,24736	PA4679				
2,44290	-3,25454	poxB blaOXA-50a				

Norges miljø- og biovitenskapelige universitet
Noregs miljø- og biovitskapelege universitet
Norwegian University of Life Sciences

Postboks 5003
NO-1432 Ås
Norway